Optical and Electrochemical Transduction of Calixarene Host-Guest Chemistry

by

Teresa Grady

B.Sc. in Analytical Science

Thesis Submitted in Accordance with the Requirements for the Degree of

Doctor of Philosophy

to

Dublin City University

Ollscoil Chathair Bhaile Átha Cliath

School of Chemical Sciences

Supervisors: Dr. Dermot Diamond & Prof. Malcolm R. Smyth

July 1996

Declaration

I hereby certify that this material, which I now submit for assessment on the programme of study leading to the award of Doctor of Philosophy is entirely my own work and has not been taken from the work of others save and to the extent that such work has been cited and acknowledged within the text of my work

Signed: Teresa Grady
Teresa Grady

ID No.: 92700535

Date: 6/9/'96

For my Parents

Teresa and Henry

Acknowledgements

Firstly, I would like to thank Dr Dermot Diamond for his support and guidance over the last four years and especially during the preparation of this thesis (maybe some day I might be able to teach you how to play squash!!!!) Thanks also for the musical interludes that kept me sane I would also like to acknowledge Prof Malcolm Smyth for his supervision during my research I am also grateful to Pfizer Ltd UK, for sponsoring my post-graduate studentship Thanks are due to Dr Steve Harris and Prof Tony McKervey for the synthesis of the calixarenes used in this research and to Paddy Kane for the molecular modelling

Sincere thanks to the technical staff of the chemistry department for all their assistance To Mick *"father-figure"* Burke, Maurice *"Linford Christie"* Burke, Damian *"sweetie-pie"* McGuirk, Veronica, Ann, Shane, Niall and not forgetting the lunchtime *God Squad.*

To the J118 crew, both past and present, Mary, Declan and Mikey, thanks for all the laughs and useful chemistry discussions!!! To the members of WG30, Tom, Joe, Aoife, Dominic and Conor, the hardest working laboratory in the department (anyone for coffee???!!!) To the Thursday night crew, Fiona, Aisling, Cormac, Pat, Joe B, Declan and Rachael, you are a great gang!!! Thanks also to Daire, Noreen R, Lorraine, Norma, Noreen T, Sinead and Josephine for being great buddies

I would also like to express my appreciation to Martin for being so patient and for always being on time to collect me at the train station!

Finally, I am indebted to my parents for all their encouragement and support over the last "22 years" of education! I love you both very much Thanks also to the other members of the Grady Bunch, especially Anne and Sean for putting up with me (putting me up!)

Go raibh mile maith agaibh go leir

Table of Contents

List of Publications

1 "*Determination of the Enantiomeric Composition of Chiral Amines Based on the Quenching of a Chiral Fluorescent Calixarene*" T Grady, S J Harris, M R Smyth, D Diamond and P Hailey, Anal Chem , 1996, in press

2 "*Sodium-Selective Electrodes Based on Triester Monoacid Derivatives of p-t-Butylcalix[4]arene Comparison with Tetraester Calix[4]arene Ionophores*" T Grady, A Cadogan, T McKittrick, S J Harris, D Diamond and M A McKervey, Anal Chim Acta, 1996, in press

3 "*Characteristics of a Europium-Selective Electrode Based on a Calix[4]arene Tetraphosphine Oxide*" T Grady, S Maskula, D Diamond, D J Marrs, M A McKervey and P O'Hagan, Anal Proc Incl Anal Commun , 1995, **32**, 471

4 "*Characteristics of Sodium-Selective Electrodes Based on a Triethylester Monoacid Derivative of p-t-ButylCalix[4]arene", D Diamond, A Cadogan,* T McKittrick, T Grady, S J Harris and M A McKervey, Anal Proc Incl Anal Commun , 1995, **32**, 137

List of Poster Presentations

1 "*Development of a Distributed Fibre Optic Ammonia Sensor*" T Butler, T Grady, D Diamond and B McCraith European Conference on Optical Sensors and Biosensors, Zurich, Switzerland, March 1996

2 "*An Optical Sensor for Gaseous Ammonia based on a Calix[4]arene with a Nitrophenylazophenol Chromophore*" T Grady and D Diamond, Research and Development Topics in Analytical Chemistry Meeting, University of Hull, UK, 10-11th July, 1995

3 "*Characteristics of a Europium-Selective Electrode Based on a Calix[4]arene Tetraphosphine Oxide*" T Grady and D Diamond, SAC '95, University of Hull, UK, 11-15th July, 1995

Abstract

The well-known selective receptor properties and ease of structural modification makes calixarene derivatives attractive materials for use in chemical sensors This thesis represents a study of the performance of a range of calixarene compounds either as the active component of an optical sensor or as the ionophore in potentiometric sensors

Determination of enantiomeric purity has become important in recent years due to increasing restrictions on the composition of pharmaceuticals whose efficacy depends on a chiral moiety With the aim of enantiomeric selectivity, three novel fluorescent calixarenes were synthesised and their interaction with R and S enantiomers of phenylethylamine and norephedrine were investigated Stern-Volmer plots were used to evaluate the calixarenes and from this it was found that the calix[4]arene with a dinaphthylprolinol group attached to the lower rim exhibited the best selectivity of the three compounds investigated Using this compound it was possible to determine the percentage of one enantiomer in the presence of the other

In keeping with the increasing popularity of optical modes of transducing host-guest interaction of calixarenes, an ammonia gas optical sensor based on the nitrophenylazophenol calix[4]arene ligand was developed The optode membranes were prepared from a PVC cocktail composition and exhibited significant colour change on exposure to gaseous ammonia Some preliminary studies involving coated optical fibres together with a mass flow controller were also carried out demonstrating the potential of this chromogenic calixarene for the detection of ppm levels of ammonia

The performance of sodium selective electrodes based on the monoacid derivatives of tetramethyl and tetraethyl *p-tert*-butylcalix[4]arenes were investigated Virtually no difference in selectivity between the monoacid derivatives and the tetraesters was found pH stability studies showed that the monoacid derivatives gave best performance at neutral pH but at alkaline pH there was a reduction in response which did not occur with the tetraesters

A PVC membrane electrode based on an alklylated calix[4]arene tetraphosphine oxide was developed and found to be selective for europium (III) in the presence of a high background of sodium and other common ions The results also suggest that there is some selectivity within the lanthanide series itself Two other tetraphosphine oxide calixarene derivatives were also evaluated but were found not to be as selective as the alkylated calix[4]arene tetraphosphine oxide

1. Literature

1.1 Calixarenes.

The origins of calixarenes can be traced back to Adolf von Baeyers discovery of phenol-formaldehyde resins in the 1870s [1] It was not until early in the twentieth century that Leo Baekeland discovered that using a small and controlled amount of base the polycondensation of phenol and formaldehyde proceeds through the *ortho* and *para* positions leading to a commercially appealing material In 1907 he filed a patent on this process for making this highly cross-linked material he called Bakelite [2] In the 1940s, Zinke and his coworker Ziegler set out to simplify the problem of variability in the product conformations, by looking not at phenols but at *para*-substituted phenols When the para position is blocked e g with an alkyl substituent, condensation is restricted to a linear progression The base-induced reaction of formaldehyde and p-tert-butyl phenol yielded a crystalline product [3] that decomposed above 300°C which Zinke assigned as the cyclic tetrameric structure shown in Figure 1 2

In 1955, John Cornforth discovered that on repeating Zinke's reaction the products were found not to be single components but mixtures He proposed that the compounds were diastereoisomers arising from hindered rotation of the phenolic nuclei around the methylene linkage [4] However in the 1970s a combination of ^{1}H, ^{13}C NMR and mass spectroscopy revealed that Zinke's procedure yielded a combination of cyclic octamers and hexamers [5, 6, 7] When Gutsche became interested in bioorganic chemistry, known as enzyme mimics, he envisaged Zinke's cyclic compounds as potential molecular baskets His group set out to examine further the one-step process of the *p-tert*-butyl phenol reaction by varying the solvents, bases and reactant ratios [8] This led to the development of reliable one-pot syntheses procedures for the cyclic tetramer, hexamer and octamer from *p-tert*-butyl phenol, formaldehyde and base Calixarenes obtained by this procedure necessarily contain the same substituent in the *para* positions

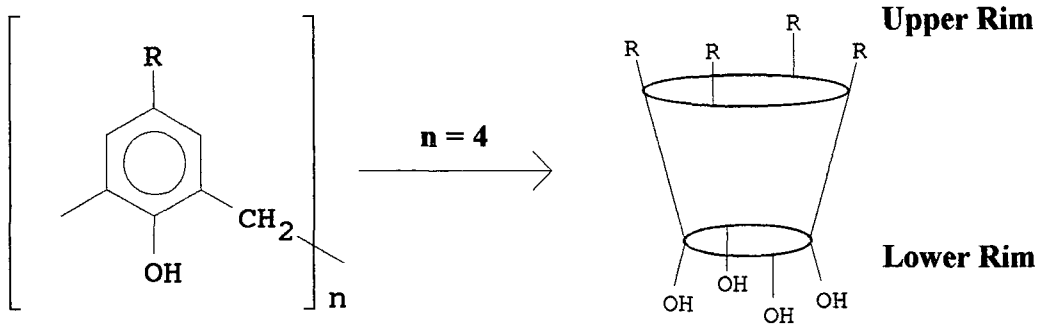

1 (i)

Figure 1.1: *General structure of calixarenes.*

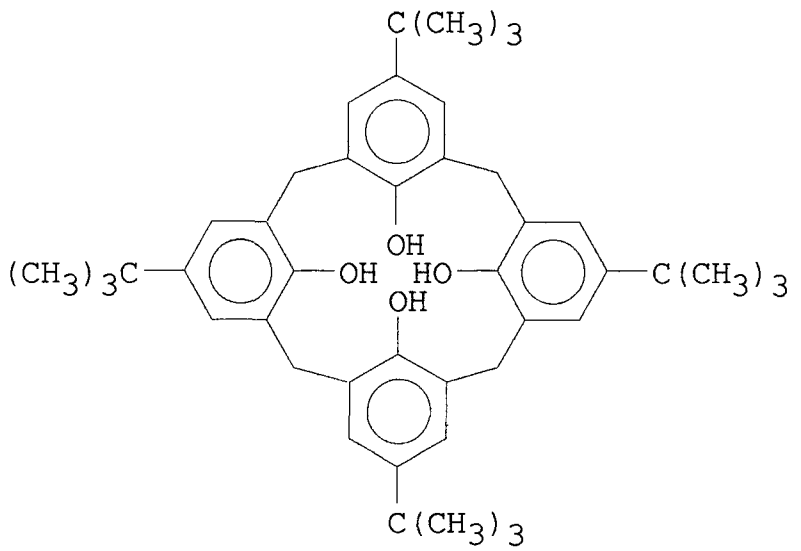

1 (ii)

Figure 1.2: *p-tert-butyl calix[4]arene*

Many names were suggested for this group of compounds but the term calixarene was the more pictorially and descriptively appealing term based on the similarity of the basket shapes to a calix (Greek vase or chalice) and the arene which denotes the presence of the aryl groups The number of aryl groups is indicated by the insertion of the number between the calix and the arene e g calix[4]arene for tetramers Then to indicate from which phenol the calixarene is derived the p-substituent is designated by the name e g the cyclic tetramer from *p-tert*-butylphenol is called *p-tert*-butyl calix[4]arene

The parent calixarenes are white crystalline materials characterised by high melting points They are insoluble in water and generally have low solubilities in most organic solvents, though with appropriate derivatisation, good solubilities can be obtained in either medium

These class of compounds have attracted appreciable attention because of their easy accessibility and interesting complexing properties The outcome of all this is the publication of three books [9, 10, 11], a conference series dedicated solely to the topic e g in Texas, USA [12] and not to mention an abundance of journal publications and patent applications

1 1 1 Conformations

The special appeal of calixarenes lies in their 3-dimensional structure Molecular models show that calixarenes can never be planar, although numerous conformations are possible by rotating the phenolic moieties about the Ar-CH_2 bonds Originally four principal conformations for calix[4]arenes were distinguished which Gutsche [13] labelled cone, partial-cone, 1,2-alternate and 1,3-alternate conformations (Figure 1 3) It is now known that calix[4]arenes prefer the cone conformation, an arrangement stabilised by a cyclic array of hydrogen bonds in which each phenolic hydroxyl group simultaneously acts as a donor and acceptor In solution, the cone conformation is indicated unequivocally by ^1H NMR e g for the tetra-tert-butyl ester of *p*-tert-butylcalix[4]arene (Figure 1 4), the aromatic protons and tert-butyl protons are singlets The four bridging methylene groups are also equivalent, but the two protons of each are non-equivalent in the cone conformation and at low temperature constitute an AB system with a coupling constant of 12-13 Hz On the basis of Nuclear Overhauser Effect experiments on simple calixarene derivatives [14] the high field doublet at δ 3 18 ppm has been assigned to the equatorial proton H_B (closer to the aromatic rings) whereas the low field singlet at δ 4 89 ppm to the axial one, H_A (closer to the phenolic oxygens) At higher temperature these signals broaden, then coalesce, and finally become a sharp singlet This behaviour is best understood as a rapid interconversion of opposite (but identical) cone conformations During this interconversion, in which the hydroxyl groups pass through the annulus, the original equatorial proton assumes the position of the axial proton and vice versa so that only an average signal is recorded in the ^1H NMR spectrum

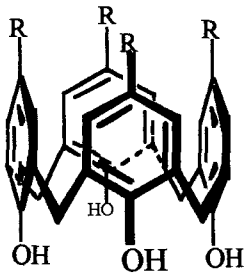

1 (iii)

Cone

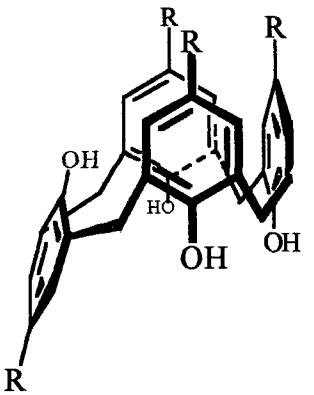

1 (iv)

Partial Cone

R ≠ H or Me

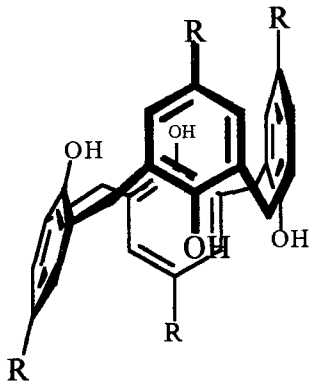

1 (v)

1,2-Alternate

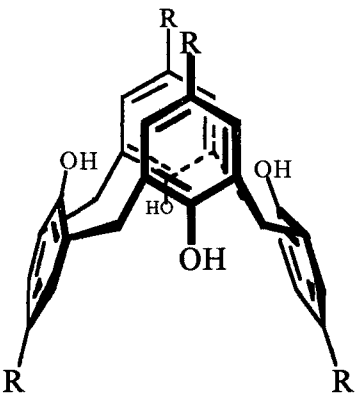

1 (vi)

1,3-Alternate

Figure 1.3: *The four principal calixarene conformations [13]*

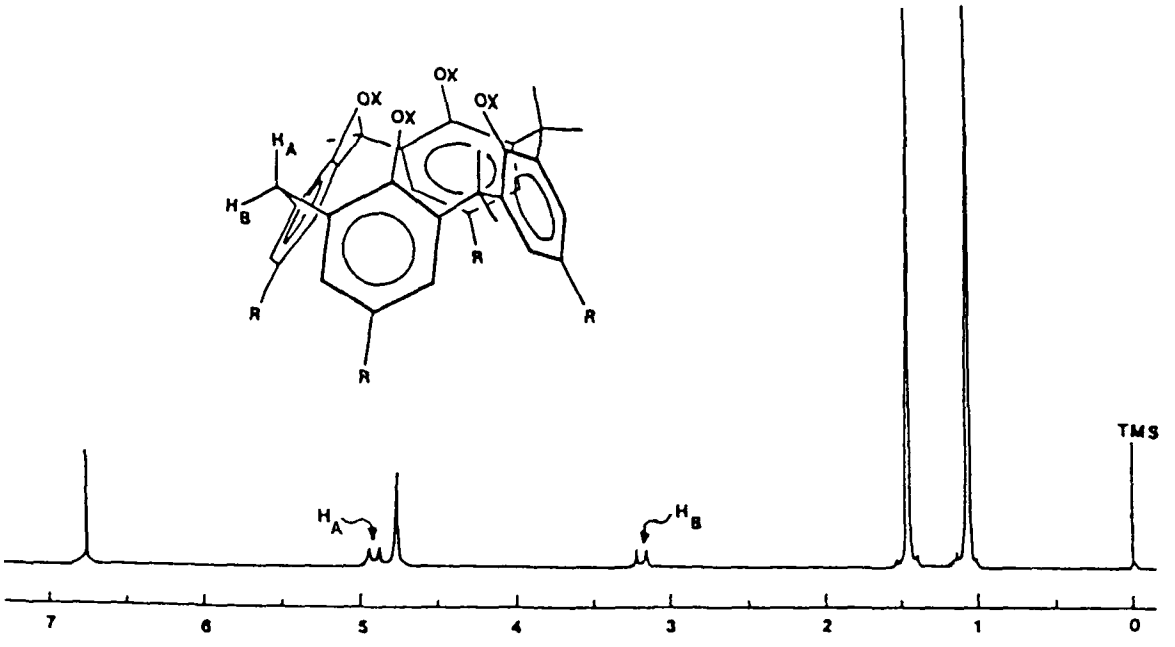

Figure 1.4: *^1H NMR spectrum of the tetrasubstituted t-butyl ester of p-tert-calix[4]arene which shows the fixed cone conformation X = CH_2COOBu^t [22]*

1 1.2 Chemical modification

The parent *p-t*-butylcalixarenes have been shown to possess very little ionophoric activity for alkali metal cations due to their inability to transport these ions from neutral aqueous solution through a chloroform membrane [15, 16] However, several workers have demonstrated that these calixarenes are amenable to chemical modification In these modifications the calixarene acts a substructure or platform to which an array of functional groups capable of acting as primary binding sites may be attached via the phenolic oxygens of the lower rim or the para positions on the upper rim (Figure 1 1) The first type of modification, lower rim functionalisation, is easily made by either alkylation or acylation The hydroxyl groups provide excellent sites for the introduction of groups which have been found to increase the ionophoric nature of the molecules [17] The second type of modification is possible because of the ease of dealkylating the *p*-tert-butylcalixarenes by Lewis-acid catalysis [18] Modification of the *p*-substituents has been shown to increase the solubility in a variety of organic solvents and in some cases render them soluble in water e g sulphonated and trimethylammonium chloride calixarenes [19, 20]

1.1 3 Receptor properties

Undoubtedly the most useful property of calixarenes is their ability to function as molecular baskets and bind neutral and ionic guests in supramolecular arrays There have been both rapid and extensive developments in the uses of the parent calixarenes and of chemically modified systems, notably in the extent to which these receptor properties are being exploited in analytical devices

The complexation of alkali and alkaline earth cations by neutral ligands of the type shown in Figure 1 5 has been examined extensively by phase transfer from water into an organic solvent (usually dichloromethane), ion transport through liquid membranes, stability constant measurements and general patterns of behaviour are beginning to emerge Thus, among the alkali cations, calix[4]arene derivatives have the highest

affinity for Na^+, exhibited as a larger stability constant (in MeOH) and through the high per cent extraction into dichloromethane Derivatives of calix[6]arenes prefer larger cations e g Cs^+ and Rb^+ while derivatives of calix[8]arenes are generally less effective as receptors due to the more open and flexible structures which leads to reduced recognition

The tetrameric calixarenes exist in a rigid cone conformation with the polar substituents grouped together at one end of the cavity and the hydrophobic moieties directed towards the upper rim thus conferring a high degree of preorganisation on the molecule The *p*-t-butyl tetramethyl ester calix[4]arene (Figure 1 5) exhibits a distorted cone conformation with two of the opposing aromatic rings essentially parallel while the other two rings are almost normal to one another The same sort of distorted cone shape is observed in the *p*-t-butyl tetraethyl ester calix[4]arene and in *p*-t-butyl-tetramethylketone calix[4]arene On complexation with an alkali metal ion, the distorted cone undergoes a slight conformational readjustment of the torsion angles, the cation being centrally located within the hydrophilic cavity defined by the four ester/ketone groups and supported electrostatically by the four etheral oxygen and four carbonyl oxygen atoms [21,22] This is demonstrated in the ^1H NMR spectrum of the free ligand, tetra t-butyl ester calix[4]arene and its sodium thiocyanate complex in Figure 1 6 By adding variable amounts of NaSCN in CD_3OD to a $CDCl_3$ solution of the ligand the ^1H NMR spectrum of the latter greatly changes in all signals The largest variation in chemical shifts is experienced by axial protons H_a which move 0 73 ppm upfield and by the aromatic protons which moves 0 38 ppm downfield Also the methylene protons of the acetate moieties move 0 37 ppm upfield whereas all ether signals shift downfield on complexation with the sodium ion This behaviour is due to the effect of the complexed cation, which induces downfield shifts on protons which are adjacent to the binding sites, and also to conformational changes The upfield shift experienced by the methylene protons of the acetate groups can be explained by assuming that upon complexation all these groups adopt a trans conformation, which brings the methylene protons out from the hydrophilic oxygen region and above the aromatic ring where they experience a shielding effect More difficult to explain is the high upfield shift (0 7 ppm) of the axial protons which appear to be very sensitive to small variations in the polar environment of the ether and ester oxygens, which are in

close proximity The involvement of the phenolic oxygens in complexation is indicated by the high downfield shift experienced by the aromatic protons This NMR titration experiment clearly indicates a 1 1 stoichiometry for the NaSCN complexing with the ligand, since all the signals remain unchanged after the salt/ligand ratio has reached the unity value (Figure 1 6c) For lower values of this ratio (Figure 1 6b) both signals for the complexed and uncomplexed are present, indicating that at room temperature, the exchange rate between the two species is slow on the NMR timescale

Numerous groups have investigated the different modifications of the phenolic groups and changes in the substituents bonded to the heteroatoms verifying the role played by phenolic and carbonyl oxygen atoms in forming complexes with alkali and alkaline earth metals This variation of cation selectivity occurs with modification of both the lower rim phenolic oxygens and upper rim *t*-butyl group and this has become the subject of a number of publications [23, 24, 25]

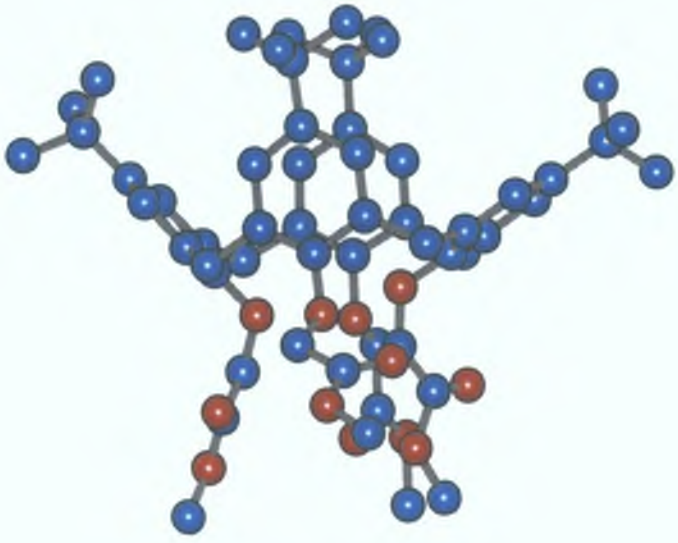

(a)

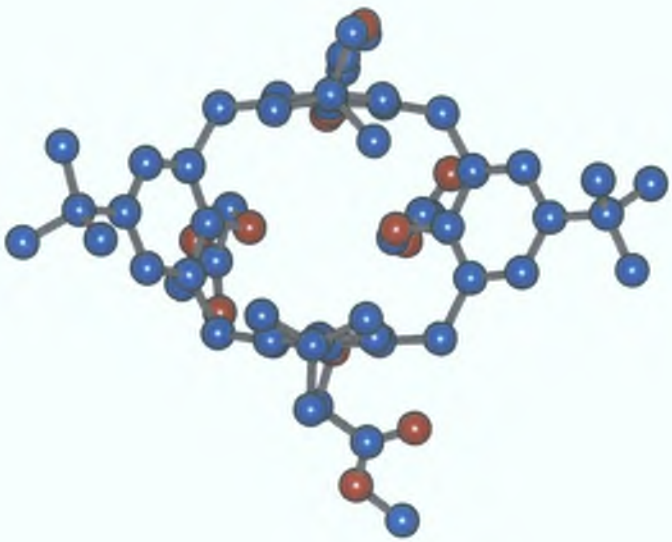

(b)

1 (vii)

Figure 1.5: *X-ray crystal structure of the tetramethyl substituted calixarene receptor [21] (a = side view and b = top view). Data obtained for structures from the Cambridge Crystallographic database and converted to Hyperchem v. 4.0. Blue = carbon atoms and red = oxygen atoms. Hydrogens not shown for clarity.*

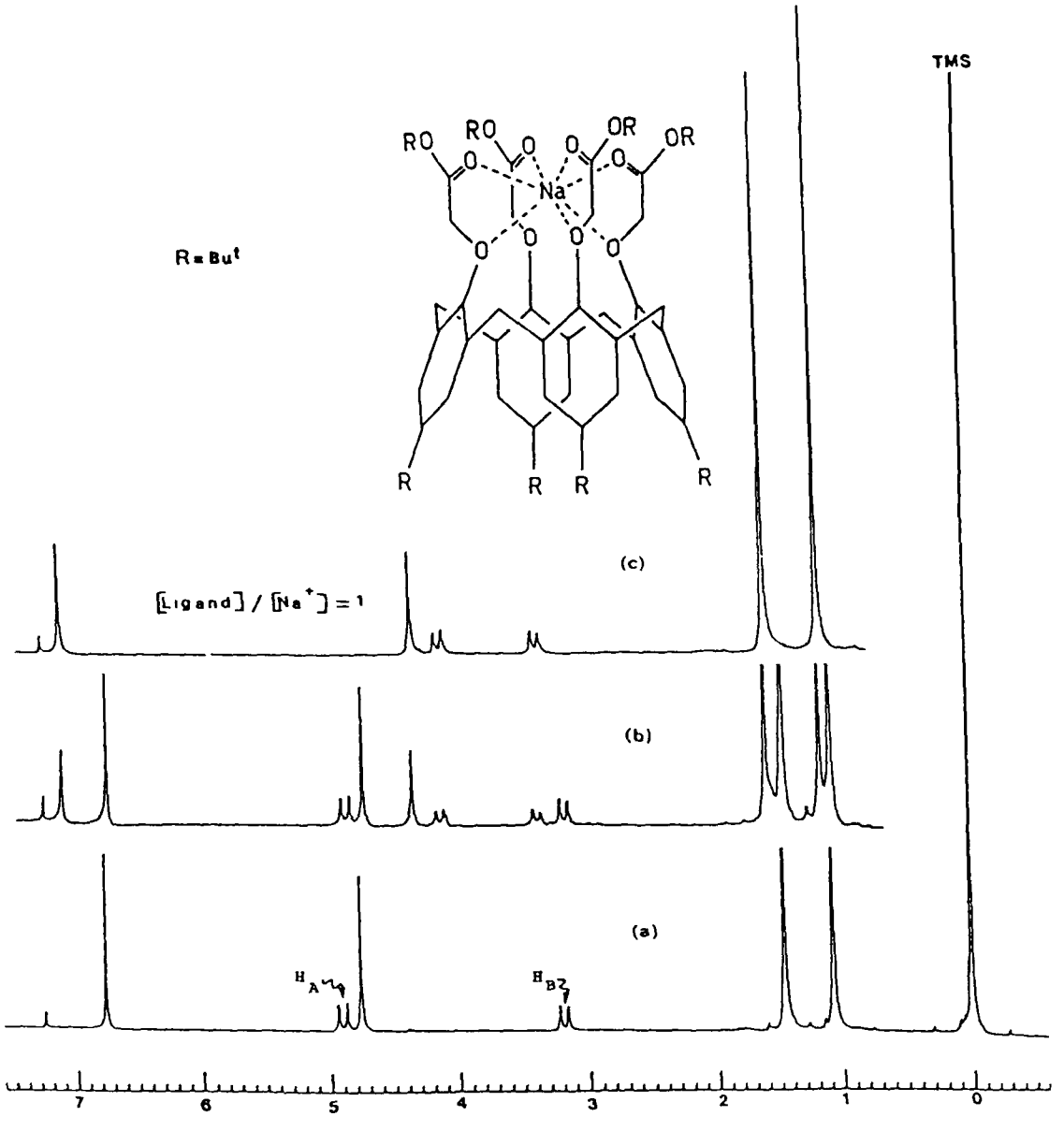

Figure 1.6: *Encapsulation of NaSCN by calix[4]arene ester ^1H NMR spectrum in $CDCl_3$ at 25 °C (a) free ligand, (b) 40% complex and (c) 100% complex [22]*

1 1 4 Applications of Calixarenes

Von Baeyer's phenolic resins were first commercially used in Bakelite Scientists in several countries are now looking for applications for calixarenes, the second generation of the phenolic resins and more than 80 patents have already been registered

One of the first applications was that of the Petrolite company in the US who in 1950 marketed the product of *O*-alkylation of *p-tert*-butyl phenol formaldehyde oligomers as a surfactant with excellent demulsifying properties Most of the more recent applications are associated with their properties as molecular receptors For example, Izatt has applied the alkali binding ability of calixarenes to the recovery of caesium from aqueous solutions containing mixtures of cations that are found in nuclear waste [26] Several Japanese patents describe the recovery of uranium from sea water by using a calix[6]arene hexacid 'super-uranophile' attached to polystyrene [27] The addition of calixarene derivatives to cyanoacrylate adhesives (super glue) is claimed to reduce fixation times and make a more durable bond [28]

Analytical applications are beginning to emerge for sensors [29, 30] and chromatography [31] Ion-selective electrodes for K^+ and Cs^+ have been successfully made using dioxacalix[4]arene [32] and calix[6]arene [33] respectively as the ionophore However, the most successful sensor application involves using calix[4]arenes to make PVC membranes which show remarkable Na^+ selectivity This material has been used to make bench and miniaturised Na^+ selective electrodes [34] and a Na^+ detector for flow injection analysis [35] These devices have been used to determine Na^+ in human blood plasma [36] and the results show excellent agreement with those obtained from laboratory analysers

Some applications in chromatography include using p-tert-butylcalix[8]arene as a stationary phase in GC for separating alcohols, chlorinated hydrocarbons and aromatics [37]

1.2 Chirality

Chirality means handedness and is based on the Greek word for hand 'cheir' A chiral molecule is one that is non-superimposable on its mirror image The human hand is probably the simplest example of chirality because it exists in two identical mirror image forms Chiral molecules, like human hands, also have a right-handed and left-handed form

If in a molecule a carbon atom is bonded to four different atoms or groups of atoms (R1, R2, R3, R4) the spatial orientation around the central carbon atom can be arranged in two ways, as can be seen in Figure 1 7 The two molecules shown are non-identical mirror images because of the opposite configuration around the chiral carbon and are called enantiomers Other words referring to such a pair of molecules are optical antipodes or optical isomers Enantiomers rotate plane-polarised light upon passage through a solution or solid under the same angle but in opposite directions (+ or −, *dextro* (d) or *laevo* (l)) for that reason they are called optical isomers A racemic mixture, or racemate, contains two equal portions of each enantiomer and, therefore, shows no net rotation of polarised light

A more general name for chemical molecules that differ in their spatial structure is stereoisomers Enantiomers are those stereoisomers that have a chiral centre and are mirror images If a molecule possesses more than one chiral centre, e g , n chiral carbon atoms, then 2^n stereoisomers are theoretically possible The relationship between stereoisomers can be seen in Figure 1 8 These may be mirror images (enantiomers) or stereoisomers that are not enantiomers but, in this case, diastereoisomers Thus all enantiomers are stereoisomers but not all stereoisomers are enantiomers

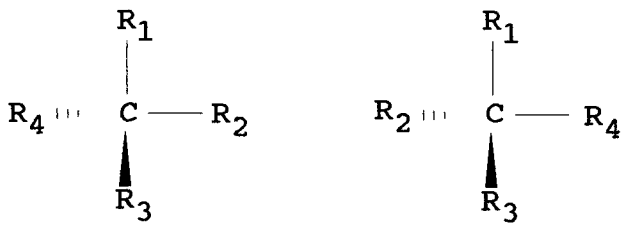

1 (viii) **1 (ix)**

Figure 1.7: *The chiral carbon atom and its two mirror-image forms*

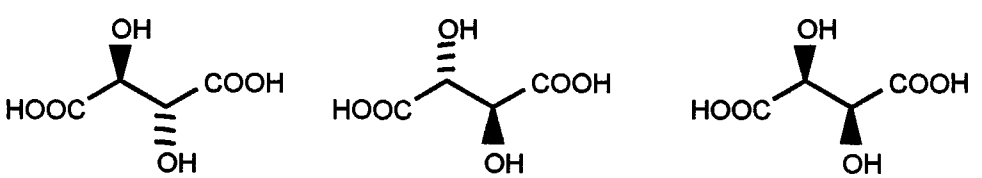

S, R *R, S* *Meso*

A **B** **C**

1 (x) **1 (xi)** **1 (xii)**

Figure 1.8: *The stereoisomers of tartaric acid A and B are a pair of enantiomers, C is a meso compound (a diastereoisomer of A and B)*

1 2 1 Labelling of chiral molecules

Enantiomers can be indicated as (+)/(-), d/l, D/L or R/S The first two refer to the direction to which the enantiomer rotates polarised light, d or (+) means rotation to the right and l or (-) signifies rotation to the left The D/L and R/S notations describe the absolute configuration around the chiral centre The D/L notation gives a correlation between the configuration of the molecule and the configuration of D/L glyceraldehyde and is mainly used for amino acids and carbohydrates [38] A monosaccharide which has its highest numbered chiral carbon with the same configuration as D-glyceraldehyde is designated D One in which it has the same configuration as L-glyceraldehyde is labelled L The R/S system is related to the Cahn-Ingold-Prelog sequence rule [39] and is based on the configuration and atomic number of the four substituents attached to the asymmetric carbon The groups around the chiral centre are ordered in a sequence according to the following basic rules

1 Higher atomic number is given priority
2 Higher atomic mass is given priority
3 *Cis* is prior to *trans*
4 Like pairs [(R,R) or (S,S)] are prior to unlike pairs [(R,S) or (S,R)]
5 Lone pair electrons are regarded as an atom with atomic number zero

By use of these rules, the groups, ordered in a sequence 1 > 2 >3 >4, are viewed in such a way that 4 (of lowest priority) is pointing backwards from the viewer The remaining groups are then counted When the group priorities follow a clockwise direction the chiral centre is labelled R and when the group priorities follow an anti-clockwise direction the chiral centre is labelled S (see Figure 1 9)

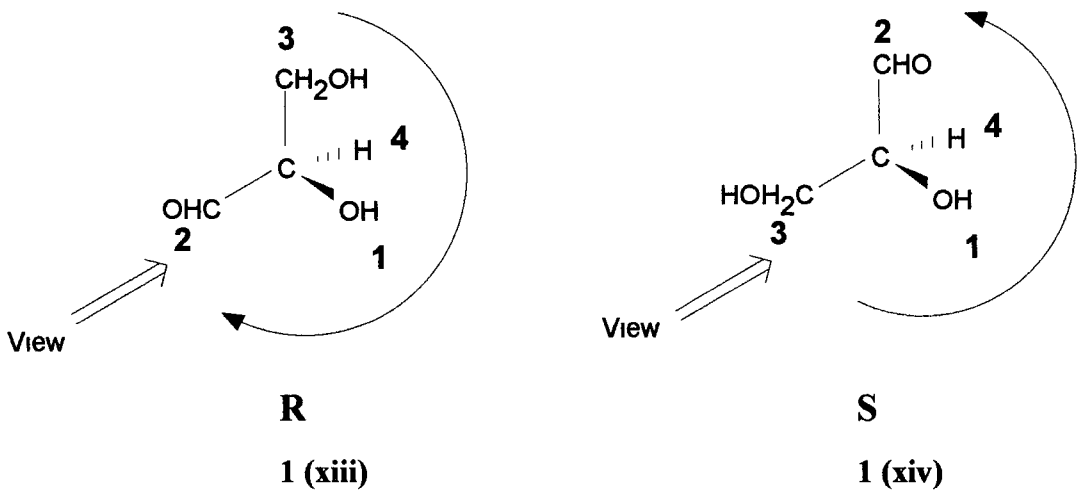

Figure 1.9: *The R and S nomenclature system [39]*

1.2.2 The importance of chirality

The existence of optical isomerism has been known since the first half of the 19th century In 1838, Jean-Baptiste Biot discovered optical activity [40] In 1850, Louis Pasteur isolated, with no more technical support than a pair of tweezers and a microscope, for the first time in history a pair of non-superimposable mirror-image crystal forms After acid treatment the isolated crystals of sodium ammonium tartrate liberated *d*- and *l*-tartaric acid [41] From Pasteur's first optical resolution of a racemate to modern sophisticated chromatographic techniques, there has been a formidable accumulation of stereochemical knowledge

Nature's well-known ability to produce and convert chiral compounds with a remarkable stereospecificity has always been fascinating The insight into enzyme structure and stereochemistry that mainly comes from kinetic and X-ray crystallographic studies has brought about a recognition of the importance of the spatial arrangement in multi-component active site-substrate interaction Similarly, the interaction between biologically active compounds and receptor proteins often shows a high or complete antipodal specificity Even more striking examples of chiral discrimination in physiological reactions are found in the hormone field e g the catecholamines Catecholamines are human endogenous compounds, which are extremely potent as regulatory hormones, affecting blood pressure and other important body functions The immediate precursor of catecholamines is L-dopa, which yields dopamine after enzymatic decarboxylation A completely stereospecific enzymatic hydroxylation then converts dopamine into a chiral compound, norepinephrine which is then converted to epinephrine The enzymes in these reactions are totally stereospecific, acting only on the L-enantiomer A common treatment for Parkinsons disease is therefore based on the administration of the L-form to increase the level of dopamine in the patients The importance of the correct configuration at the chiral centre of epinephrine and its analogues is evident from the fact that the natural R-(-)-epinephrine is at least twenty times as active as its enantiomer

More importantly, from our point of view, numerous drugs are synthetic racemic compounds and used as such Although this has often been quite adequate, there may exist the possibility that one of the two enantiomers is undesirable A tragic example was the use of thalidomide, a sedative and sleeping drug used in the 1960s, which caused serious malformations in the new-born of women who had taken the drug during the early phase of pregnancy In 1979 it was shown that it was only the (S)-(-)-enantiomer of thalidomide that possessed the tetratogenic action Furthermore, this enantiomer was without importance for the desired sedative or sleep-inducing property Therefore if the (R)-(+)-enantiomer alone had been given, no tetratogenic effects would have appeared and the drug might perhaps still have been used For such reasons the pharmaceutical industry is becoming more and more interested in methods to resolve racemates into optical antipodes in order to be able to subject these individually to pharmacological testing

Nowadays dramatic cases such as that of thalidomide are rare, reflecting the strict procedures laid down by the regulatory authorities, and the appropriate manufacturing and control procedures adopted by most companies before a drug is commercialised Moreover, major advances in asymmetric synthesis, preparative chiral purification methods and chiral chromatographic separation techniques, have helped drug companies to produce stereochemically pure drug compounds that show optical pharmacotherapy

Chiral chromatography is the main method for the resolution of enantiomers Analysts in the pharmaceutical industry now face the challenge of monitoring the stereoisomeric composition of potential drugs during both the discovery and development stages They usually need to characterise the drug stereochemically for purity and/or purity profiling after asymmetric synthesis, for determining the fate of a chiral molecule and it's metabolites (which may also be chiral) during *in vivo* and *in vitro* studies, and for preparative chromatographic separation of enantiomers for pharmacological evaluation While chiral chromatography has many advantages, its main disadvantage lies in the fact that it does not provide the chemist with real-time information on the resolution of the racemates, in the pharmaceutical industry

1.3 Resolution of enantiomers by host-guest interaction.

A host-guest relationship involves a complimentary stereoelectronic arrangement of binding sites in the "host" and "guest" The host component is defined as an organic molecule or ion whose binding sites converge in the complex, the guest component is defined as any molecule or ion whose binding sites diverge in the complex [42] Cyclodextrins, their derivatives, and chiral crown ethers, are hosts which spatially enclose the guests (analytes) or at least part of them Because of this property, these molecules have been extensively used in enantiomer resolution in HPLC, GC, CZE and chiral sensors

1.3.1 Cyclodextrins

Cyclodextrins—cycloamyloses, cycloglucans, or cyclomaltooligoses— were isolated as degradation products of starch by Villers as long ago as 1891 [43], but it was not until 1904 that they were characterised by Schardinger as cyclic oligosaccharides [44] Almost two decades before Pedersen's synthesis of crown ethers [45], Freudenberg and Cramer in 1948 recognised the ability of cyclodextrins to form molecular inclusion complexes [46] Cyclodextrins (CDs) are a homologous series of non-reducing cyclic oligosaccharides made up of six, seven or eight D-(+)-glucopyranose units connected via α-1,4,-glycoside bonds and designated as α-, β-, and γ- respectively The structure of β-cyclodextrin is shown in Figure 1 10 The inner diameter of the cavity measures 5 7, 7 8 and 9 5 angstroms for α-, β-, and γ- respectively

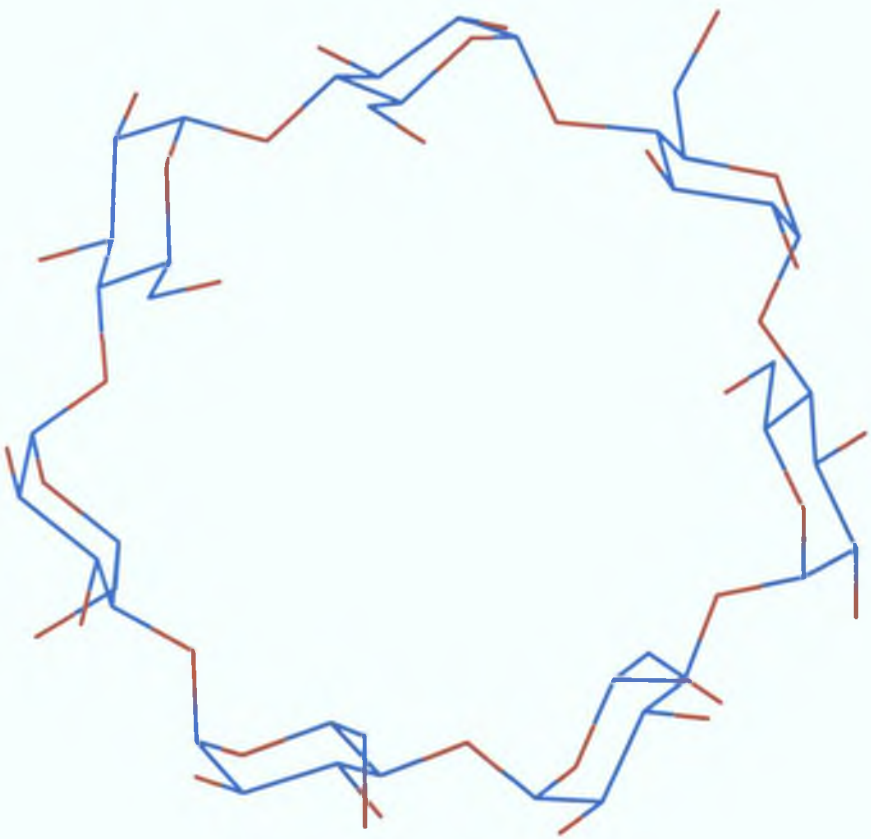

1 (xv)

Figure 1.10: *Structure of* β*-cyclodextrin [47]. Data for structures obtained from the Cambridge Crystallographic Database and converted to Hyperchem (v. 4.0). Blue = carbon atoms and red = oxygen atoms. Hydrogens not shown for clarity.*

They are obtained biotechnologically via enzymatic degradation of the glucose units of the polysaccharide starch These CDs are chiral molecules as each glucose unit contains five chiral atoms This means that the β-CD contains 35 chiral atoms These compounds, which have the shape of a truncated cone, have a hydrophobic inner cavity The chiral cavity, lined by hydrogen atoms and glycosidic oxygen bridges, is rimmed by secondary 2- and 3-hydroxyl functionalities at the larger opening and by primary 6-hydroxyl groups at the smaller orifice The surface of the molecule is relatively hydrophilic and therefore CDs are soluble in aqueous systems The solubility of CDs in both water and organic solvents can be substantially increased by derivatisation the protons of the hydroxyl groups are replaced by one or more methyl groups e g methyl-CD, dimethyl-CD, trimethyl-CD, hydroxyethyl-CD and hydroxypropyl-CD, leading to extended CDs Enantiorecognition of CDs is based on the inclusion of an aromatic functional group of the guest in the hydrophobic cavity (host-guest complexation) Additional hydrogen bondings between the substituents (at the chiral centre) in proper spatial orientation, and the secondary hydroxyl groups at the cavity entrance contribute to the inclusion-complex stability For maximum recognition the chiral centre of the analyte must be close to the entrance of the cavity

1 3 2 Crown ethers.

The discovery of crown ethers by Pedersen [48] opened the door to a new field of chemistry They are macrocyclic polyether ring systems consisting of several oxygens joined by ethylene bridges and are also classed as ionophores because they are able to form stable and selective complexes with various inorganic and organic cations The first identified crown ether, named "dibenzo-18-crown-6" (Figure 1 11) was not the target of synthesis in his experiment but a slight amount of unexpected by-product in a 0 4% yield However his appreciation of the importance of the discovery, followed by energetic research in the area established the foundation for the present status of crown ethers in chemistry

Pedersen named these macrocyclic polyethers with specific characteristics "crown ethers", because of their chemical structure as well as the fact that the shape of the complexes resembled a crown The conformation of the crown ether molecule is very flexible, and this confers very good solubility, not only in hydrophilic solvents such as water and alcohols, but also in hydrophobic solvents like benzene and chloroform

These ligands, which are classified in the family of coronands, are able to form stable and selective complexes with alkali, alkaline-earth and primary ammonium cations A second, more sophisticated generation of macrocycles are the cryptands of Lehn [49] and spherands of Cram [50] (Figure 1 12) As an acknowledgement of the substantial contributions they made host-guest chemistry, Pederson, Lehn and Cram were awarded the Nobel Chemistry Prize in 1987

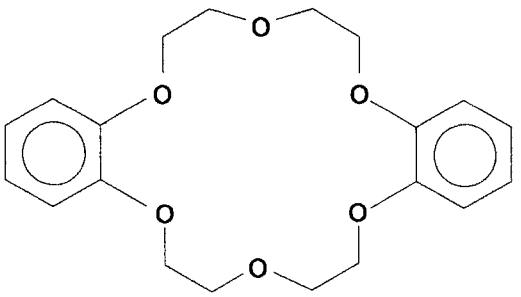

1 (xvi)

Figure 1.11: *dibenzo-18-crown-6 [48]*

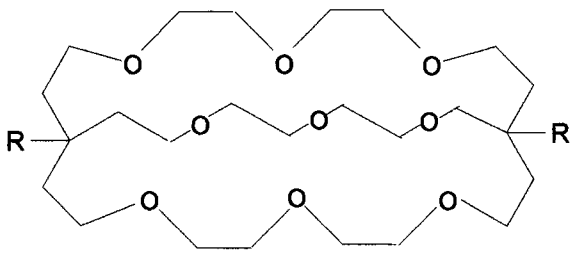

1 (xvii)

Cryptand

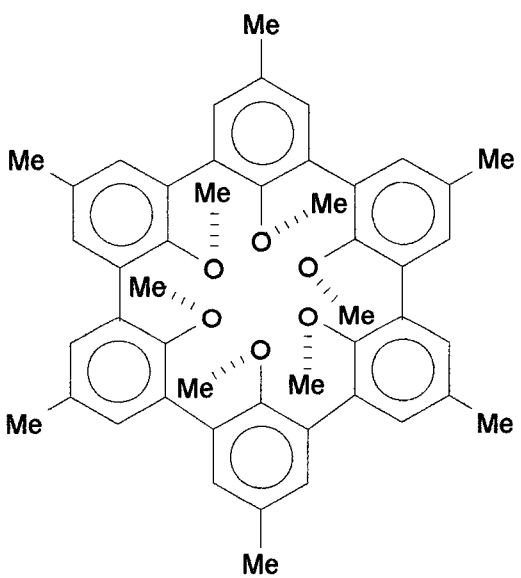

1 (xviii)

Spherand

Figure 1.12 *Structure of typical cryptand and spherand [49, 50]*

1 3 2 1 Chiral crown ethers

The first chiral crown ethers to exhibit chiral recognition towards enantiomeric substrates were described by Cram [51] in 1973 They were prepared from optically pure 2,2'-dihydroxy-1,1'-binapthyl and examples are shown in Figure 1 13 The isolation of optically pure enantiomers of this diol reflects its axis of chirality resulting from hindered rotation about its naphthalene-naphthalene bond A chloroform solution of the chiral receptor molecule, bisbinaphthyl-22-crown-6 (**1 xx**), is capable of extracting twice as much or the (R) enantiomer as of the (S) enantiomer from racemic α-amino-ester hexafluorophosphate salts [52] D-mannitol and L-tartaric acid served as precursors to the first chiral 18-crown-6 derivatives (Figure 1 14, **1 xxi-1 xxiv** and **1 xxv-1-xxviii** respectively) reported in 1975 [53] Simultaneously with the publication of these, Lehn and coworkers [54] described the preparation of chiral 18-crown-6 derivatives containing four carboxamide groups from L-tartaric acid (**1 xxix**)

Prelog and coworkers [55] chose 9,9'-spirobifluorene as a starting material for synthesising chiral crown ethers since (i) it has a more rigid carbon skeleton than the 1,1'-binaphthyl unit and (ii) it can be substituted easily in the 2 and 2' positions by electrophilic reagents (Figure 1 15)

More recently, Izatt and coworkers [56] have studied the equilibrium constant, enthalpy change and entropy change values for the interactions of a series of chiral pyridino-18-crown-6 type ligands with enantiomers of several primary alkylammonium salts in various solvents The extent of enantiomeric recognition and the stabilities of the chiral crown ether-ammonium salt complexes were found to depend on the many factors including the following

1 the ligand should be able to form reasonably stable complexes with the chiral guests If the conformation of a chiral ligand is twisted such that the three point hydrogen bond cannot form between the primary ammonium cation and the ligand, the ability of the ligand to recognise guest enantiomers will be poor
2 the ligand molecule should be rather rigid If the ligand is too flexible, it will be able to match both enantiomers of a guest equally well by adjusting the conformation

3 the chiral centre must be positioned to influence the R group on the ammonium cation, but not the three point hydrogen bonding

The classes of chiral crown ethers discussed thus far are the most common However they may also be prepared from a great many other chiral starting materials, including glycerol derivatives, optically active cyclohexanediols and D-ephedrine [57]

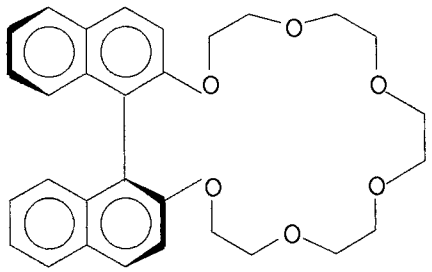

1 (xix)

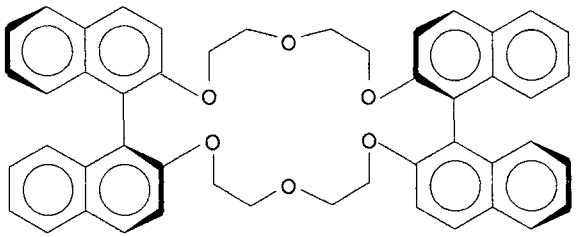

1 (xx)

Figure 1.13: *Cram's substituted binaphthyl-20-crown-6 and bisbinaphthyl-22-crown-6 [51]*

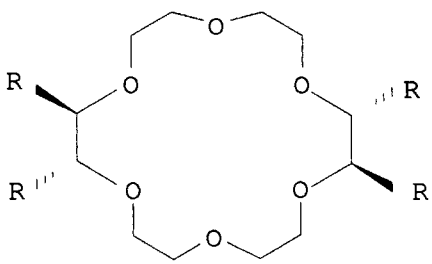

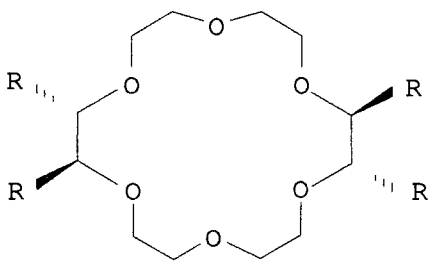

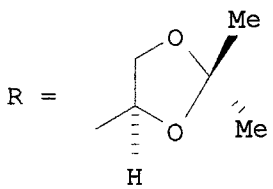

1 (xxi)

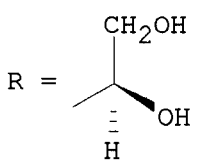

1 (xxii)

1 (xxv) R = CH_2Ph

1 (xxvi) R = H

1 (xxvii) R = CH_2OAc

1 (xxviii) R = CPh_3

1 (xxix) R = $CONMe_2$

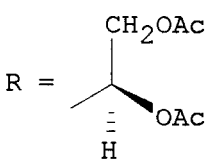

1 (xxiii)

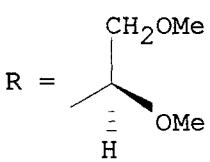

1 (xiv)

Figure 1.14: *Chiral crown compounds obtained from D-mannitol and L-tartaric acid [53, 54]*

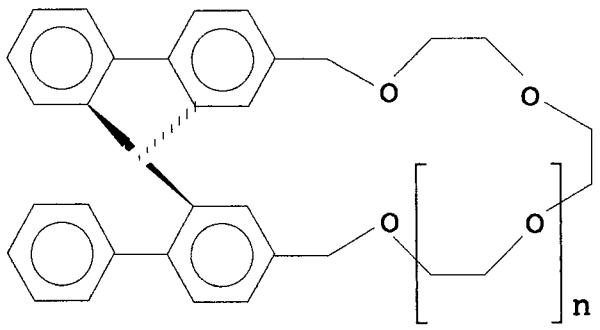

1 (xxx)

Figure 1.15: *Crown Compound containing chiral 9,9'-spirobifluorene units [55]*

1.3.3 Chiral chromatography

Over the last decade HPLC and GC have been used extensively to perform chiral separations There are principally three methods for resolving enantiomers by HPLC Two exploit conventional column technology, either by formation of diastereomeric derivatives, or by the use of chiral mobile phase additives A third method involves the use of chiral stationary phases which is also used in GC for enantiomeric separation The use of cyclodextrins and crown ethers in the formation of inclusion complexes with enantiomers either as chiral stationary phases or as mobile phase additives will now be discussed

1 3 3 1 Cyclodextrins in chiral chromatography

The major development in chiral liquid chromatography (LC) with cyclodextrins started with the technique of using them as mobile phase additives in TLC experiments [58,59] This technique was then applied with success to column chromatography where the CD was used as a chiral selector in the mobile phase together with an achiral column The CD was mainly used in the β-form in conjunction with a column working in reversed phase mode employing C_{18}-silica and an aqueous buffer system [60,61]

HPLC separation of compounds containing chiral centres with chiral stationary phases (CSPs) has seen a tremendous increase in recent years In the past decade, much research has centered on the use of cyclodextrins as CSPs for the LC separation of enantiomers CD CSPs were prepared by immobilising CD in polymeric structures [62,63] or on silica gel [64], the later showing good performance on an analytical scale Optimisation of the enantioselectivity can be achieved by modifying different factors, such as the concentration and nature of organic modifiers, pH, temperature and buffer concentration Although reversed phase modes are usually employed with the cyclodextrin-based CSPs, analytical applications in the normal mode have also been reported [65]

Much of the early work on the use of native cyclodextrins as GC stationary phases was done by Smolkova-Keulemansova and coworkers [66,67] and Sybilska [68] Native cyclodextrins sometimes were difficult to use as capillary stationary phases and generally inefficient due to their limited temperature range (maximum 70°C) and low theoretical plate numbers of about 950-1250 for columns two metres long (CD columns in HPLC give about 8000 theoretical plates for a length of 25 cm) Meanwhile, other researchers advanced two rather universal approaches using cyclodextrin derivatives In 1987, Novotny and Schurig introduced permethylated β-cyclodextrin, dissolved in a moderately polar polysiloxane, for the enantiomeric separation of many classes of compounds at a temperature range of 0-220 °C [69] In 1988, Konig, Wenz and colleagues [70], and in 1990, Armstrong [71], reduced the minimum working temperature of the stationary phase by using undiluted, low-melting cyclodextrin derivatives containing *n*-pentyl groups

An easy way to create enantioselectivity in capillary electrophoresis is by adding chiral selectors to the buffer solution Cyclodextrins are by far the most common of all chiral additives in capillary zone electrophoresis Derivatised cyclodextrins are usually employed at a low pH where the electroosmotic flow is minimal and the uncharged cyclodextrin does not migrate Basic compounds can migrate towards the detector once protonated and can form inclusion complexes on route with the cyclodextrins Enantioseparation is based on the premise that one enantiomer has a higher inclusion complex stability constant and migrates more slowly through the capillary, effecting a chiral resolution Examples of the use of this method for the separation of racemic mixtures of pharmaceutical products and amino acids are well documented in the literature [72,73] Cyclodextrins are also employed in micellar electrokinetic chromatography Cyclodextrins are solubilised by sodium dodecyl sulphate giving rise to micelles with enantioselective centres [74] Another method recently developed involves fixing the cyclodextrin on the capillary surface Thus the high efficiency of CE can be combined with the enantioselectivity of permethylated β-cyclodextrin polysiloxane phase [75], chemically bonded by an octamethylene spacer

1 3 3 2 Crown ethers in chiral chromatography

Cram and coworkers were the first to recognise the potential of optically active crown ethers for the separation of enantiomers in liquid chromatography [76, 77] The staggered arrangement of the binaphthyl rings in the structure of Cram's crown ethers behaves like a chiral barrier for the enantiomers The chiral crown ether was used either in the mobile phase or covalently bonded to a silica support Such a chiral host is able to discriminate between enantiomeric ammonium compounds, such as esters of D- and L-amino acids, because the multiple hydrogen bonds formed between the ammonium group and the ether oxygens will, for steric reasons, lead to a less stable complex with one of the enantiomers Separation of a variety of optically active amines using chiral crown ether stationary phases have subsequently been reported [78,79]

Kuhn *et al* [80] described for the first time the separation of racemic amino acids by means of CZE using 18-crown-6-tetracarboxylic acid, a chiral crown ether derivative (Figure 1 16) This molecule was also used for the separation of primary amines [81] The cavity of crown ethers shaped by the ring is able to form complexes with cations if their size fits in the cavity In particular 18-crown-6 forms complexes with potassium, ammonium or protonated alkyl amines [45] All six oxygens of the polyether are inside the cavity and roughly define a plane [76] As discussed in detail by Cram [76, 77] and Lehn [82] the ammonium cation forms complexes through three $^{+}$NH O hydrogen bonds in a tripod arrangement Enantiorecognition depends on a second interaction In the case of chiral alkyl amines e g α-amino acids, as guest molecules the plane formed by the oxygens is perpendicular to the N-C* bond axis of the amino acid, where C* represents the chiral centre of the guest The substituents of the crown ether are also arranged perpendicular to the plane and act like barriers dividing the space available for the three remaining functional groups of C* Thus two diastereomeric complexes with different equilibrium constants are formed depending on the size and steric arrangement of the substituents

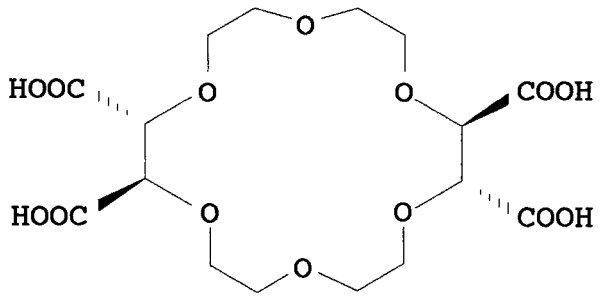

1 (xxxi)

Figure 1.16: *The structure of [18]-crown-6 tetracarboxylic acid [80]*

1.3.4 Chiral sensors.

Cyclodextrins and crown ethers have also been used as the active component of chiral sensors in the determination of enantiomeric purity either as the ionophore in potentiometric sensors or in optical sensors. While there have been a number of publications in this area it was necessary to be critical of some of the reported results.

1.3.4.1 Cyclodextrins in chiral sensors.

Potentiometric chiral sensors based on functionalised cyclodextrins have been developed by Parker and coworkers [83,84]. They synthesised peroctylated cyclodextrins which are lipophilic and suitable for incorporation into solvent polymeric membranes and investigated their ability to measure enantiomeric purity of chiral molecules incorporating aryl rings e.g., ephedrine. The ion-selective electrodes were calibrated using a constant dilution technique and a fixed interference method was used for selectivity coefficient measurements with a background of serum levels of NaCl, KCl and $CaCl_2$. Using bis(1-butylpentyl)adipate (BPPA) they obtained calibration graphs for electrodes with α-CD-BPPA membranes with NH_4Cl inner filling solution that were conditioned in either in (+) or (-) ephedrine hydrochloride (Eph.HCl) in the presence and absence of serum levels of the cations (Figure 1.17). On the basis of these calibration plots the authors claimed that the slope of the (-)-Eph.HCl sensor was 10 mV/decade lower than that of the (+)-Eph.HCl sensor (in the absence of cations). The difference in electrode potentials between enantiomeric electrodes ΔE[(+) - (-)] in the appropriate 0.1 mol dm^{-3} solutions was found to be 26.0 mV which the authors erroneously claimed to be $-\log K^{pot}_{(+)/(-)}$ 2.7 where:

$$-\log K^{pot}_{(+)/(-)} = [E_{(+)} - E_{(-)}]/S. \text{ where S = electrode slope.} \qquad \textbf{Eq. 1.1}$$

However, by our calculations $-\log K^{pot}_{(+)/(-)} = 0.44$. This value is very small compared to conventional ion-selective electrodes where good selectivity usually results in a value of the $-\log K^{pot}_{(i)/(j)}$ being between 2 and 3. On examination of the calibration plots in the absence of cations (3 and 4 on the graph), the (-)-Eph.HCl sensor has a higher potential than the (+)-Eph.HCl sensor at a concentration of -log[6.5] up to about -

log[3 5] where the two plots overlap and cross At ≈ -log[1] the (+)-Eph HCl sensor has a higher potential than the (-)-Eph HCl sensor This may be due to a shift in reference electrode potential or error in the readings This difference in electrode potential at either ends of the concentration scale and the absence of standard deviation (error bars) would suggest that the data for these plots is questionable

The performance of the electrode was also assessed in solutions containing ephedrine of varying enantiomeric purity The electrodes were conditioned overnight in the appropriate Eph HCl solution (Figure 1 18) From their data, the (-)-Eph HCl sensor appears to be more sensitive of the two as it gives a near linear e m f response However, the difference of 20 mV between 100% of one enantiomer and 100% of the other enantiomer is a very small range and would prove difficult to perform analytical measurements without a significant error being involved No analytical measurements were carried out to determine the enantiomeric purity of some simulated samples so it would be difficult to assess how this method could be used with good accuracy and precision

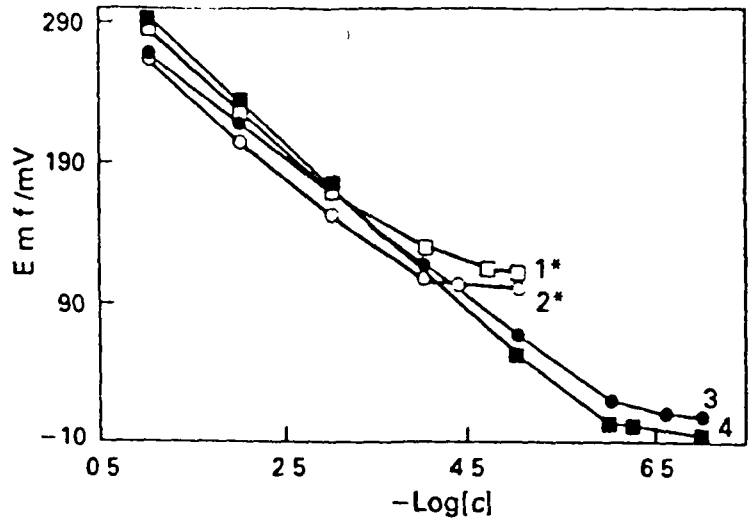

Figure 1.17: *Calibration graphs for electrodes with α-CD-BPPA membranes with NH_4Cl inner filling solutions 1*, (+)-Eph HCl, 2*, (-)-Eph HCl, 3, (-)-Eph HCl, 4, (+)-Eph HCl * Background of serum levels of Na^+, K^+ and Ca^{2+} [84]*

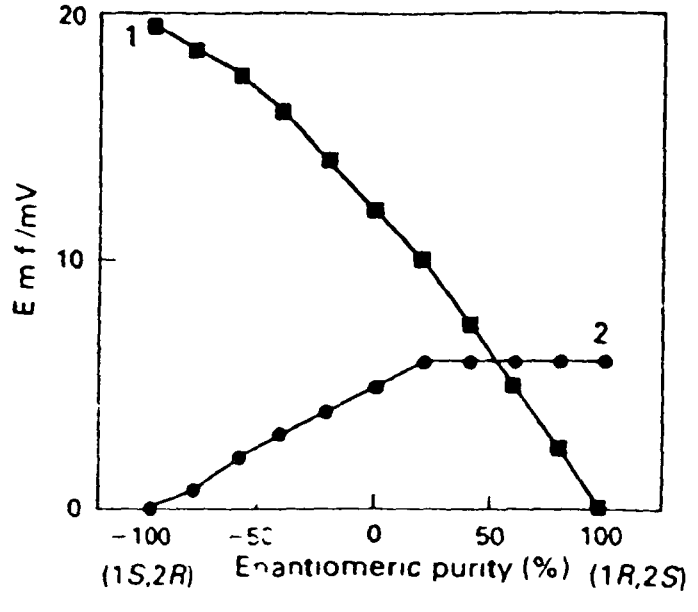

Figure 1.18: *Behaviour of the electrode in solutions of varying enantiomeric excess Electroactive membrane α-CD-BPPA, inner filling solution 1.0 mmol dm^{-3} NH_4Cl, conditioned in 1.0 mmol dm^{-3} (+)- or (-)-Eph HCl 1, (-)-Eph HCl-BPPA and 2, (+)-Eph HCl-BPPA [84]*

1 3 4 2 Crown ethers in chiral potentiometric sensors

The ability of chiral crown ethers to bind chiral ammonium ions with differing enantiomer selectivity prompted their use in potentiometric sensors Yasaka [85] reported on the enantiomer selectivity of chiral crown ethers with tartaric acid and phenylalanine methyl ester as chiral units by a membrane electrode method The enantiomer selectivity for both hydrochloride salts of phenylalanine methyl ester and phenylethylamine were investigated They reported K_{RS}^{pot} values of 1 4 (-log K_{RS}^{pot} = 0 15) are given for the selectivity of the crown ether with phenylalanine methyl ester residues attached for R- and S-phenylalanine methyl ester salts which is a very low and would seriously limit practical applications This sensor is also limited by their sensitivity to high Na^+ and K^+ and therefore cannot be used in a clinical background of serum cations The enantiomer selectivity of a series of chiral crown ethers (e g **1 (xx)** and **1 (xxx)** in Figure 1 13 and Figure 1 15) was also investigated by the same method using ammonium salts as substrates [86] The ΔE [(+) – (-)] (0 01 mol/dm^3) for phenylethylamine, for example, using a membrane electrode incorporating compound **1 (xx)** was found to be 12 1 mV and an enantiomer selectivity factor of 1 6 The enantioselectivity observed with the other chiral crown ethers in the experiment with substrates such as ephedrine and phenylglycine methyl ester, were below this value This implies that the electrodes did not exhibit good enantiomer selectivity Solvent polymeric membranes containing another chiral crown ether (Figure 1 19) have shown a slightly higher enantiomer selectivity for R- over S-phenylethylammonium ions [87] than that discussed above A ΔE [(+) – (-)] value of 25 1 mV at 0 1 mol/dm^3 and an enantiomer selectivity factor of 2 6 was reported

The best data reported is based on polymeric membrane electrodes incorporating another chiral crown ether (Figure 1 20) [88] The electrodes based on R- and S-forms of the crown ether exhibited a Nernstian response to D and L-phenylglycine methyl ester (PGM), respectively, in the range above 10^{-4} mol /dm^3 The S-electrode showed a greater response to L-PGM than D-PGM The potential difference between the responses to 10^{-2} mol /dm^3 L-PGM and D-PGM with the S-electrode reaching a value of 66 mV The enantiomer-selectivity factor for PGM was calculated to be 13 1

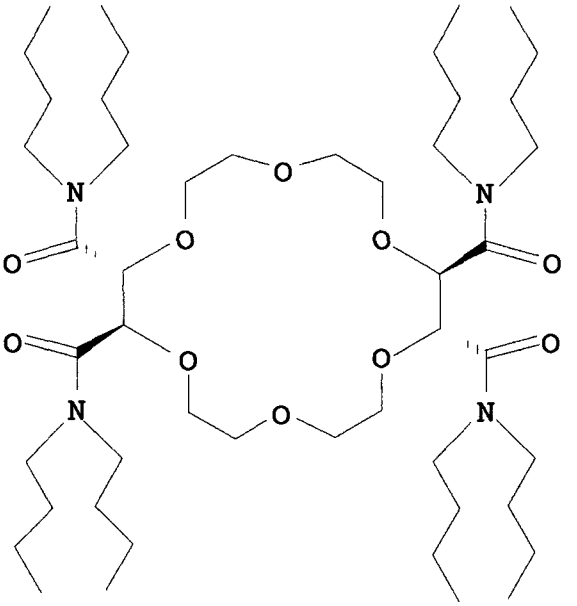

1 (xxxii)

Figure 1.19: *Tetracarboxamide chiral crown ether [87]*

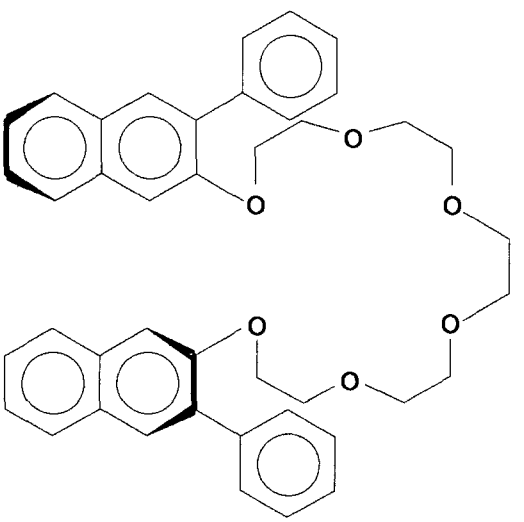

1 (xxxiii)

Figure 1.20: *(S)-2,3 4,5-bis[1,2-(3-phenylnaphtho)]-1,6,9,12,15,18-hexaoxacycloeicosa-2,4-diene [88]*

1 3 4 3 Crown ethers as optical sensors for chiral compounds

The breakthrough in differentiating between the enantiomers of chiral amines by UV/Vis spectroscopy was achieved in 1985 by Misumi [89] The chiral hosts such as that shown in Figure 1 21 could be prepared through a combination of the acid (phenolic) crown ethers with 2,4-dinitroazobenzene units as colour-giving component Addition of amines (e g phenylethylamine and napthylethylamine) to ethanolic solutions of the chiral crown ether afforded violet solutions of the ammonium phenolates and distinct shifts of absorption maxima in the UV/VIS spectra (up to 11 nm) between complexes with the enantiomeric forms of the guest The visual differentiation between the enantiomers of a guest with the host molecule was, however, not possible because the difference in wavelength of the absorption maxima of the diastereomeric complexes was too slight

More recently Shinkai *et al* [90] were able to intensify the effects for the chiral recognition of optically active ammonium ions by chiral crown ethers They utilised the property that the wavelength of reflection for incident light in cholesteric liquid crystals depends on the pitch of the helical structures in the liquid crystalline phase Hence, introduction of complexes of steroid crown ether (Figure 1 22) with chiral ammonium compounds into a cholesteric liquid-crystal matrix gave visible colour changes The difference in wavelength of reflection between the diastereomeric complexes was up to 65 nm and thus capable of observation with the naked eye The conventional chromophoric group was no longer required, as in this case the whole system of crown-ether complex and liquid crystal functions as (supramolecular) chromophore

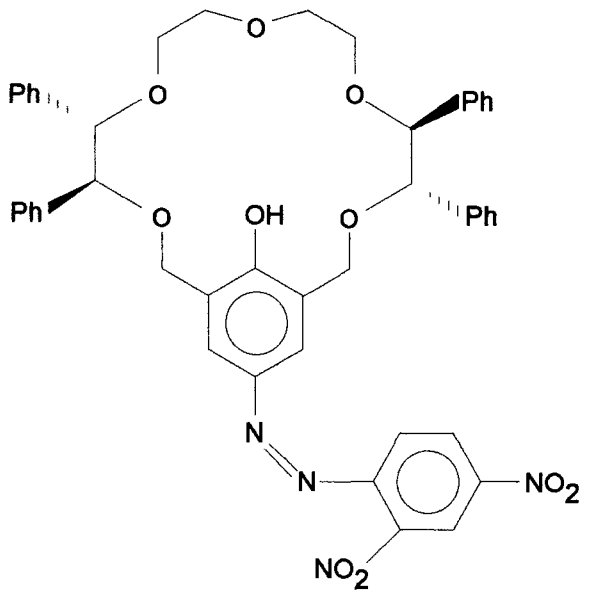

1 (xxxiv)

Figure 1.21: *An example of a chiral azophenolic crown ether [89]*

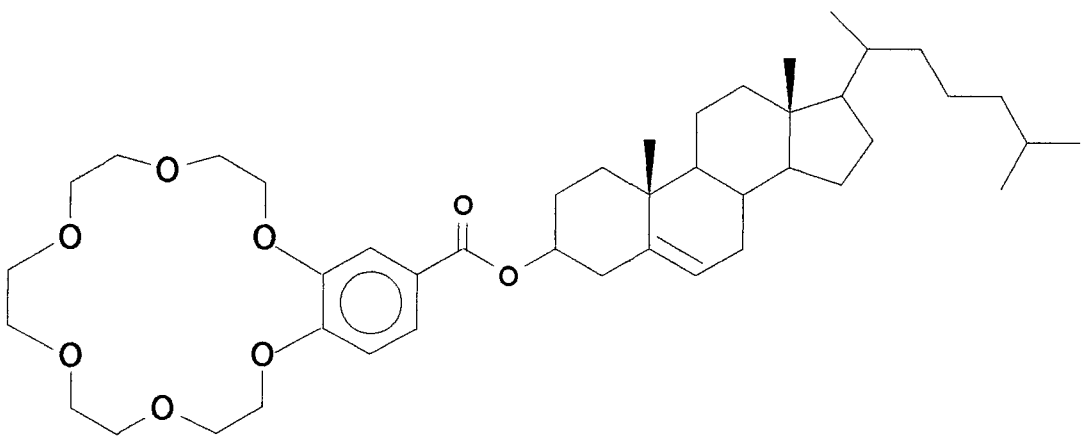

1 (xxxv)

Figure 1.22: *Steroidal crown ether [90]*

Over the past few years, considerable effort has been directed towards the development of chemical sensors based on optical transduction (optodes or optrodes) The general principle of ion-selective optode membranes, based on conventional ionophores , was employed by Simon and coworkers [91] to design a new approach to the determination of enantiomeric excess A highly lipophilic chiral crown derivative (Figure 1 23) which is known to exhibit high selectivity for a chiral organoammonium guest cation, is combined with a H^+-selective chromoionophore, ETH 5294 in a plasticised PVC membrane Two pairs of optical membranes (mounted on glass plates in a flow through cell), one incorporating the R-enantiomer of the crown ether (a) and the other the S enantiomer (b), were equilibrated with pH-buffered solutions containing different concentrations of (R)-PEA and (S)-PEA ions Figure 1 24 represents the absorbtion spectra for each pair of enantiomers The protonated form of the chromoionophore ETH 5294 shows two absorption bands with maxima at 610 nm and 660 nm and the deprotonated form absorbs at 540 nm A high concentration of PEA ions leads, therefore, to a decrease in absorbance at 610 nm and 660 nm The R enantiomer of the crown ether is more selective for (R)-PEA and the S enantiomer is more selective for (S)-PEA

Enantioselective optical sensors for protonated 1-phenylethylamine, propranolol and norephedrine have also been developed by Wolfbeis [92] based on the use of lipophilic (R,R)-tartrates as carriers and a longwave-fluorescent lipophilic dye which is used as a proton carrier The sensing scheme (which is similar to that discussed above) is based on the selective extraction of the organo-ammonium ions into a PVC membrane and on the concomitant release of a proton from the protonated dye, contained in the PVC membrane, into the sample solution Upon deprotonation, the dye undergoes a colour change which is optically detected The differences in the free energy of the two enantiomeric complexes ($\Delta\Delta G$) and the selectivity coefficient (K^{opt}) are calculated as follows

$Q = k_R/k_S$ (Q = enantiomer distribution constant)

$k_R = [RNH_3^+/ligand]_{(org),\,R}/\,[RNH_3^+]_{(aq),\,R}$

$k_S = [RNH_3^+/ligand]_{(org),\,S}/\,[RNH_3^+]_{(aq),\,S}$

$\Delta\Delta G = -RT \ln Q$

$K^{opt} = [RNH_3^+]_{(aq),\,R}/\,[RNH_3^+]_{(aq),\,S} = 1/Q$

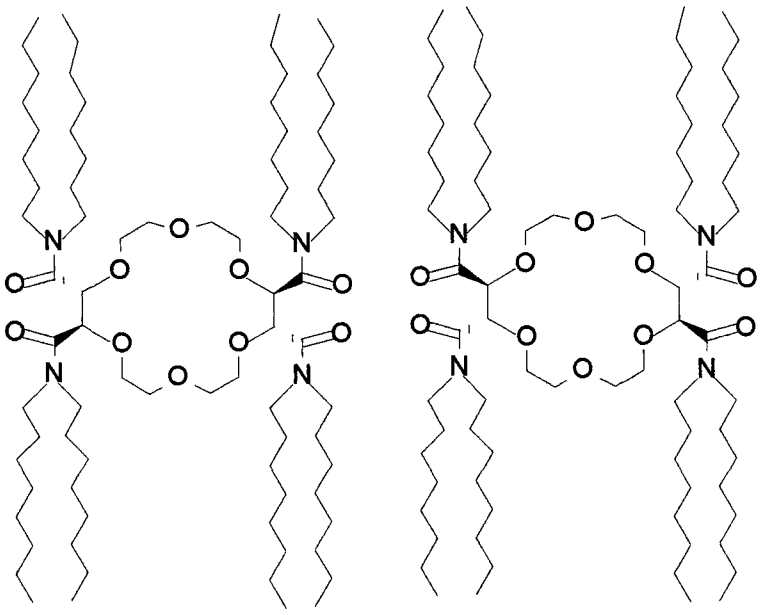

1 (xxxvi) **1(xxxvii)**

Figure 1.23: *R and S enantiomers of the highly lipophilic crown ether which was incorporated into the membranes with the chromoionophore ETH 5294 [91]*

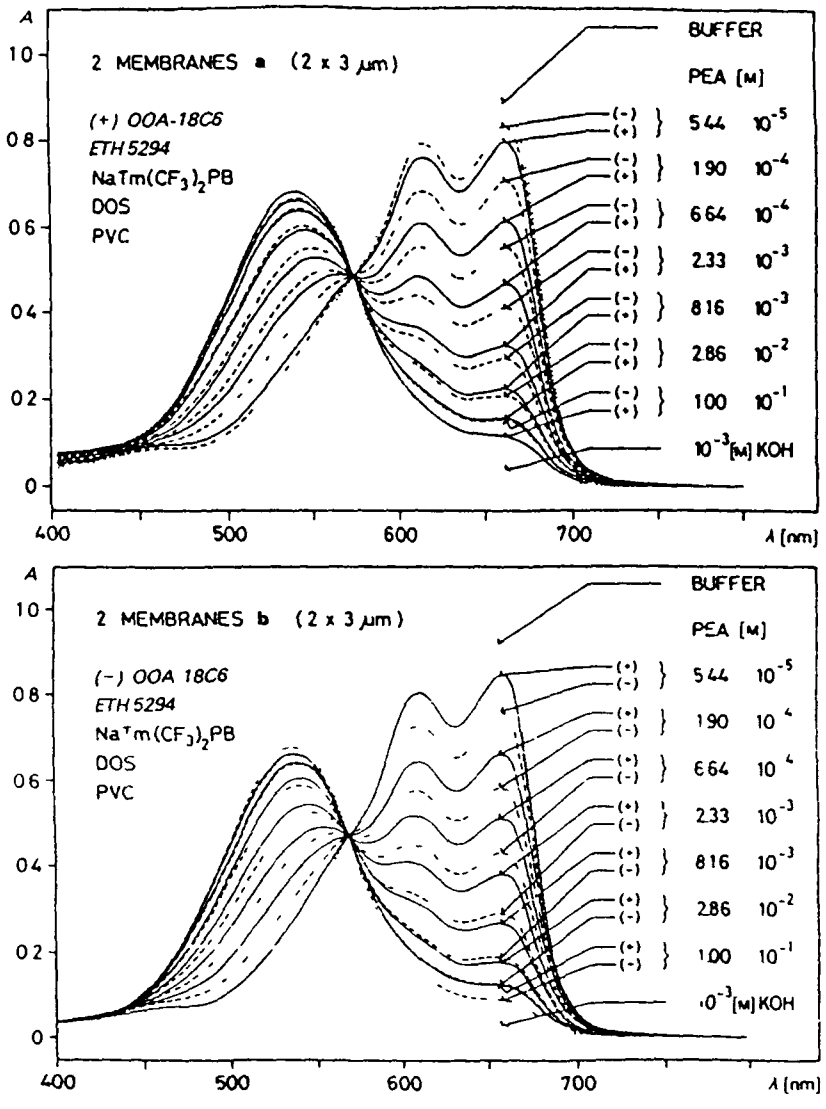

Figure 1.24: *Absorbtion spectra of two 3 µm thick optode membranes a and b, after equilibration with pH buffered solutions containing different concentrations of (R)- and (S)-PEA [91]*

$\Delta\Delta G$ values for the PVC membrane incorporating di-*tert*-butyl tartrate as carrier were calculated to be equal to 0 2, 0 2 and 0 3 kcal/mol for phenylethylamine, propranolol and norephedrine respectively K^{opt} values were quoted to be 0 8, 0 7 and 0 6 for phenylethylamine, propranolol and norephedrine respectively The K^{opt} values for the other tartrate esters were 0 9 or 1 proving that they were not as enantiomerically selective as the di-*tert*-butyl tartrate ester

1.4 Chiral calixarenes

Of particular interest in the chemistry of cyclodextrins is their ability to sustain asymmetric inclusion and catalysis owing to the presence of the chiral cavity made up of D-glucose units As calixarenes are capable of forming host-guest type complexes it seemed an attractive and creative possibility to introduce some asymmetric factors into the molecule and assess the new materials as optically responsive chiral receptors

There are two main ways in which calixarenes can be rendered chiral The first involves attaching chiral substituents either to the upper or lower rim of the calixarene macrocycle The second method is based on the synthesis of inherently chiral calixarenes where the chirality arises from the absence of a plane of symmetry in the molecule

1.4 1 Derivatives with chiral substituents

Just like any other molecules calixarenes can be converted into chiral derivatives by the introduction of optically-active groups In the case of calixarenes derived from phenols, this can be done either at the phenolic OH group or at the *p*-positions Examples for this have been described mainly by Shinkai *et al* [93, 94] and include compounds such as those shown in Figure 1 25

Shinkai found that in chiral water-soluble calixarenes (e g **(1 xxxviii)**) the circular dichroism (CD) spectra change sensitively on guest binding [95] The CD technique is one of the most useful tools to evaluate asymmetric interactions between host and guest molecules in solution The spectral change was easily explained by the conformational change in the host calixarene induced by inclusion of guest molecules

With this approach, the use of enantiomerically pure reagents leads directly to pure enantiomeric products Larger quantities thus become available in a quite

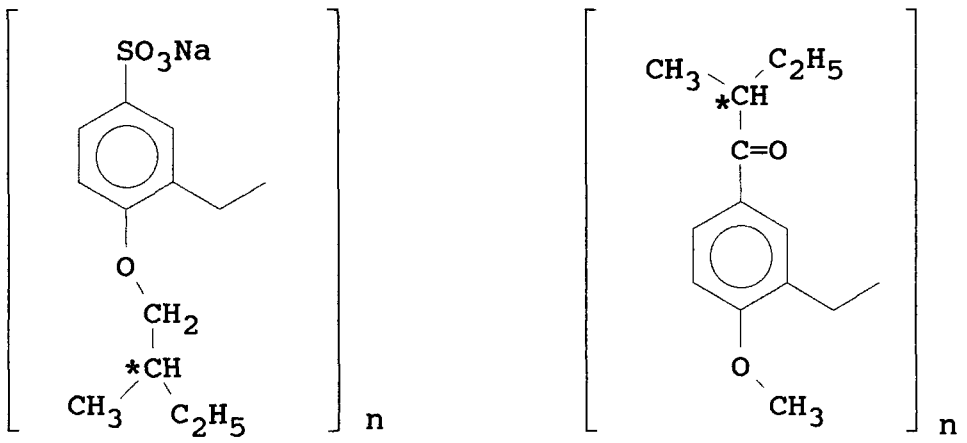

1 (xxxviii) **1 (xxxix)**

Figure 1.25: *Calixarene derivatives with chiral substituents [93,94]*

straightforward way, which is advantageous in comparison to the inherently chiral calixarenes where the yields tend to be smaller

1 4.2 Inherently chiral calixarenes

The chirality of the calixarenes shown in Figure 1 25 is due solely to the chirality of the substituent groups However, due to their non-planar shape, calixarenes offer numerous additional possibilities for producing chiral host molecules, which are not based on a chiral sub-unit but on the absence of a plane of symmetry or an inversion centre in the molecule as a whole In other words, opening up of the macrocyclic structure would lead to an achiral linear molecule Examples of such inherently chiral calixarenes have so far been members of the calix[4]arene family

The first attempts involved the synthesis of calix[4]arenes with three (in the sequence AABC) [96] or four [97] different *p*-substituted phenolic units by Bohmer *et al* Molecules of this type (Figure 1 26) can be obtained by fragment condensation of suitable trimers with bisbromomethylated phenols or suitable dimers with bisbromomethylated dimers

Asymmetric calix[4]arenes also result from the incorporation of a single *meta*-substituted phenolic unit, an idea first realised by Vicens and coworkers [98] It is quite interesting that the introduction of only one methyl group makes the calix[4]arene chiral (Figure 1 27)

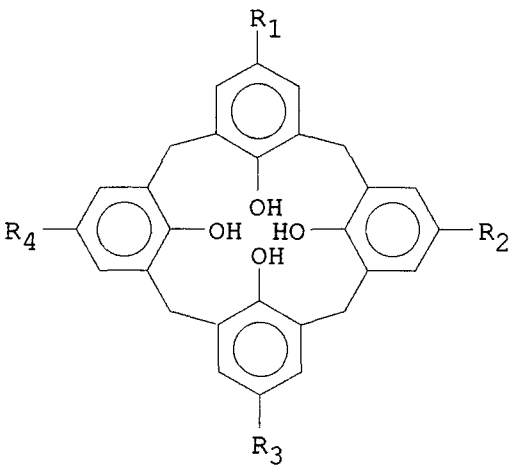

	R1	R2	R3	R4
1 (xl)	C_6H_5	*t*-but	$CO_2C_2H_5$	CH_3
1. (xli)	C_6H_5	*t*-but	CH_3	$CO_2C_2H_5$
1 (xlii)	CH_3	*t*-but	$CO_2C_2H_5$	C_6H_5
1 (xliii)	CH_3	*t*-but	C_6H_{11}	C_8H_{17}
1 (xliv)	CH_3	CH_3	C_8H_{17}	C_6H_{11}
1 (xlv)	CH_3	CH_3	C_8H_{17}	Cl

Figure 1.26: *Asymmetric Calix[4]arenes with different phenolic units [96, 97]*

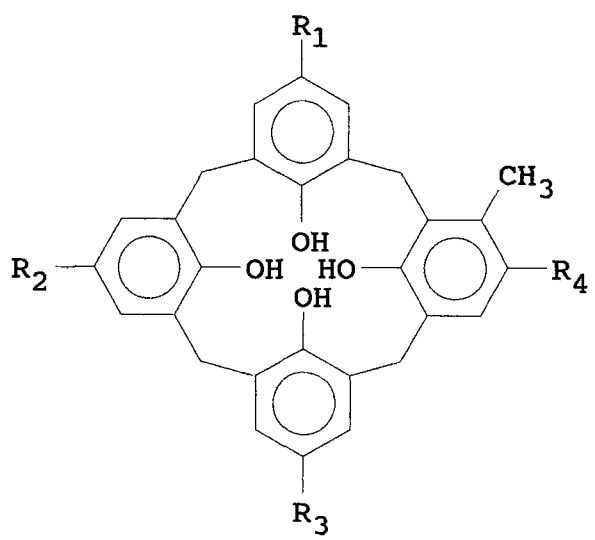

1 (xlvi)

Figure 1.27: *Asymmetric calix[4]arene with a methyl group in the meta-position [98]*

Temperature-dependant ^{1}H NMR experiments have shown that a rapid interconversion of the various conformers of calixarenes occurs at room temperature [99] For chiral calixarenes this means racemisation, since one cone conformation is the mirror image of the other cone conformation (Figure 1 28) Therefore a separation into enantiomers is impossible, unless the conformation is "fixed" This is possible by the introduction of bulky substituents at the phenolic hydroxyl groups, which cannot penetrate through the annulus Indeed the cone conformation is fixed in most of the known derivatives which are obtained by reaction of the phenolic hydroxyl group, e g , ethers or esters [100, 101] Therefore it should be possible to obtain enantiomeric host molecules having an "enforced cavity" from calix[4]arenes with differently substituted phenolic units But because of the asymmetry of such calixarenes, it is necessary to achieve complete conversion of all the OH groups in the cone conformation, and this can cause problems, leading to a mixture of conformational isomers which are difficult to separate [102] However the tetrapropyl ether of a calix[4]arene containing one 3-methyl-4-isopropylphenol unit (Figure 1 29) has been prepared in the cone conformation and separated into its enantiomers by HPLC using chiral stationary phases [103, 104] This is the first example of a successful optical resolution of an asymmetrically substituted calix[4]arene

The same asymmetric pattern can in principle be achieved by *O*-alkylation (or *O*-acylation) when different residues are added to the phenolic oxygen atoms This strategy has the additional advantage that (with residues larger than ethyl) the conformation is simultaneously fixed and racemisation becomes impossible

For an *all-syn* arrangement of the *O*-alkyl groups, at least two different residues are necessary (Figure 1 30,**1 li**), but additional possibilities exist if the *O*-alkyl groups are in an *anti* position Thus, compounds **1 (lii)** and **1 (liii)** with one kind of *O*-alkyl groups are asymmetric or disymmetric respectively Examples of these types have been prepared mainly by Shinkai [105] and Pappalardo [106], and some have been resolved by chromatographic techniques [107, 108, 109,]

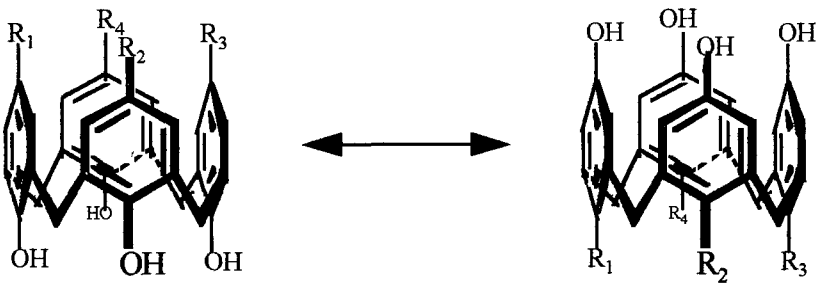

1 (xlvii) **1 (xlviii)**

Figure 1.28: *One cone conformation is the mirror image of the other [99]*

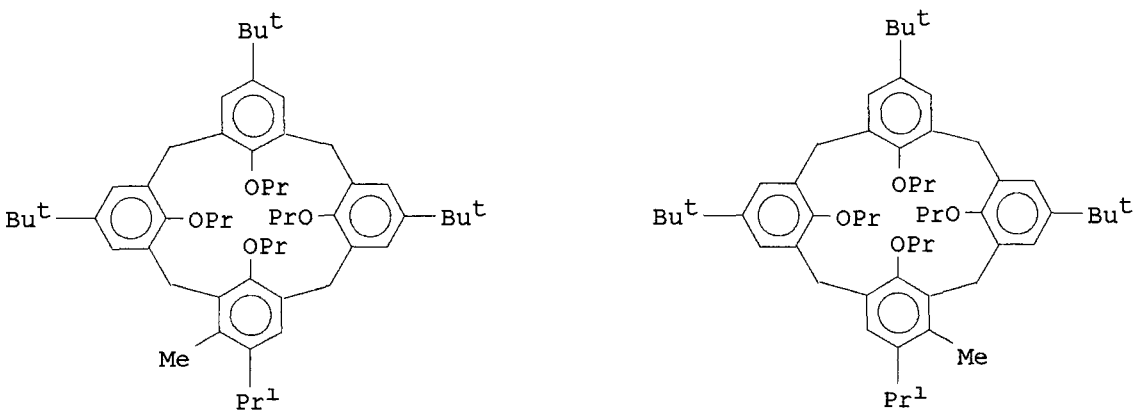

1 (il) **1 (l)**

Figure 1.29: *Racemates possible for cone-conformation of tetrapropyl ether of a calix[4]arene [103, 104]*

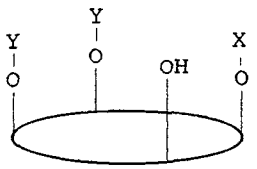

1 (li)

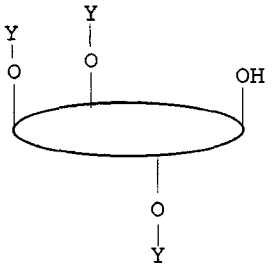

1 (lii)

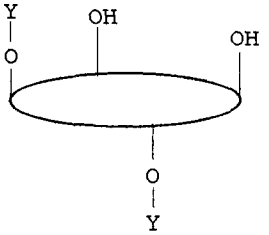

1 (liii)

Figure 1.30: *Possible arrangements obtained from O-alkylation of the calix[4]arenes [105, 106]*

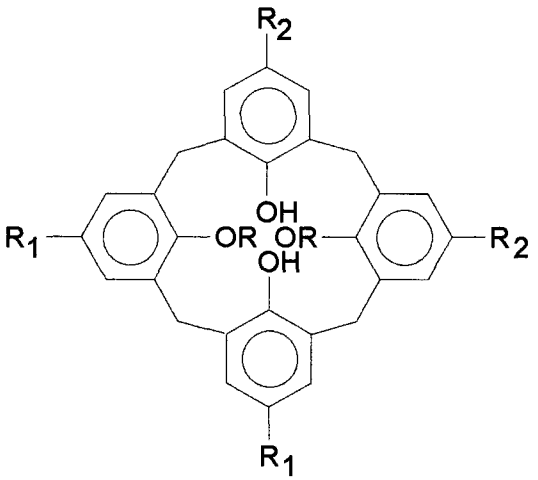

1 (liv)

Figure 1.31: *Alkylation of the phenolic hydroxy groups in the 1,3-position [111]*

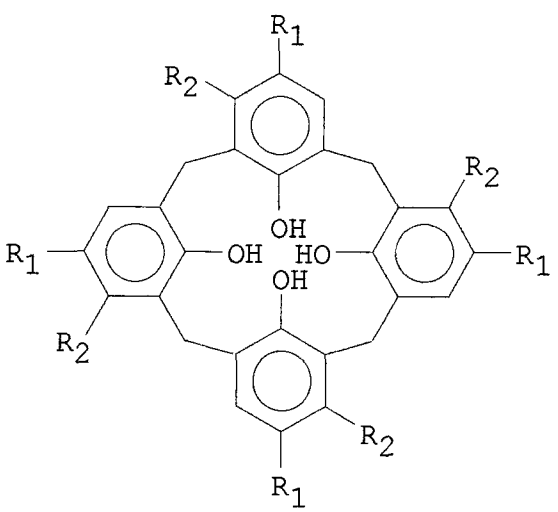

1 (lv)

Figure 1.32: *Disymmetric calix[4]arene with C_4 symmetry [112]*

Using different *O*-alkyl residues, 34 types of tetraalkylethers, 13 types of trialkylethers and 8 types of alkylethers are possible, among which 17, 9 and 3 are chiral [110]

Alkylation of the phenolic hydroxy groups in the 1,3-position in calix[4]arenes consisting of two different phenolic units arranged in the order AABB leads to a new type of chiral calix[4]arene [111] which is in the cone conformation (Figure 1 31)

Disymmetric calixarenes having an *n*-fold symmetry axis have also been synthesised Several calix[4]arenes with C_4 symmetry (Figure 1 32) have been obtained from 3,4-disubstituted phenols with yields of up to 30% [112] Because of the equivalence of their phenol units all the *O*-alkylation products (from mono- to tetraethers) are available in a defined manner 1,3-diether derivatives in particular (which have C_2 symmetry) have been prepared in good yields and separated into their enantiomers [113]

This demonstrates the huge potential which is available in the calixarene family for obtaining chiral host molecules or chiral building blocks for the construction of even larger molecular systems

1.5 References

1 A Baeyer, *Ber* , 1872, **5**, 25

2 L H Baekeland, U S Patent 942, October 1908, 699

3 A Zinke and E Ziegler, *Ber* , 1944, 77, 264

4 J W Cornforth, P D'Arcy Hart, G A Nicholls, R J W Rees and J A Stock, 1955, *Br J Pharmacol* , 1955, **10**, 73

5 H Kammerer, G Hapel and F Caesar, *Makromol Chem* , 1972, **162**, 179

6 G Happel, B Mathiasch and H Kammerer, *Makromol Chem* ,1975, **176**, 3317

7 J H Munch, *Makromol Chem* , 1977, **178**, 69

8 C D Gutsche and R Murthukrishnan, *J Org Chem* , 1978, **43**, 4905

9 C D Gutsche "*Calixarenes*", Monographs in Supramolecular Chemistry, Vol 1, R S C Cambridge, 1989

10 J Vicens and V Bohmer (edts), "*Calixarenes - A Versatile class of Macrocyclic Compounds*", Topics in Inclusion Science, Kluwer Academic Publishers, 1991

11 J Vicens, Z Asfari and J M Harrowfield (edts), *Calixarenes 50th Anniversary Commemorative Volume*, Kluwer Academic Publishers, 1994

12 3rd International Calixarene Conference, Fort Worth, Texas, May 1995

13 C D Gutsche, B Dhawam, J A Levine, K H No and L J Bauer, *Tetrahedron*, 1983, **39**, 409

14 A Arduini, A Pochini, S Reverberi and R Ungaro, *J Chem Soc , Chem Commun* , 1984, 981

15 R M Izatt, J D Lamb, R T Hawkins, P R Brown, S R Izatt and J J Christensen, *J Am Chem Soc* , 1983, **105**, 1782

16 C Alfieri, E Dradi, A Pochini, R Ungaro and C D Andreetti, *J Chem Soc , Chem Commun* , 1983, 1075

17 M A McKervey, E M Seward, G Ferguson, B Ruhl and S J Harris, *J Chem Soc , Chem Commun* , 1985, 389

18 O Aleksiuk and S E Biali, *Tetrahedron Lett* , 1993, **34**, 4857

19 S Shinkai, H Kawabata, T Arimura, T Matsuda, H Satoh and O Manabe, *J Chem Soc, Perkin Trans 1*, 1989, 1073

20 S Shinkai, Y Shirahama, T Tsubaki and O Manabe, *J Chem Soc, Perkin Trans 1*, 1989, 1859

21 F Arnaud-Neu, E M Collins, M Deasy, G Ferguson, S J Harris, B Kaitner, A J Lough, M A McKervey, E Marques, B L Ruhl, M J Schwing-Weill, E M Seward, *J Am Chem Soc*, 1989, **111**, 8681

22 A Arduini, A Pochini, S Reverberi, R Ungaro, C D Andreetti, F Ugozzoli, *Tetrahedron*, 1986, **42**, 2089

23 G Barrett, V Bohmer, G Ferguson, J F Gallagher, S J Harris, R G Leonard, M A McKervey, M Owens, M Tabatabai, A Vierengel and W Vogt, *J Chem Soc, Perkin Trans 2*, 1992, 1595

24 F Arnaud-Neu, G Barrett, S Cremin, M Deasy, G Ferguson, S J Harris, A J Lough, L Guerra, M A McKervey, M J Schwing-Weil, P Schwinte, *J Chem Soc, Perkin Trans 2*, 1992, 1119

25 E M Collins, M A McKervey, E Madigan, M B Moran, M Owens, G Ferguson, S J Harris, *J Chem Soc, Perkin Trans 1*, 1991, 3137

26 R M Izatt, J J Christensen and R T Hawkins, *US Patent* 4,477,377, 16 Oct 1984

27 S Shinkai, O Manabe, Y Kondo and T Yamamoto, *Jpn Kokai Tokkyo Koho* JP 62/136242 A2, 19 June 1987

28 S J Harris, M A McKervey, D Melody, J Woods and J Rooney, *US Patent* 4,556,700, 21 Nov 1984, assigned to Loctite (Ireland) Ltd

29 D Diamond, *J of Inclu Phenom*, 1994, **19**, 149

30 K M O'Connor, D W Arrigan and G Svehla, *Electroanalysis*, 1995, **7**, 205

31 J D Glennon, E Horne, K O'Connor, G Kearney, S J Harris and M A McKervey, *Anal Proc Including Anal Commun*, 1994, 31, 33

32 A Cadogan, D Diamond, S Cremin, M A McKervey and S J Harris, *Anal Proc*, 1991, **28**, 13

33 A Cadogan, D Diamond, M R Symth, G Svehla, M A McKervey, E M Seward and S J Harris, *Analyst*, 1990, **115**, 1207

34 D Diamond, G Svehla, S M Seward and M A McKervey, *Anal Chim Acta*, 1988, **204**, 223

35 M Teltıng-Dıaz, D Diamond and M R Symth, *Anal Chim Acta*, 1991, **251**, 149

36 M Teltıng-Dıaz, F Regan, D Diamond and M R Symth, *J Pharm Biomed Anal*, 1990, **8**, 695

37 R Ungaro, A Pochını, A Mangıa and G D Andreettı, *Anal Lett*, 1983, **16**, 1027

38 E L Elıel, S H Wılen and L N Mander *"Stereochemıstry of Organıc Compounds"*, Wıley Interscıence, New York, 1994

39 R S Cahn, C K Ingold and V Prelog, *Experıentıa*, 1956, **12**, 81

40 J B Bıot, *Mem Acad Scı Inst Fr*, 1838, **15**, 93

41 L Pasteur, *Ann Chım Phys*, 1850, **38**, 56

42 D J Cram, *J Incl Phenom*, 1988, **6**, 397

43 A Vıllers, *C R Acad Scı*, 1891, **112**, 536

44 F Schardınger, *Wıen Klın Wochenschr*, 1904, **17**, 207

45 C Pedersen, *J Am Chem Soc*, 1967, **89**, 2495

46 K, Freundenburg and F Cramer and Z Naturforsch, *B3*, 1948, 464

47 K Lındner and W Saenger, *Carbohydr Res*, 1982, **99**, 103

48 C J Pedersen, *J Am Chem Soc*, 1967, **89**, 7017

49 J M Dıetrıch, J M Lehn and J P Sauvage, *Tetrahedron Lett*, 1969, 2885

50 D J Cram, T Kaneda, R C Helgeson and G M Leın, *J Am Chem Soc*, 1979, **101**, 6752

51 E P Kyba, M G Sıegel, L R Sousa, G D Sogah and D J Cram, *J Am Chem Soc*, 1973, **95**, 2691

52 R C Helegson, J M Tınko, P Moreau, S C Peacock, J M Mayer and D J Cram, *J. Am Chem Soc*, 1974, **96**, 6762

53 W D Curtıs, D A Laıdler, J F Stoddart and G H Jones, *J Chem Soc, Chem Commun*, 1975, 833

54 J M Gırodeau, J M Lehn and J P Sauvage, *Angew Chem Int Ed Engl* 1975, **14**, 764

55 V Prelog, *Pure Appl Chem*, 1978, **50**, 893

56 R M Izatt, T Wang, J K Hathaway, X X Zhang, J C Curtis, J S Bradshaw C Y Zhu and P Huszthy, *J of Incl Phenom* , 1994, **17**, 157

57 J F Stoddart in ", E L Eliel and W Wilen (edts), " *Topics in Stereochemistry"*,Wiley Interscience, New York, vol 17, 1987

58 D W Armstrong, *J Liquid Chromatogr* , 1980, **3**, 895

59 W L Hinze and D W Armstrong, *Anal Lett* , 1980, **13**, 1093

60 D Sybilska, J Zukowski and J Bojarski, *J Liquid Chromatogr* , 1986, **9**, 591

61 M Gazdag, G Szepesi and L Huszar, *J Chromatogr* , 1986, **371**, 227

62 A Harada, M Furue and S I Nozakura, *J Polym Sci* , 1978, **16**, 189

63 B Zsadon, L Decsei, M Szilasi and F Tudos, *J Chromatogr* , 1983, **270**, 127

64 K Cabrera and D Lubda, *GIT Spezial Chromatogr* , 1992, **2**, 77

65 D W Armstrong, M Hilton and L Coffin, *LC-GC Int* , 1992, **5**, 28

66 E Smolkova-Keulemansova, H Kralova, S Krysl and L Felti, *J Chromatogr* , 1982, **241**, 3

67 E Smolkova-Keulemansova, L Felti and S Krysl, *J Incl Phenom* , 1985, **3**, 183

68 T Koscielski, D Sybilska and J Jurczak, *J Chromatogr* , 1983, **280**, 131

69 V Schurig and H -P Nowotny, *J Chromatogr* , 1988, **441**, 155

70 W A Konig, S Lutz, P Mischnick-Lubbecke, B Brassat and G Wenz, *J Chromatogr* , 1988, **447**, 193

71 D W Armstrong, W Y Li and J Pitha, *Anal Chem* , 1990, **62**, 214

72 M Tanaka, S Asano, M Yoshinaga, Y Kawaguchi, T Tetsumi and T Shono, *Fresinus J Anal Chem* , 1991, **339**, 63

73 M Yoshinaga, S Asano, M Tanaka and S Toshiyuki, *Anal Sci* , 1991, **7**, 257

74 S Terabe, H Ozaki, K Otsuka, T Ando, *J Chromatogr* , 1985, **332**, 211

75 S Mayer and V Schurig, *J Liq Chromatogr* , 1993, **16**, 915

76 E P Kyba, J M Timko, L J Kaplan, F de Jong, G W Gokel and D J Cram, *J Am Chem Soc* , 1978, **100**, 4555

77 L S Sousa, G D Y Sogah, D H Hoffman, D J Cram, *J Am Chem Soc*, 1978, **100**, 4569

78 D W Armstrong, T Ward, B Czech and R Bartsch, *J Org Chem*, 1985, **50**, 5557

79 M Hilton and D W Armstrong, *J Liq Chromatogr*, 1991, **14**, 9

80 R Kuhn, F Stocklin and F Erni, *Chromatographia*, 1992, **33**, 32

81 R Kuhn, F Erni, T Bereuter and J Hausler, *Anal Chem*, 1992, **64**, 2815

82 J P Behr, J M Girodeau, R C Heyward, J M Lehn and J P Sauvage, *Helv Chim Acta*, 1980, **63**, 2096

83 P S Bates, R Kataky and D Parker, *J Chem Soc, Chem Commun*, 1992, 153

84 R Kataky, P S Bates and D Parker, *Analyst*, 1992, **117**, 1313

85 Y Yasaka, T Yamamoto, K Kimura and T Shono, *Chem Lett*, 1980, 769

86 A P Thoma, A Vivian-Nauer, K H Schellenburg, D Bedekovic, E Pretsch, V Prelog and W Simon, *Helv Chim Acta*, 1979, **62**, 2303

87 W Bussmann, J-M Lehn, U Oesch, P Plumere and W Simon, *Helv Chim Acta*, 1981, **67**, 657

88 T Shinbo, T Yamaguchi, K Nishimura, M Kikkawa and M Sugiura, *Anal Chim Acta*, 1987, **193**, 367

89 T Kaneda, K Hirose and S Misumi, *J Am Chem Soc*, 1989, **111**, 742

90 T Nishi, A Ikeda, T Matsuda and S Shinkai, *J Chem Soc, Chem Commun*, 1991, 339

91 P Holy, W E Morf, K Seiler and W Simon, *Helv Chim Acta*, 1990, **73**, 1171

92 H He, G Uray and O S Wolfbeis, *Anal Chim Acta*, 1991, **246**, 251

93 T Arimura, S Edamitsu, S Shinkai, O Manabe, T Muramatsu and M Tashiro, Chem Lett, 1987, 2269

94 T Arimura, H Kawabata, T Matsuda, T Muramatsu, H Satoh, K Fujio, O Manabe, S Shinkai, *J Org Chem*, 1991, **56**, 301

95 A Ikeda, T Nagasaki and S Shinkai, *J Phys Org Chem*, 1992, **5**, 699

96 V Bohmer, L Merkel, U Kunz, *J Chem Soc, Chem Commun*, 1987, 896

97 V Bohmer, F Marschollek, L Zetta, *J. Org Chem*, 1987, **52**, 3200

98 H Casabianca, J Royer, A Satrallah, A Taty-C and J Vicens, *Tetrahedron Lett*, 1987, **28**, 6595

99 C D Gutsche and L J Bauer, *J Am Chem Soc*, 1985, **107**, 6052

100 C D Gutsche and J A Levine, *J Am Chem Soc*, 1982, **104**, 2652

101 C D Gutsche, J A Levine and P K Sujeeth, *J Org Chem*, 1985, **50**, 5802

102 L Zetta, A Wolff, W Vogt, K L Platt and V Bohmer, *Tetrahedron*, 1991, **47**, 1911

103 S Shinkai, T Arimura, H Kawabata, H Murakami, K Araki, K Iwamoto, T Matsuda, *J Chem Soc, Chem Commun*, 1990, 1734

104 S Shinkai, T Arimura, H Kawabata, H Murakami, K Iwamoto, T Matsuda, *J Chem Soc, Perkin Trans* 1, 1991, 2429

105 K Iwamoto, A Yanagi, T Arimura, T Matsuda and S Shinkai, *Chem Lett*, 1990, 1901

106 S Pappalardo, L Guinta, M Foti, G Ferguson, J F Gallagher and B Kaitner, *J Org Chem*, 1992, **57**, 2611

107 K Iwamoto, H Shimizu, K Araki and S Shinkai, *J Am Chem Soc*, 1993, **115**, 3997

108 S Papppalardo, S Caccamese and L Giunta, *Tetrahedron Lett*, 1991, **32**, 7747

109 S Caccamese and S Papppalardo, *Chirality*, 1993, **5**, 159

110 V Bohmer, D Kraft and W Vogt, *Supramol Chem*, 1994, **3**, 299

111 V Bohmer, A Wolff and W Vogt, *J Chem Soc, Chem Commun*, 1990, 968

112 A Wolff, V Bohmer, W Vogt, F Ugozzoli, and G D Andreetti, *J Org Chem*, 1990, **55**, 5665

113 S T Pickard, W H Pirkle, M Tabatabai, W Vogt and V Bohmer, *Chirality*, 1993, 5, 310

2. Determination of the Enantiomeric Composition Based on the Quenching of a Chiral Calixarene

2.1 Introduction

Determination of enantiomeric purity has become important in recent years due to increasing restrictions on the composition of pharmaceuticals whose efficacy is dependant upon a chiral moiety [1,2] The behaviour of the enantiomers of a chiral drug may show striking differences in terms of biological activity, potency, toxicity, transport mechanisms and routes of metabolism [3] Therefore analysts in the pharmaceutical industry now face the challenge of assessing the stereoisomeric composition of potential drugs during both the discovery and development stages The characterisation of the drug for enantiomeric purity is required after synthesis and also during *in vivo* and *in vitro* studies for determining the fate of a chiral molecule and its metabolites There are several methods commonly employed in the pharmaceutical industry for the determination of enantiomeric purity including circular dichroism [4] and specific rotation [5], separation techniques such as liquid and gas chromatography [6,7] and more recently, capillary electrophoresis [8]

None of these techniques are amenable to real-time analysis and while the separation methods can offer good analytical performance in terms of precision and accuracy, they are expensive techniques in terms of reagent consumption and cost of instrumentation, and in addition generate significant waste In contrast, sensor-based analysis provides real-time analysis, low cost of instrumentation, amenability to automation, no expensive reagents and virtually no waste

Our aim is to develop a sensor which can distinguish between enantiomers of the same molecule This is a difficult task, as enantiomers usually exhibit very similar chemical properties, and in contrast to chromatography, sensor-based analysis involves determination of the target species in the sample matrix without separation The power of chromatography arises from the dynamic interaction of analytes between the mobile phase and stationary phase, which, over the length of a typical column, can greatly magnify any small differences in relative affinity for the two phases which may exist between enantiomers of the same compound In contrast, however, a sensor can only rely on a single partitioning or exchange event to

generate the selectivity required Hence development of successful materials for sensors is extremely challenging as the host-guest properties of receptors are difficult to predict accurately from a theoretical point of view, as the overall observed selectivity is the sum of many subtle interactions which may, or may not be interdependent

However, broad predictions can be made about the type of features which should be present if a ligand is to have any chance of performing the required task These can be summarised as follows,

1 The substance must contain features which allow it to interact reversibly with the target species For example, polar groups, acidic/basic groups or groups capable of hydrogen bonding
2 These groups must be pre-organised in such a manner that they provide the basis for the required selectivity
3 The interaction between the host and the guest must also provide a signal which enables it to be observed and quantified from the outside world [9] A variety of signalling options are available including electrochemical (e g potentiometry, amperometry) and spectroscopic (e g fluorescence, absorbance) For our purposes, fluorescence is the most attractive because of its sensitivity and variety of signalling modes (e g quenching, enhancement or half-life selectivity) which can be employed
4 The groups conferring recognition and signal transduction must be arranged in an interactive conformation so that binding with the target species will result in a signal

With these guidelines in mind, our strategy was to investigate whether we could use a calixarene macrocycle as a template for producing materials which in principle satisfy the above criteria In choosing which fluorescent labels and chiral moieties to attach to the calixarene template, and which chiral guests to investigate, previous workers in the area have provided useful guidance

2.1 1 Fluorescence as a signal transduction mechanism

Optical based sensing is attractive for many reasons and offers several advantages over electrochemical sensors These optical sensors can measure concentrations without perturbing the sample and can be used for continuous sensing Because the signal is optical these sensors are not subject to electrical interference and do not require a "reference" like electrochemical sensors The referencing is carried out optically by using wavelength ratioing, in which part of the conducted light not affected by the measurement variable can be used to correct for other optical variations The coupling of optical sensing techniques with optical fibres has promoted rapid progress and great interest in this sensing technology

There are many reasons why fluorescence might be identified as the optimal signal transduction mechanism for sensing applications Fluorescence is a very sensitive technique, in large part because the observing wavelength is always longer than that of the exciting wavelength Thus, a signal may be measured versus zero or near-zero background Fluorescence signalling also permits the monitoring of excitation and emission wavelengths The emission signal may be observed in the form of intensity, intensity ratio, or lifetime measurements Fluorescence is usually non-destructive and is an ideal signal transduction mechanism for fibre optic remote sensing applications

Substances which display significant fluorescence generally possess delocalised electrons formally present in conjugated double bonds Some typical fluorescent substances (fluorophores) are shown in Figure 2 1 A number of fluorescent sensors for metal ions have been developed by several groups during the last decade [10] Many of these sensing supramolecules contain anthracene **(2 (i))** as a fluorescent subunit for its strong and well characterised emission and its chemical stability

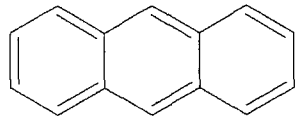

2 (i)

Anthracene

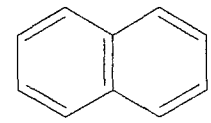

2 (ii)

Naphthalene

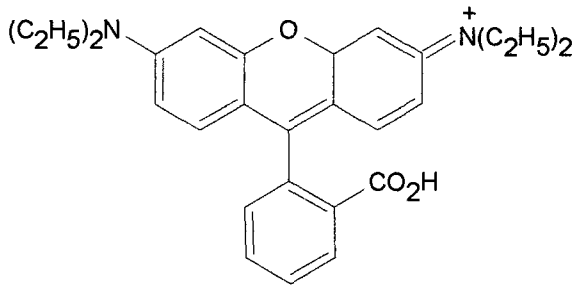

2 (iii)

Rhodamine B

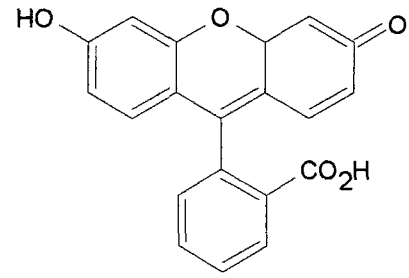

2 (iv)

Fluorescein

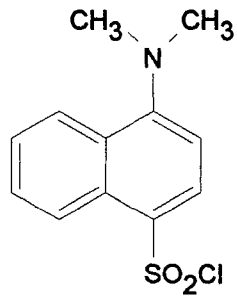

2 (v)

Dansyl chloride

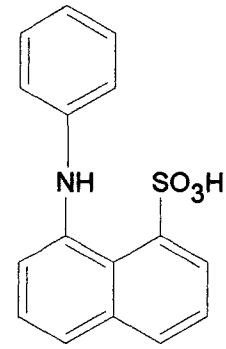

2 (vi)

1-anilino-8-naphthalene-sulfonic acid

Figure 2.1: *Structures of typical fluorescent substances*

2 1 2 Quenching of fluorescence

Fluorescence quenching refers to any process which decreases the fluorescence intensity of a given substance A variety of processes can result in quenching These include excited state reactions, energy transfer, complex formation and collisional quenching

Collisional or dynamic quenching results from collisional encounters between the fluorophore and quencher The collisional quenching process involves the formation of a non-fluorescent complex between the excited state fluorophore and quencher This complex, sometimes known as an exciplex, absorbs the energy from the excited state and results in the non-radiative decay of the fluorophore This is a time dependant process Static quenching results from the formation of a non-fluorescent ground state complex between the fluorophore and quencher When this complex absorbs light it immediately returns to the ground state without the emission of a photon Lifetimes or temperature dependence measurements of the quenching process can be used to distinguish between static and collisional quenching contributions

A wide variety of substances act as quenchers of fluorescence One of the best known collisional quenchers is oxygen [11] The mechanism by which oxygen quenches fluorescence has been the subject of considerable research and it is clear that contact between the oxygen molecule and the fluorophore is a requirement of quenching [12] Aromatic and aliphatic amines are efficient quenchers of most unsubstituted aromatic hydrocarbons [13] For example, anthracene fluorescence is effectively quenched by diethylaniline In this instance the mechanism of quenching is the formation of a charge transfer complex when the excited state fluorophore accepts an electron from the amine

The efficiency of the quenching of a fluorescent species by a quenching species follows the Stern-Volmer relationship, if the fluorophore and quencher concentrations are in the appropriate range

$$I_0/I = 1 + K_{sv}[Q] \qquad \textbf{Eq. 2.1}$$

where I_0 is the fluorescence in the absence of the quencher, I is the fluorescence in the presence of quencher at a concentration [Q], and K_{sv} is the Stern-Volmer constant which is a measure of quenching efficiency This relationship holds for both excited state and ground state quenching processes

If a system obeys the Stern-Volmer equation, a plot of I_0/I *versus* [Q] will give a straight line with a slope of K_{sv} and an y-axis intercept of 1 K_{sv} is therefore a measure of quenching efficiency and a large value for this parameter equates to a sensitive response

2.1 3 Chiral discrimination in fluorescent quenching

Early work by Irie and coworkers [14] demonstrated that specific geometry is required for the fluorescence quenching of 1,1'-binaphthyl by N,N,-dimethyl-α-phenylethylamine (Figure 2 2) Both **2 (vii)** and **2 (viii)** are chiral molecules The use of chiral compounds as excited molecules and quenchers enables one to examine pure steric effect upon the quenching rate without being disturbed by the electronic factor, since enantiomers have inherently the same electronic nature i e , oxidation-reduction potential or bulkiness Photoexcited 1,1'-bmaphthyl gives a fluorescence around 360 nm The fluorescence of which can be quenched by adding N,N,-dimethyl-α-phenylethylamine No difference was found in the Stern-Volmer plots for the fluorescent quenching of a racemic mixture of 1,1'-binaphthyl by enantiomers, S(-)- and R(+)- N,N,-dimethyl-α-phenylethylamines On the other hand, a significant difference in quenching was observed for the quenching of R(-)-,1'-binaphthyl by the enantiomers The ratio of the quenching rates, k_q(R-S)/ k_q(R-R), was determined to be 1 90 The difference in the rate clearly indicates that quenching occurs in the contact pair of an excited molecule and a quencher, and specific orientation is required in the quenching process Solvent polarity is also believed to alter the quenching mechanism [15] In nonpolar solvents, exciplex formation is dominant in

the quenching process, in polar solvents, quenching by electron transfer in an encounter of loose structure dominates This mechanism was examined by measuring the quenching rate of the two enantiomers as a function of the polarity of the solvent The ratio, k_q(R-S)/ k_q(R-R), was found to decrease with increasing solvent polarity The Stern-Volmer constant also depends on polarity and increases with increasmg solvent polarity

Irie and coworkers extended their study to other quenchers having bulky substituents and compared the effect of substituents on the quenching rate and the ratio of the quenching rates of the two enantiomers k_q(R-S)/k_q(R-R) [16] Significant differences in the quenching rate were observed for the quenching of (R)-(-)-1,1'-binaphthyl fluorescence by (S)-(-)- and (R)-(+)- N,N,-dimethyl-1-phenylethylamines, N,N,-dimethyl-α-phenyl-2-methylpropylamines and N,N,-dimethyl-α-phenyl-2,2-dimethylpropylamines, while no difference was discerned for the fluorescent quenching of the racemic mixture of 1,1'-binaphthyl The ratios of the quenching rates, k_q(R-S)/ k_q(R-R), increased as the bulkiness of the amine increased and were found to be 1 9, 2 7 and 4 0, respectively This difference in the quenching rate indicates that specific orientation is required in the quenching process between 1,1'-binaphthyl and the amines

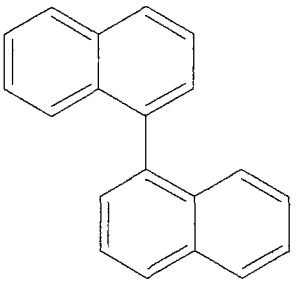

2 (vii)

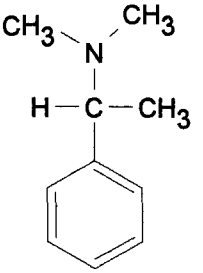

2 (viii)

Figure 2.2: *Structure of the 1,1'-binaphthyl molecule, 2 (vii) and N,N-dimethyl-α-phenylethylamine, 2 (viii) [14]*

More recently, James *et al* [17] showed that chiral recognition of saccharides could be achieved and signalled by fluorescence to the outside world They used a chiral tertiary amine to provide the potential for chiral discrimination and a binaphthyl group to transduce the host-guest interaction into a fluorescent signal (Figure 2 3) In addition, they suspected that twisting of the binaphthyl moiety might provide additional chirality Efficient photoelectron transfer from the amine to the binaphthyl occurred in the absence of the guest, and facilitated an efficient quenching mechanism for the fluorescence, provided the nitrogen atom was suitably oriented Boronic acid groups were sited near the chiral amine group and on binding with the saccharide target groups, a strong lewis acid interaction occurred between the boronic acid group and the amine, which drastically affected the latters ability to quench the binaphthyl fluorescence Both steric and electronic chiral recognition is clearly demonstrated by **2 (ix)** With the (R) form of this compound, the 1 1 complex stabilities of D-fructose, D-glucose and D-Mannose are greater than those of L-fructose, L-glucose and L-Mannose With the (S) form of the compound the 1 1 complex stabilities of L-fructose and L-glucose are greater than those of D-fructose and D-glucose This differences were attributed to steric effects With the (R) form of this compound the PET (photoinduced-electron-transfer) quenching efficiency on saccharide binding is effected most strongly by D-fructose and D-glucose, the least by L-fructose and L-glucose With the (S) form of this compound, the PET quenching efficiency on saccharide binding is affected most strongly by L-fructose and L-glucose and least by D-fructose and D-glucose This demonstrates the electronic effects of complexation This work elegantly demonstrated that chiral discrimination and signal transduction could be achieved by the placement of groups with the required functionalities in a suitable conformation

Parker *et al* [18] recently used the fluorescent emission from the formation of a diastereoisomeric complex between a chiral fluorescent acid (2,2'-dihydroxy-1,1'-binaphthalene, see Figure 2 4) in its excited state and a non-fluorescent chiral base (1-phenylethylamine) A linear relationship between the intensity of this emission and the enantiomeric composition of the non-fluorescent base was shown and this was used to determine the enantiomeric composition of two unknown samples of the

base The limit of quantification of one enantiomer in the presence of another was found to be 5%

The same group also developed a method using the same molecule (Figure 2 4) for the determination of the enantiomeric composition of phenylethylamine [19] A linear relationship between the efficiency of the energy transfer measured in terms of quenching of the molecule with the enantiomeric composition has been shown A limit of detection of one enantiomer in the presence of another has been calculated to be 10 %

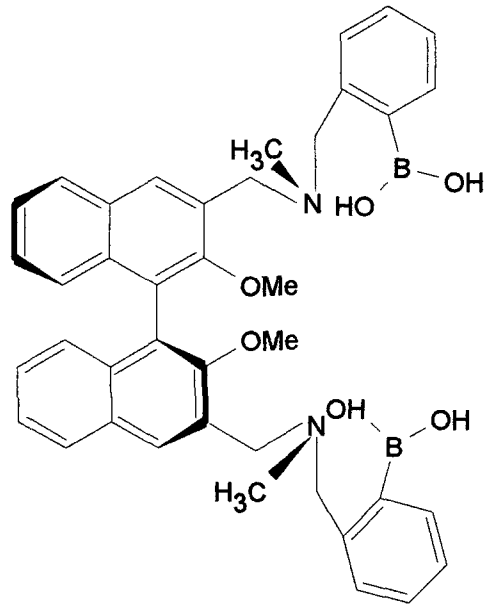

2 (ix)

Figure 2.3: *Chiral diboronic acid [17]*

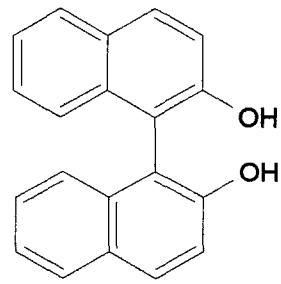

2 (x)

Figure 2.4: *2,2'-Dihydroxy-1,1'binapthalene [18,19]*

Bearing this in mind, we synthesised three receptors with substituent groups which were both chiral and fluorescent attached to the lower rim of a calixarene macrocycle Compound **2 (xi)** is based on the attachment of the chiral fluorescent moiety, S-di-2-naphthylprolmol, to the four positions at the lower rim of the calix[4]arene molecule whereas compounds **2 (xii)** and **2 (xiii)** involve the attachment of (R/S)-1-(9-anthryl)-2,2,2-trifluoroethanol to three of the lower rim positions in the tetramer, and four of the lower rim positions in a hexamer, respectively

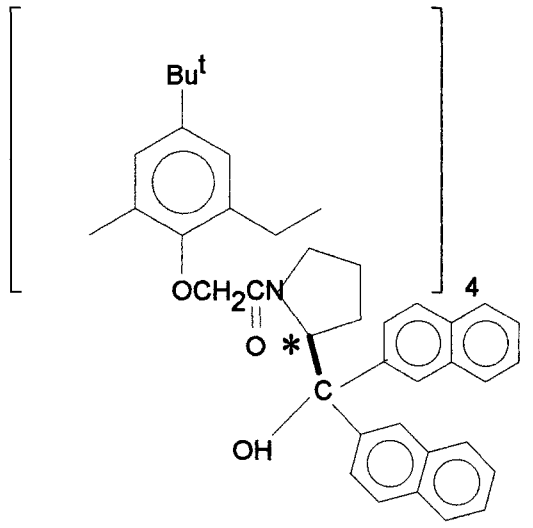

2 (xi)

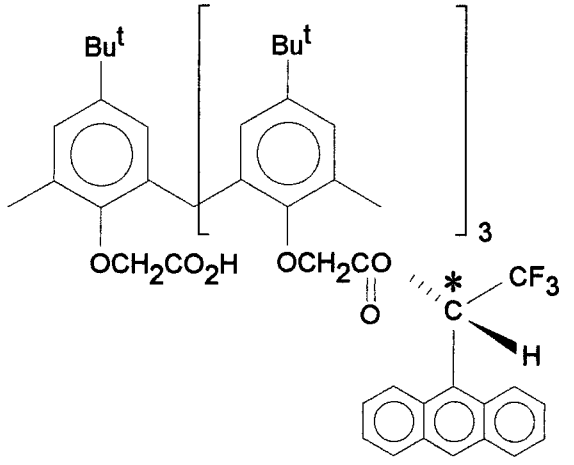

2 (xii)

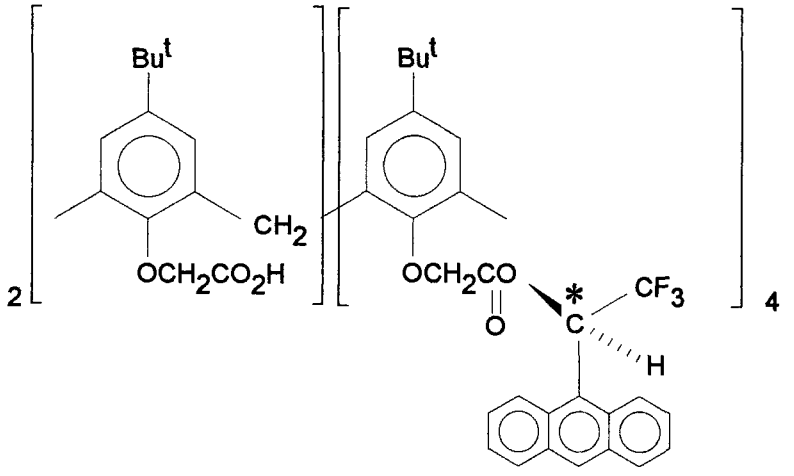

2 (xiii)

* = chiral centre

Figure 2.5: *Structures of synthesised chiral fluorescent calixarenes*

2.2 Experimental

2 2 1 Apparatus and Reagents

All experiments were performed using a Perkin Elmer Luminescence Spectrometer LS 50B interfaced with an Elonex PC-466 which employs fluorescence data manager software Post-run data processing was performed using Microsoft Excel v 5 0 after importing the spectra as ascii files

The R- and S- forms of 1-phenylethylamine (PEA) were of puriss grade obtained from Sigma and all solvents were of HPLC grade obtained from Labscan Ltd The S-Di-2-naphthylprolinol was obtained from Oxford Asymmetry and the enantiomers of 1-(9-anthryl)-2,2,2-trifluoroethanol were obtained from Fluka

2 2 2 Synthesis of the calixarenes

(i) Compound **2 (xi)** was synthesised as follows 2 48g (2 5 mmol) of the tetraethyl ester was prepared as described previously [20] and hydrolysed to its carboxylic acid potassium salt by refluxing with 2 5 g KOH in 50 mL of ethanol followed by filtration and acidification with 37% aqueous HCl to give 2 1g (95%) of product This was subsequently converted to the acid chloride by a 2 hour reflux in 10 mL of thionyl chloride followed by removal of volatiles (the last traces under reduced pressure) to give a quantitative yield To 0 238g (0 25 mmol) of the acid chloride in 5 mL of dry THF was added 0 353g (1 mmol) of S-di-2-naphthylprolmol and 0 079g (1 mmol) of dry pyridine with stirring at room temperature for 24 hours 0 528 g (95%) of a pale brown product was isolated which was purified by chromatography on basic alumina using chloroform to give 211 mg (40%) yield of the compound as a buff coloured solid mp 198-200°C, IR (KBr) γ(C=O) 1634 cm^{-1}, ^1H NMR (400 MHz, $CDCl_3$), δ

1 24 [s, 36H, C(CH_3)$_3$] , δ 2 0-2 40 [m, 16H CH_2CH_2], δ 2 90 [m, 4H, NCH_2], δ 3 25 [m, 4H, NCH_2], δ 3 50 [d, 2H, NC*H*], δ 4 06 [d, 4H, H_BArCH$_2$Ar], δ 4 40 [d, 2H, NC*H*], δ 4 70 [m, 4H, NCHCO*H*], δ 5 16 [d, 4H, H_AArCH$_2$Ar], δ 5 30 [m, 8H, OCH_2], δ 6 76-8 11 [m, 64H, *ArH*], δ 7 27 [s, $CHCl_3$] Anal Calcd for $(C_{38}H_{37}O_3N)_4$ $CHCl_3$ C, 78 45, H, 6 41, N, 2 39 Found C, 78 04, H, 6 59, N, 2 40 $[\alpha]_D^{20}$ -304 $\pm$ 2° (c = 25 mg in 2 mL Chloroform)

(ii) Compound **2 (xii)** was synthesised as follows To 0 238g (2 5 mmol) of the acid chloride in 5 mL of dry THF was added 0 276 g (1 mmol) R(-)-1-(9-anthryl)-2,2,2-trifluoroethanol (Fluka) and 0 079 g (1 mmol) dry pyridine This was allowed to stir at room temp for 48 hours afterwhich the volatiles were removed and the residue taken up into dichloromethane which was washed with 1% aqueous HCl 0 4 g (97% yield) of a pale yellow solid **2 (xii)** was obtained The product appeared exceptionally sensitive to base catalysed cleavage mp 59-61°C, IR (KBr) γ(C=O) 1740 cm^{-1}, γ(CO_2H) 3298 cm^{-1}, ^{1}H NMR (400 MHz, $CDCl_3$), δ 0 90 [s, 12 H, C(CH_3)$_3$] , δ 1 25 [s, 12H, C(CH_3)$_3$], δ 1 29 [s, 12H, C(CH_3)$_3$], δ 1 83 [m, 3H, C*H*CF_3], δ 3 24 [d, 4H, H_BArCH$_2$Ar], δ 3 72 [m, 8H, OCH_2], δ 4 3-4 7 [br, 1H, COO*H*], δ 4 52 [d, 4H, H_AArCH$_2$Ar], δ 6 65-9 00 [m, 35H, *ArH*], δ 5 29 [s, CH_2Cl_2] Anal Calcd for ($C_{100}H_{91}F_9O_{12}$) CH_2Cl_2 C, 69 69, H, 5 39 Found C, 69 33, H, 5 73

The reaction scheme for the synthesis of ligand **2 (xi)** and **2 (xii)** is summarised in Figure 2 6

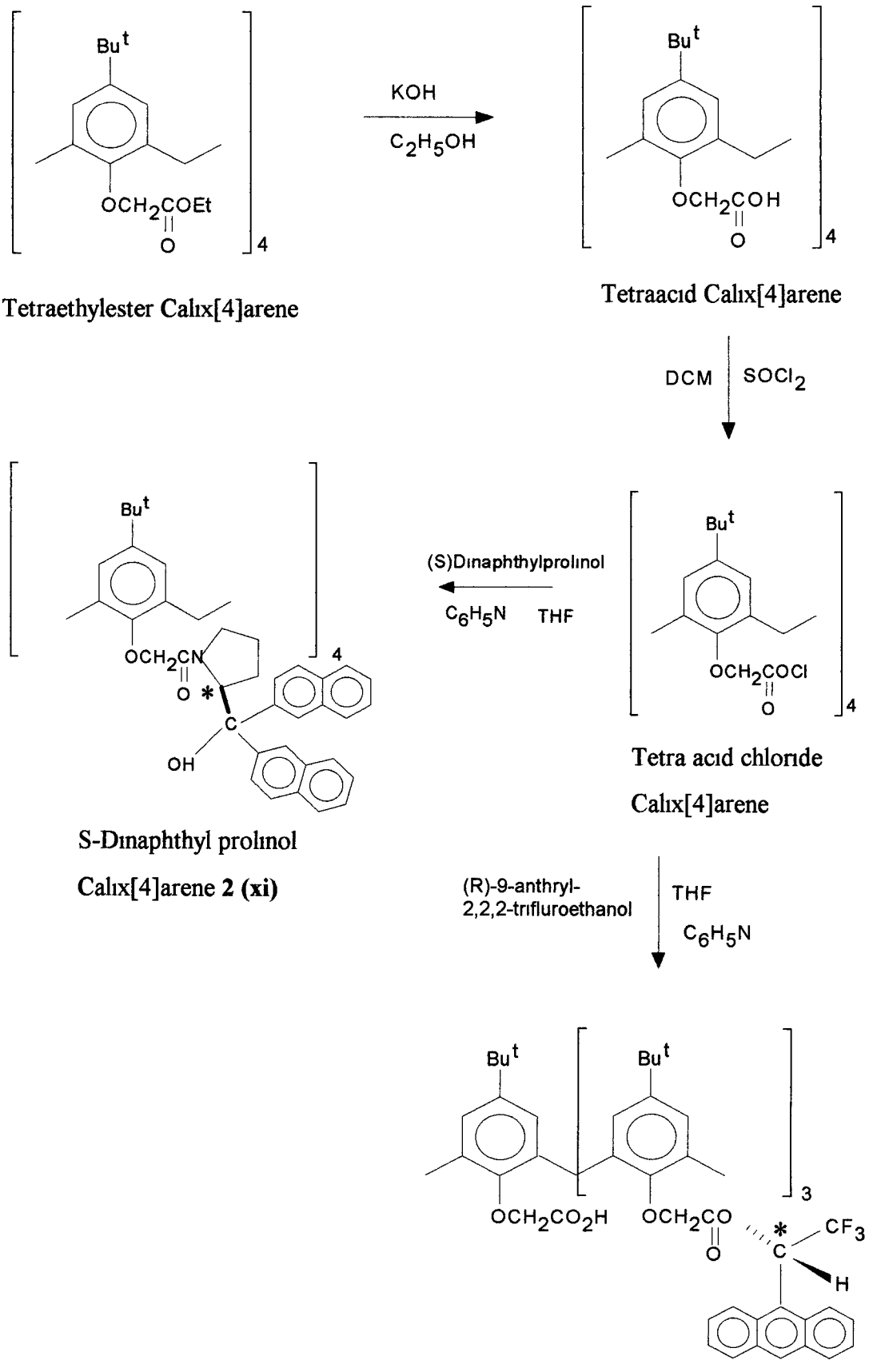

Figure 2.6: *Reaction scheme for the synthesis of the calix[4]arenes*

(iii) The synthesis of **2 (xiii)** was as follows 2 48 g (16 7 mmol) of the hexaethyl ester calixarene was prepared as described previously [20] and hydrolysed to its potassium carboxylate by refluxing with 2 5 g KOH in 50 mL of ethanol followed by filtration and acidification with 37% aqueous HCl to give 2 0 g (91% yield) This was then converted to the acid chloride by refluxing for 2 hours in 10 mL of thionyl chloride To 0 238g (0 16 mmol) of the acid chloride in 5 mL of dry THF was added 0 276 g (1 mmol) S(+)-1-(9-anthryl)-2,2,2,-trifluoroethanol (Fluka) and 0 079 g (1mmol) dry pyridine The entire was allowed to stir at room temperature for 48 hours afterwhich all volatiles were removed and the residue taken up in dichloromethane which was washed with 1% aqueous HCl After removal of the solvent, 0 38 g (92% yield) of the compound **2 (xiii)** was obtained as a pale yellow solid Like the tetramer the compound is sensitive to base catalysed cleavage mp 77-79°C, IR (KBr) γ(C=O) 1738 cm^{-1}, $\gamma(CO_2H)$ 3396 cm^{-1}, ^1H NMR (400 MHz, $CDCl_3$), δ 1 24 [s, 54H, $C(CH_3)_3$] ,δ 1 80 [m, 4H, $CHCF_3$], δ 3 30 [d, 6H, H_BArCH_2Ar], δ 3 70 [m, 12H, OCH_2], δ 4 2-4 5 [br, 2H,COOH], δ 4 39 [d, 6H, H_AArCH_2Ar], δ 6 53-9 00 [m, 48H, *ArH*], δ 5 28 [s, CH_2Cl_2] Anal Calcd for ($C_{142}H_{132}F_{12}O_{18}$) $2CH_2Cl_2$ C, 68 51, H, 5 43 Found C, 68 43, H, 5 68

2 2 3 Procedure for fluorescence measurements

Solutions giving concentrations of the dinaphthyl calix[4]arene **2 (xi)** of 1 μmol dm^{-3} and 1-phenylethylamine in the range of 1-12 5 mmol dm^{-3} in chloroform were prepared as follows A 50 μmol dm^{-3} stock solution of the calixarene was prepared by dissolving 11 7 mg in 100 mL of chloroform A 25 mmol dm^{-3} solution of the 1-phenylethylamine was prepared by dissolving the required combination of the two enantiomers, totalling 1 515 g in 50 mL of chloroform A 10 mL volume of this solution was diluted to 100 mL with chloroform to a working stock solution Test solutions were prepared by placing a 1 mL aliquot of the calixarene stock solution in a 50 mL volumetric flask, adding 5, 10, 15, 20 or 25 mL of 1-phenylethylamine stock solution and making up to volume with chloroform For the preparation of solutions

containing calixarenes **2 (xii)** and **2 (xiii)** the same general procedure was followed The concentration of calixarene in both cases was 0 2 μmol dm^{-3}

The fluorescence intensity of solutions containing **2 (xi)** were measured at an excitation wavelength of 274 nm The fluorescent intensity readings were compared to a solution containing 1 μmol dm^{-3} calixarene of **2 (xi)** and no 1-phenylethylamine An excitation wavelength of 258 nm was used for the fluorescent measurements of **2 (xii)** and **2 (xiii)**

2.3 Results and Discussion

2 3 1 Excitation and emission spectra

The excitation and emission spectra of the S-dinaphthyl calix[4]arene (**2 (xi)**) in the presence and absence of 0 33 mol dm^{-3} 1-phenylethylamine are shown in Figure 2 7 The maximum of the excitation spectrum is at 274 nm (Figure 2 7a) and the emission spectrum obtained using an excitation wavelength of 274 nm is 337 nm (Figure 2 7b) The presence of the 1-phenylethylamine alters these spectra considerably, and the maximum is shifted in the excitation spectrum (274 nm in the absence of the 1-phenylethylamine and 280 nm in the presence of 1-phenylethylamine, (see Figure 2 7a)

The broad nature of the excitation spectrum of **2 (xi)** arises from the S-dinaphthylprolinol label, as a very similar excitation spectrum is obtained with the free ligand (Figure 2 8) In the presence of PEA the same quenching effect is seen as with the calixarene There are two fluorophores in the dinaphthylprolinol label arising from the naphthyl groups, which are in different environments due to the effect of the bridging prolinol group and hence the excitation spectrum is considerably broadened compared to that of naphthalene for example (Figure 2 9) This is so for the free label and the labelled calixarene **2 (xi)** Molecular modelling suggests that hydrogen bonding between the prolinol OH and the PEA amine groups allows one of the naphthyl and the PEA aryl groups to stack, leaving the other naphthyl group unaffected (the one absorbing at longer wavelengths) as shown in Figure 2 10 This would explain the partial quenching of the excitation spectrum

Alternatively, the effect could arise from PEA which absorbs in the range 240-270 nm The apparent quenching could therefore be due to absorbance by the PEA of incident radiation from the source and of photons emitted by the calixarene over this range, leading to less observed fluorescence Above this range, the PEA no longer competes for available energy and the excitation spectrum is much less affected

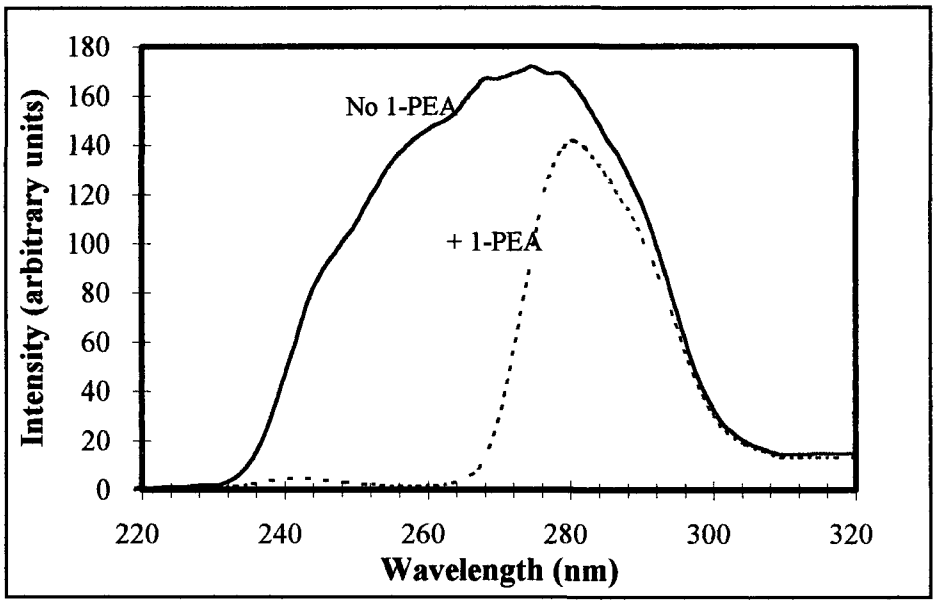

(a)

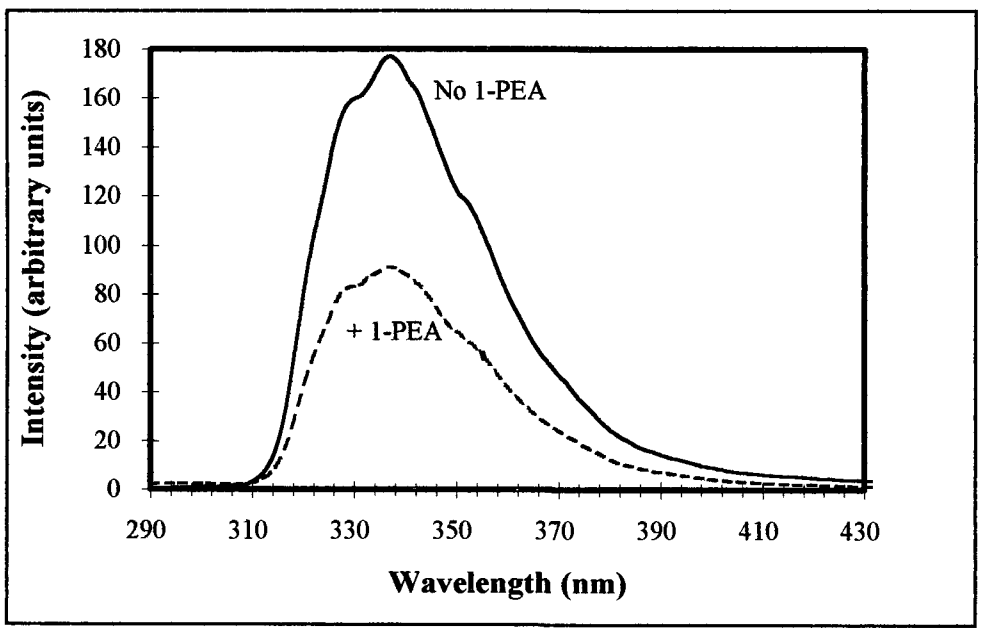

(b)

Figure 2.7 *Excitation and emission spectra of the dinaphthyl calix[4]arene (2 (xi)) at a concentration of 2 μmol dm^{-3} in the presence and absence of racemic 1-phenylethylamine (a) Excitation spectra of the calixarene with and without 0 33 M 1-phenylethylamine using an emission wavelength of 340 nm (b) Emission spectra of the calixarene and also with 0 33 M 1-phenylethylamine using an excitation wavelength of 274 nm*

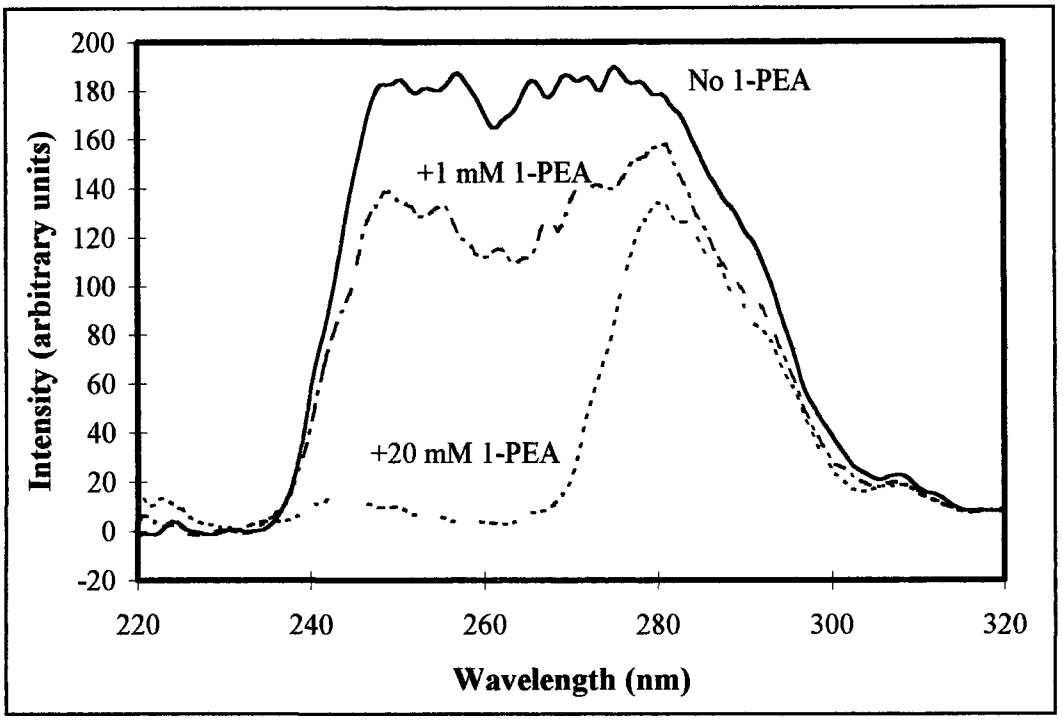

Figure 2.8: *Excitation spectra of the S-dinaphthyl prolinol label alone (1 μM dm^{-3}) and in the presence of 1 mM and 20 mM 1-PEA using an emission wavelength of 340 nm*

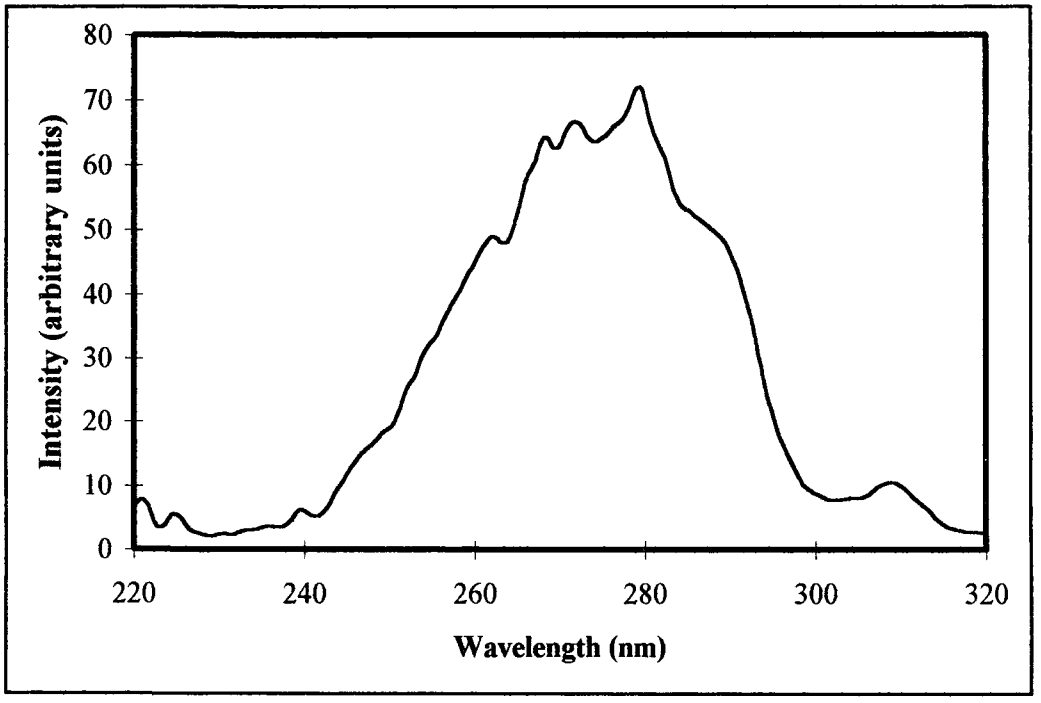

Figure 2.9: *Excitation spectrum of naphthalene at an emission wavelength of 340 nm and at a concentration of 1 μmol dm^{-3}*

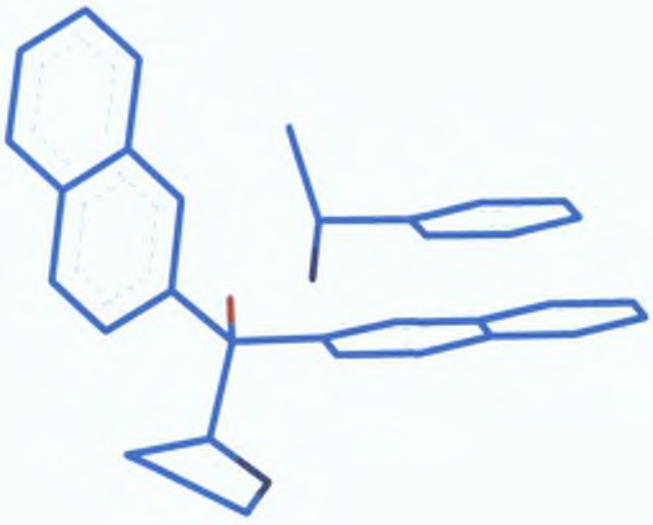

Figure 2.10: *Molecular model demonstrating the interaction between the dinaphthyl prolinol and the PEA suggesting that hydrogen bonding between the prolinol OH and the PEA amine groups allows one of the naphthyl and the PEA aryl groups to stack. This may explain the partial quenching seen in the excitation spectrum (Figure 2.7a). This 3-d model was obtained using Hyperchem v. 4.0.*

Light blue = C-C bonds

Red = Oxygen atoms

Dark blue = Nitrogen atoms

Hydrogens not shown for clarity.

Examination of the excitation spectra from the anthryl-labelled compounds **2 (xii)** and **2 (xiii)** tends to support the case for the PEA absorbance mechanism (Figure 2 11) In these compounds, the main emission band (240-270 nm) coincides with the absorbance of PEA Once again, a quenching effect is observed in the excitation spectrum in this region but not at the less intense anthracene fingerprint region (320-400 nm) These compounds have a maximum emission intensity at an excitation wavelength of 258 nm and an emission wavelength of 416 nm

The background fluorescence of the calixarene ring using tetraesters for comparison was checked, and the fluorescence is insignificant (Figure 2 12) Therefore we do not believe that the calixarene fluorescence quenching is an important factor - it is more to do with the inherently broad excitation spectrum of the dinaphthylprolinol group as outlined above

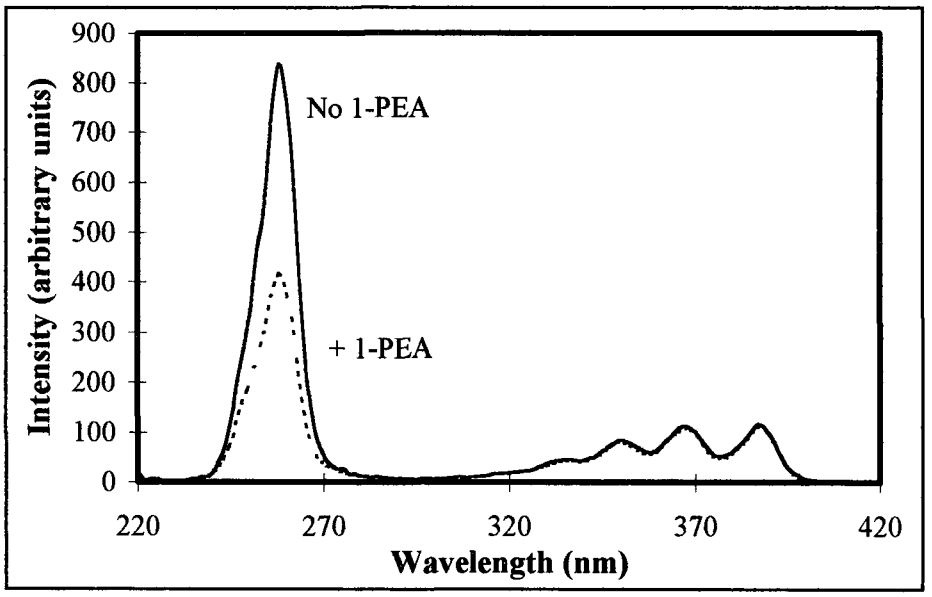

(a)

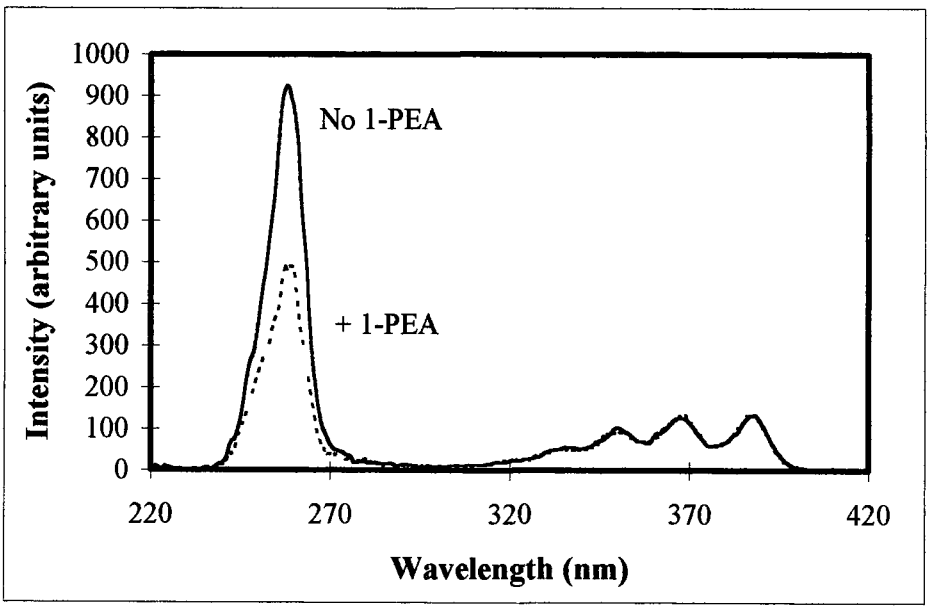

(b)

Figure 2.11: *Excitation spectra (a) of the tetraanthryl calix[4]arene* **2** ***(xii)*** *(0 2 μmol dm^{-3}) and the hexaanthryl calix[6]arene (b)* **2** ***(xiii)*** *(0 2 μmol dm^{-3}) in the presence and absence of 2 5 mmol dm^{3} 1-PEA at an emission wavelength of 416 nm*

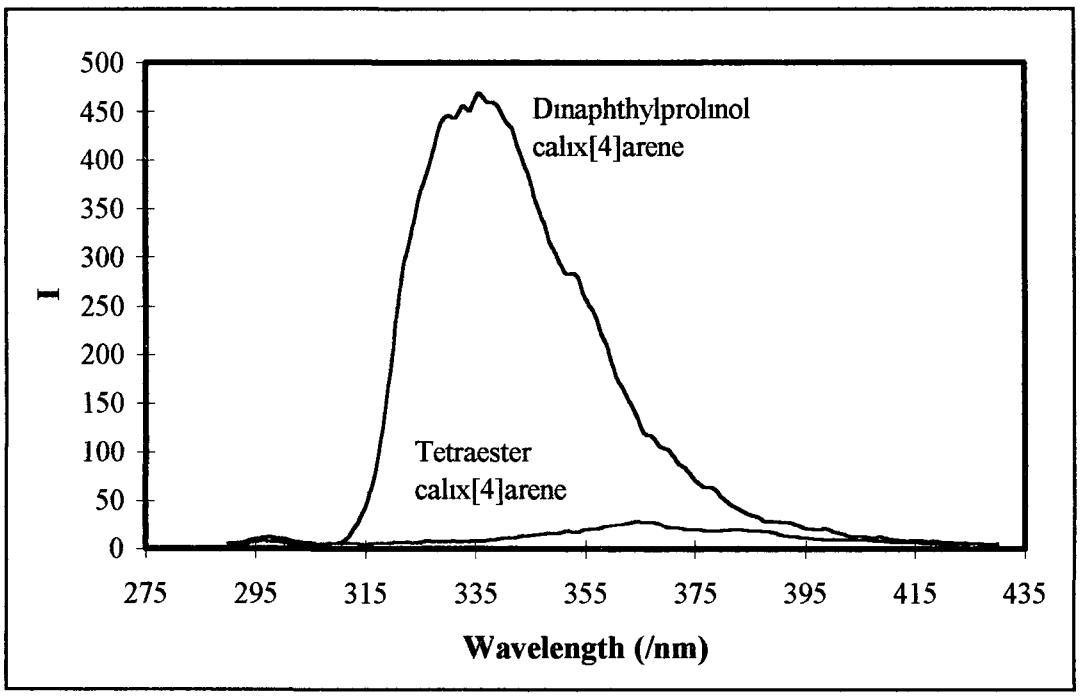

Figure 2.12: *Fluorescence emission spectra of the dinaphthylprolinol calix[4]arene (1 μmol dm^{-3}) and the tetraester calix[4]arene (1 μmol dm^{-3}), demonstrating how the fluorescence of the later is insignificant*

2.3.2 Linear response range

The linear response range of fluorescence intensity to concentration of **2 (xi)** is shown in Figure 2 13(a) and was found to be 0-1 2 μmol dm^{-3} (r = 0 9997, n = 6) at an excitation wavelength of 274 nm It is important to use a concentration of the calixarene within the linear range in order to ensure that no self-quenching occurs and therefore no alternative self-quenching mechanisms are present A concentration of 1 μmol dm^{-3} was chosen for subsequent experiments with calixarene **2 (xi)** to examine the effect of 1-PEA, and hence any quenching observed can be related to the effect of the target species on the ligand The linear response range of **2 (xii)** (Figure 2 13(b)) was 0-0 4 μmol dm^{-3} (r = 0 9988, n = 5) and **2 (xiii)** (Figure 2 13(c)) was 0-0 3 μmol dm^{-3} (r = 0 9992, n = 5) A concentration of 0 2 μmol dm^{-3} was chosen for subsequent measurements for both these compounds

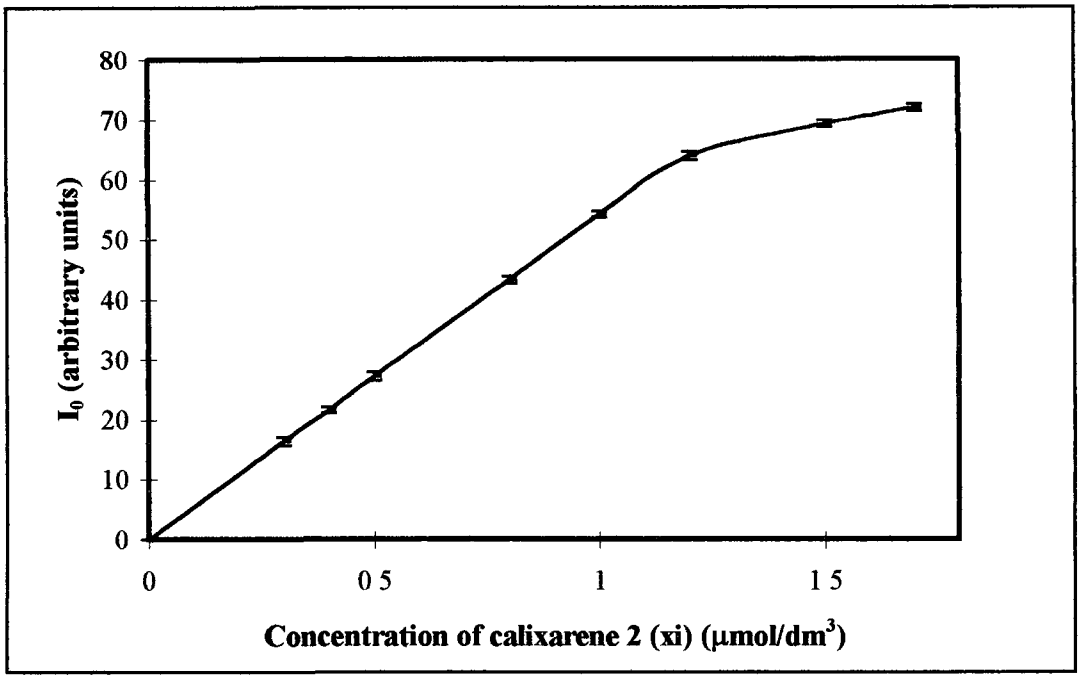

Figure 2.13 (a): Fluorescent response of calixarene **2 (xi).**

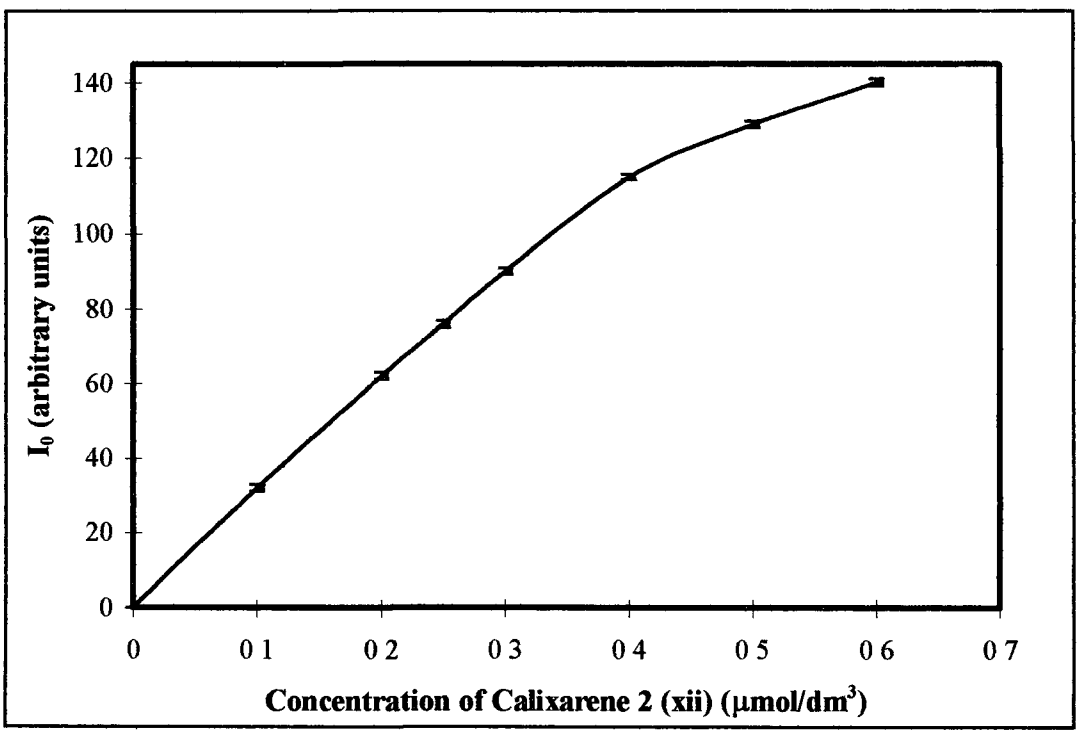

Figure 2.13 (b): Fluorescent response of calixarene **2 (xii)**

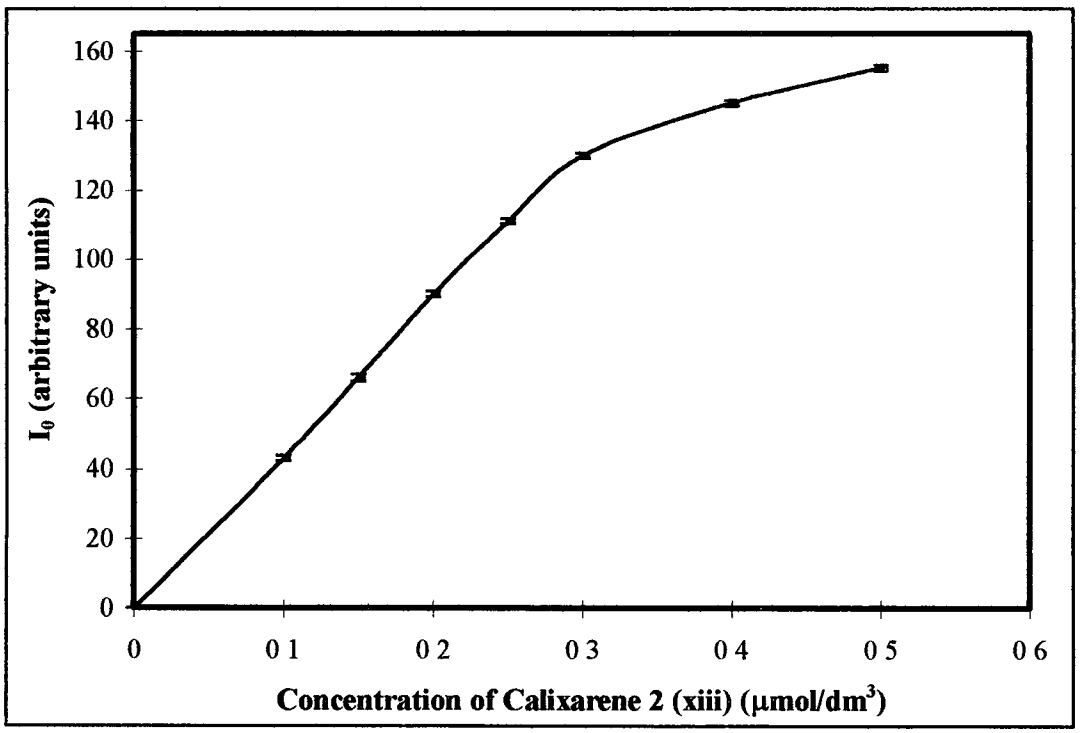

Figure 2.13 (c): Fluorescent response of calixarene **2 (xiii)**

Figure 2.13: *Investigation of linear range of the calixarenes Change in the fluorescent intensity of* **2 (xi)** *(a),* **2 (xii)** *(b) and* **2 (xiii)** *(c) with concentration, standard deviations shown as error bars*

2.3.3 Linear range of Stern-Volmer plot

The Stern-Volmer plot of **2 (xi)** was found to be linear over the range investigated (0-13 5 mmol dm^{-3} of racemic phenylethylamine, (Figure 2 14a) The Stern-Volmer plot of **2 (xii)** was found to be linear over the measured range of 0-2 5 mmol dm^{-3} of racemic phenylethylamine (Figure 2 14b) and for compound **2 (xiii)** (Figure 2 14c) 0-2 5 mmol dm^{-3} of racemic phenylethylamine

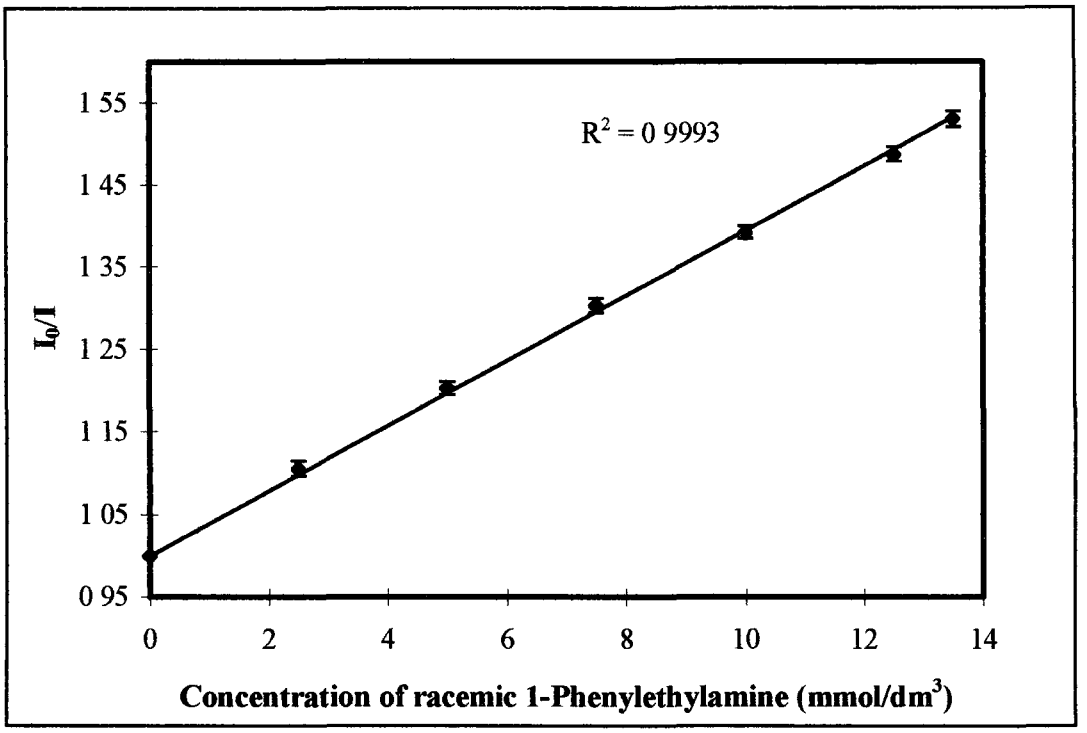

Figure 2.14 (a): Stern-Volmer plot of calixarene **2 (xi)**

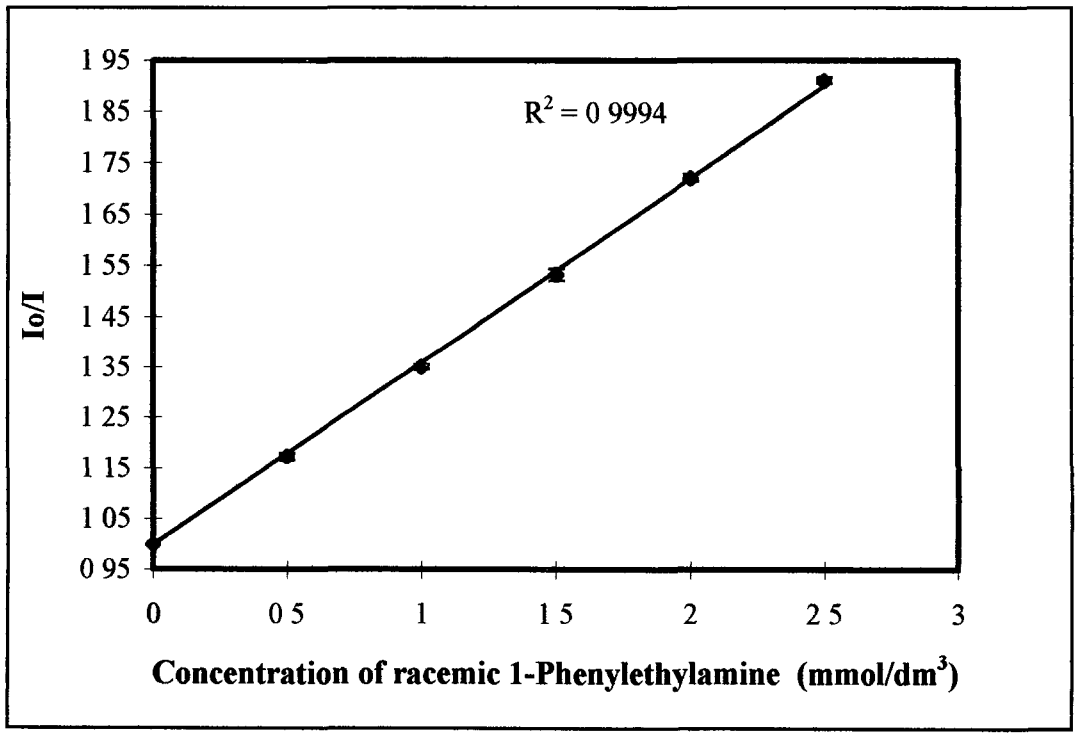

Figure 2.14 (b): Stern-Volmer plot of calixarene **2 (xii).**

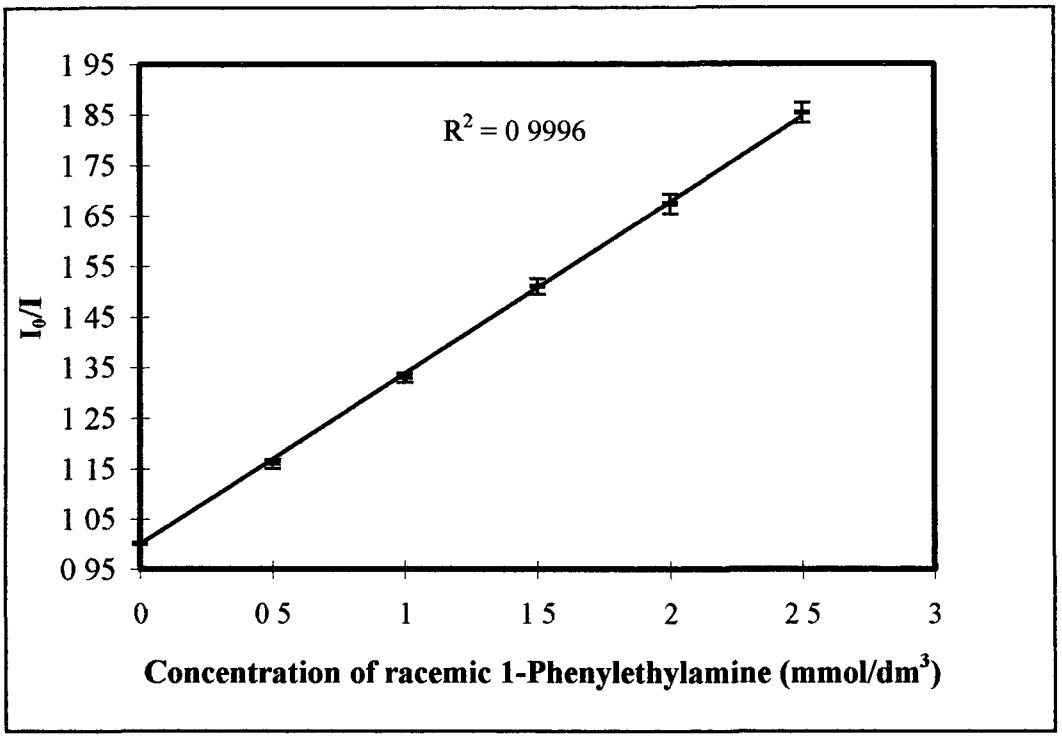

Figure 2.14 (c): Stern-Volmer plot of Calixarene **2 (xiii).**

Figure 2.14: *Stern- Volmer plot obtained for the addition of racemic 1-phenylethylamine to* ***2 (xi)*** *(a),* ***2 (xii)*** *(b) and* ***2 (xiii)*** *(c), standard deviations shown as error bars*

2 3 4 Variation of Stern-Volmer plot with enantiomeric composition

Figure 2 15 illustrates the difference in the Stern-Volmer plots of the three fluorescent calixarenes on addition of PEA of several enantiomeric compositions varying from 100% (S) to 100% (R) Values for K_{SV} for 100% (S) to 100% (R) for each ligand is summarised in Table 2-1 From these results we can conclude that unlike **2 (xi)** which exhibits a much larger difference in K_{sv} values, **2 (xii)** and **2 (xiii)** do not exhibit any enantiomeric selectivity under the conditions used in this study, (100%(S)/100%(R) K_{sv} ratios are 1 856, 0 962 and 1 040, for **2 (xi)**, **2 (xii)**, and **2 (xiii)**, respectively Figure 2 15d shows the Stern-Volmer plot for the dinaphthylprolinol label on its own (i e not attached to Calixarene **2 (xi)**) This demonstrates that the free label by itself cannot distinguish between the PEA enantiomers (slopes are virtually the same), and that the mechanism does not obey the Stern-Volmer equation (intercept does not pass through one) The non-linearity in the Stern-Volmer plot is reproducible and must arise from the structural differences in the free label and the labelled calixarene, and may involve hydrogen bonding between the amine and hydroxyl groups of the label and the PEA More importantly from the point of view of our investigations however, these results suggest that the chiral recognition exhibited by **2 (xi)** is not an inherent characteristic of the label itself, but rather that it arises from the 3-d effect of the substituted calixarene

The Stern-Volmer constant for compound **2 (xi)** was shown to vary linearly with the enantiomeric composition of 1-phenylethylamine ($r = 0\ 9980$, $n = 5$) as shown in Figure 2 16 which suggests that it may be possible to use this technique for the determination of enantiomeric composition

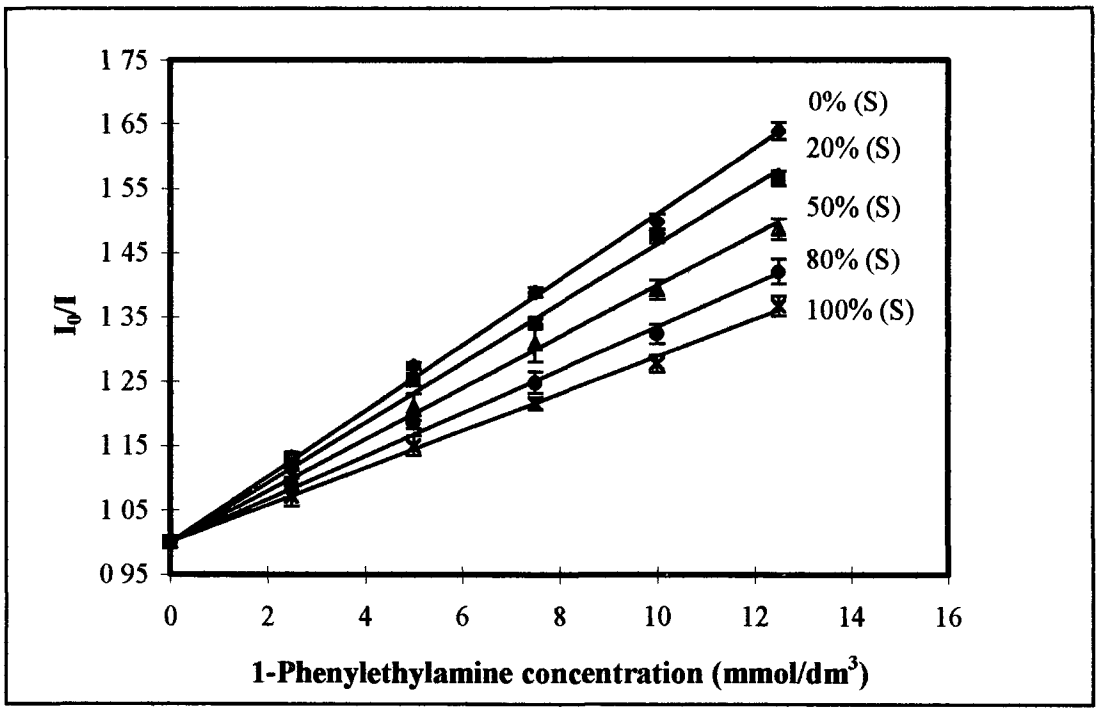

Figure 2.15 (a): Stern-Volmer plots for calixarene **2 (xi)**

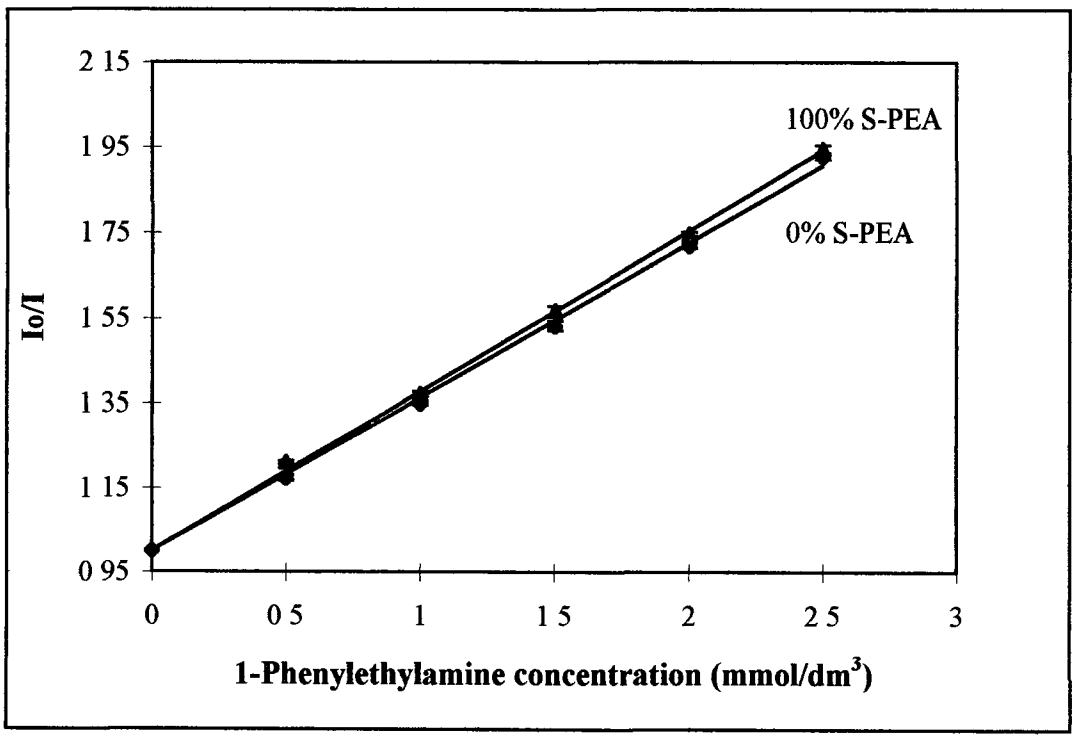

Figure 2.15 (b): Stern-Volmer plots for Calixarene **2 (xii)**

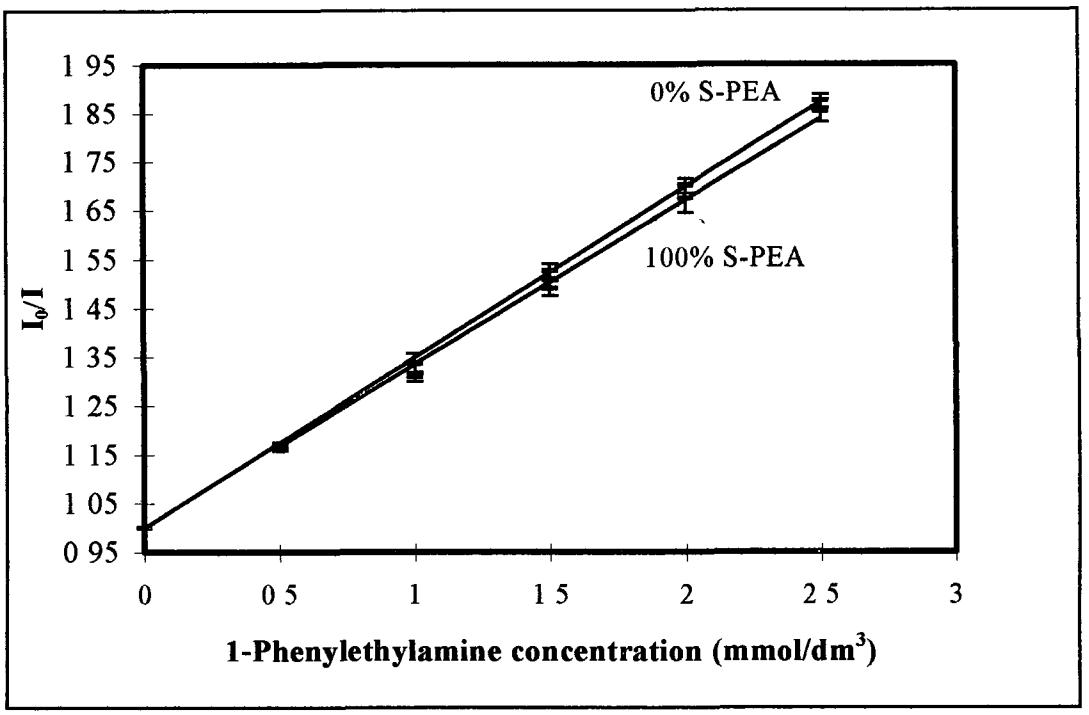

Figure 2.15(c): Stern-Volmer plots for calixarene **2 (xiii)**

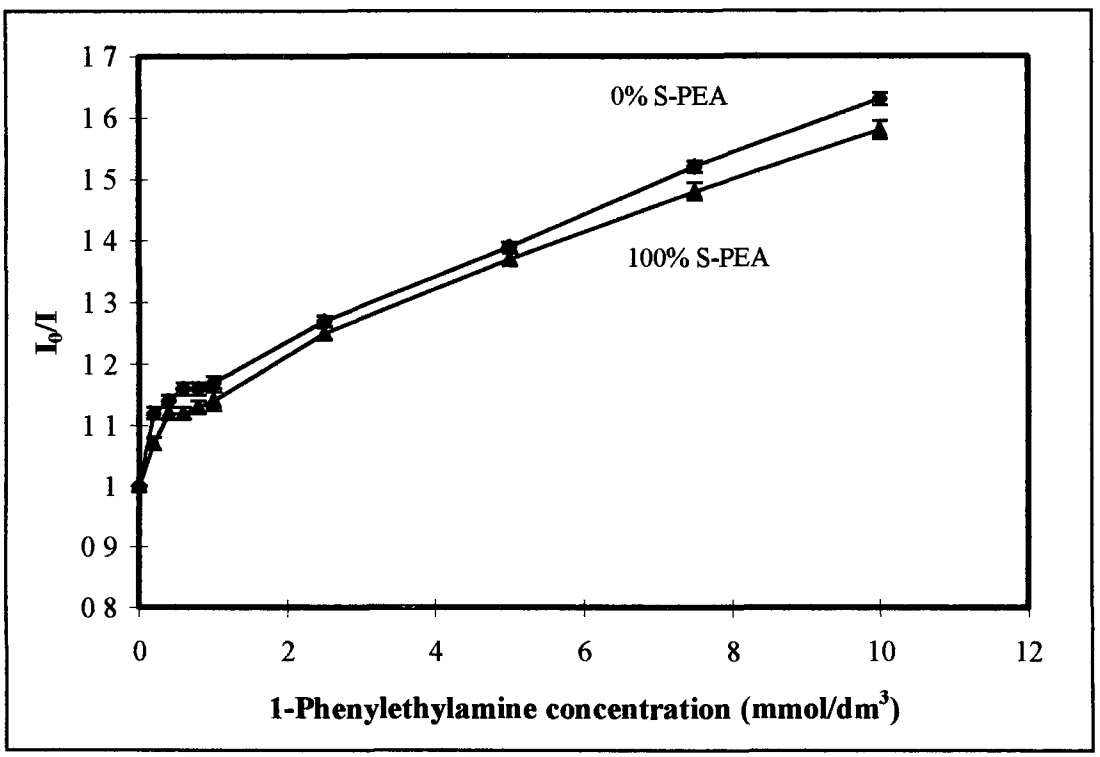

Figure 2.15(d): Stern-Volmer plots for S-dinaphthylprolinol label

Figure 2.15 *Stern-Volmer plots for the quenching of calixarenes* ***2 (xi)*** *(a),* ***2 (xii)*** *(b),* ***2 (xiii)*** *(c) and S-di-naphthyl prolinol (d) upon addition of 1-PEA containing 0-100% of the S-form Standard deviations shown as error bars*

Compound	*Composition*	K_{SV}	*St.Dev.*
2 (xi)	0%S,100%R	0 052 (0 9983)	0 0005
2 (xi)	100%S, 0%R	0 028 (0 9962)	0 0007
2 (xii)	0%S,100%R	0 363 (0 9976)	0 0007
2 (xii)	100%S, 0%R	0 377 (0 9984)	0 0006
2 (xiii)	0%S,100%R	0 3485 (0 9993)	0 0005
2 (xiii)	100%S, 0%R	0 3350 (0 9963)	0 0006

Table 2-1: *Stern-Volmer slopes , correlation coefficients and standard deviations for curves in Figure 2 15 (n=6)*

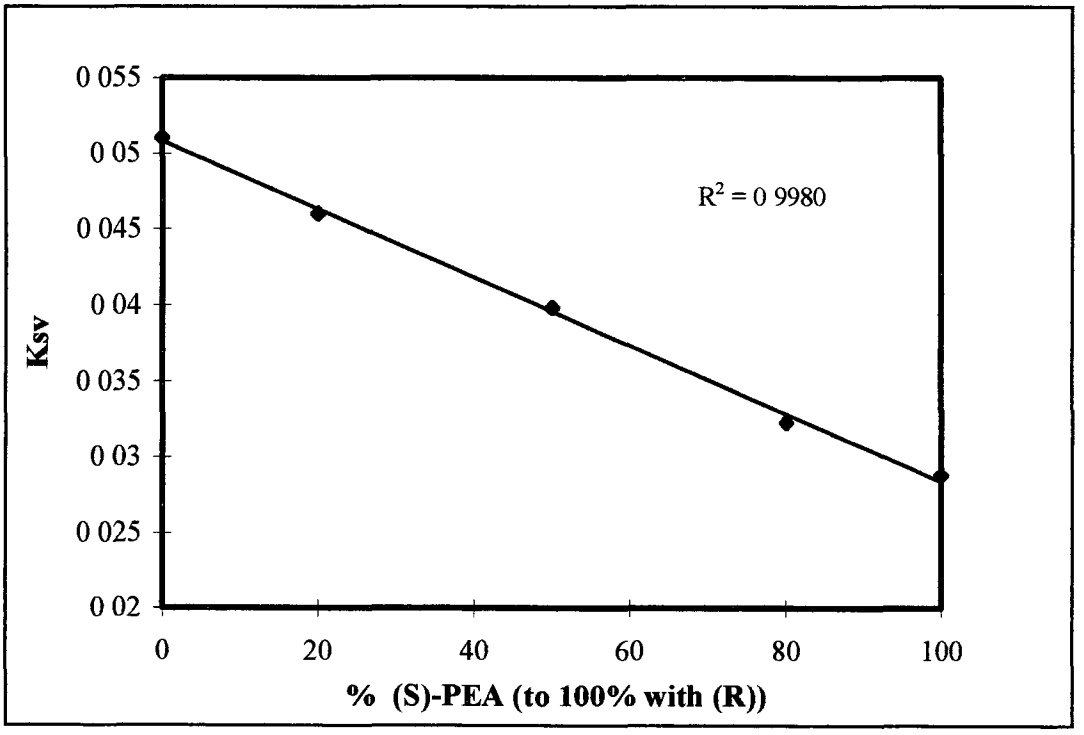

Figure 2.16 *The variation of the Stern-Volmer constant for the quenching of the fluorescence of calixarene 2 (xi) (1 μmol dm^{-3}) with enantiomeric composition of 1-Phenylethylamine*

However, this chiral discrimination is not exhibited by the (R/S)-1-(9-anthryl)-2,2,2-trifluoroethanol tetramer and hexamer derivatives, **2 (xii)** and **2 (xiii)**, respectively It is the general case that calixarene hexamers like **2 (xiii)** are more open and flexible structures than tetramers [21] The energy minimised structures of the three compounds are shown in Figure 2 17 and confirm this All energy-minimised structures were generated using Hyperchem v 4 0 using MM^{+} Each calixarene subunit was individually energy minimised, and the subunits subsequently linked to provide the appropriate macrocycle which was then energy minimised Interatomic distances and bond angles obtained with the macrocycles compare favourably with X-ray data from similar calixarenes suggesting that these are reasonable structures However, as X-ray structures for **2 (xi)**, **2 (xii)**, and **2 (xiii)** are not available at present, the exact conformations are not known

The energy minimised structures suggest that the four (S)-di-naphthylprolinol groups in **2 (xi)** are much more closely arranged than the three (R)-1-(9-anthryl)-2,2,2-trifluoroethanol groups in **2 (xii)** and the four (S)-1-(9-anthryl)-2,2,2-trifluoroethanol groups in **2 (xiii)** There is also evidence for this on comparing the interatomic distances between similar pairs of atoms on the energy minimised calix[4]arene macrocycles (Table 2-2 and Table 2-3) For example, these interatomic distances are similar for calixarenes **2 (xi)** and **2 (xii)** at the upper rim, down to, and including the phenolic oxygen atoms at the lower rim (distance between the phenolic oxygen atoms of opposing rings of **2 (xi)** are 5 55 and 3 35 Å and for **2 (xii)**, 5 44 and 3 53 Å) However, there is striking difference in the distance between the two opposing chiral carbon centres for calixarene **2 (xi)** (9 064 Å for both pairs) and for the single pair in **2 (xii)** (13 558 Å) This could be a significant factor influencing the dramatic difference in chiral discrimination exhibited by these tetramers In the case of **2 (xi)**, there is a relatively well-defined 3-d chiral space through which the enantiomers must pass in order to facilitate quenching (see discussion below) Clearly, if this is the case, then the (R)-PEA enantiomer must be better predisposed to passing through the chiral space than the (S)-PEA enantiomer, leading to a more efficient transfer of energy from the (S)-di-naphthylprolinol group, and a greater slope for the Stern-Volmer plot

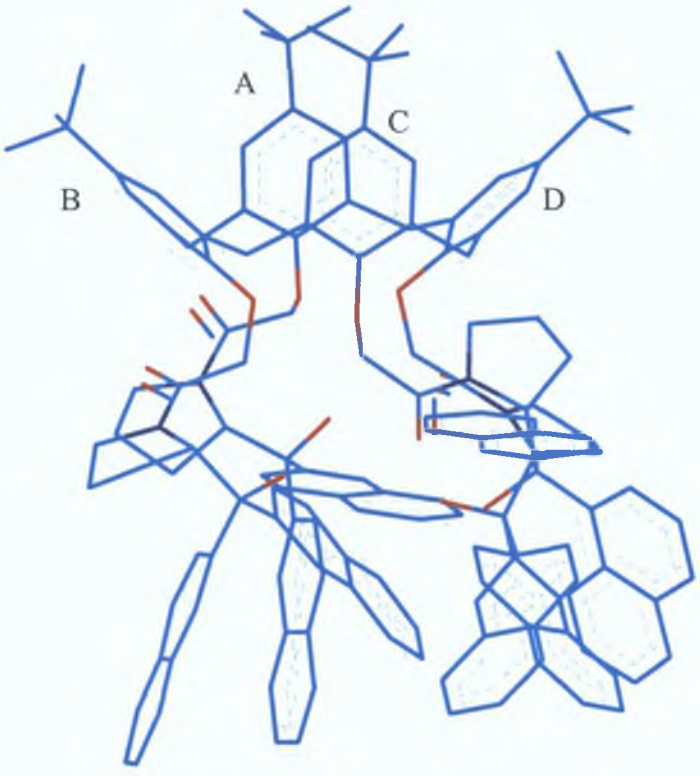

Calixarene 2 (xi)

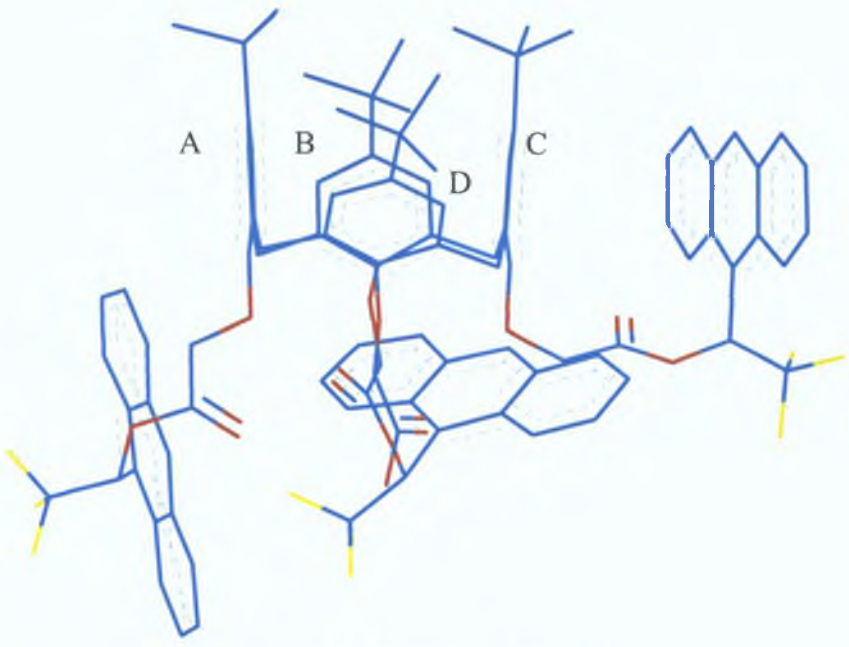

Calixarene 2 (xii)

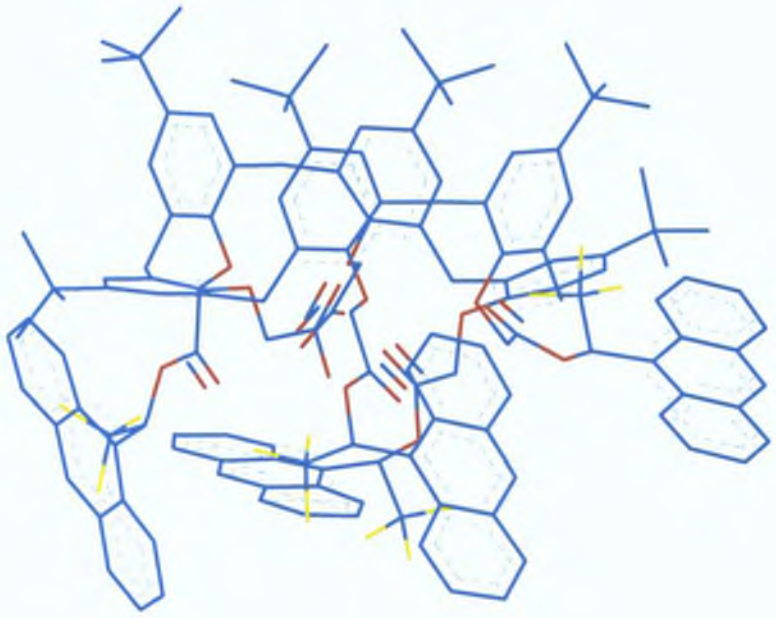

Calixarene 2 (xiii)

Figure 2.17: *Energy minimised structures of calixarene* ***2 (xi)****,* ***2 (xii)*** *and* ***2 (xiii)*** *obtained using molecular mechanics in Hyperchem v 4.0. The chiral region on the lower rim is clearly much more defined in* ***2 (xi)*** *than in* ***2 (xii)*** *or* ***2 (xiii)****.*

Light blue = C-C bonds

Red = Oxygen atoms

Dark blue = Nitrogen atoms

Yellow = Fluorine atoms

Hydrogens not shown for clarity.

Distances	Carbon of t-butyl	Phenoxy oxygen	Carbonyl oxygen	Nitrogen	Chiral Carbon
A-C	5 414	3 350	7 014	8 207	9 064
B-D	11 929	5 547	10 024	10 343	9 899

Table 2-2: *Distances (in angstroms) between opposing groups on the dinaphthyl calix[4]arene (2 (xi))*

Distances	Carbon of t-butyl	Phenoxy oxygen	Carbonyl oxygen	Chiral Carbon
A-C	5 802	3 535	6 142	13 558
B-D	11 491	5 437	9 021	N/A

Table 2-3: *Distances (in angstroms) between opposing groups on the anthryl trifluoro-calix[4]arene (2 (xii))*

2 3.5 Determination of enantiomeric composition

From Figure 2 16 it is clear that the enantiomeric composition of mixtures of PEA can be determined from the slope of the Stern-Volmer plots However, a faster and less tedious method can be employed which involves only a single fluorescence measurement of the sample if the total PEA concentration is known We examined this possibility by making up PEA samples of varying enantiomeric composition and fitting to a calibration plot similar to Figure 2 16 In addition, we repeated the procedure for another chiral amine, norephedrine, in order to determine whether this recognition was restricted to PEA For these measurements, 12 5 mmol dm^{-3} total PEA concentration was chosen as this gives good discrimination in the Stern-Volmer plots and also provides a reasonable fluorescent signal From Figure 2 15a, this is 12 5 mmol dm^{-3} Figure 2 18 shows the linear relationship between fluorescence intensity and enantiomeric composition at a constant total PEA composition of 12 5 mmol dm^{-3} and from this plot, the enantiomeric composition of some unknowns have been calculated (Table 2-4) The results were obtained to within ca 4% error of the known composition The same method was carried out using norephedrine as the substrate at a fixed total concentration of 12 5 mmol dm^{-3} (Figure 2 19) and varying the ratio of the L- and D- enantiomers Again, good linearity is evident In Table 2-5 results obtained for the determination of several unknown mixtures of these enantiomers are displayed and in this case, the relative error is less than 3% However, we are confident that these results can be further improved by more detailed optimisation of the analytical conditions and experimental design, and by improved technique

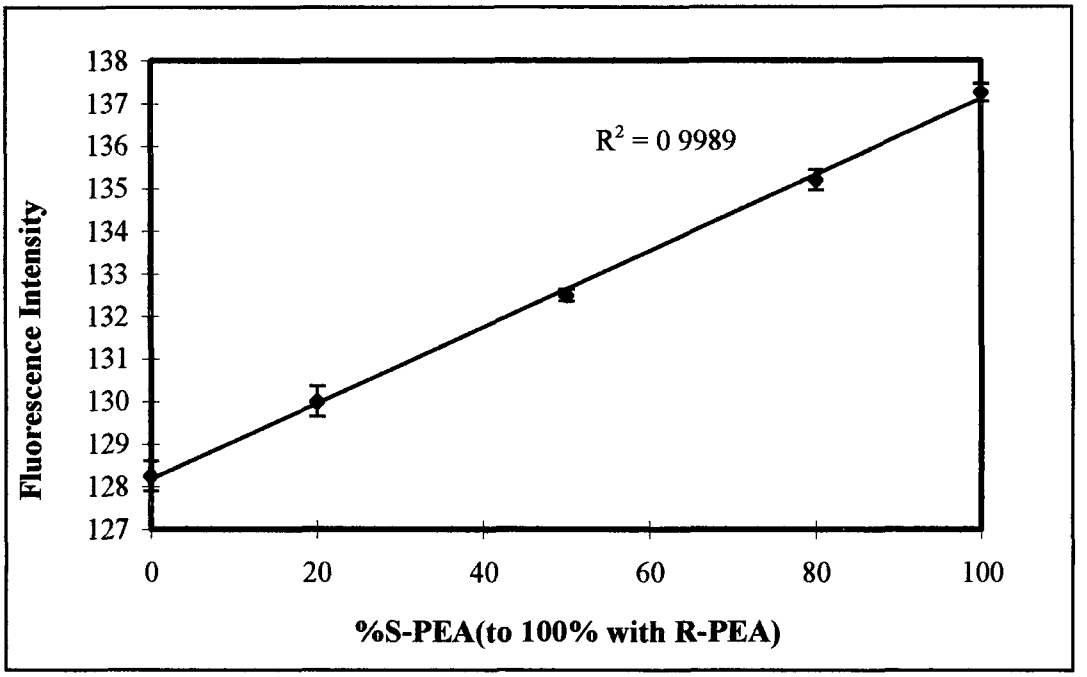

Figure 2.18: *Calibration plot of fluorescence Vs enantiomeric composition of 1-phenylethylamine at a concentration of 12 5 mmol dm^{-3} Standard deviations shown as error bars*

% S-PEA	Mean Φ	St deviation	% Estimated	% Error
10	129 1	0 28	10 32	-3 25
40	131 6	0 07	38 38	4 04
60	133 3	0 14	58 58	2 35
90	136 1	0 353	89 45	0 61

Table 2-4: *Determination of % phenylethylamine in simulated unknown samples*

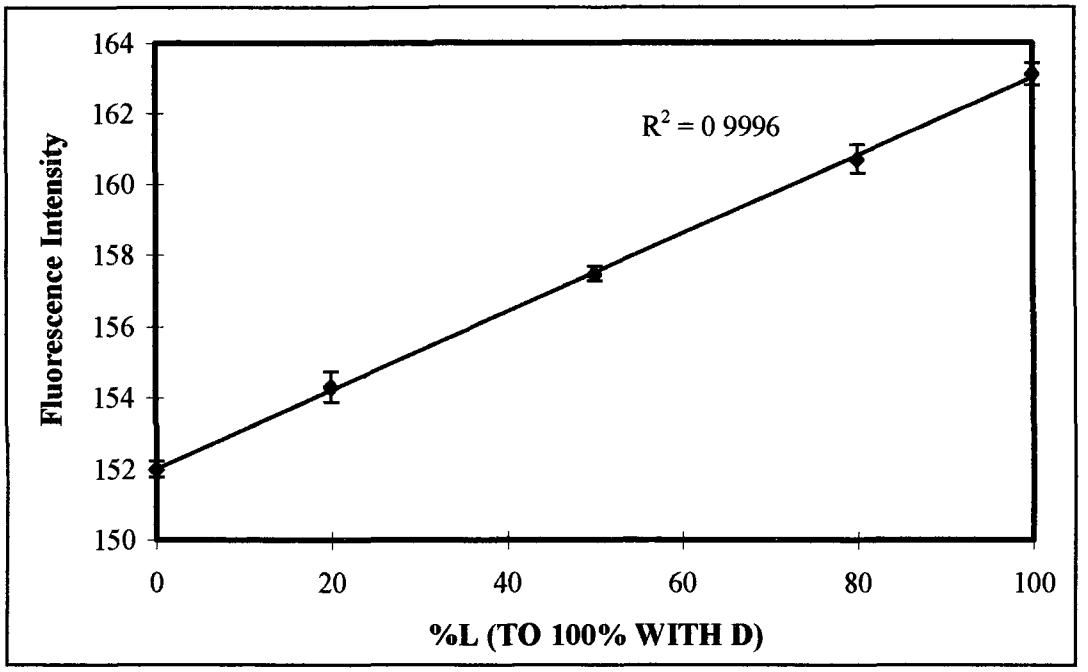

Figure 2.19: *Calibration plot of fluorescence Vs enantiomeric composition of norephedrine at a concentration of 12 5 mmol dm^{-3} Standard deviations shown as error bars*

% L-Norep	Mean Φ	St deviation	% Estimated	% Error
10	153 1	0 30	9 83	1 73
40	156 4	0 26	39 85	0 36
60	158 5	0 12	59 26	1 22
90	162 17	0 21	92 33	-2 58

Table 2-5: *Determination of % norephedrine in simulated unknown samples*

We do not, at present, have any definitive explanation for the enantiomeric selectivity displayed by **2 (xi)** However, the two target molecules (Figure 2 20) are structurally similar in that both contain a group capable of hydrogen bonding (primary amine in PEA, hydroxyl in norephedrine) as part of a chiral centre attached directly to an aryl group This arrangement could facilitate simultaneous π-π interactions between the dinaphthyl groups on **2 (xi)** and the PEA aryl group, and hydrogen bonding between the prolinol hydroxyl group on **2 (xi)** and the PEA amine (see Figure 2 21) However, the presence of this arrangement of structural features on its own does not explain the enantiomeric selectivity displayed by **2 (xi)**, as the S-di-2-naphthylprolinol (Figure 2 20 (**2 xviii**)) does not exhibit this behaviour when unattached to the calixarene macrocycle (see Figure 2 15(d))

3-d energy minimised structures suggest that in PEA, the methyl group is more accommodated within the region of the S-di-naphthylprolinol in the case of the (R)-enantiomer, whereas with the (S)-enantiomer, it is more exposed This feature, coupled with the rather crowded arrangement of the four pendent S-di-naphthylprolinol groups, could be the source of the enantiomeric selectivity displayed by **2 (xi)** It should also be appreciated that the 3-d region around the lower rim of **2 (xi)** is chiral not only because of the asymmetric carbon of the prolinol moiety, but also because of the possibility of chiral twisting of the naphthyl groups about the bridging carbon Furthermore, the amine group of the PEA could be involved in hydrogen bonding with the carbonyl oxygen adjacent to the prolinol, as well as the hydroxyl group on the dinaphthyl bridging carbon, in contrast to the situation with the free S-di-naphthylprolinol (Figure 2 20 **(2 xviii)**) Moreover, while **2 (xii)** and **2 (xiii)** both possess a chiral centre immediately adjacent to an aryl group, the structures are much more open as discussed above, minimising any chiral steric effects arising from clustering of the chiral substituents around the calixarene lower rim which might enhance enantiomeric selectivity

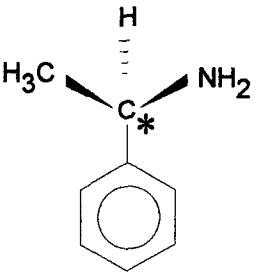

2 (xiv)

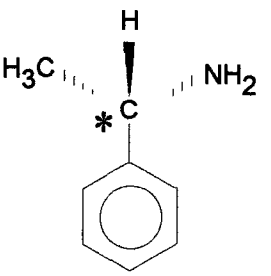

2 (xv)

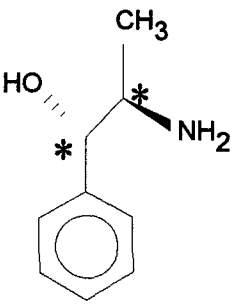

2 (xvi)

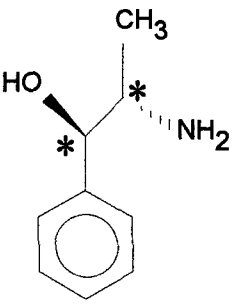

2 (xvii)

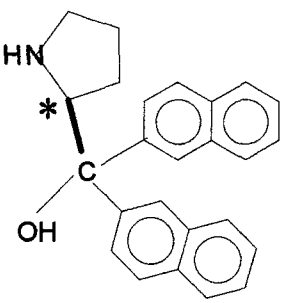

2 (xviii)

Figure 2.20: *Structures of the both enantiomers of target molecules and the chiral fluorescent groups* ***(2 xiv)*** *and* ***(2 xv)*** *are (R)- and (S)-phenylethylamine respectively* ***(2 xvi)*** *and* ***(2 xvii)*** *represent (D)- and (L)-norephedrine repectively* ***(2 xviii)*** *is the free S-di-naphthylprolinol group*

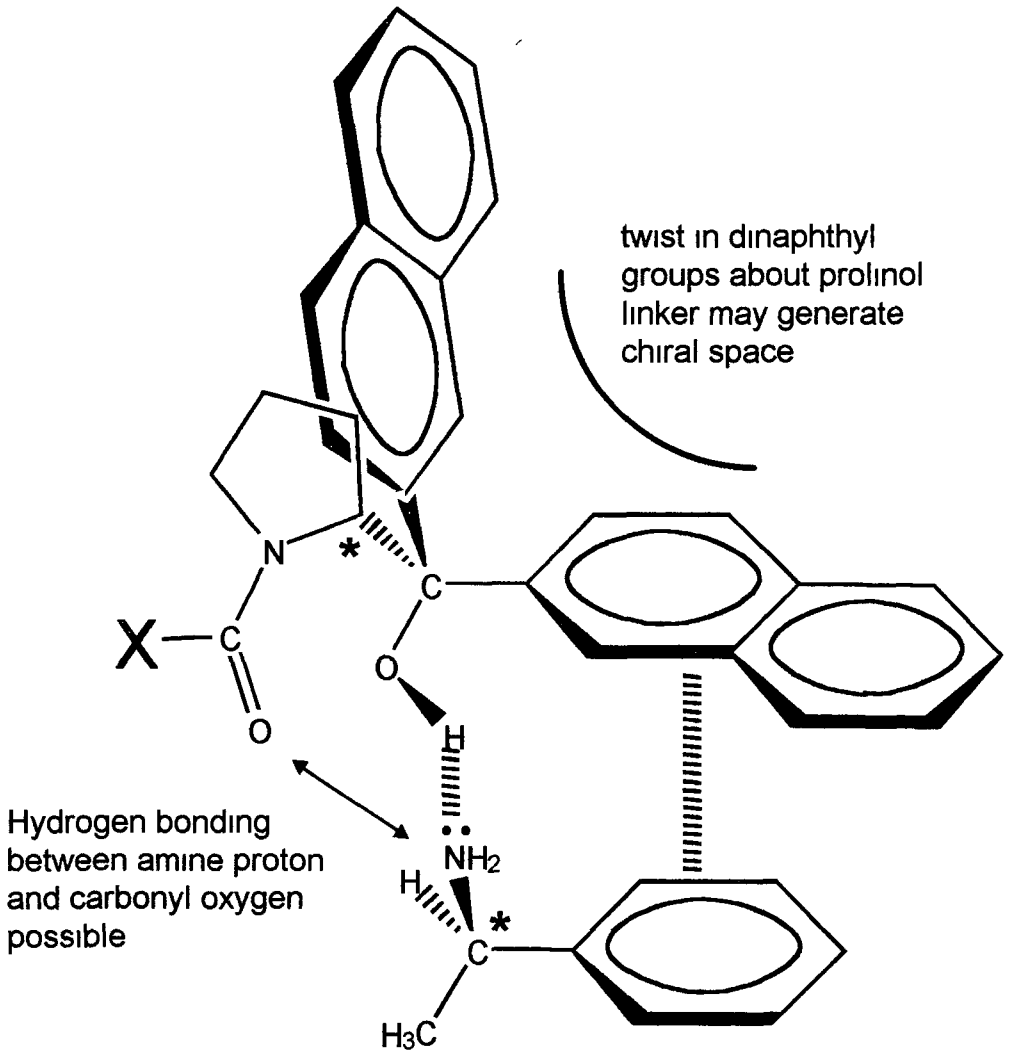

Figure 2.21: *A possible explanation for the origin of the enantiomeric selectivity of 2 (xi) may lie in hydrogen bonding between the PEA amine group and the hydroxyl group of one of the S-di-2-naphthylprolinol groups of 2 (xi) which would be favoured by parallel alignment of the aryl groups of the PEA molecule and the dinaphthyl fluorophore Simultaneous hydrogen bonding from the amine to the nearby carbonyl oxygen is also possible*

UV-VIS spectra show that while the addition of PEA to **2 (xii)** and **2 (xiii)** produces a simple additive effect (Figure 2 22 and Figure 2 23 respectively), this is not the case with **2 (xi)** (Figure 2 24) This supports the view that a different mechanism is involved with **2 (xi)**, and that this probably involves ground state complexation rather than an excited state interaction

Norephedrine (Figure 2 20 (**2 xvi**) and (**2 xvii**)) also possesses the combination of aryl group adjacent to a chiral carbon which is attached to a hydrogen bonding group (hydroxyl), and so the same arguments can be applied in its case While this is a plausible explanation for the observed enantiomeric quenching selectivity exhibited by PEA and norephedrine with **2 (xi)**, an alternative mechanism could involve photoelectron transfer between the amine groups of the target molecules and the dinaphthyl moiety [17]

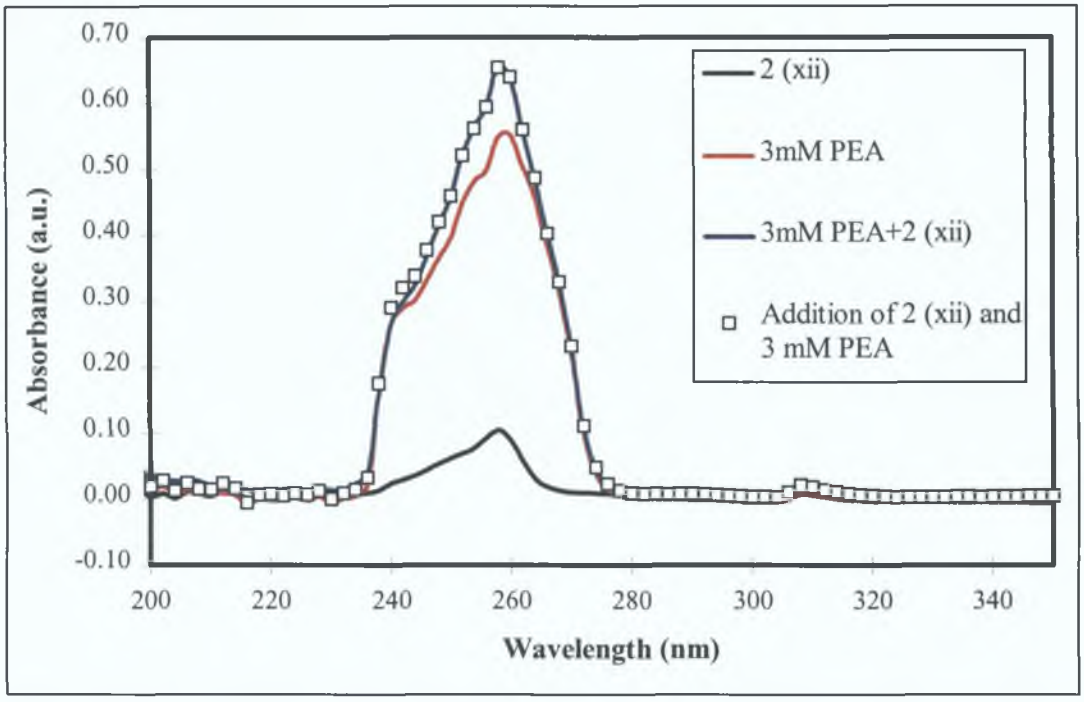

Figure 2.22: *UV-Vis spectra of the anthryl substituted tetramer* ***2 (xii)*** *(0.2 μmol dm^{-3}) in the presence and absence of 3 mmol dm^{-3} PEA, demonstrating the additive effect.*

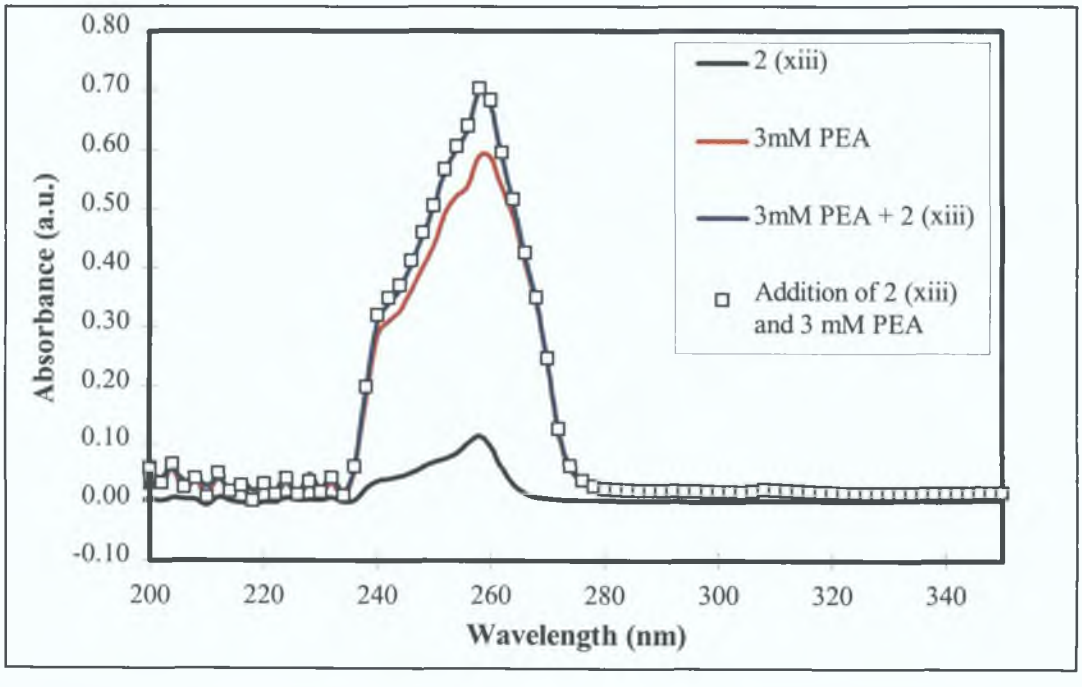

Figure 2.23: *UV-Vis spectra of the anthryl-substituted hexamer* ***2(xiii)*** *(0.2 μmol dm^{-3}) in the presence and absence of 3 mmol dm^{-3} PEA which also demonstrates the additive effect.*

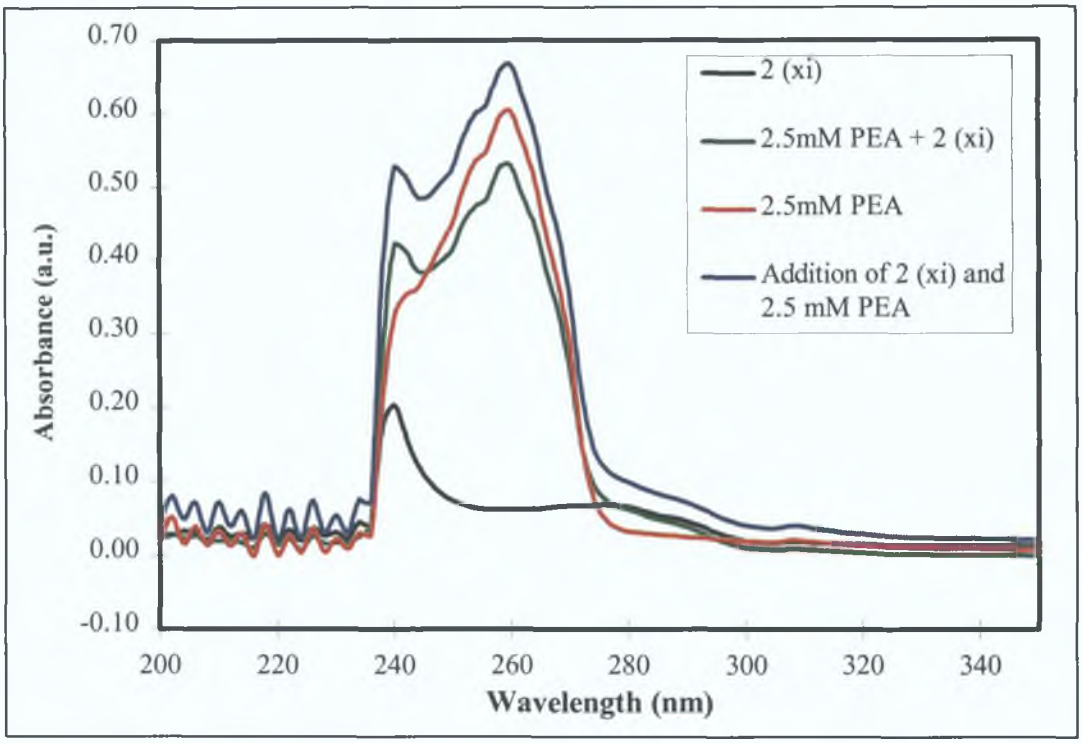

Figure 2.24: *UV-Vis spectra of the dinaphthyl prolinol tetramer* ***2 (xi)*** *(1 μmol dm^{-3}) in the absence and presence of 2.5 mmol dm^{-3} PEA.*

2.4 Conclusions

The Stern-Volmer plots obtained demonstrate that the fluorescent tetra-S-di-2-naphthylprolinol calix[4]arene **2 (xi)** is the most enantiomerically selective The (R)-PEA was seen to have greater efficiency as a quencher, proving that the calixarene was more sensitive to the presence of (R)- than the (S)-PEA Enantiomeric selectivity was also observed for (L) and (D) norephedrine which has a similar structural conformation to PEA It is possible to determine the enantiomeric composition of samples of (R)- and (S)-PEA and (L)- and (D)-norephedrine to within a few %, if the total concentration of both enantiomers is known While the mechanism underlying the chiral recognition displayed by **2 (xi)** is not fully understood at present, it would appear to arise from a combination of hydrogen bonding recognition sites located within a 3-d chirally restricted space defined by tight clustering of the four S-di-2-naphthylprolinol groups around the calixarene lower rim

2.5 Future work

Further research into host-guest properties of the dinaphthyl calix[4]arene chiral receptor **2 (xi)** and its analytical applications are continuing The preliminary data show that the compound may be used to differentiate enantiomers of a number of chiral amines Hence sensor applications would be restricted to those in which relatively pure samples are to be evaluated (e g in pharmaceutical formulations) However, it is possible that the receptor may prove to be a useful component in capillary electrophoresis or chiral HPLC separations by the attachment of silyl groups to the upper rim of the calixarene

With respect to compounds **2 (xii)** and **2 (xiii)**, the situation is more complicated The PEA does unfortunately absorb at the main excitation waveband and we have looked at the data with and without correction However, as the correction represents a constant weighting factor for both enantiomers, it does not affect the relative slopes of the Stern-Volmer plots (i e there is no recognition with or without correction) It would be important to repeat the study by focusing on the fingerprint region of the anthracene labels in order to provide additional information

2.6 References

1 U Hacksell and S Ahlenius, *Trends Biotechnol*, 1993, **11**, 73

2 D T Witte, K Ensing, J -P Franke and R A De Zeeuw, *Pharmacy World Sci*, 1993, **15**, 10

3 A K Scott, *Drug Safety*, 1993, **8** 149

4 L Velluz, M Legrand and M Grosjean, *Optical Circular Dichroism Principles, Measurements and Applications*, Verlag Chemie, Weinheim, 1965

5 G Consiglio, P Pino, L I Flowers and C U Pittman, *J Chem Soc, Chem Commun*, 1983, 612

6 V Schurig and M Jung, *Recent Advances in Chiral Separations*, Plenum Press, New York, 1990

7 S G Allenmark, *Chromatographic Enantioseparation Methods and Applications*, 2nd edition, Ellis Horwood, Chichester, 1991

8 T L Bereuter, *LC-GC Int*, 1994, **7**, 78

9 L Fabbrizzi and A Poggi, *Chem Soc Reviews*, 1995, 197

10 A W Czarnik (ed) "*Fluorescent Chemosenosrs for Ion and Molecule Recognition*", ACS Symposium Series 538, American Chemical Society, Washington DC, 1993

11 H Kautsky, *Trans Faraday Soc*, 1939, **35**, 216

12 J R Lakowicz, "*Principles of Fluorescent Spectroscopy*"Plenum Press, New York, 1983

13 H Knibbe, D Rehm and A Weller, *Ber Bunsenges*, 1968, **72**, 257

14 M Irie, T Yorozu and K Hayashi, *J Am Chem Soc*, 1978, **100**, 2236

15 N Mataga, T Okada, H Masuhara, N Nakashima, Y Sakata and S Misumi, *J Lumin*, 1976, **12/13**, 159

16 T Yorozu, K Hayashi and M Irie, *J Am Chem Soc*, 1981, **103**, 5480

17 T D James, K R A Samankumara Sandanayake and S Shinkai, *Nature*, 1995, **374**, 345

18 K S Parker, A Townshend and S J Bale, *Anal. Proc*, 1995, **32**, 183

19 K S Parker, A Townshend and S J Bale, *Anal Proc*, 1995, **32**, 329

20 F Arnaud-Neu, E M Collins, M Deasy, G Ferguson, S J Harris, B Kaitner, A J Lough, M A McKervey, E Marques, B L Ruhl, M J Schwing-Weill and E M Seward, *J Am Chem Soc*, 1989, **111**, 8681

21 C D Gutsche "*Calixarenes*", Monographs in Supramolecular Chemistry, Vol 1, R S C Cambridge, 1989

3. Determination of Gaseous Ammonia using a Nitrophenylazophenol Calix[4]arene.

3.1 Introduction

This chapter deals with preliminary research carried out on the development of an optical sensor for ammonia in the gaseous state using a chromogenic calixarene An introduction is given on chromogenic ionophores This is followed by a section outlining the experimental procedure used in this work Finally the results obtained on the use of this calixarene are presented

3.1.1 Chromoionophores

3 1 1 1 Chromogenic Crown Ethers

In 1977 Takagi *et al* synthesised the first coloured crown ether anions [1, 2] Mono (Figure 3 1) and diprotic chromophores were attached to the crown ether in such a way so that the complexation of positively charged metal ions was accompanied by the dissociation of protons of the chromophore The colour effect is primarily due to the spectral differences of the protonated and deprotonated species with very little difference observed between the absorption spectra of different cations Extraction studies of metal ions from an aqueous phase into a basic-chloroform layer containing the chromogenic ligands resulted in an ease of extraction in the order of $K^+ > Rb^+ > Cs^+ > Na^+ >> Li^+$ The photometric determination of 10-800 ppm of K^+ was possible in the presence of other alkali and alkaline earth metal ions

Pacey *et al* examined the effect of varying the chromophore substituents on the picrylaminobenzene[15]crown-5 derivatives e g replacing the nitro group with nitrile or trifluoromethyl [3] By changing these groups it was hoped to increase the spectral separation of the protonated and deprotonated species making the effective molar absorptivity for the deprotonated species greater and improving the reagent sensitivity The addition of trifluoromethyl group was found to improve aqueous

solubility and exhibit potassium selectivity The analytical range which the analysis covered was within the normal 137-207 ppm range for human blood serum

Misumi *et al* incorporated a dinitrophenylazophenol group into a crown ether molecule [4] In this case, the ionisable phenolic proton, was found within the crown ether cavity (Figure 3 2) Upon lithium complexation, a colour change from yellow to purple-red was observed when n = 1

Pyridine was used as the base to facilitate the uptake of the phenolic proton upon complexation with lithium The observed lithium ion-characteristic colour change is dependant on various factors e g , cavity size, acidity of the azophenol group, basicity of added amine and polarity of the solvent

By increasing n to 2 in **3 (iv)**, and attaching this reagent to an optical fibre, a system was developed for the determination of K^+ in the presence of Na^+ [5] This potassium sensor was capable of determining potassium ions in the concentration range 10^{-3}-10^{-1} M However the K^+/Na^+ selectivity of 6 4 was not sufficient for clinical use

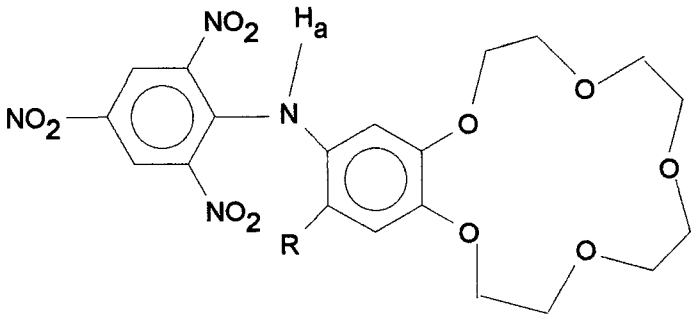

3 (i) R = H

3 (ii) R = NO_2

3 (iii) R = Br

Figure 3.1: *Picrylaminobenzene[15]crown-5 derivatives [1]*

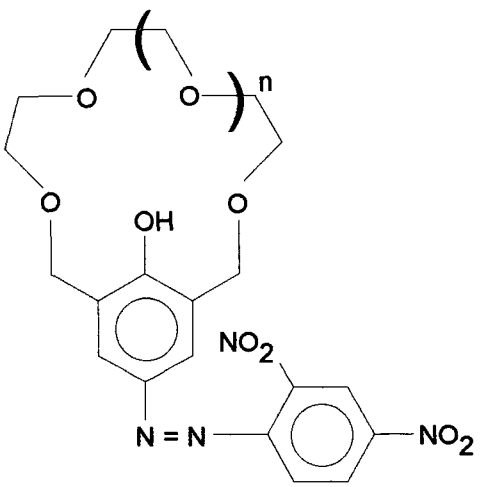

3 (iv)

Figure 3.2: *"Crowned" dinitrophenylazophenol [4]*

Misumi *et al* developed amine selective crown ethers which were also based on the dinitrophenylazophenol chromophore [6] The coloured complexes of these crowns with metal or ammonium ions are differentiated from simple ion-dipole type complexes by an additional binding force, that is, coulombic interaction between the phenolate anion and the guest cation The nitrophenylazophenol crowns investigated were capable of producing colour changes with primary, secondary and tertiary amines The crown shown in Figure 3 3 is an example of one of the compounds investigated which apart from the chromophore also contains the nitrogen atom of a pyridine ring in the crown cavity

Van Gent and coworkers [7] synthesised a 18-crown-5 incorporating a phenol, onto which was attached a dimethylquinolinium iodide group, with the phenolic hydroxyl group in the crown cavity as before In this work the importance of the coulombic interaction between the phenolate anion and , along with electrostatic interaction with the crown oxygens, for cation selectivity was expressed Complexation with Ca^{2+} caused the greatest shift in wavelength in the absence of base and was suggested to be due to Ca^{2+} ion being compatible with the cavity size and therefore in close contact with the phenolate anion

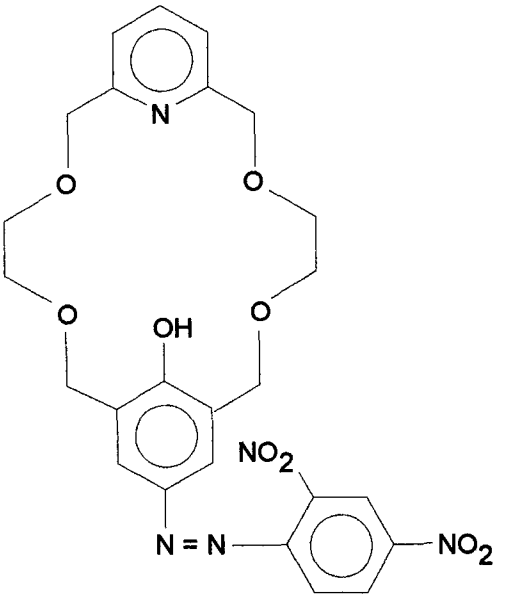

3 (v)

Figure 3.3: *Amine selective "crowned" dinitrophenylazophenol [6]*

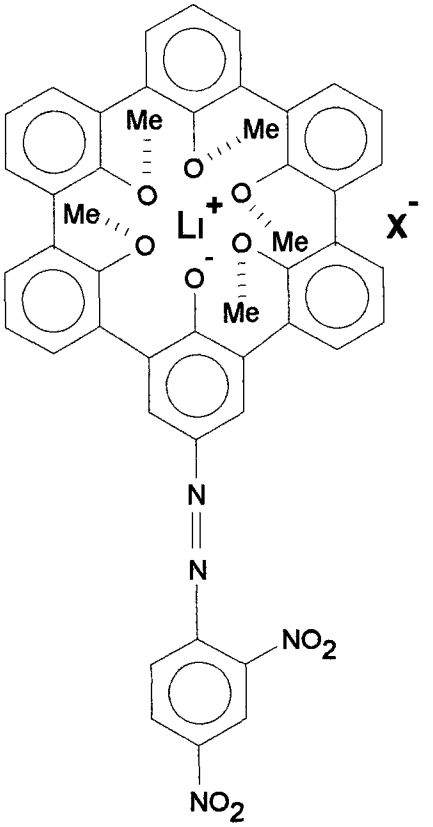

3 (vi)

Figure 3.4: *Complex formed between Na^+ and the dinitrophenylazophenol spherand [8]*

3 1 1 2 Chromogenic Spherands

In 1988, a six-membered spherand incorporating a dinitrophenylazophenol moiety was synthesised by Cram *et al* [8] and was shown to exhibit high Li^+ binding power (Figure 3 4) The pK_a of the phenolic proton varied depending on which cation was complexed with the ligand The lowest pK_a was found for the Li^+ complex (5 9) compared to values of 6 9, 12 7 and 13 for the Na^+, K^+ complexes and the free ligand respectively Therefore by careful choice of base, selectivity could be introduced

Picrylamine chromogenic groups were attached to one of the spherand rings in a Na^+ and K^+ selective cryptaspherand [9] These molecules were targeted because of the selective nature of their analogous non-chromogenic cryptaspherands for either Na^+ or K^+ The inclusion of the cation into the central cavity was sufficient to increase the acidity of the monobasic proton Selectivities of greater than 1000 for both $[K^+]/[Na^+]$ and $[Na^+]/[K^+]$ were obtained with these compounds

Sholl and coworkers reported on a chromogenic cryptand which contained a phenolic hydroxy group in the central cavity, attached to a nitrophenylazophenol group [10] This compound exhibited a Li^+ Na^+ selectivity ratio of ca 10^4 on the basis of spectroscopic response at pH 9 No response to Na^+ was seen even at a 1M concentration Zazulak et al [11] described another lithium selective chromogenic cryptand similar to the one described by Sholl An association constant of 3200 M^{-1} in 10% DEGMEE/TMA(OH) (diethylene glycol monoethyl ether/tetramethyl ammonium hydroxide) for a lithium chromogenic cryptand complex was determined, but a value could not be obtained for Na^+ or K^+ due to lack of chromogenic response

3 1 1 3 Chromogemc Calıxarenes

In 1984, Bohmer *et al* descnbed a lıthıum selectıve colour change for a calıx[4]arene whıch had not been functıonalısed at the hydroxyl group on the phenolıc unıts However, these calıxarenes contaıned one hydroxylnıtrophenylene group adjacent to alkylhydroxyphenylene[12]

The first report on the ıncorporatıon of a nıtrophenylazophenol unıt onto the upper rım of the calıx[4]arene macrocycle was ın 1989 [13] (Fıgure 3 5, **3 (vii)).** The pK_a values of each of the phenolıc protons of a tetrachromogenıc derıvatıve were evaluated by measurıng the pH-dependant spectral change

$$CalixH_4 \rightleftharpoons CalixH_3^- + H^+ \qquad pK_{a1} = 0\,5$$

$$CalixH_3^- \rightleftharpoons CalixH_2^{2-} + H^+ \qquad pK_{a2} = 2\,0$$

$$CalixH_2^{2-} \rightleftharpoons CalixH^{3-} + H^+ \qquad pK_{a3} = 10\,0$$

$$CalixH^{3-} \rightleftharpoons Calix^{4-} + H^+ \qquad pK_{a4} = 13\,0$$

where H^+ is the acıd proton removed from the phenol groups

Thıs pK_a splıt was explaıned by the strong hydrogen-bondıng ınteractıons characterıstıc of calıx[4]arenes The catıon bındıng abılıty of a monochromogenıc calıx[4]arene bearıng one nıtrophenylazophenol group as a coloratıon sıte and the trıester moıety as a metal-bmdıng sıte was later ınvestıgated by the same group [14] (Fıgure 3 5, **3 (viii))** Thıs compound was found to be more selectıve for Li^+ over Na^+ ın the presence of ımıdazole whıch was added to facılıtate the metal ınduced proton dıssocıatıon The Li^+ acts as a countercatıon of the azophenolate anıon and ınteracts wıth the three phenolıc oxygens Nakamoto *et al* descrıbed a sımılar molecule whıch contaıned a 2,4-dınıtrophenylazophenol group rather than a tetrasubstıtuted calıxarene [15] Thıs compound also gave a colour change on complexatıon wıth Li^+ ın the presence of trıethylamıne

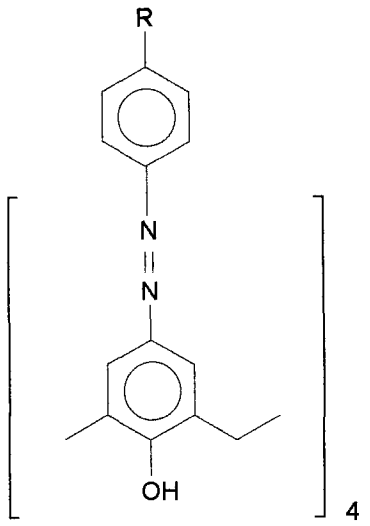

3 (vii)

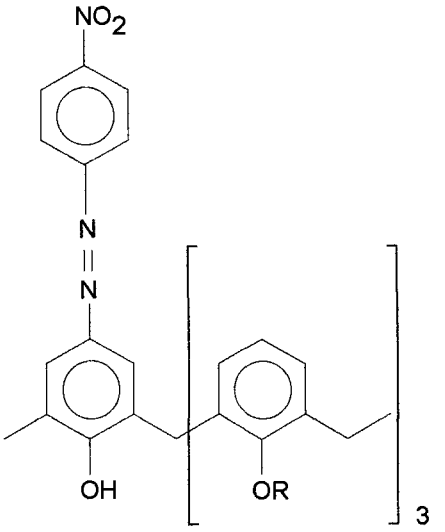

3 (viii)

Figure 3.5: *Tetranitrophenylazophenol Calix[4]arene [13] and Mononitrophenylazophenol calix[4]arene [14]*

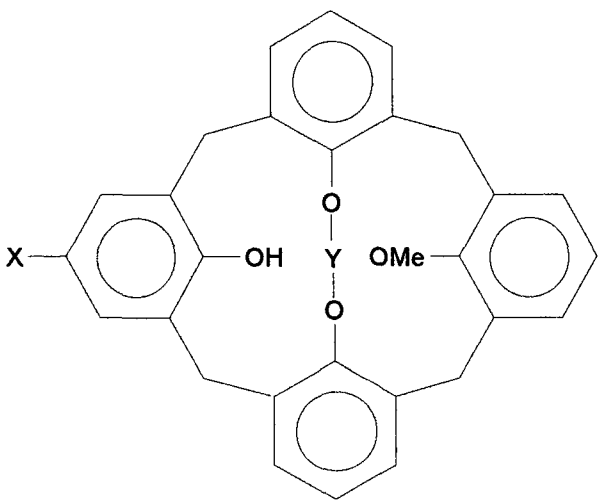

3 (ix)

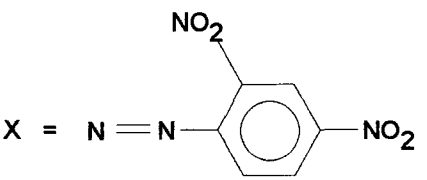

Y = $OCH_2(CH_2OCH_2)_3CH_2O$

Figure 3.6: *Bridged chromogenic Calixarene [16].*

Sutherland and coworkers used a tetrameric bridged structure with the same chromophore [16, 17] (Figure 3 6) which had previously been reported to show selectivity for K^+ over Na^+ in the purely ionophoric form [18] It was found that the pK_a of the azophenol chromophore could be adjusted by changing the substitution pattern of the chromogenic aromatic group with a corresponding change in sensitivity to K^+ at a given pH Improved extraction ability for K^+ from a buffered pH aqueous solution to $CHCl_3$ was demonstrated when the chromogenic group was a dinitrophenylazophenol as opposed to the nitrophenylazophenol The addition of a second electron withdrawing NO_2 group would appear to give further stabilisation to the deprotonated phenolic form of the chromogenic group [16] When the size of the bridge was reduced by changing the number of OCH_2 groups from 5 to 4 the compound became more selective for Na^+ than K^+ [17]

Kubo *et al* used indoaniline as a chromophore in conjunction with calixarenes for cation analysis [19, 20] The calix[4]arene shown in Figure 3 7 exhibited a high selectivity for sodium A bathochromic shift was observed upon complexation with the sodium cation and this was explained in terms of the well tailored electrostatic interactions existing between Na^+ surrounded by OCH_2COO^- groups and the indoaniline carbonyl oxygen segment [19] A 1,3-bis(indoaniline)-derived calix[4]arene shown in Figure 3 8 was found to display Ca^{2+} induced colour change with a wavelength change greater than 100 nm [20] The preferential binding of Ca^{2+} compared to Na^+, which have similar ionic radii, is due to the higher charge density of the Ca^{2+} which should react more strongly with the polar donor groups, especially those of the two quinone oxygens

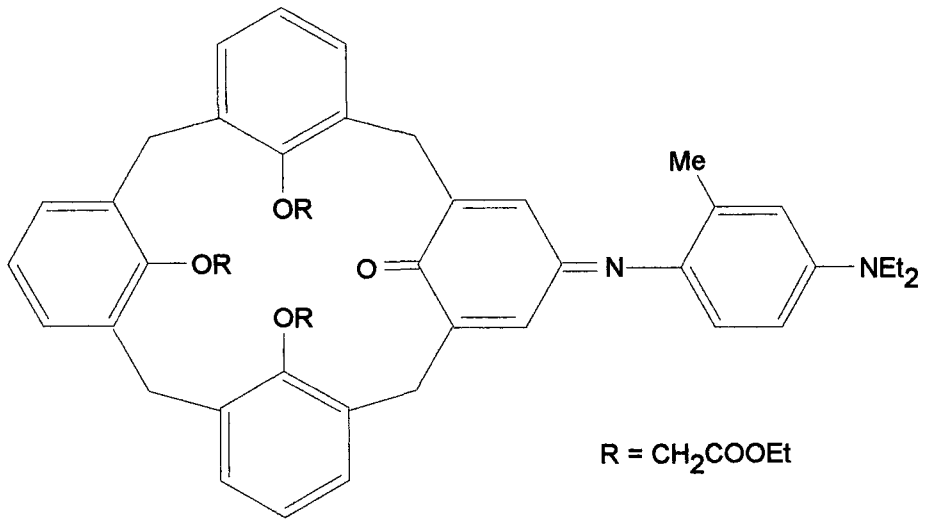

3 (x)

Figure 3.7: *Monosubstituted indoaniline calix[4]arene [19]*

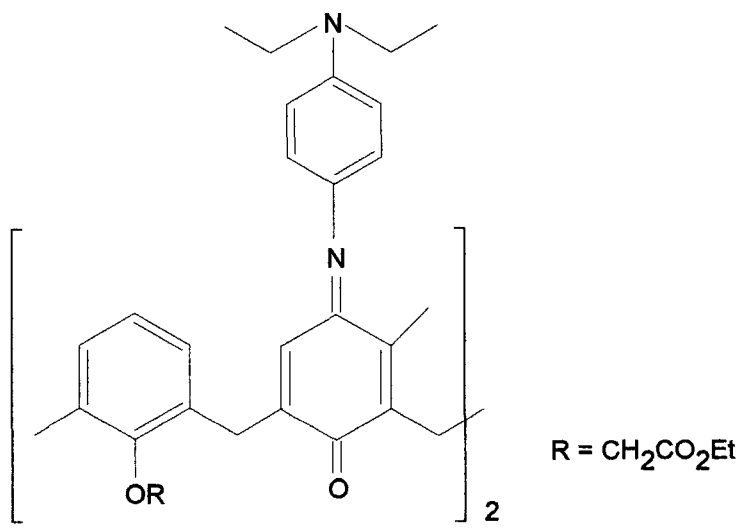

3 (xi)

Figure 3.8: *1,3-Bis(indoaniline) derived Calix[4]arene [20]*

With the increasing interest in the development of optical sensors for the determination of clinically important metal ions, McCarrick et al synthesised a range of chromogenic calixarenes and investigated their selectivity for various cations In a preliminary publication [21], two new chromogenic calix[4]arene tetraesters bearing nitrophenol residues adjacent to the polar cavity (Figure 3 9), display a striking cation-selective shift in absorbance maximum from the ultraviolet to the visible region in the presence of morpholine upon addition of lithium and to a lesser extent, sodium ions The metal salt causes a colour change from colourless to yellow with the colour density being concentration dependant The crucial role played by the base in generating the optical response was confirmed by the total lack of spectral changes on addition of metal salts in the absence of morpholine Deprotonation of the phenol is therefore an integral part of the process and the fact that an optical response is also found with the monophenol ligand **(3 (xiii))** indicates that only one deprotonation is sufficient for the effect to be observed

The calixarenes shown in Figure 3 9 as well as the calixarene (C_{18} groups in the *para* position) in Figure 3 10 were the subject of another publication by McCarrick and coworkers [22] Ligand **3 (xiv)** was also found to be selective for lithium in the presence of morpholine ^1H NMR experiments provided information on complexation Ligand **3 (xii)** appears to be in the cone conformation since the ^1H NMR spectrum reveals the presence of two tert-butyl signals which are replaced by a singlet on addition of NaSCN which is indicative of complexation of the cation within a more symmetrical environment defined by the four equivalent ligating arms, as are changes in the positions of the aromatic protons and bridging methylene protons However, no colour change occurred in these measurements, indicating that complexation without deprotonation was occurring This lack of colour change upon complexation in the absence of base confirms that deprotonation of the nitrophenol is a prerequisite for colour generation Therefore the colour change occurs only if a suitable base is available for uptake of the phenolic proton All three ligands are capable of extracting metal ions from an aqueous phase into an immiscible organic phase (which contained tridodecylamine) Leaching of the complex from the organic to the aqueous phase was greatly reduced with ligand **3 (xiv)** (C_{18} on upper rim)

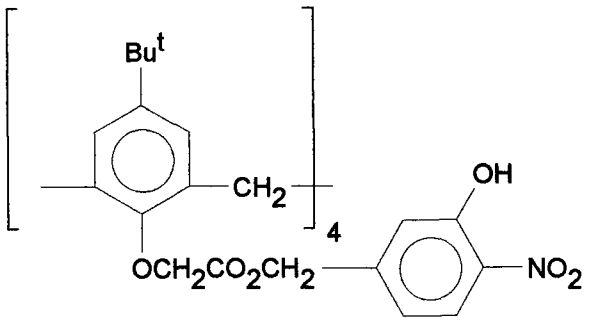

3 (xii)

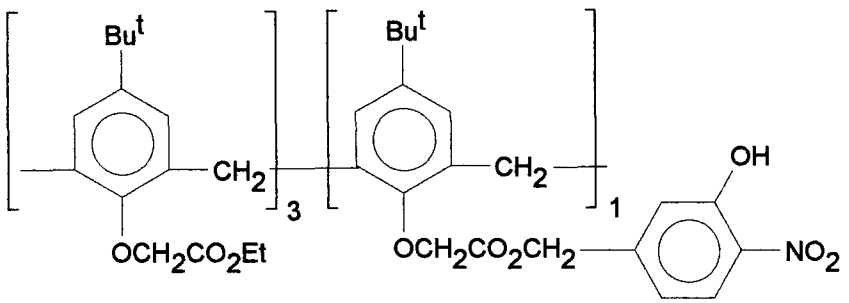

3 (xiii)

Figure 3.9: *Chromogenic tetraesters bearing four or one nitrophenol residues [21, 22]*

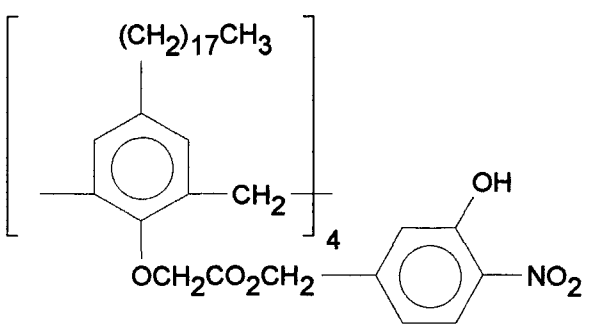

3 (xiv)

Figure 3.10: *Chromogenic calix[4]arene with C_{18} alkyl chain in para position [22]*

In an attempt to create compounds whose complex would have a longer wavelength absorbance maximum than the compounds containing the nitrophenol group, tetrameric calixarenes have been synthesised which incorporate a nitrophenylazophenol group as the chromogenic moiety in the ester portion of the molecule Compounds with a longer absorbance maxima such as these are more useful from an optical sensor point of view owing to cheap availability of blue light emitting diodes, which emit light in the range of the absorbance maxima of the azophenol group Therefore instrumentation development for these sensors is much simpler than for shorter wavelength compounds in which more complex excitation sources are required

Three novel cone conformational calix[4]arene tetraesters bearing nitrophenylazophenol residues (mono-, di- and tetrasubstituted) (Figure 3 11) were synthesised and shown to display a dramatic change in absorption spectrum upon complexation with lithium, and to a lesser extent sodium , in the presence of a base (tridodecylamine) [23] An instantaneous colour change from yellow to red corresponding to a wavelength shift from 380 to 520 nm, occurs upon the addition of lithium perchlorate to a solution containing any of the three ligands with the intensity of the colour being concentration dependant As with the nitrophenyl substituted calixarenes discussed above [22], no colour change was observed in the absence of base The best selectivity for lithium was exhibited by the mono-substituted derivative **3 (xvi).**

McCarrick *et al* developed a rapid and sensitive visual method for the detection of gaseous trimethylamine (TMA) using the tetrasubstituted nitrophenylazophenol calix[4]arene **3 (xv)** [24] TMA is a degradation product of bacteria such as *Pseudomanas* upon trimethylamine oxide in marine fish after death [25] The development of a non-instrumental indicator system which would respond quickly to gaseous amines would obviously be of great benefit to the food industry A solution containing the ligand and $LiClO_4$ in butanol were placed in a test tube in a gas tight vessel

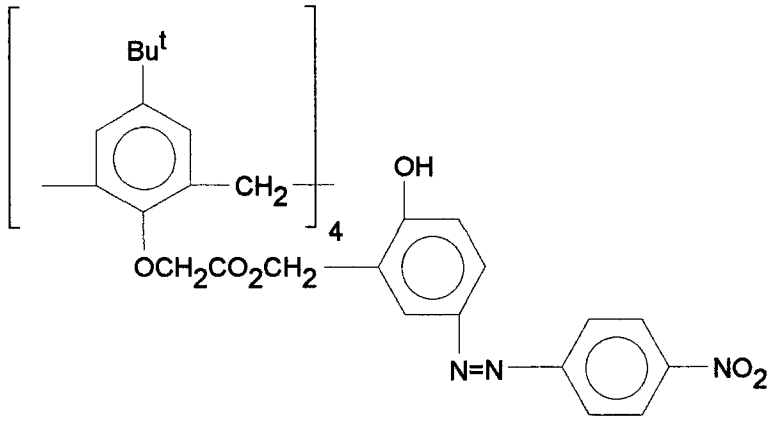

3 (xv)

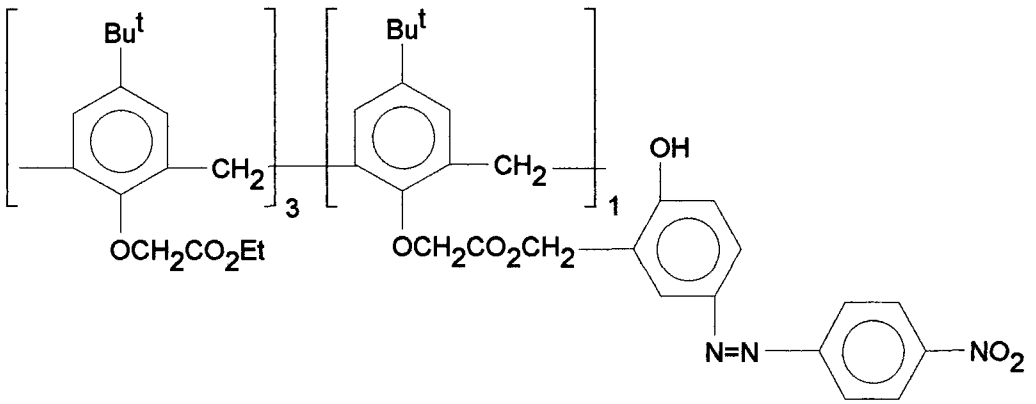

3 (xvi)

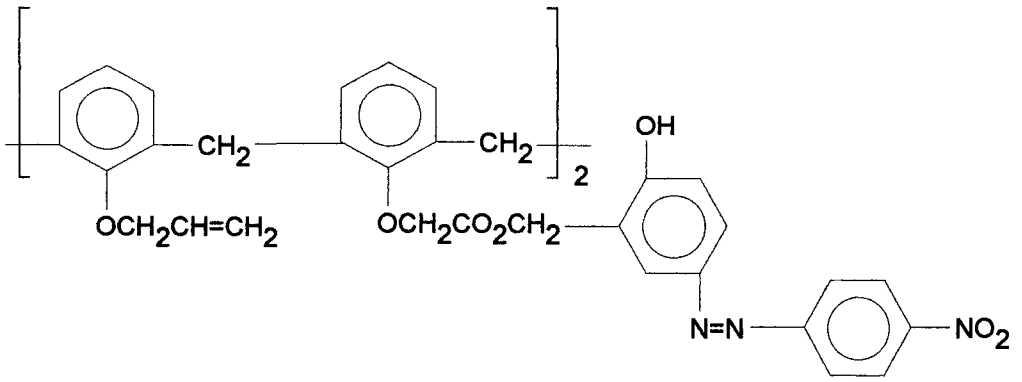

3 (xvii)

Figure 3.11: *Chromogenic cone conformation calix[4]arene tetraesters bearing nitrophenylazophenol residues (mono- di- and tetra-substituted [23]*

Fixed volumes of aqueous TMA were injected into the vessel through a supa seal cap, ensuring that none of the liquid entered the test tube containing the indicator solution The vessel was heated gently to aid the evolution of gaseous TMA The colour of the indicator solution changed from yellow to red, with the colour density and time taken for the colour to develop to be dependant on TMA concentration The colour changes were measured using UV-VIS spectroscopy where an increase in absorbance occurred at 490 nm (from the deprotonated form of the complexed calixarene) and a decrease in absorbance at 376 nm (from the protonated form of the complexed calixarene) in butanol Using filter paper as the support, the complex was immobilised by carefully adding 0 2 mL of tetrahydrofuran (THF) solution containing the ligand and $LiClO_4$ onto the paper Evaporation of the THF yielded a paper with a yellow tinge These test strips were placed inside a gas-tight vessel and varying volumes of TMA added Striking colour changes were observed from yellow to red on the test strips for concentrations above 0 020 ppm up to 30 ppm were no further change in colour intensity was visually discernible At the lower concentrations, the colour change occurred in under 2 minutes As the ultimate application of these test strips were in the food industry, experiments were carried out to determine whether the test strips could react to the presence of gaseous TMA when enclosed in a gas permeable membrane such as Cling Film Visually no colour change was observed below 0 4 ppm TMA on exposure of up to 8 h Full colour changes were observed after 20 min for 2 5 ppm TMA and instantaneous colour changes occurring above 10 ppm TMA The colour density is much greater and reaction times are much shorter for the test strips compared to the liquid phase experiments This arises because in the liquid phase experiments, the experimental design is such that the amine must partition into the butanol phase and diffuse throughout to generate the colour, whereas, with the test strip, only the coated surface of the paper is involved and not bulk diffusion processes, therefore colour generation is much faster

It is the ability of this compound to detect gaseous TMA that prompted us to investigate the effect of ammonia gas on a PVC membrane which incorporated the nitrophenylazophenol calix[4]arene ligand **3 (xv)**

3.1 2 Colour Generation in Chromogenic Ligands

The basic idea behind the colour change in the chromogenic ligands discussed in the previous sections is the same The vital role played by a suitable base in the ionisable chromogenic system has been highlighted by McCarrick and coworkers [22,23] as discussed in section (3 1 1 3) The ligand under investigation in this study belongs to a series of chromogenic materials in which the colour generation process essentially arises from deprotonation of the acidic chromophore (-COH) attached near the ligand (L-) polar cavity and can be used to detect a variety of metal ions (M^+) Usually with these materials, formation of the metal ligand complex by itself does not generate the colour change as a proton receptor is required for the acid-base colour generating reaction

$$L—COH + M^+ \rightleftharpoons LM^+—COH \qquad \textbf{Eq. 3.1}$$

Confirmation of metal complexation in the absence of base was carried out by proton NMR spectroscopy as shown in Figure 3 12 Upon addition of 1 molar equivalent of sodium thiocyanate, a complex sequence of peaks between 0 9 and 1 3 ppm due to the non-equivalence of the tertiary butyl protons in the free ligand are resolved into a singlet at 1 2 ppm, indicating that a more ordered symmetry is forced on the molecule on complexation The characteristic AB quartet of the bridging methylene protons of the calix[4]arene at 3 2 and 4 6 ppm were found to shift to 3 4 and 4 4 ppm respectively, which is again indicative of metal complexation conferring a more ordered structure on the molecule However the positive metal ion in the ligand cavity increases the acidity of the ionisable chromophores (as seen with the chromogenic crown ethers and spherands discussed in the previous sections) and in the presence of a suitable base (B) these are more easily deprotonated, shifting their absorbance maxima to longer wavelengths in the process

$$LM^+—COH + B \overset{K_{a\,(C)}}{\rightleftharpoons} LM^+—CO^- + BH^+ \qquad \textbf{Eq. 3.2}$$

Hence for metal ion detection, the base must be chosen carefully, as if it is too strong, deprotonation of the ligand may occur independently of the presence of metal ions

$$L\text{—}COH + B \underset{}{\overset{K_{a\,(L)}}{\rightleftharpoons}} L\text{—}CO^{-} + BH^{+} \qquad \textbf{Eq. 3.3}$$

The ideal base will therefore react with the complex but not with the free ligand, therefore enabling the metal ion to be detected optically Equations **3.2** and **3.3** evoked the successful investigation of the potential of the ligand-metal complex to produce a colour change upon reaction with gaseous trimethylamine [24] As the complex is a stronger acid than the free ligand [i e $K_{a(C)} > K_{a(L)}$], this was used in the subsequent experiments In other words the ligand-metal-base system previously used to detect the presence of metal ion is being reversed, the complex is used to detect the base

In the same way, we envisaged using the complexed form of the nitrophenylazophenol calix[4]arene to detect gaseous ammonia

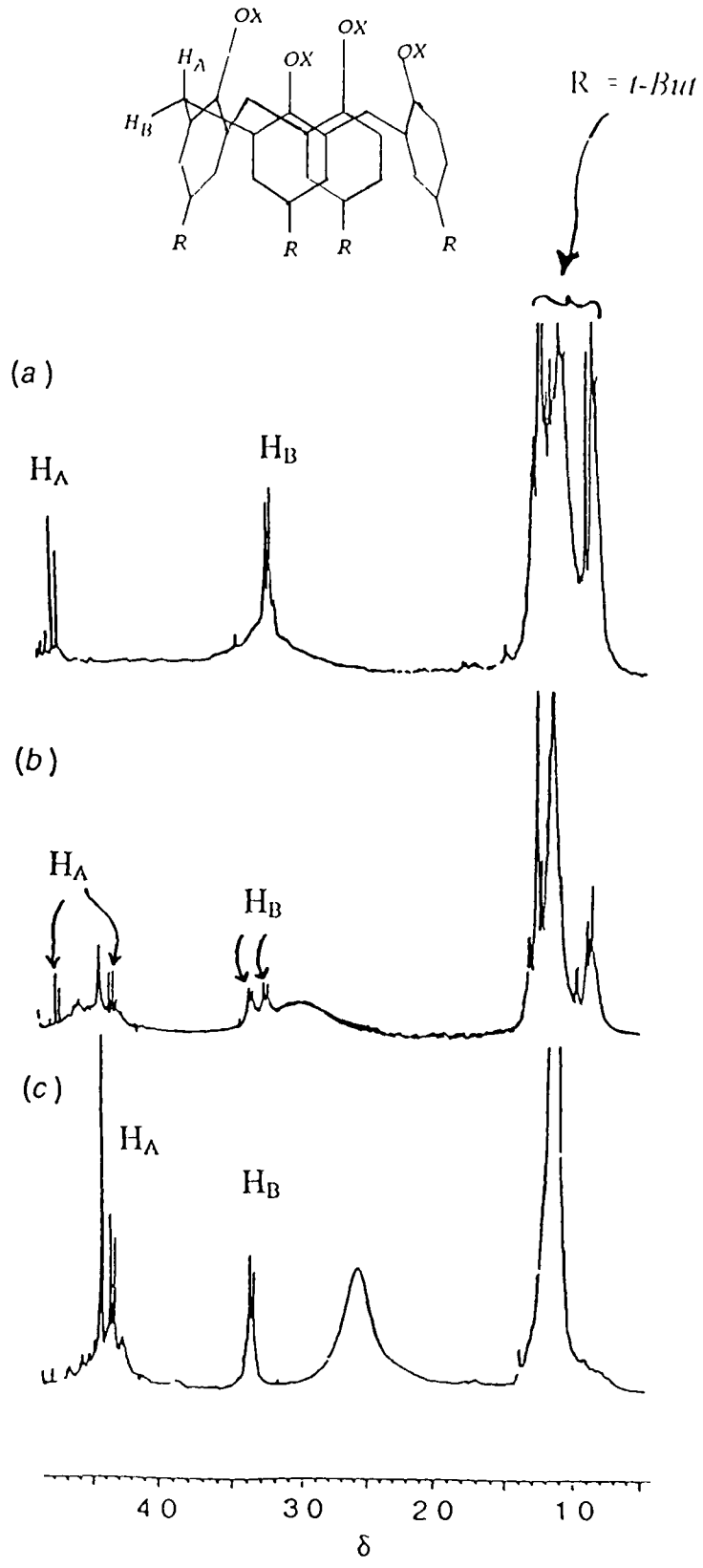

Figure 3.12: *Partial proton NMR spectra for the nitrophenylazophenol calix[4]arene in $CDCl_3$ (a) Before addition of NaSCN (b) After addition of 0 5 molar equivalent of NaSCN in CD_3OH (c) After addition of 1 molar equivalent of NaSCN [26]*

3 1 3 Determination of Gaseous Ammonia

The determination of ammonia gas is important in clinical, environmental and industrial process analyses Ammonia is recognised as one of the primary irritants to humans as it affects skin and mucus membranes of the eye, nose, throat and lungs Concentrations of 25 ppm in air have been recommended as threshold limit value for human exposure [27]

Ammonia plays an important role in atmospheric chemistry It is the most important alkaline gas in the atmosphere, although its average residence time is only 7-14 days due to aerosol formation and neutralisation by the more abundant acidic species [28] These reactions make the measurement of ammonia important in studies of smog and acid rain formation Higher ammonia levels are of analytical interest in indoor environments where industrial operations such as refrigeration or fertiliser manufacture are carried out It has been found that excess emissions of ammonia cause damage to the ecosystem For example, the influence of ammonia in contact with soil leads to acidification and unbalance of nutrients, resulting in destruction or change in natural vegetation [29]

Another major concern is the presence of ammonia in agriculture and animal shelters The ammonia problem in agriculture consists of two parts, on one side there is the in-building ammonia concentration, which has potential physiological effects on animals and health effects on workers On the other side, the emission of ammonia from the animal buildings into the atmosphere contributes much to the air pollution, both chemically and through the generation of offensive agricultural odour

Apart from being present in the atmosphere, it is also present in waters High levels of ammonia in river water are indicative of pollution and can pose hazard to aquatic life Measurement of ammonia is also important to assess the freshness of meat and other food products

The use of optical sensors for ammonia gas determinations have drawn considerable attention owing to their inherent advantages over electrochemical sensors

pH sensitive indicators are highly specific for ammonia determination Exposure to ammonia increases the pH of an indicator based sensor and the extent of the reaction between the ammonia and the indicator dye depends on the concentration of ammonia in the sample Several approaches have been reported for preparing optical ammonia sensors based on pH indicators [30,31,32]

The use of receptor molecules coordinating the gaseous compounds instead of immobilised dyes being deprotonated during the reaction with the gas were found to be a successful alternative in the development of optochemical sensors to determine ammonia e g metalloporphyrins immobilised in nitrocellulose membranes [33]

Simon and coworkers [34,35] have reported on an optical sensor that responds selectively to ammonia gas These sensors consist of an optical indicator and an ionophore contained in a thin plasticised PVC membrane which is cast on a glass or quartz plate so it can be easily mounted into a flow through cell in a spectrophotometer The ionophore is a neutral carrier (nonactin or ETH 157) and the indicator is a H^+ selective neutral chromoionophore that dramatically changes its absorption spectrum in the UV-Vis region on protonation/deprotonation When exposed to the air sample, ammonia diffuses into the membrane A reaction occurs in which the indicator is deprotonated and ammonia is protonated The degree of deprotonation of the indicator at equilibrium is mediated by the complexation of the resulting ammonium ion by the ionophore This complexation induces selective response to gases which can be protonated to form a cation The ratio of the protonated to deprotonated form of the indicator is a function of the ammonia concentration which can be deduced by measuring the absorbance at an appropriate wavelength for either form This optode has a range from 0 002 to 100 ppm ammonia and is unaffected by changes in humidity

3.2 Experimental

3.2.1 Apparatus and materials

3.2.1.1 Materials

The nitrophenylazophenol calix[4]arene **3 (xv)** was synthesised as described previously [23]. The ammonia solution and lithium perchlorate and potassium perchlorate salts were obtained from Riedal-de Haen. Membrane plasticiser, *o*-nitrophenyl octyl ether (*o*-NPOE) and dibutyl sebacate (DBS), ion-exchanger, potassium tetrakis (p-chlorophenyl)borate, (KTp1PB) poly(vinyl chloride) (PVC) and selectophore grade tetrahydrofuran (THF) were obtained from Fluka. Deionised Milli-Q grade water was used throughout.

3.2.1.2 Energy minimised structures

The 3-dimensional energy minimised structure of the molecule is shown in Figure 3.13. This structure was minimised using Hyperchem v. 4.0 which employs molecular mechanics with the force field MM^{+}. The following algorithms were also employed, Steepest Decent, Polak-Ribiere and Newton-Raphson. Light blue = carbon atoms, red = oxygen atoms, dark blue = nitrogen atoms. Hydrogens not shown for clarity.

3.2.1.3 Membrane preparation

The optode membranes were prepared from a PVC cocktail composition as follows: ligand, 10mg; ion-exchanger, 2mg; o-NPOE, 200mg; PVC, 100mg. A reference membrane was also prepared that omitted the ligand from the cocktail. The membrane components were dissolved in 1.5 mL of THF. A portion of 400 μL of this solution was injected onto a rotating dust-free glass slide. The spinning device

used was a Laurell WS-200 series (Lansdale, PA 19446, USA) with a rotating frequency of 600 rpm This allows the preparation of glass-supported membranes having controlled and reproducible thickness (c 10 μm) After a spinning time of 5 seconds the glass slides with the yellow optical sensing membrane was removed and left to dry for 10 minutes in the dark

3 2 1 4 Preparation and coating of optical fibre

The plastic clad silica optical fibre of 600 μm diameter was prepared as follows A 12 cm length of the optical fibre was polished at both ends and the primary (outer) coating was removed with a blade The cladding was then removed using a commercial etcher (Lumer O E Stripper) The remaining glass silica core was then cleaned with acetone and water

The fibre was then coated by dipping into the PVC cocktail containing the same components and amounts as used to prepare the membranes on the slides The only difference being the plasticiser which was dibutyl sebacate The refractive index (R I) of a series of plasticisers (with PVC) were measured using ellipsometry (Table 3-1) and it was found that the refractive index of DBS is the only one of those investigated that had an R I just below the maximum value allowed for these experiments so as to provide total internal reflectance of light (1 46) along the optical fibre Above this value the light would escape from the fibre

Plasticiser	Refractive Index
2-NPOE	1 52
Dioctyl phthalate	1 51
Dioctyl adipate	1 47
Dioctyl sebacate	1 46
Dibutyl sebacate	1 45

Table 3-1: *Refractive index of plasticiser coatings on silicon using ellipsometry*

Experiments were also carried out where lithium perchlorate or potassium perchlorate were included in the cocktail 5 mL (in total) of THF was added to the cocktail The dip coating process involves an automated system which allows the withdrawal speed to be varied In our case a the speed was set to 1mm/s 5 cm of unclad fibre was coated

3 2 1 5 Equipment

UV-Vis absorbance spectra were obtained using a Hewlett Packard 845 2A photodiode array specrophotometer The cuvettes used to carry out the measurements had a platform of glass in the bottom so that the coated glass slides could be held securely in place The lid of the cuvette was also cut so that it fitted between both slides (Figure 3 14)

The characterisation setup for the fibre optic measurements is shown in Figure 3 15 The white light source is a tungsten halogen lamp Both the launch optics and collection optics contain two lens, one lens is used to collimate the light and the other is a microscope objective lens to focus the light The mass flow controller allows known concentrations of ammonia gas to be passed over the optical fibre The mask shown here in the setup is placed at the end of the optical fibre where the light is launched The function of the mask is to block the low order modes of light, which is the light that passes straight through the optical fibre and has no significance in the evanescent wave motion Higher order light enters the fibre optic at greater angles and dominates evanescent wave measurements By filtering out the lower order light, the fraction of light that is absorbed is increased which causes an increase in sensitivity The Ocean Optics Spectrophotometer is used to collect the light that is coming from the fibre and disperses it across a linear range of 1024 CCD detectors

3 2 2 Experimental procedure

Two coated glass plates were mounted in the cuvette The coated slides which did not contain the ligand were used as the blank scan 5 μL of aqueous ammonia of varying concentrations (0 1M to 5M) were injected carefully onto the bottom of the cuvette taking care not to touch the membranes The spectra were recorded after 30 s To investigate the time response of the membranes, three concentrations were chosen and the spectra were recorded at various time intervals

The optical fibre measurements were carried out using the coated fibre in nitrogen as a reference Various concentrations of ammonia were passed through the cell and an interval of one hour was allowed before the absorbance spectra were recorded An experiment was also carried out to investigate the time response of the coated fibre to the ammonia gas The ocean optics spectrometer was set to monitor one wavelength (the wavelength of maximum absorbance)

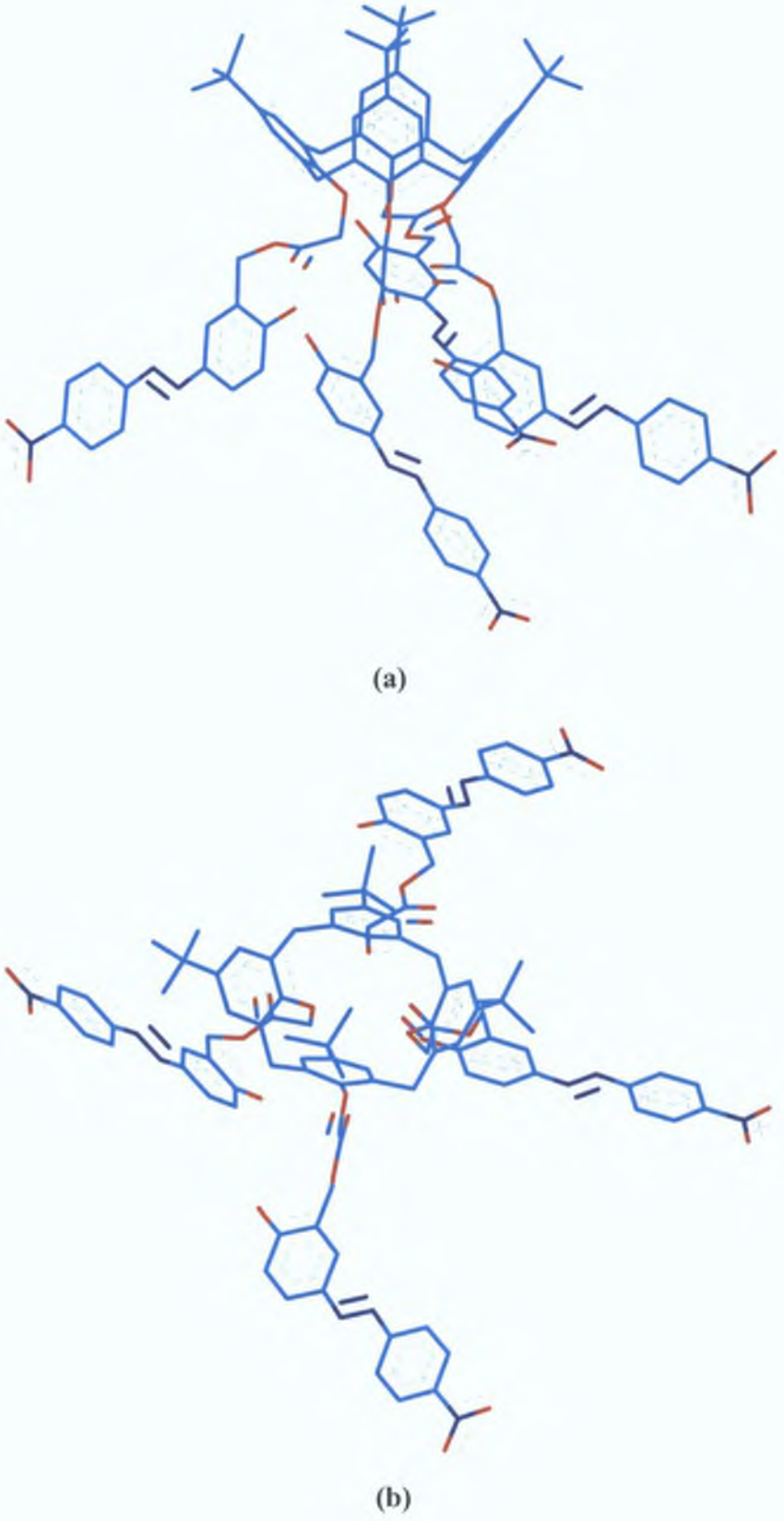

Figure 3.13: *Molecular model of the nitrophenylazophenol calix[4]arene* ***3 (xv)*** *using Hyperchem (v.4.0) showing side (a) and top view (b) of molecule. Refer to experimental section for further details (3.2.1.2).*

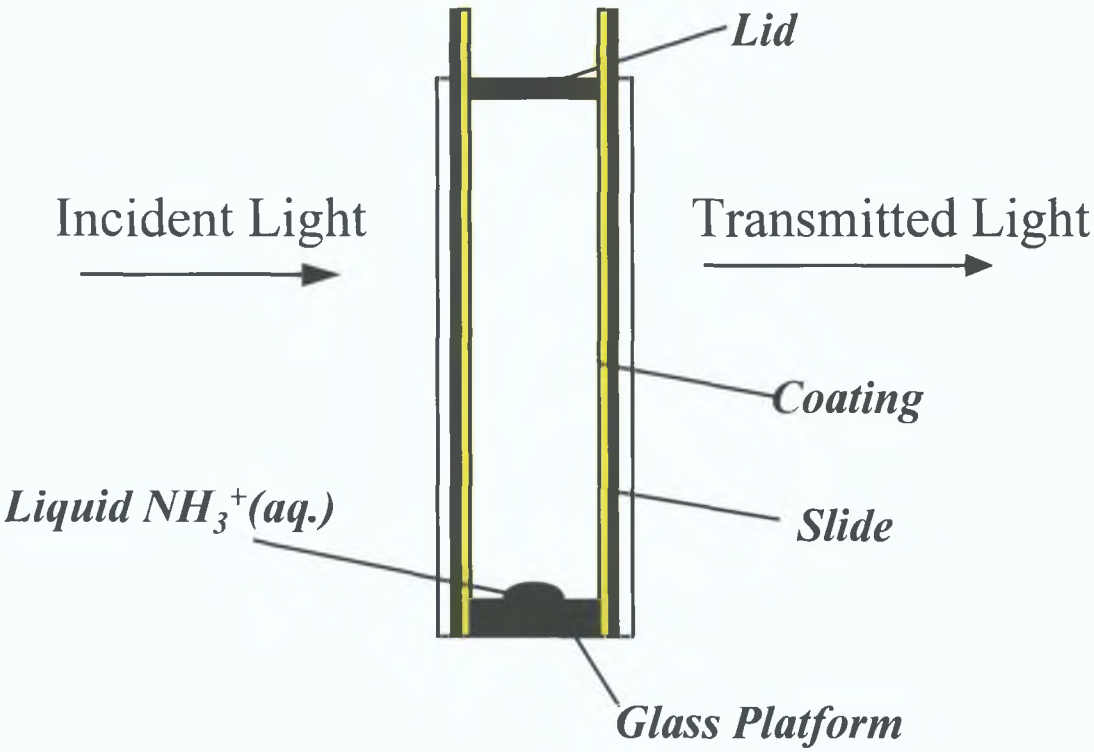

Figure 3.14: 1 cm *cuvette used in the UV-VIS measurements.*

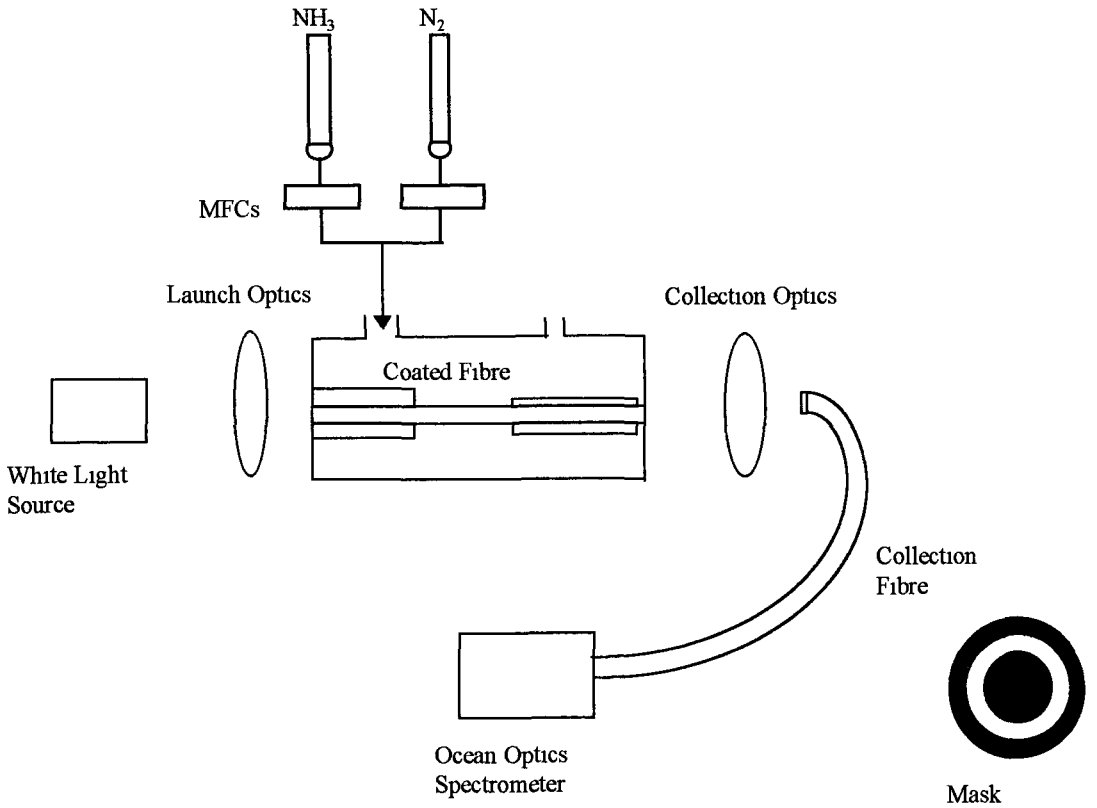

Figure 3.15: *Schematic diagram of the instrumental set-up used for the optical fibre measurements*

3.3 Results and Discussion

3 3 1 Cuvette-based experiments

The 3-d representations of the molecule shown in Figure 3 13 clearly show the four pendant nitrophenylazophenol groups pointing downwards from the calix[4]arene backbone and emphasising the polar ester cavity The distances between the phenolic oxygen atoms on opposing rings is 5 29 and 3 57 angstroms The angles were also measured between the aryl groups The angle was 4 5° for the parallel aryl groups and 86 5° between the angular aryl groups These measurements emphasise the 'two in two out' conformation which is characteristic of the cone conformation

An immediate visible colour change from yellow to red could be identified once the membranes were exposed to the ammonia gas Once the slides were removed from the ammonia atmosphere in the cuvette the original yellow colour returned immediately proving the reversibility of the reaction The difference spectra obtained on exposure of the coated slides to the various concentrations of ammonia are shown in Figure 3 16 A decrease in absorption occurs at 394 nm and this is accompanied by an increase in absorbance at 500 nm with an isosbestic point at 418 nm Eventhough the difference in absorbance is quite small (0 01 for 0 1 M to 0 30 for 5 M), this experiment demonstrates the potential application of this chromogenic ligand in the determination of ammonia in the gas phase Obviously the concentration of ammonia in the gas phase in the cuvette is much smaller than the aqueous solutions that were added in 5µL quantities implying that the ligand may be employed for the detection of trace quantities of gaseous ammonia

As discussed in the introduction, this ligand belongs to series of chromogenic materials in which the colour generation is caused by the deprotonation of the acidic chromophore (-COH) attached near the ligand polar cavity In previous experiments involving this ligand (L) [23], the presence of a suitable base causes deprotonation

In our experiment, the basic nature of the NH_3^+ results in the deprotonation of the OH of the chromophore and hence the colour change occurs (Figure 3 18)

$$L — COH + NH_3^+ \rightleftharpoons L — CO^- + NH_4^+ \qquad \textbf{Eq. 3.4}$$

We have no evidence as to whether there is only deprotonation occurring in one of the chromogenic groups or if the other groups are also involved Figure 3 18(a) illustrates the deprotonation of one group with the protonated cation then entering the cavity of the calixarene Alternatively, the ammonium cation may also form a loose association with the deprotonated group as shown in Figure 3 18(b) An ^1H NMR titration experiment would distinguish between these two mechanisms of interaction

The response *vs* time curves at an absorbance maximum of 500 nm are presented in Figure 3 17 These results demonstrate that it takes about 30 seconds before the final steady state absorbance maximum is reached for each of the three concentrations investigated It maintains this absorption maximum for up to 3 min

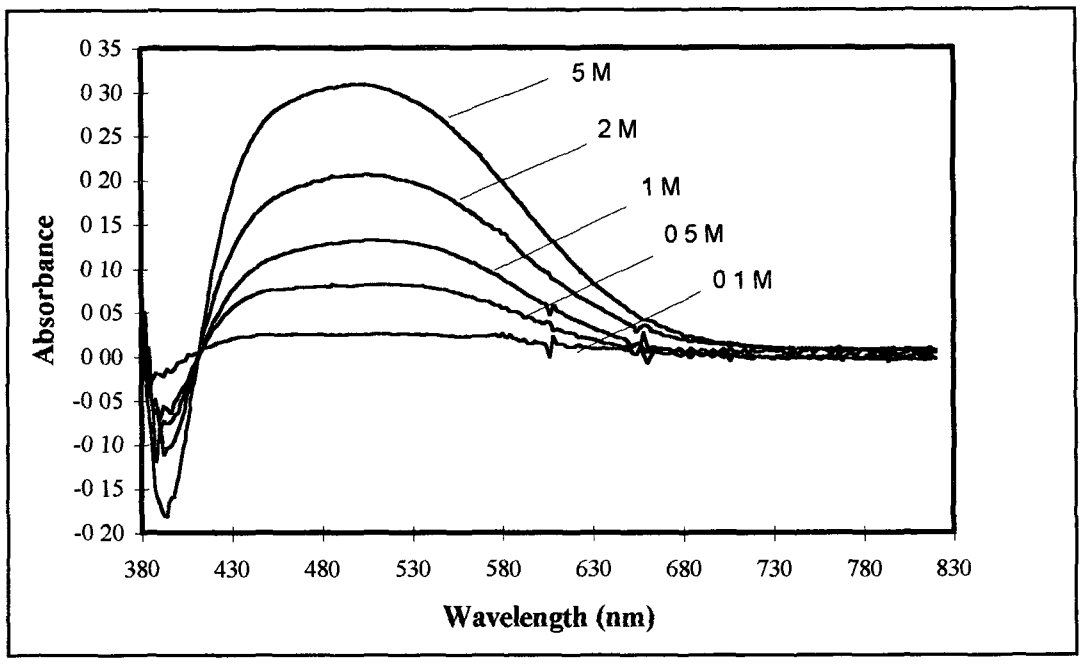

Figure 3.16: *Difference absorption spectra of the plasticised PVC membrane containing the nitrophenylazophenol calix[4]arene upon addition of 5 μL of various concentrations of aqueous ammonia to the bottom of the cuvette*

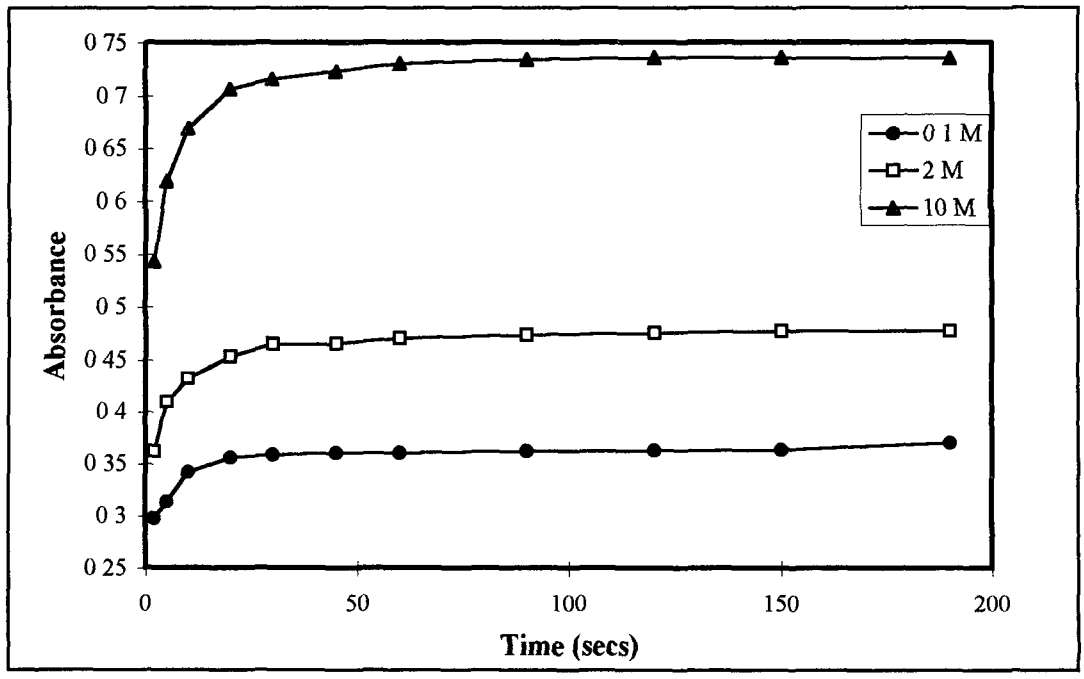

Figure 3.17: *Absorbance Vs Time recorded at a wavelength of 500 nm for the addition of 5 μL of 0 1 M, 2 M and 10 M aqueous ammonia into the bottom of the cuvette.*

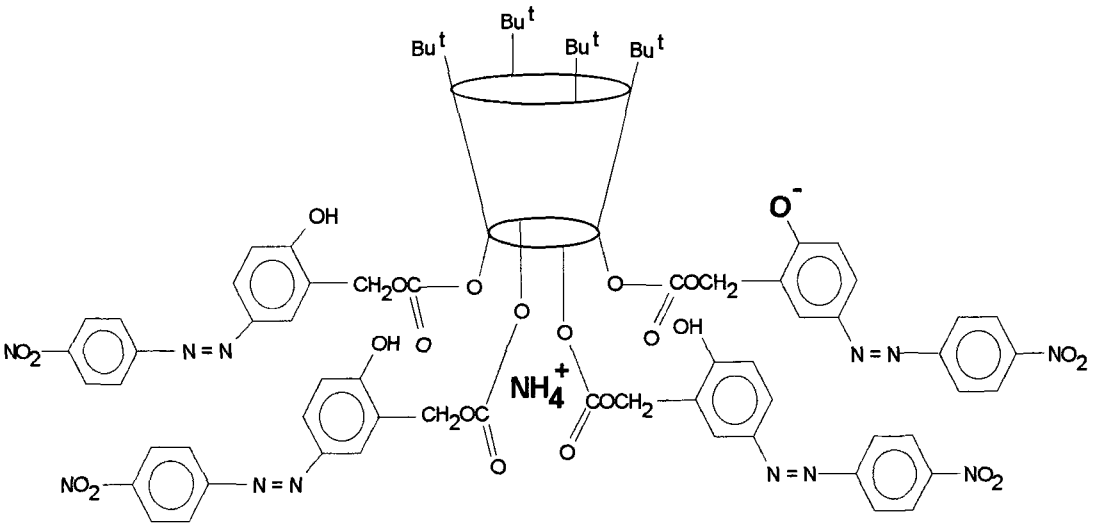

(a)

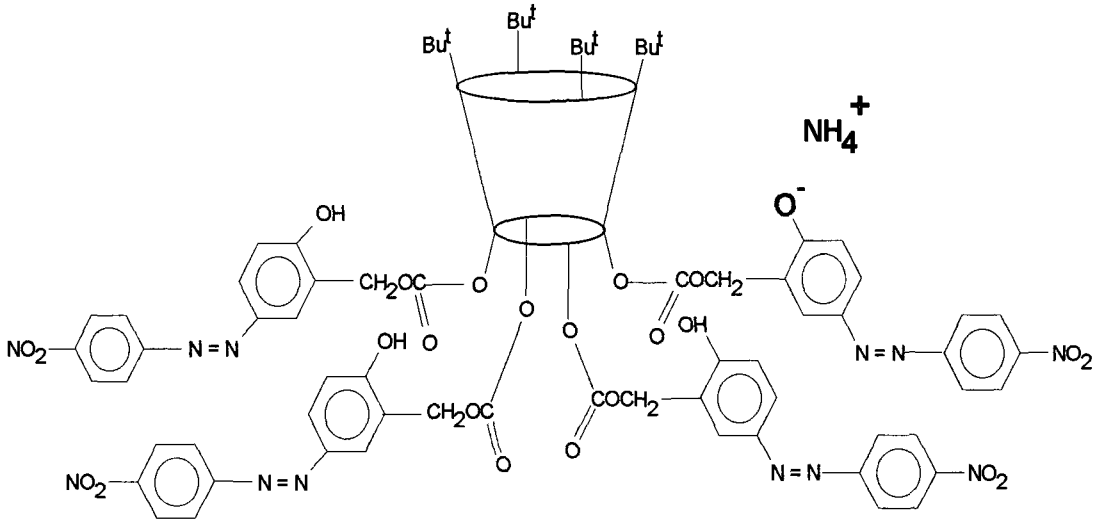

(b)

Figure 3.18: *Representations of the deprotonation of the nitrophenylazophenol calix[4]arene brought about by the basic nature of the ammonia gas (a) The ammonium ion enters the cavity or (b) the ammonium cation forms a loose association with the deprotonated anion*

3.3.2 Fibre-optic experiments

The results obtained using the cuvette experiments evoked interest in the development of a more sensitive method for the detection of gaseous ammonia. The use of an optical fibre system in conjunction with a mass flow controller was investigated and some preliminary results are presented here demonstrating the potential of this compound. The nitrophenylazophenol group is a suitable chromophore for fibre optic measurements due to its long wavelength absorbance maximum in the deprotonated form.

We envisaged using the lithium-complex to increase the sensitivity for the detection of gaseous ammonia in the same way as it was used to detect gaseous trimethylamine [24] as discussed in section 3.1.2. As the ligand has been shown to be more selective for Li^+ over sodium with a $K_{Li/Na}$ of 31.5 [36], $LiClO_4$ was included in the PVC cocktail. The effect of potassium in the PVC coating was also investigated.

Four different coatings for the optical fibre were investigated in the following experiments:
Coating **1** contained ligand, ion-exchanger, DBS and PVC
Coating **2** contained same as **1** plus a 1 mole equivalent of $LiClO_4$ to the ligand.
Coating **3** contained same as **1** plus a 0.5 mole equivalent of $LiClO_4$ to the ligand.
Coating **4** contained same as **1** plus a 0.5 mole quivalent of $KClO_4$ to the ligand.
Coatings were prepared as described in section 3.2.1.3.

3.3.2.1 Spectral characteristic of optical fibre with coating 1.

Figure 3.19 shows the absorbance spectra of the PVC coated optical fibre incorporating the nitrophenylazophenol calix[4]arene for different ammonia concentrations in the wavelength range of 400 to 750 nm. All spectra were recorded relative to a scan of the coated fibre in nitrogen. The same trend can be seen as was found with the cuvette experiments, with the added advantage that the concentration

of gaseous ammonia flowing through the system is known The characteristic shift of absorbance maximum to 500 nm occurs on the addition of varying concentrations of ammonia gas in the range of 5 ppm to 500 ppm which represents the deprotonated form of the azophenol group This λ_{max} increases with increasing concentration of ammonia but the absorbance values are quite small, (the addition of 500 ppm leads to an absorbance of 0 12 a u) The noisy signal at the lower wavelengths is due to two main factors At lower wavelengths the sensitivity of the system is low Coupled with this is the small signal obtained at these wavelengths due to the large absorbance of the calixarene which would result in a low signal to noise ratio

A plot of the correlation coefficient versus wavelength is shown in Figure 3 20 It appears that the correlation coefficient is the largest in the wavelength range of 550 to 590 nm

The graph of absorbance at three different wavelengths within this range (550 - 590 nm) versus concentration of ammonia is shown in Figure 3 21 There is no linearity within the concentration range of ammonia investigated The linear range may be at the lower ppm values Further experiments in the lower ppm region would be required in order to confirm this

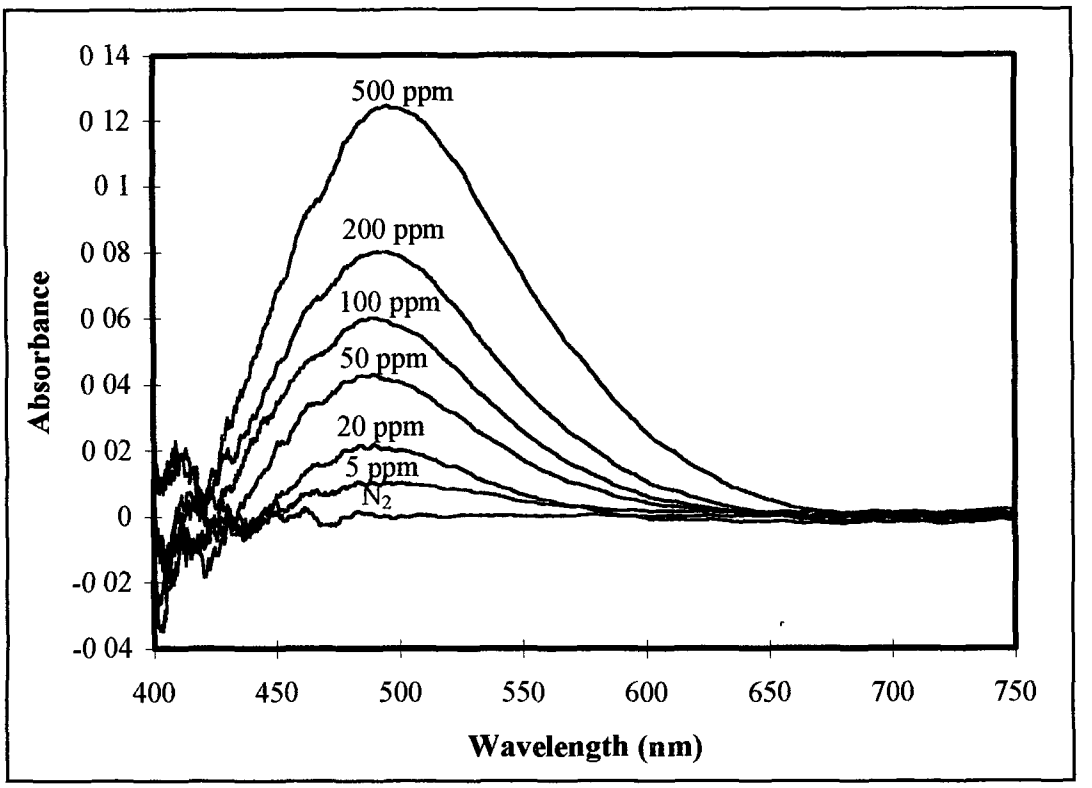

Figure 3.19: *Absorption spectra of the optical fibre with coating 1 for different concentrations of ammonia A scan of the coated fibre in nitrogen is used as the reference*

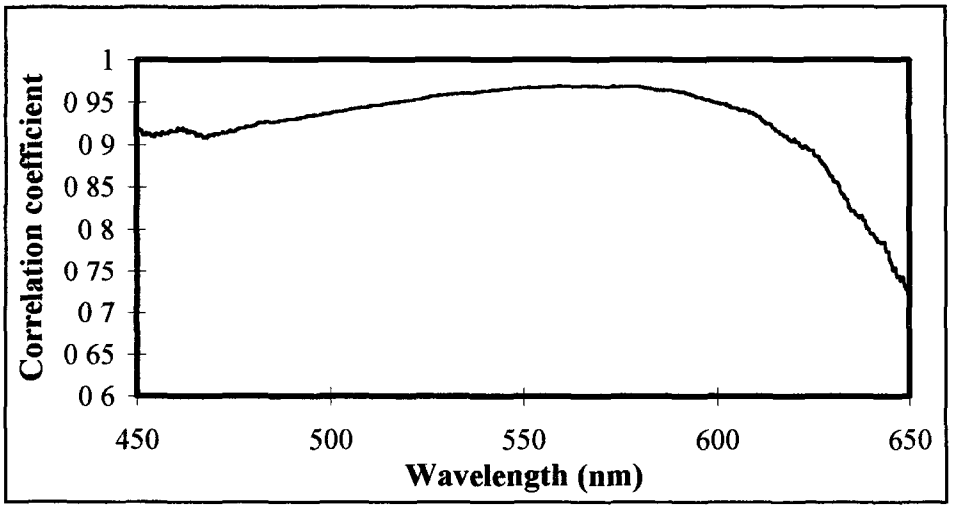

Figure 3.20: *The variation of correlation coefficient over the wavelength range from 450 to 650 nm for coating 1*

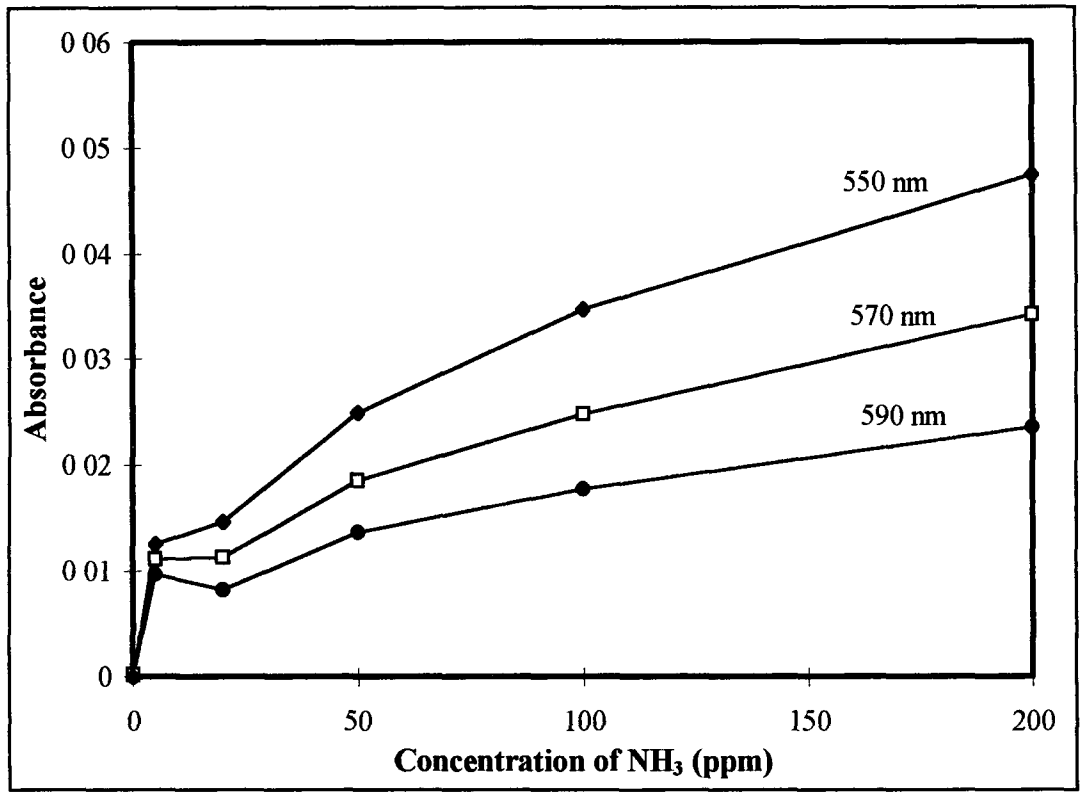

Figure 3.21: *Comparison of the absorbance at 550, 570 and 590 nm versus the concentration of gaseous ammonia in ppm using optical fibre with coating 1*

3 3 2 2 Spectral characteristic of optical fibre with coating 2

Figure 3 22 shows the absorption spectrum of the optical fibre with coating **2** over the wavelength range of 400-750 nm The addition of $LiClO_4$ to the cocktail has greatly increased the sensitivity to gaseous ammonia as expected, with the absorbance at the λ_{max} reaching 1 2 a u on exposure of the optical fibre to 100 ppm NH_3^+ On investigation of the variation of correlation coefficient (Figure 3 23) over the wavelength range, it was found that the highest values were in the wavelength range of 580 -620 nm

Figure 3 24 illustrates the change in absorbance over the concentration range of ammonia at three wavelengths There appears to be some linearity at the lower concentrations (0-10 ppm) Further experiments in this range would be required to investigate this linearity

The inclusion of a metal cation into the calixarene cavity is exerting an effect on the ionisable chromophore, thereby lowering its pK_a and facilitating proton uptake by NH_3^+ The ammonium cation may then form an association with the perchlorate anion in the non-polar environment of the membrane (Figure 3 25)

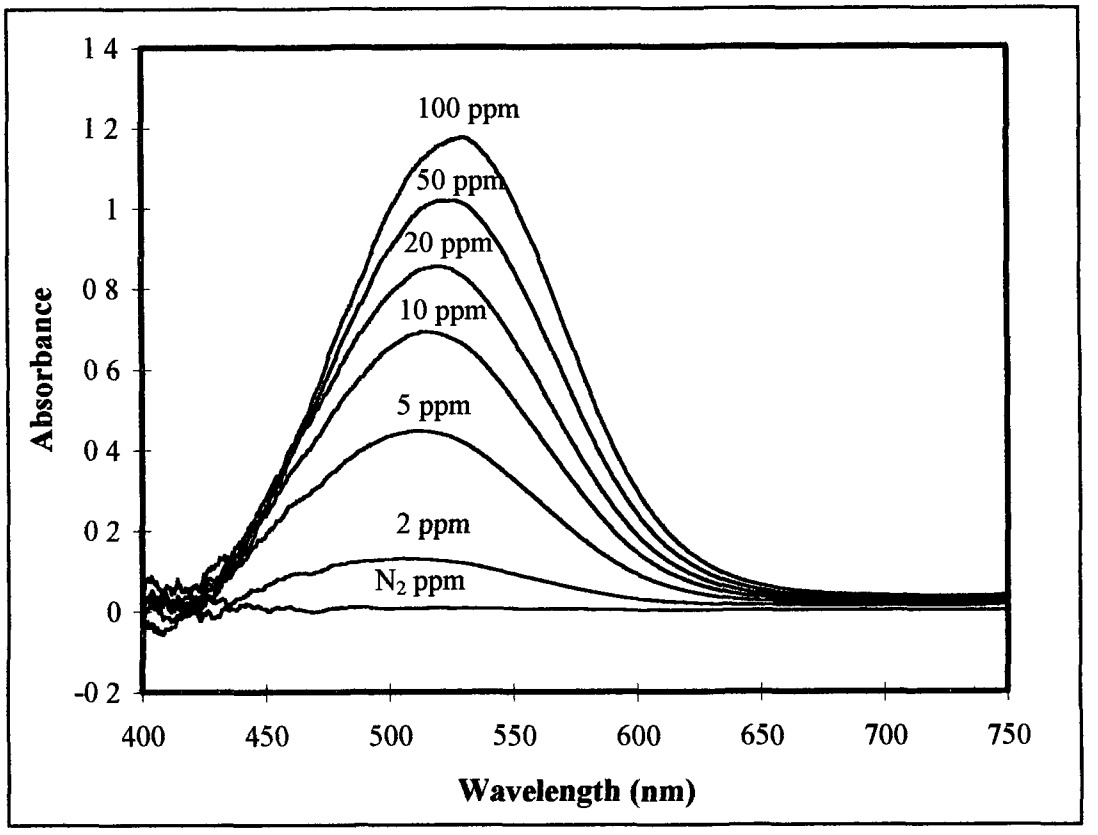

Figure 3.22: *Absorption spectra of the optical fibre with coating 2 containing $LiClO_4$ for different concentrations of ammonia A scan of the coated fibre in nitrogen is used as the reference*

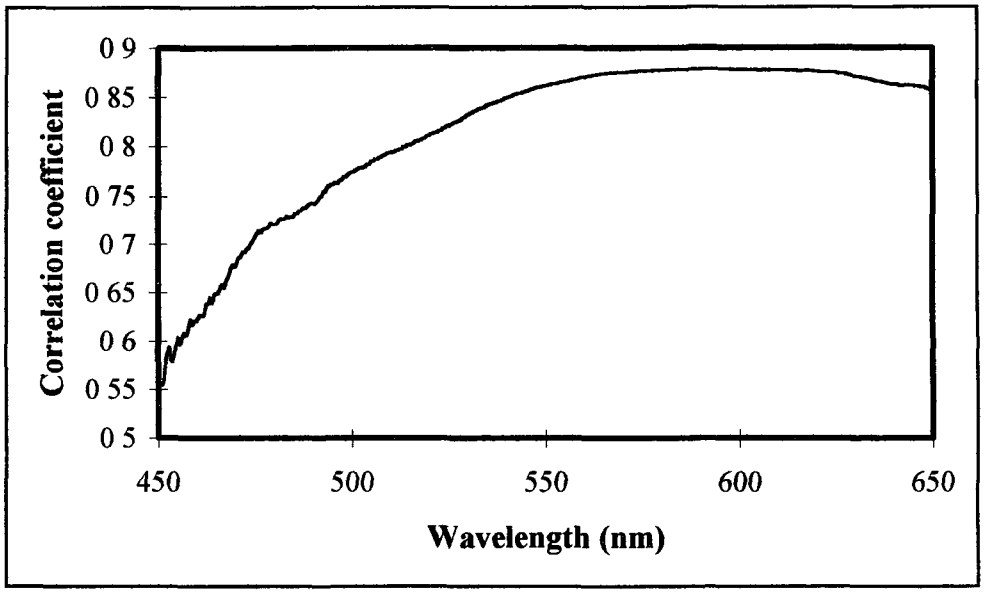

Figure 3.23: *The variation of correlation coefficient over the wavelength range from 450 to 650 nm of the optical fibre with coating 2*

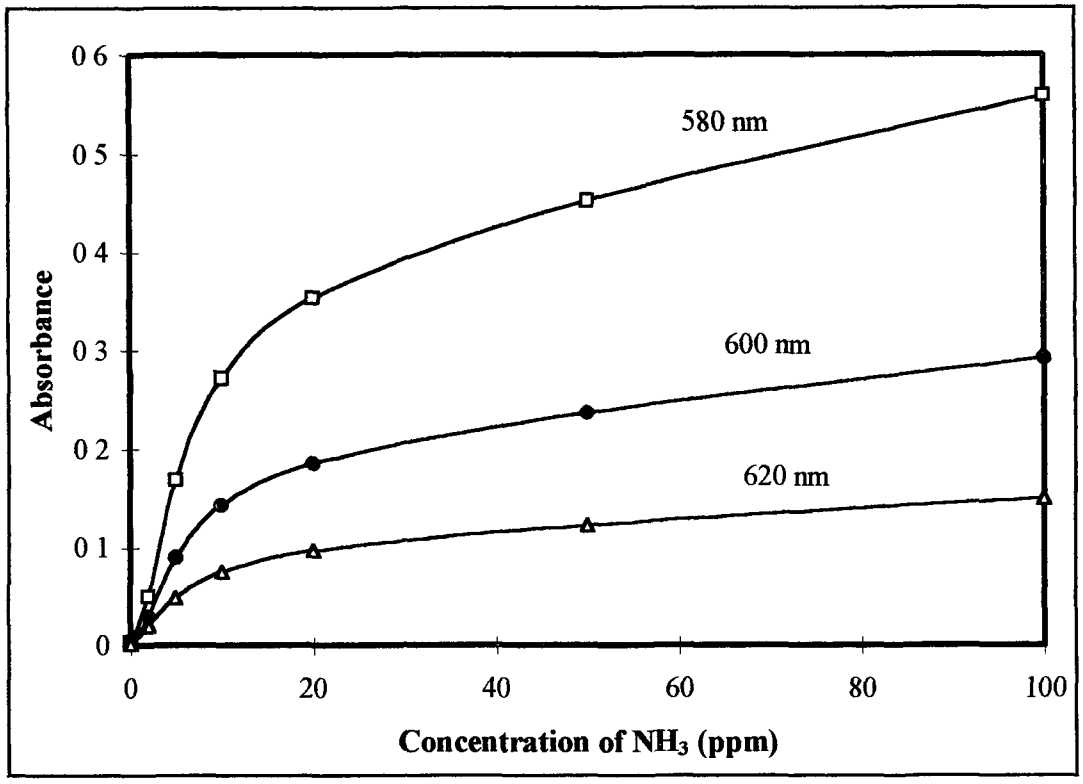

Figure 3.24: *Comparison of the absorbance at 580, 600 and 620 nm versus the concentration of gaseous ammonia in ppm of the optical fibre with coating 2*

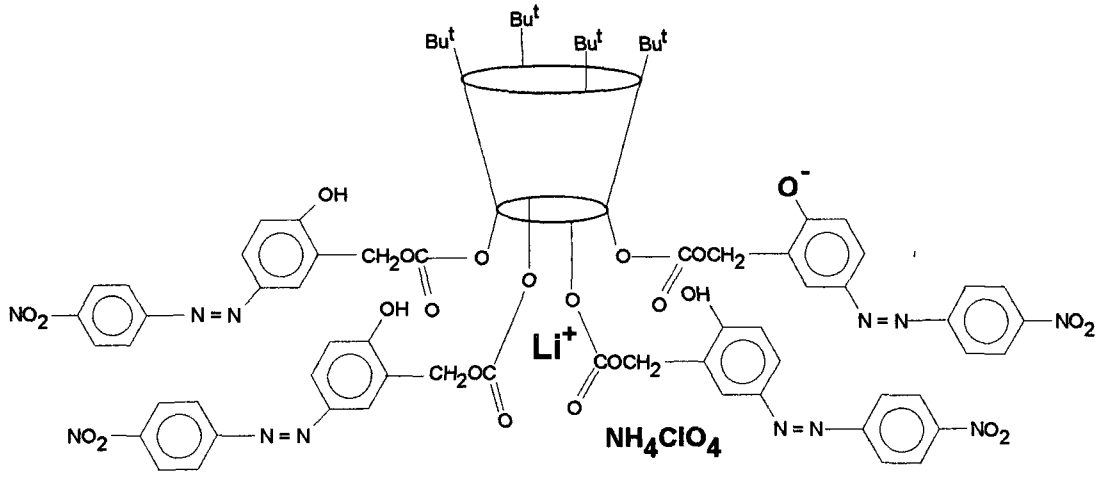

Figure 3.25: *Representation of the deprotonation of the lithium nitrophenylazophenol calix[4]arene complex brought about by the basic nature of the ammonia gas and the formation of ammonium perchlorate*

3 3 2 3 Spectral characteristic of optical fibre with coating 3

In this case the effect of decreasing the concentration of $LiClO_4$ (0 5 mole eq) in the PVC coating was investigated Figure 3 26 shows the absorbance spectra obtained The sensitivity has decreased compared to coating **2** but is more sensitive than coating 1 which is in the absence of $LiClO_4$ On exposure to 500 ppm ammonia the absorbance at the maximum wavelength is 0 3 a u On analysis of the data, the correlation coefficient appears to be the biggest in the wavelength range around 600 nm (Figure 3 27) The plot of absorbance at 580, 600 and 620 nm versus concentration of NH_3^+ (Figure 3 28) suggests that as in Figure 3 24 there is some degree of linearity in the lower concentration range of ammonia

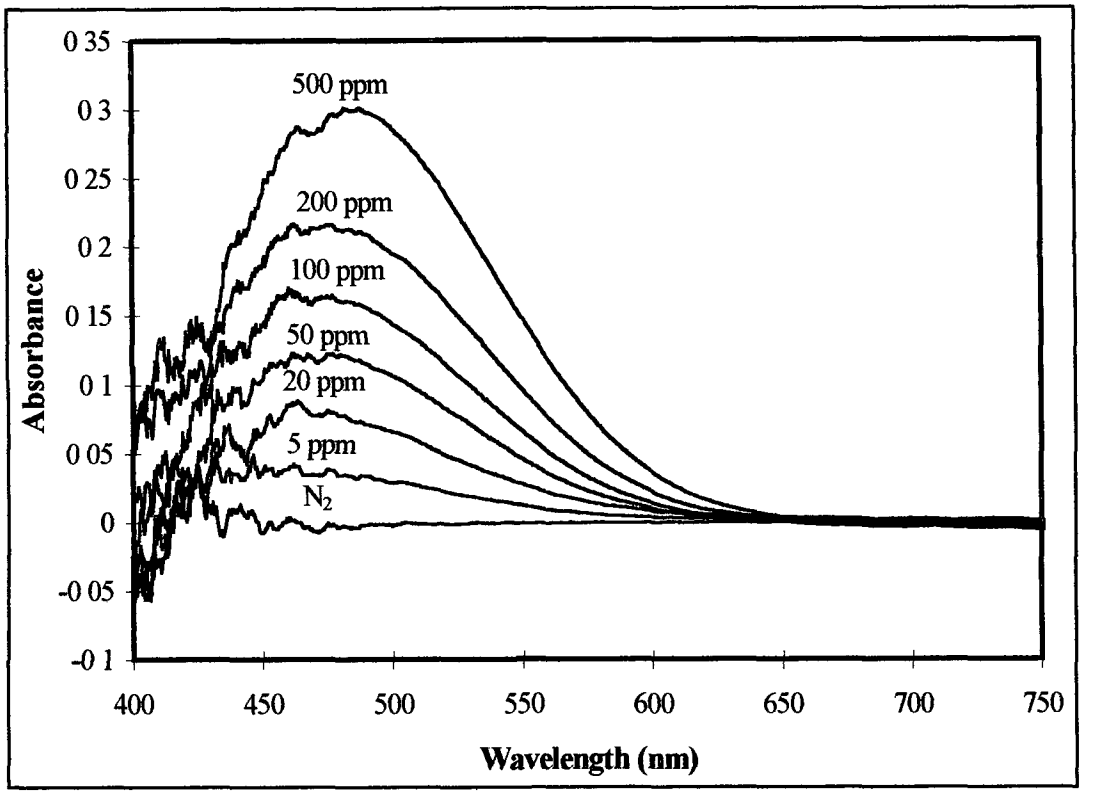

Figure 3.26: *Absorbtion spectra of the coated optical fibre containing 0 5 mole eq $LiClO_4$ (coating 3) for different concentrations of ammonia A scan of the coated fibre in nitrogen is used as the reference*

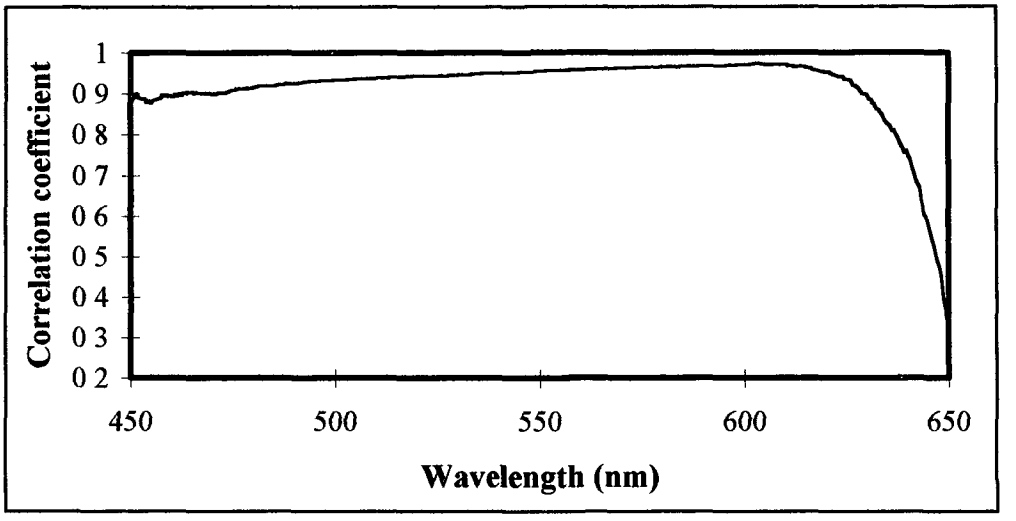

Figure 3.27: *The variation of correlation coefficient over the wavelength range from 450 to 650 nm for optical fibre with coating 3*

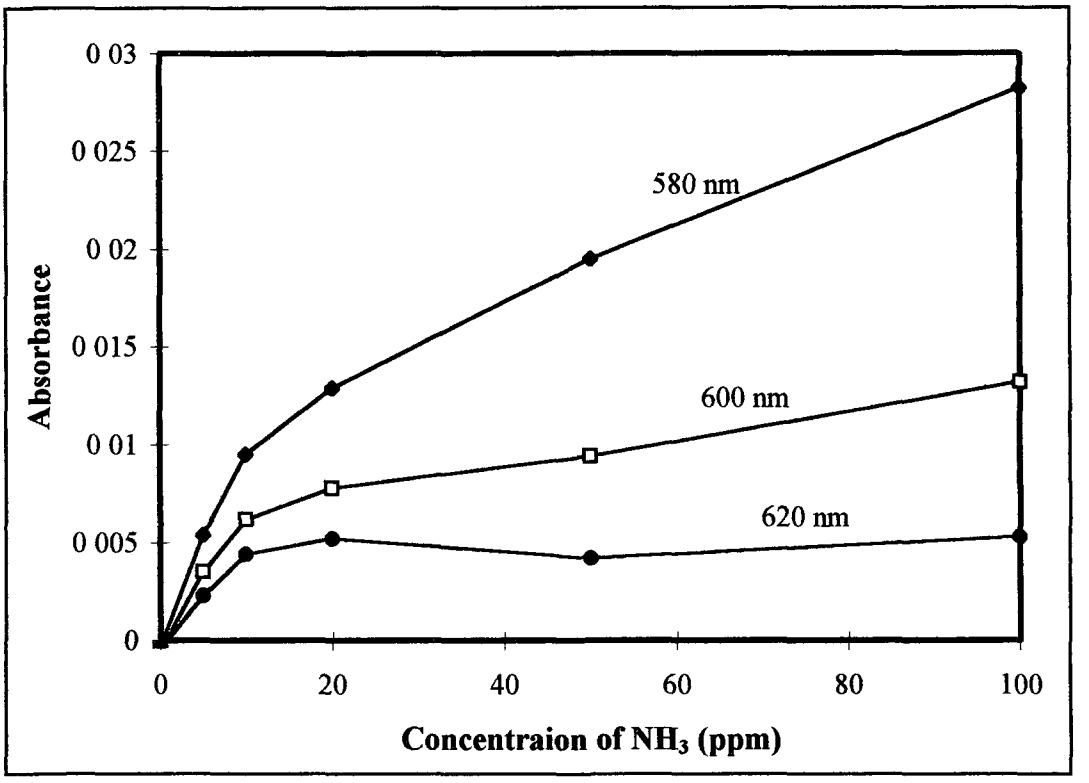

Figure 3.28: *Comparison of the absorbance at 580, 600 and 620 nm versus the concentration of gaseous ammonia in ppm for optical fibre with coating 3*

3 3 2 4 Spectral characteristic of optical fibre with coating 4

Figure 3 29 illustrates the absorbance spectra obtained using the coating which included 0 5 mole eq of $KClO_4$ The sensitivity is slightly decreased when compared to coating 3, with the maximum absorbance on exposure to 500 ppm approaching 0 2 at a wavelength of 480 nm The correlation coefficient is poor over the entire range (Figure 3 30), never rising above 0 8 except around 450 nm where the signal is very noisy Figure 3 31 shows the non-linear responses obtained at three wavelengths

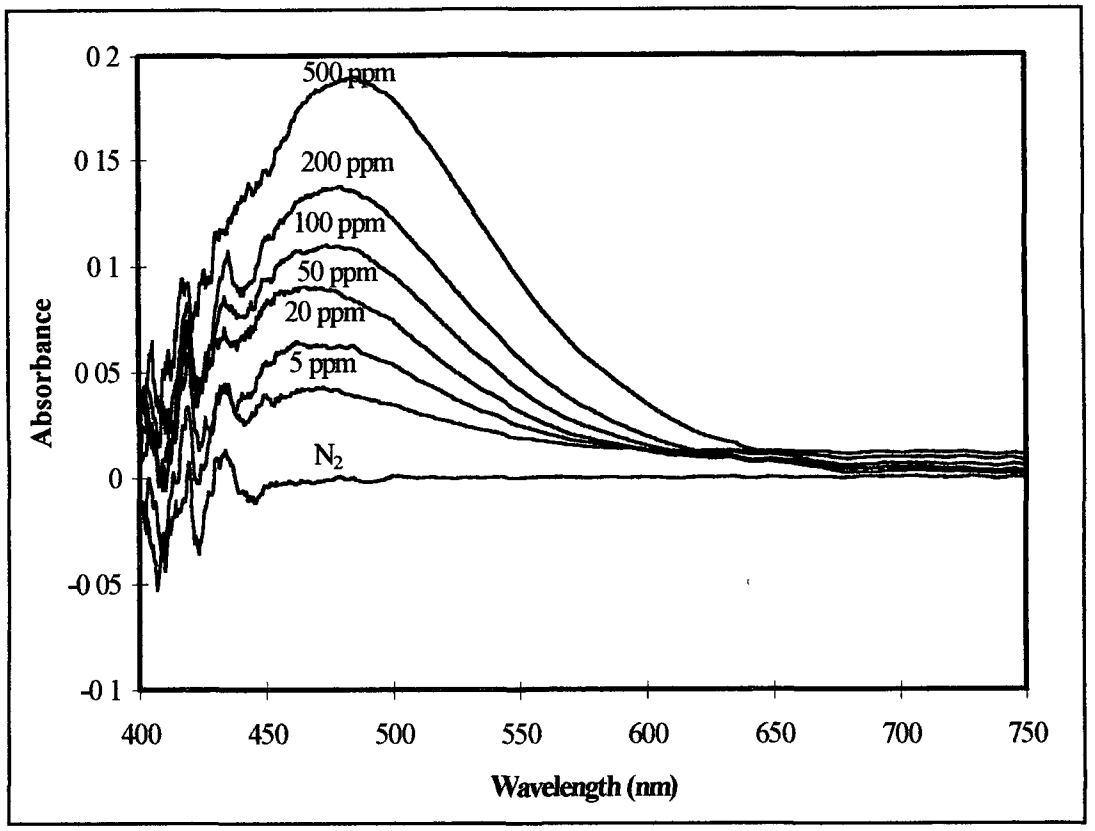

Figure 3.29 *Absorbtion spectra of the coated optical fibre containing 0 5 mole eq $KClO_4$ (coating 4) for different concentrations of ammonia A scan of the coated fibre in nitrogen is used as the reference*

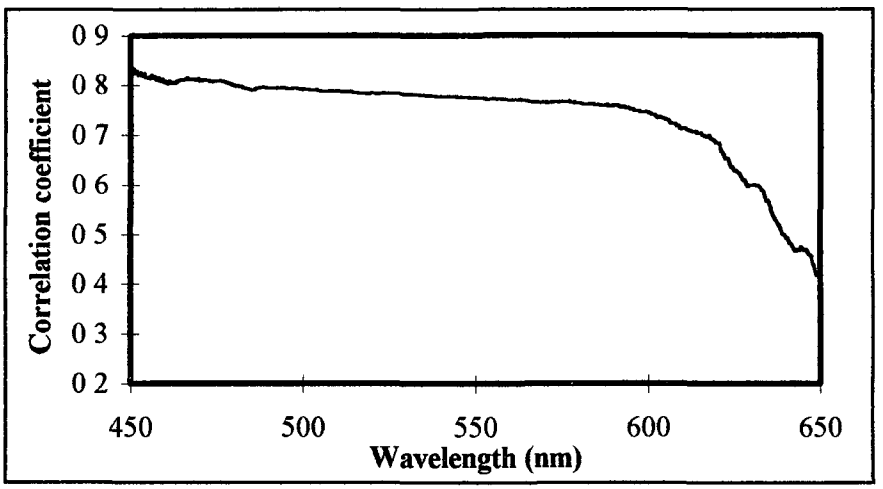

Figure 3.30 *The variation of correlation coefficient over the wavelength range from 450 to 650 nm of optical fibre with coating 4*

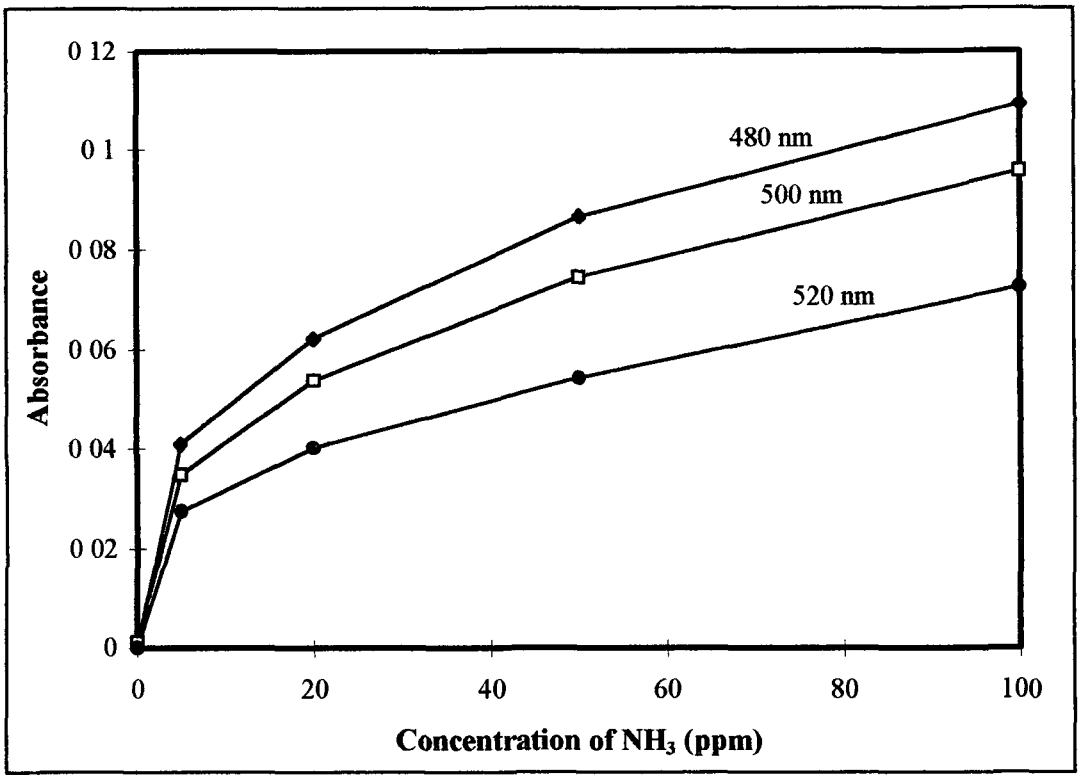

Figure 3.31: *Comparison of the absorbance at 480, 500 and 520 nm versus the concentration of gaseous ammonia in ppm of optical fibre with coating 4*

3 3 2 5 Comparison of the four coatings

Figure 3 32 compares the absorbance of the four coatings at a concentration of ammonia of 50 ppm This clearly demonstrates that the presence of a 1 mole eq of $LiClO_4$ to the calixarene in the PVC membrane (coating **2**) increases the sensitivity to the gas However, there is also a shift in the maximum wavelength from 490 nm which is the λ_{max} for the other three coatings to 520 nm for coating **2** This shift to higher wavelengths may indicate that further deprotonation is also occurring with the other chromogenic groups that are present within the molecule Variations in the concentration of $LiClO_4$ would be expected to result in different deprotonated spectra in the presence of the same concentration of ammonia This was found in the TMA detection experiments carried out with the same complexed ligand, with the concentration of $LiClO_4$ having a large bearing on the concentration range of TMA concentrations which could be determined [37] In the same way, coating **3** which contains 0 5 mole eq $LiClO_4$ exhibits a large decrease in absorbance at the deprotonated complex λ_{max} for the same concentration of ammonia relative to coating **2**

By changing the metal cation to $KClO_4$ in the membrane (coating **4**), the response to 50 ppm is even further decreased McCarrick and coworkers found a spectral response to Li^+ at lower concentrations than for Na^+ for this ligand [23] The variation in response to different cations is a function of both the stability constant of the complex and of the effect the inclusion of a cation has on the pK_a of the dissociating proton Undoubtedly complexation occurs with Na^+ as shown by the proton NMR experiments discussed earlier, but the less densely charged Na^+ cation cannot quite exert the same effect on the pK_a of the phenolic proton of the chromophore It is well known that tetraesters do not form stable complexes with K^+ which has a larger atomic radius than Na^+ and is even less densely charged and so would explain the decrease in response with coating **4**

As would be expected, the absence of $LiClO_4$ in coating **1** results in a sensor that has the least response of all four coatings to gaseous ammonia

Figure 3 33 shows the comparison of the absorbance at the wavelength maximum of the deprotonated ligand over the concentration range of ammonia investigated for the four coatings This reinforces what has been discussed above in demonstrating the effect of the presence of Li^+ in the coating on the detection of the gas

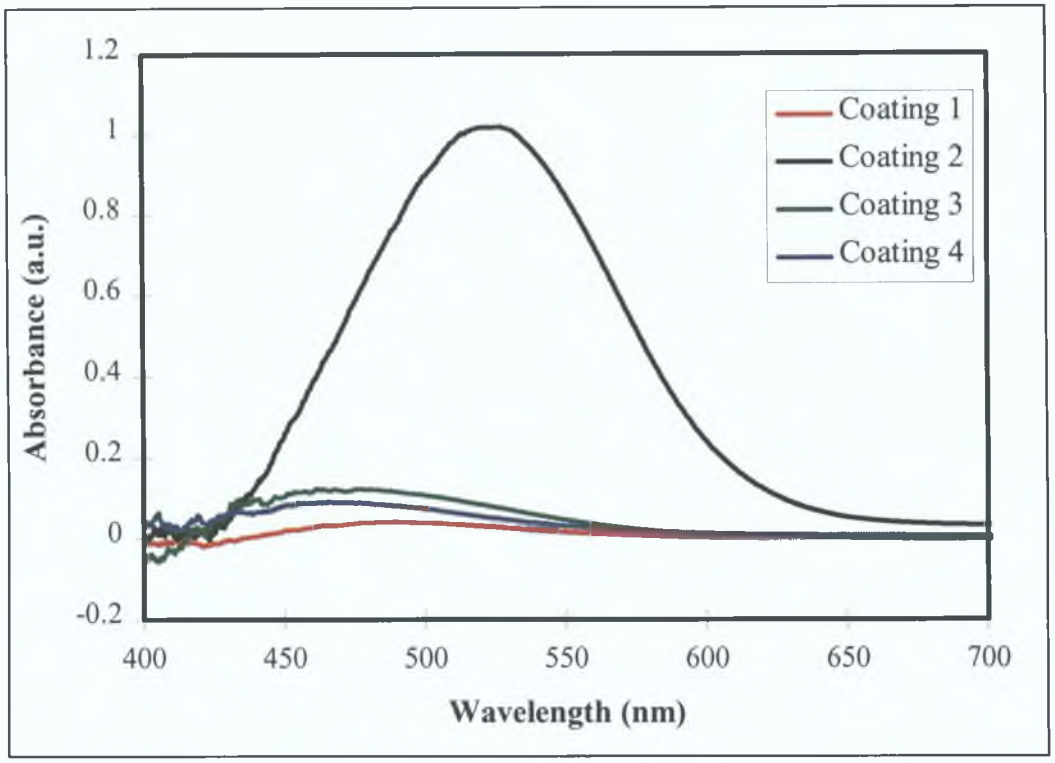

Figure 3.32: *Absorbtion spectra of the four different coated optical fibres at a 50 ppm concentration of gaseous ammonia.*

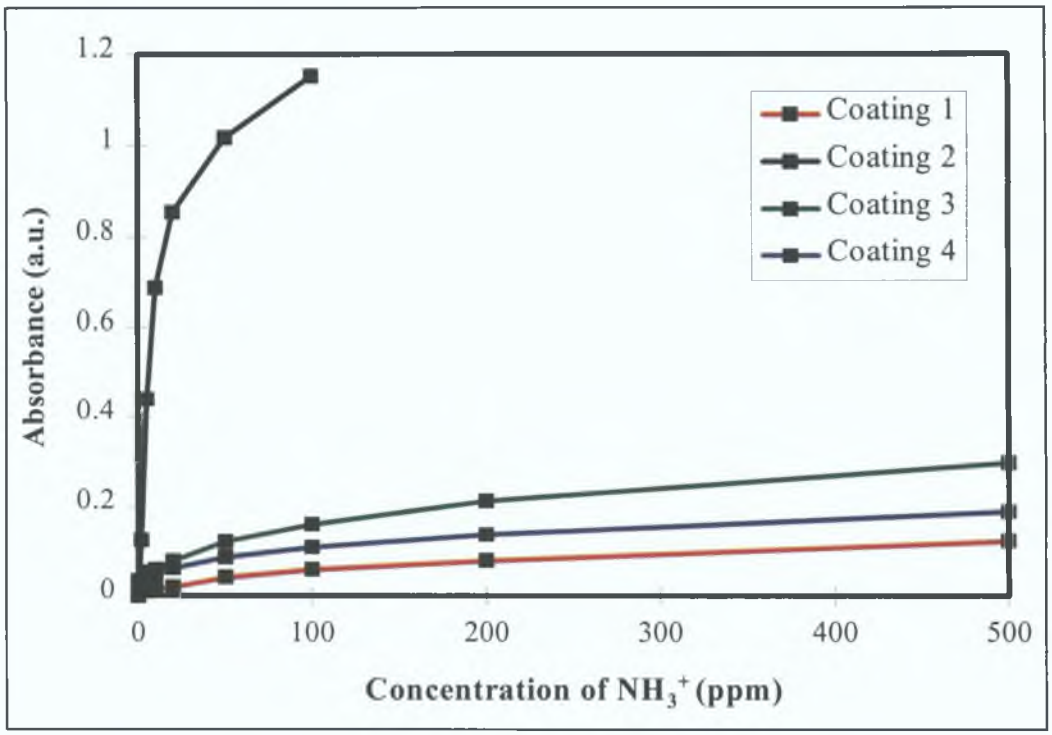

Figure 3.33: *Comparison of the absorbance at the λ_{max} versus concentration of ammonia for the four coated optical fibres.*

3 3 2 6 Time response on exposure to ammonia

The response time of these coated optical fibres were investigated and some preliminary results were obtained

Figure 3 34(a) shows a plot of absorbance at 490 nm versus time on the addition of 20 and 100 ppm ammonia using the optical fibre which was coated with the ligand only (coating **1**) For a concentration of 20 ppm ammonia the t_{90} time is 7 minutes (t_{90} is the time needed to reach 90% of the final value) There is an immediate response on exposure to 100 ppm but there is considerable drift in the signal This drift is also apparent when nitrogen is passed through the system which may be due to the presence of ammonia in the pipes

In Figure 3 34(b) the absorbance is measured at 520 nm over time using the optical fibre coated with coating **2** (i e 1 mole eq $LiClO_4$) The time response on exposure to 5 ppm ammonia is very long with the signal beginning to stabilise ≈60 minutes When the concentration is increased to 50 ppm, the time it takes for the signal to stabilise is obviously quicker but the signal is extremely slow to return to baseline when the ammonia is replaced by nitrogen

When the fibre used has a coating which contains 0 5 mole eq of $LiClO_4$ (coating **3**), a slower time response to that in Figure 3 34(a) is seen (Figure 3 34(c)) The absorbance is measured at a maximum of 480 nm Again there is considerable drift in the signals with the time it takes for the signal to return to baseline ≈ 40 minutes

In Figure 3 34(d) the absorbance is of a fibre with coating **4** is measured at 480 nm over time The time response is very similar to the fibre which did not contain any lithium in the coating (Figure 3 34(a))

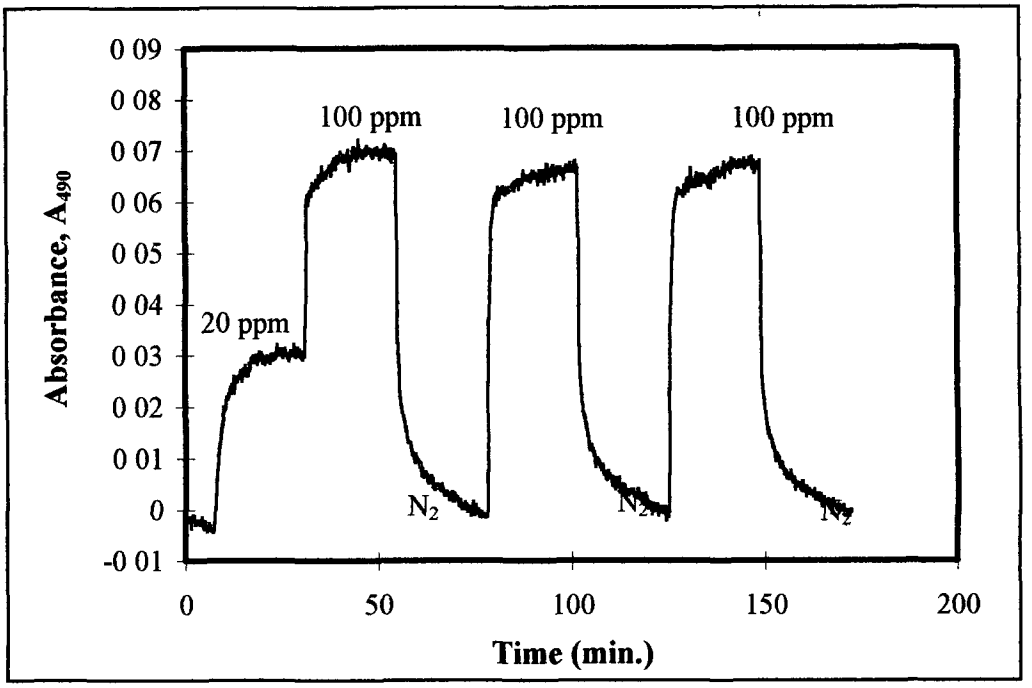

Figure 3.34(a): *Time response using coating 1*

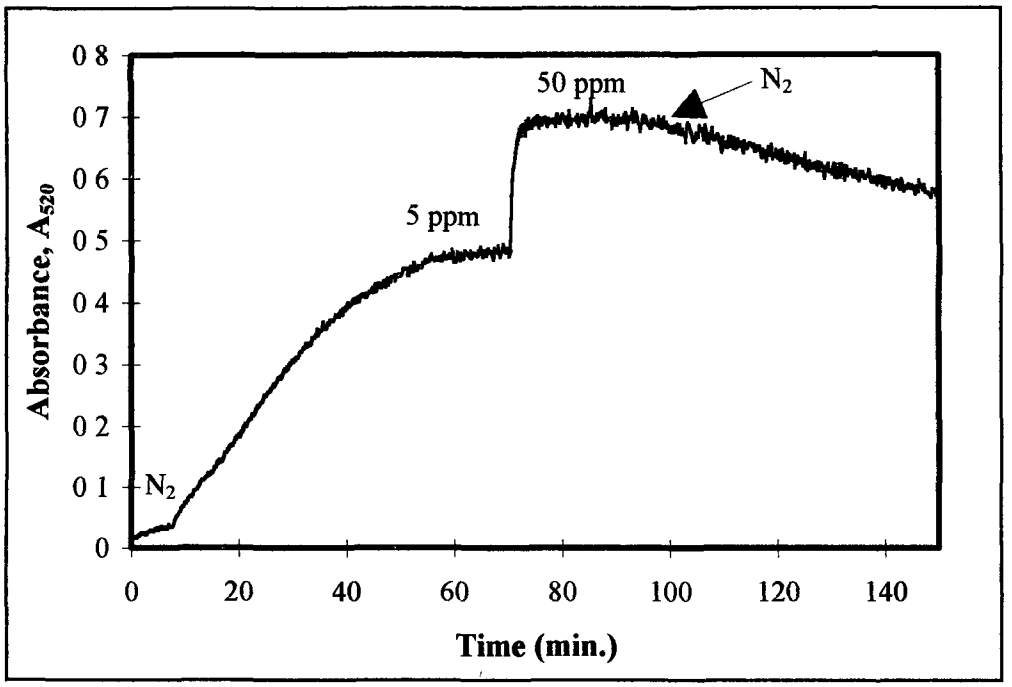

Figure 3.34 (b): *Time response using coating 2*

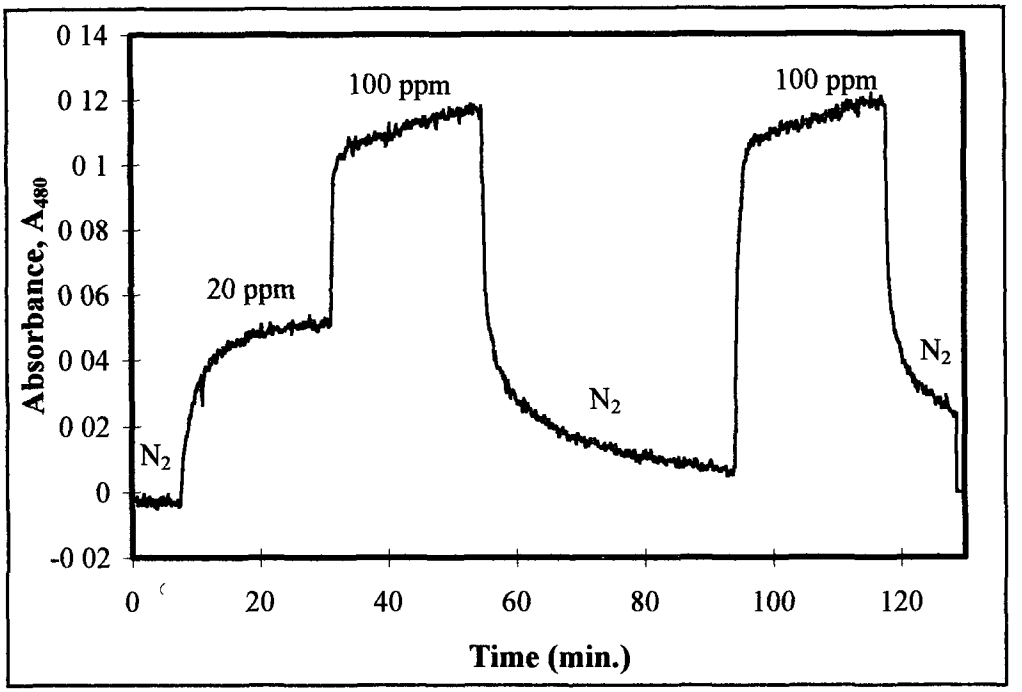

Figure 3.34(c): *Time response using coating 3*

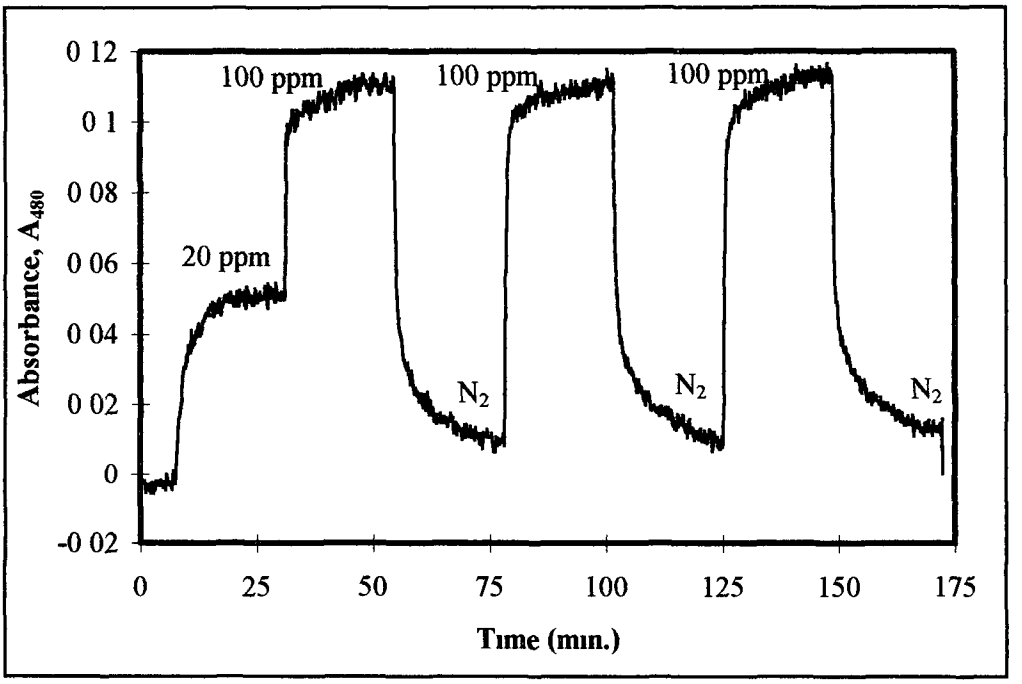

Figure 3.34(d): *Time response using coating 4*

Figure 3.34: *Investigation of the optical response at the λ_{max} of the optical fibres with coating 1 (a), coating 2 (b), coating 3 (c) and coating 4 (d) with time*

3.4 Conclusions

The preliminary results presented in this chapter demonstrate the potential of the nitrophenylazophenol calix[4]arene as the active component of an optical sensor for the detection of gaseous ammonia and the main features are discussed below

- In the cuvette-based experiments, a colour change from yellow to red was clearly visible when the coated membranes were exposed to gaseous ammonia which resulted in a shift in the absorbance maximum from 390 nm to 500 nm which was shown to be concentration dependant The results demonstrated that it took 30 s before an steady-state absorbance maximum was reached Once the slide was removed from the ammonia atmosphere the original yellow colour returned
- The sensitivity to ammonia was significantly improved when an optical system was used which involved coating optical fibres The Li^+-calixarene complex demonstrated the largest response to ammonia as compared to the coatings which did not contain $LiClO_4$ The Li^+ in the cavity lowers the pK_a of the ionisable chromophore and facilitates proton uptake by the ammonia
- The response times of the sensors to ammonia were slow (typically 60 minutes for lower concentrations) and there was considerable drift occurring The signal was slow (> 40 minutes) to return to baseline when nitrogen was passed through the system

3 4.1 Future Work

No optimisation studies were carried out on any aspect of this work so there is much scope for improvement in the general specification of the sensor Further work could include,

- Optimisation of coating thickness on the optical fibre by varying the components of the PVC cocktail e g diluting the cocktail and varying the amount of THF and varying the withdrawal speed in the dip-coating process
- Investigation of the effect of other cations in the coating and using higher mole equivalents to ligand
- Measurement of the pKa of the complexed ligand with varying concentrations of Li^+ using a non-aqueous pH titration, which may give some insight into the degree of deprotonation occurring
- Proton NMR titration studies which would give some insight into the fate of the ammonium cation once the colour change has occurred
- Examine the effect of other strategies for immobilising the calixarene onto the fibre e g other polymers, plasticisers, covalent attachment via silyl groups on upper rim of the calixarene

3.5 References

1 M Takagı, H Nakamura and K Ueno, *Anal Lett*, 1977, **10**, 1115

2 H Nakamura, M Takagı and K Ueno, *Talanta*, 1979, **26**, 921

3 B P Bubnıs, J L steger, Y P Wu, L A Meyers and G E Pacey, *Anal Chım Acta*, 1982, **139**, 307

4 T Kaneda, K Sugıhara, H Kamıya and S Mısumı, *Tet Lett*, 1981, **22**, 4407

5 J F Alder, D C Ashworth, R Narayanaswamy, R E Moss and I O Sutherland, *Analyst*, 1987, **112**, 1191

6 S Mısumı and T Kaneda, *J Incl Phenom and Mol Recog*, 1989, 7, 83

7 J Van Gent, E J R Sudholter, P V Lambeck, T J A Popma, G J Gerrıtsma and D N Reınhoudt, *J Chem Soc, Chem Commun*, 1988, 893

8 D J Cram, R A Cramack and R C Helgeson, *J Am Chem Soc*, 1988, **110**, 571

9 R C Helgeson, B P Czech, E Chapoteau, C R Gebauer, A Kumar and D J Cram, *J Am Chem Soc*, 1989, **111**, 6339

10 A F Sholl and O Sutherland, *J Chem Soc, Chem Commun*, 1992, 1716

11 W Zazulak, E Chapoteau, B P Czech and A Kumar, *J Org Chem*, 1992, **57**, 6720

12 V Bohmer, E Schade and W Vogt, *Makromol Chem, Rapıd Commun*, 1984, **5**, 221

13 S Shınkaı, K Arakı, J Shıbata, D Tsugawa and O Manabe, *Chem Lett*, 1989, 931

14 H Shımızu, K Iwamoto, K Fujımoto and S Shınkaı, *Chem Lett*, 1991, 2147

15 Y Nakamoto, T Nakayama, T Yamagıshı and S Ishıda, *Workshop on Calıxarenes and Related compounds*, Maınz, Germany, August 1991

16 A M Kıng, C P Moore, K R A S Sandanayake and I O Sutherland, *J Chem Soc, Chem. Commun*, 1992, 582

17 K R A S Sandanayake and I O Sutherland, *Sens and Act B*, 1993, **11**, 331

18 E Ghidini, F Ugozzoli, R Ungaro, S Harkema, A Abu El-Fadl and D N Reinhoudt, *J Am Chem Soc*, 1990, **112**, 6979

19 Y Kubo, S Hamaguchi, K Kotani and K Yoshida, *Tet Lett*, 1991, **32**, 7419

20 Y Kubo, S Hamaguchi, A Niimi, K Yoshida and S Tokita, *J Chem Soc, Chem Commun*, 1993, 305

21 M McCarrick, B Wu, S J Harris, D Diamond, G Barrett and M A McKervey, *J Chem Soc, Chem Commun*, 1992, 1287

22 M McCarrick, B Wu, S J Harris, D Diamond, G Barrett and M A McKervey, *J Chem Soc, Perkin Trans*, 1993, 1963

23 M McCarrick, S J Harris, D Diamond, *Analyst*, 1993, **118**, 1127

24 M McCarrick, S J Harris, D Diamond, *J Mater Chem*, 1994, **4**, 217

25 C K Simmonds and E C Lamprecht, in "*Microbiology of Frozen Foods*", ed R K Robinson, Elsevier Applied Science Publishers, London and New York, 1985, p 169

26 Mary McCarrick, Ph D thesis, Dublin City University, 1995, 145

27 A Sharma, Z Ali and I J Higgins, *Environ Proc Monitor Tech*, 1992, 107

28 S H Cadle, R J Countess and N A Kelly, *Atmos Environ*, 1982, **16**, 2501

29 E Bijsman and J W Erisman, *J Atmos Chem*, 1988, **6**, 265

30 Q Zhou, D Kritz, L Bonnell and G H Sigel, *Jr Appl Opt*, 1989, **28**, 2022

31 P Caglar and R Narayanaswamy, *Analyst*, 1987, **112**, 1285

32 R A Potyrailo, S P Golubkov, P S Borsuk and P M Talanchuk, *Analyst*, 1994, **119**, 443

33 A Morales-Bahnik, R Czolk and H J Ache, *Sensors and Acutuators B*, 1994, 493

34 S Ozawa, P C Hauser, K Seiler, S S Tan, W E Morf and W Simon, *Anal Chem*, 1991, **63**, 640

35 S J West, S Ozawa, K Seiler, S S Tan and W Simon, *Anal Chem*, 1992, **64**, 533

36 Mary McCarrick, Ph D Thesis, Dublin City University, 1995, 138

37 Mary McCarrick, Ph D Thesis, Dublin City University, 1995, 155

4. Sodium-Selective Electrodes Based on Triester Monoacid Derivatives of *p*-tert-Butylcalix[4]arene

4.1 Introduction

This chapter deals with another means of transduction of calixarene host-guest chemistry, that of potentiometry An introduction to the theory of potentiometry is given as well as a brief literature survey on calixarene-based sodium selective electrodes This is followed by a section outlining the experimental procedures used in this work Finally the results of the work carried out on the characterisation of sodium-selective electrodes incorporating triester monoacid derivatives of *p*-tert-butylcalix[4]arene are presented

4.1 1 Potentiometry

Potentiometry is one of the most widely used electroanalytical methods The term potentiometry pertains to the technique of measuring the potential difference of a galvanic cell or electromotive force (emf) The simplest electrochemical cell consists of two electrical conductors or electrodes immersed in an electrolyte solution

In potentiometry the voltage source is a form of a galvanic cell in which electrochemical reactions occur spontaneously at the electrolyte/electrode interface when the electrodes are connected by a conductor The two electrodes are known as the ion-selective electrode (ISE) and reference electrode respectively The overall cell potential is measured when the reversible electrode reactions have reached thermodynamic equilibrium Hence the true values of this potential can only be measured under zero current conditions The main task in analytical potentiometry is to relate changes in cell potential to shifts in a particular ion activity arising from its reversible exchange at the ISE membrane/sample interface boundary This can only be achieved if all other potentials arising in the cell are independent of the solution composition

4.1.2 Conventional Ion-Selective Electrodes

The conventional cell arrangement for potentiometric measurements using an ion-selective electrode (ISE) is shown in Figure 4 1 [1]

In the conventional configuration, the ISE is filled with an aqueous reference solution which contains the ions necessary to maintain constant potentials at both the internal reference electrode (e g Ag/AgCl) and the inner surface of the ion-selective membrane In a simple system where the reference electrode does not have a liquid junction such as an Ag/AgCl reference electrode, the overall cell potential (E_{cell}) would be given by

$$E_{cell} = E_{ISE} - E_{Ref} \qquad \textbf{Eq. 4.1}$$

where E_{ISE} is the ion selective electrode potential and E_{ref} is the reference electrode potential If the sensing electrode responds in a Nernstian fashion to the analyte ion (i^{z+}) then

$$E_{ISE} = E^{o} + 2.303\frac{RT}{z_1 F}\log a_1 \qquad \textbf{Eq. 4.2}$$

where i is the analyte of interest, of charge z_1 and activity a_1, R, T and F are the gas constant, the absolute temperature and the Faraday constant respectively and E^{o} is the standard electrode potential, which is ideally constant under the conditions of use If E_{ref} is independent of the sample composition (i e constant) then by combining equation **4.1** and **4.2** and the following equation can be written

$$E_{cell} = constant + 2.303\frac{RT}{z_1 F}\log a_1 \qquad \textbf{Eq. 4.3}$$

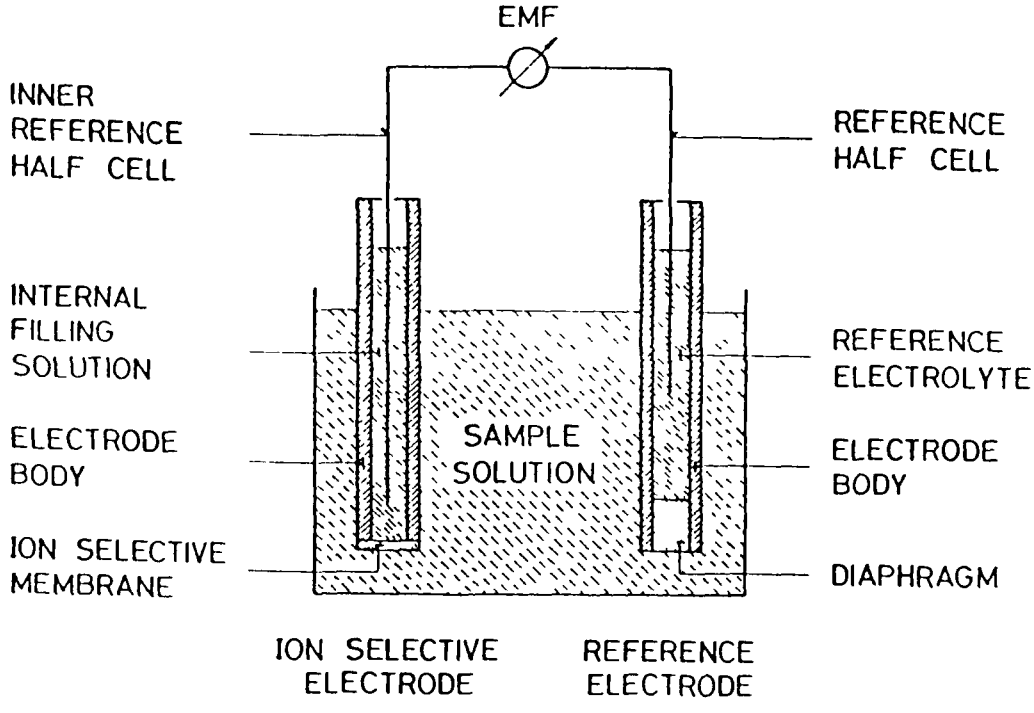

Figure 4.1 *-Schematic diagram of a membrane electrode measuring circuit and cell assembly [1]*

Hence the cell will respond in a Nernstian manner to changes in a_1 However the reference electrode must often be separated from the sample solution because the reference electrode potential is affected by the sample composition or because of cell design considerations The electrical contact between the reference half-cell and the sample solution is achieved by means of a salt bridge Such a bridge/solution boundary gives rise to ionic diffusion which introduces a liquid-junction potential into the system Liquid junction potentials are a direct result of the differences in ionic mobilities of the positive and negative ions constituting the bridge electrolyte resulting in a charge separation For example if the positive ions migrate faster into the sample solution than the negative ions, a charge separation soon develops at the sample/bridge junction The magnitude of the resulting potential difference is dependent on a number of factors, such as the type of the bridge ions, the composition of the sample solution, the geometry of the bridge and the temperature

As the junction potential contributes to the overall cell potential, it is important that it be as small as possible, or at least constant over the period of use Due to the similar mobilities of K^+ and Cl^-, saturated KCl solutions are frequently used in the preparation of bridges as only relatively small junction potentials will arise [2] A mathematical description of the junction potential is given by the Henderson Equation **(Eq. 4.4)** [1],

$$E_D = \left(\frac{\sum z_1 u_1 a_1(0) - \sum z_1 u_1 a_1(d)}{\sum z_1^2 u_1 a_1(0) - \sum z_1^2 u_1 a_1(d)} \right) x2\,303 \frac{RT}{F} \log \left(\frac{\sum z_1^2 u_1 a_1(0)}{\sum z_1^2 u_1 a_1(d)} \right) \qquad \textbf{Eq. 4.4}$$

The summation terms include contributions by all the ionic species (i) that are present within the membrane, the absolute value of the charge numbers z_1, mobilities u_1 and activities a_1 and assumes a linear diffusion gradient, and (d) and (o) are due to the diffusion layer between the internal reference solution and the external sample respectively

4.1 3 Activity Coefficient

From the Nernst equation (**Eq 4.2**) it can be seen that the electrode response is related to the activity of the ion of interest a_1 The activity of an ion in solution is not identical to its concentration but can be related to it by the equation

$$a_1 = f_1 c_1 \qquad \textbf{Eq. 4.5}$$

where for an ion (i), a_1 is the activity, (c_1) is the concentration and (f_1) is an activity coefficient As the concentration of a species tends to zero, the activity coefficients tends to unity and so the activity and concentration become identical in infinitely dilute solutions The activity coefficient (f_1) quantifies the degree of deviation of an ideal solution from the ideal situation Its value depends on the ionic strength of the solution

$$I = \frac{1}{2}\sum c_i z_i^2 \qquad \textbf{Eq. 4.6}$$

where c_1 = molar concentration of i

The ionic strength may be related to the activity coefficient by means of the Davies model [3],

$$\log f_i = -Az_i^2\left(\frac{\sqrt{I}}{1+\sqrt{I}} - 0\,2I\right) \qquad \textbf{Eq. 4.7}$$

where A is a solvent dependency constant (0 512 for water)

4.1 4 Membrane Potentials

In an ideal potentiometric cell, where effectively the contributions from the reference electrode, and the junction potential are constant, changes in the membrane potential

E_m can be monitored as changes in overall cell potential The membrane potential is determined by the boundary potentials at the two membrane/solution interfaces and any diffusion potential which arises as a result of variation in the ion composition through the membrane This is shown diagramatically in Figure 4 2 where E'_B is the potential at the internal solution boundary, E''_B the potential at the sample boundary and E_D is the diffusion potential which arises from the spontaneous transport of charged species across the membrane so that a potential gradient is formed The full membrane potential is then given by

$$E_m = E''_B - E'_B + E_D \qquad \textbf{Eq. 4.8}$$

4 1 4 1 Boundary Potential

The phase boundary potential arises from the non-uniform distribution of electrically charged species between the two phases Both chemical and electrical potential contributions must be taken into account in descriptions of ion transport or ion distribution For an ion i of charge z_i exchanging reversibly across an aquo-liquid membrane boundary, the work done in establishing equilibrium can be described by

$$-\Delta G = z_i F E_B \qquad \textbf{Eq. 4.9}$$

where ΔG is the change in Gibb's free energy, F is the Faraday constant and E_B is the electrical potential established over the boundary The decrease in Gibb's free energy is given by the difference in the partial molar Gibb's free energy (μ) for the ion i in the membrane (m) and the aqueous (aq) phases

$$-\Delta G = \mu_{i(aq)} - \mu_{i(m)} \qquad \textbf{Eq. 4.10}$$

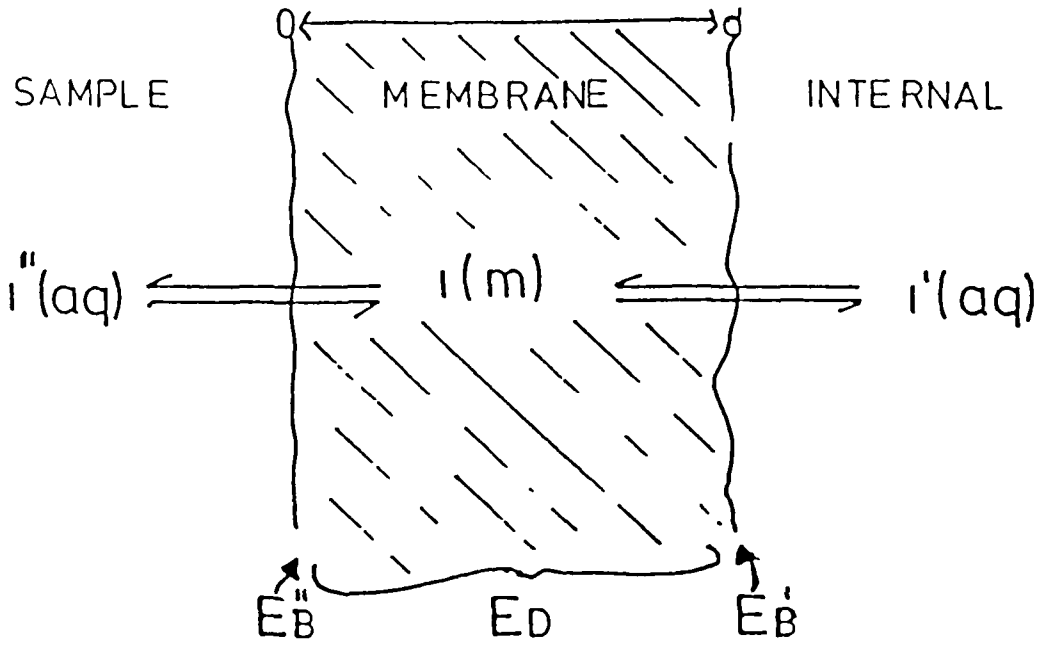

Figure 4.2: *Boundary and diffusion potentials of ion-selective liquid-membranes*

While measurements are usually carried out under a wide variety of conditions, these are conventionally related to the work done to bring about the same charge under standard conditions by

$$-\Delta G^{o} = \mu^{o}_{i(aq)} - \mu^{o}_{i(m)} = z_i F E^{o}_{B} \qquad \textbf{Eq. 4.11}$$

and the standard state ^{o} is related to other states by

$$\mu_i = \mu^{o}_i + RT \ln a_i \qquad \textbf{Eq. 4.12}$$

So substituting into **Eq. 4.10** above

$$-\Delta G = \mu^{o}_{i(aq)} - \mu^{o}_{i(m)} + RT \ln \frac{a_{i(aq)}}{a_{i(m)}} \qquad \textbf{Eq. 4.13}$$

The electrical potential at the interface is thus

$$E_B = \left(\frac{\mu^{o}_{i(aq)} - \mu^{o}_{i(m)}}{z_i F} \right) + \frac{RT}{z_i F} \ln \left(\frac{a_{i(aq)}}{a_{i(m)}} \right) \qquad \textbf{Eq. 4.14}$$

If $\mathbf{E^{o}_{B}}$ the standard potential $= \frac{\left[\mu^{o}_{i(aq)} - \mu^{o}_{i(m)} \right]}{z_i F}$, then the boundary potential at any particular membrane interface is,

$$E_B = E^{o}_{B} + \frac{RT}{z_i F} \ln \left(\frac{a_{i(aq)}}{a_{i(m)}} \right) \qquad \textbf{Eq. 4.15}$$

As there are two membrane interfaces, (') the internal interface and (") the external interface Two equations can be written for the boundary potentials E'_B and E''_B from **(Eq. 4.15)** above

$$E'_B = E^o_B + \frac{RT}{z_1 F} \ln\left(\frac{a'_{1(aq)}}{a'_{1(m)}}\right) \qquad \textbf{Eq. 4.16}$$

$$E''_B = E^o_B + \frac{RT}{z_1 F} \ln\left(\frac{a''_{1(aq)}}{a''_{1(m)}}\right) \qquad \textbf{Eq. 4.17}$$

Combining **(Eq. 4.16)** and **(Eq. 4.17)** the net boundary potential across the membrane is

$$E''_B - E'_B = E^{o''}_B - E^{o'}_B + \frac{RT}{z_1 F} \ln\left(\frac{a''_{1(aq)} a''_{1(m)}}{a'_{1(aq)} a'_{1(m)}}\right) \qquad \textbf{Eq. 4.18}$$

Assuming the activity of the ion a_1 is the same at both interfaces in the membrane i e $a'_{1(m)} = a''_{1(m)}$ then

$$E''_B - E'_B = E^{o''}_B - E^{o'}_B + \frac{RT}{z_1 F} \ln\left(\frac{a''_{1(aq)}}{a'_{1(aq)}}\right) \qquad \textbf{Eq. 4.19}$$

4 1 4 2 Diffusion Potential

Although the membrane is considered to be a uniform phase, the free energies of the membrane components undergo variation with time and this gives rise to diffusional fluxes of ions within the membrane Although more commonly used for the

estimation of junction potentials, the Henderson approximation can be used to describe the diffusion potential across the membrane This allows easy and rather close characterisation of the diffusion potential in terms of boundary concentrations and mobilities of diffusing ions, (see **Eq. 4.4**)

Relating this equation to Figure 4 2 , x = 0 for the sample boundary ("), x = d at the internal boundary (') and the thickness of the membrane is d If we assume there is a negligible drop in primary ion activity across the membrane i e

$$a_{i(o)} \approx a_{i(d)} \qquad \textbf{Eq. 4.20}$$

and that there is virtually no penetration of the membrane by interfering ions (j)

$$a_j \sim a_{j(d)} \sim 0 \qquad \textbf{Eq. 4.21}$$

then the substitution into the Henderson equation leads to the approximation

$$E_D \sim 0 \qquad \textbf{Eq. 4.22}$$

4 1 4 3 The Complete Membrane Potential

Since E_D can be approximated to zero or is at least constant, variations in the overall membrane potential will be determined by the values of the boundary potentials As the internal electrolyte activity a'_i is constant, substitution of **eq. 4.22** into **eq. 4.8** and **eq. 4.19** gives an expression for the overall membrane potential

$$E_M = E_M^o + \left(\frac{RT}{z_i F}\right) \ln a_i'' \qquad \textbf{Eq. 4.23}$$

where E^{o}_{M} is a standard membrane potential and includes contributions from E_D, $E^{o''}_{B}$ and E'_{B} Provided that the junction potential (E_{jn}) and the reference potential (E_{ref}) remain constant the overall cell potential will depend on the activity of the primary ion a_i'' in solution and can be defined by

$$E_{cell} = \text{constant} + S \log a_i'' \qquad \textbf{Eq. 4.24}$$

For a ten-fold change in primary ion activity (a_i) the ideal slope (S) is 2 303 $\frac{RT}{z_1F}$

This is 59 2 mV for a monovalent ion and 29 6 mV for a divalent ion at 25°C Hence overall changes in cell potential will be ideally determined by changes in E''_B

4 1 5 The Nikolskii-Eisenman Equation

Thus far in our discussion the change in electrode potential has been discussed in terms of the ideal situation where the electrode responds solely to the presence of the analyte ion In reality all electrodes are exposed to interfering ions, both cationic and anionic in nature The response of the electrode must also be considered in terms of these interfering ions, which will interact with the electrode to varying degrees The Nikolskii equation [3] introduces a term for the presence of interfering ions into the Nernst equation -

$$E_M = E^{o}_{M} + 2\,303\frac{RT}{z_1F}\log\left[a_1 + \sum k^{pot}_{ij}\left(a_j\right)^{z_i/z_j}\right] \qquad \textbf{Eq. 4.25}$$

where a_1 = activity of the primary ion (i) in the sample solution, a_j = the activity of the various interfering ions (j) in the sample solution, E^{o}_{M} = a standard boundary

potential of the membrane, incorporating other potentials besides the external boundary potential, k_{ij}^{pot} (the selectivity coefficient) is a weighting factor to include contributions from interfering ions (j) to the total membrane potential (E_M) In the absence of other ions ($a_j = 0$) or an ideal electrode ($k_{ij}^{pot} = 0$, for all interferents j) the equation reduces to a Nernstian form for the primary ion

4.1 6 Ion-Selective Membrane Components

The key to successful design of a potentiometric sensor is to select a membrane that exhibits a selective and reproducible change in the presence of the desired species Sensors are classified by the nature of the membrane and one of the largest groups of such sensors contain liquid membranes

The membrane material can be a non-polar liquid or polymer/liquid system with mobile ion-exchange sites that can move throughout the membrane but which are trapped within the boundaries of the membrane because of their lipophilic nature This generates a membrane potential via ion transfer from the aqueous to the membrane phase at the aquo/liquid boundary and forms the basis of the potentiometric measurement of ions adjacent to the liquid membrane Two main types of ion-selective compounds are used as dissolved components in liquid membrane sensors

(i) Organic ion-exchangers such as organophosphates or tetraphenylborate (cation exchanger) and tetraalkylammonium ions (anion exchangers)

(ii) Uncharged molecules (neutral carriers) capable of selectively complexing metal ions and drawing them into the membrane

In general , these selective membranes also consist of a polymer, usually poly-vinyl chloride (PVC) and a plasticiser which acts as the organic solvent The role of the PVC is to provide an inert solid support structure in which the rest of the components are contained Different plasticisers will effect the lipophilicity of the

membrane which would alter the distribution coefficients (k) of the different species Other additives include fixed ion-exchange sites such as potassium tetrakis(4-chlorophenyl)borate (KTpC1PB) which functions as an anion excluder, preventing negative charged ions getting into the polymer membrane and helping to obtain a more ideal Nernstian response

4 1.7 Neutral Carrier ISEs

Various classes of neutral carrier ionophores have been used in potentiometric ISE work such as crown ethers, spherands, and calixarenes The traditional barrel configuration ISEs shown in Figure 4 1 containing these neutral carrier ionophores as the membrane recognition components have been used in numerous analytical situations over the last 30 years or so The huge developments in ISE research over this period has been driven m part by the speed and ease of ISE use, the wide dynamic range possible and the relatively low cost of the devices

For an extensive list of neutral carrier based ISEs and their current applications one should look to the excellent reviews [4,5,6,7]

4.1 8 Estimation of Selectivity Coefficients

A selectivity constant or coefficient is used to express the extent to which an interfering ion (j), interferes with the response of an electrode to its primary ion (i) and has already been defined by the Nikolskii Equation **(Eq. 4.25)**

$$E_M = E_M^o + \frac{2\,303RT}{z_1F} \log\left[a_1 + \sum k_{ij}^{pot} a_j^{zi/zj}\right] \qquad \textbf{Eq. 4.25}$$

where z_1 and z_J are the charges on the ion i and j respectively and E^O is the standard potential of the electrode or a constant The term selectivity coefficient can be misleading in several ways This may result in coefficients that are not highly reproducible or precise being quoted Firstly, the selectivity coefficients for any interfering ions are dependent on the ionic strength of the solution and the activity level at which the primary and interfering ions are measured They also depend on whether potentials are taken in mixed or separate solutions containing the two ions The actual method/equation used to obtain the final result has an effect on the calculated selectivity coefficient value Finally, the membrane composition of the electrode e g the amount and type of ionophore, plasticiser and additives which is mainly determined by the membrane manufacturer, will affect the selectivity characteristics of a particular electrode

Therefore it is crucial when quoting selectivity coefficient values that the composition of the membrane, the conditions under which the measurements were made and the methods used in the calculations are stated A number of methods have been outlined for obtaining estimates of k_{ij}^{pot}, with the most frequently used methods being the separate and mixed solution methods which have been described in full by Moody and Thomas [5]

4 1 8 1 Separate Solution Method

A calibration curve is obtained for the primary ion (i) over the concentration range usually from 10^{-1} to 10^{-5} M A similar curve is prepared for the interfering ion (j), (see Figure 4 3) The selectivity coefficient can then be calculated by either of two methods (a) equal activities or (b) equal potentials

(a) Equal Activities

The electrode potential, E_i, to the primary cation (i) only , is given by the Nernst equation

$$E_1 = E^o + S \log a_1 \qquad \textbf{Eq. 4.2}$$

where $S = 2\ 303\ RT/Z_iF$

The electrode response to a mixture of cations is given by the Nikolskii equation **(Eq.4.25)** above If the electrode is placed in a solution containing the interfering cation (j) only then can the potential (E_2) to cation (j) be obtained from **eq. 4.25** by letting $a_1 = 0$, and

$$E_2 = E^o + S \log k_{ij}^{pot} a_j \qquad \textbf{Eq. 4.26}$$

When $a_1 = a_j$ and provided the valency of the cations is the same i e $z_1 = z_j$ then k_{ij}^{pot} can be calculated from

$$\log k_{ij}^{pot} = \frac{(E_2 - E_1)}{S} \qquad \textbf{Eq. 4.27}$$

when the potentials E_1 and E_2 have been measured Since the selectivity coefficients are activity dependent, for comparison purposes the chosen activity should always be reported (usually 10^{-2} or 10^{-1} M)

(b) Equal Potentials

Alternatively a method of equal potentials may be used When $E_1 = E_2$, **eq. 4.2** and **eq. 4.26** may be combined to give

$$k_{ij}^{pot} = \frac{a_1}{a_j} \qquad \textbf{Eq. 4.28}$$

The activities a_i and a_j can be read from the calibration curve (Figure 4 3), where the potentials E_1 and E_2 are equal If the primary and interfering ions have different charges, the equation may be modified to

$$k_{ij}^{pot} = \frac{a_1}{a_j^{z1/zj}} \qquad \textbf{Eq. 4.29}$$

4 1 8 2 Mixed Solution Method

Here the calibration curve is recorded in the presence of a fixed level of interfering ion (e g a_j = 0 01 M) throughout the calibration range of the primary ion As the activity of the primary cation falls, the interfering ion j exerts its influence until complete interference sets in, and is seen as a horizontal plateau at which the potential is constant (Figure 4 4) The two linear portions are extrapolated to calculate the activity of the primary ion a_i at the intercept and the selectivity coefficient is calculated from **eq.4.29** where a_j is the constant background interference activity If drift of the potential is observed in the plateau region when ion (j) provides high interference, then the value of a_i can be taken at the point where the two curves differ by 18 mV In the case where z_j = 2 i e divalent ion selectivity a value of 8 9 mV should be used

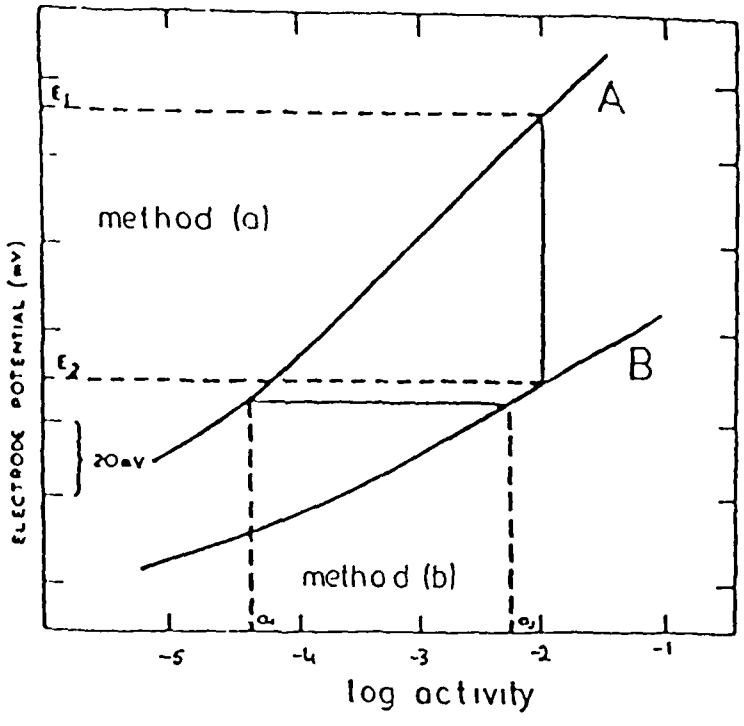

Figure 4.3: *Estimation of the selectivity coefficient k_{ij}^{Pot} using separate solution method (A) Response to primary ion (i) only, (B) response to interfering ion (j) only [3]*

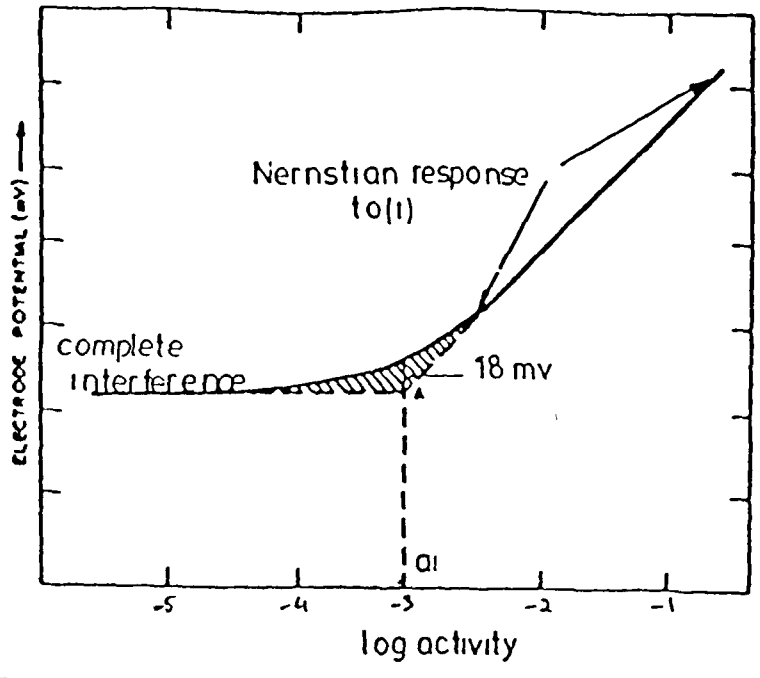

Figure 4.4: *Estimation of selectivity coefficient (k_{ij}^{Pot})using the mixed solution method [3]*

4.1.9 Sodium ISEs based on calixarenes

The analysis of sodium using PVC electrodes based on neutral carriers has received much attention in the last ten years, especially in the area of clinical chemistry Apart from the very important clinical analysis of blood electrolytes and urine for sodium there are many other applications where sodium ion-selective electrodes are used in chemical analysis The amount of sodium in various water sources such as potable water, rivers, effluents and boiler feeds may be monitored for reasons of health, safety and efficiency The sodium content of some food stuffs, beverages and agricultural products may also be of interest and can be conveniently measured using ion-selective electrodes

Complexation studies in solution (by phase transfer experiments, membrane transport and stability constant measurements) show that functionalised calix[4]arenes have a general selectivity for sodium ions

The first calixarene-based ISE was reported by Diamond in 1986 [8] The sodium ISEs reported employed *p-tert*-butylated calix[4]arene methyl and ethyl esters as neutral carriers The ISEs exhibited selectivity over a range of alkali metal cations such as potassium, lithium and caesium and gave Nernstian response slopes A second publication early in 1987 by Diamond and Svehla [9] again highlighted the excellent selectivity of the tetramethyl calix[4]arene tetraacetate for sodium against potassium and a range of other interferents which can affect the measurement of sodium in blood Detailed studies on the properties of PVC membrane ISEs based on the same compounds confirmed their usefulness as sodium sensors [10]

Kimura et al reported on other related calix[4]arenes (amide functionalised) as sodium sensors [11], and the effect of varying substituent groups on the esters was examined by Cadogan and coworkers [12] More recently, Cunningham reported the *p-t*-butylcalix[4]arene methoxymethyl ester as producing the most selective sodium electrode so far [13]

Of the thirty three calix[4]arenes that have been studied in ISEs, twenty five are either symmetrical calixarenes containing 4 pendant ester groups or mixed functionality calixarenes containing at least one ester group Such functionality has been shown to give the best selectivity for sodium ions

Mini sodium ISEs incorporating the calix[4]arene methyl ester have been employed for dip measurements of sodium in blood plasma [14,15] The results were compared to a SMAC-Technicon Analyser and good correlation was found but a systematic error was apparent due to the calibration methodology used in the study

Other ligands were assessed for use in sodium-selective electrodes, including the methyl, butyl and adamantyl ketone tetramers of *p-t*-butylcalix[4]arene However only the methyl ketone derivative produced satisfactory PVC membrane electrodes [12] These were subsequently applied to the analysis of sodium in plasma samples [16] However as before a bias in the results was apparent

Obviously, when trying to establish a new analytical device, any bias in results is unacceptable One way to reduce the effect of drift and error in the results would be to use flow-injection analysis (FIA) PVC membranes incorporating the methylketone and methyl ester derivatives were assessed in an FIA system for blood sodium analysis and the results demonstrated that the bias described above could be greatly reduced [17] The methyl ester tetramer was used in an ISE array both in conventional dip-type experiments [18] and in a FIA system [19,20] Using sophisticated calibration and sensor modelling techniques, it was demonstrated that the methylester tetramer could be applied to the analysis of sodium in blood with excellent results Calixarene-based ISEs have also been incorporated into arrays for batch injection analysis [21]

4 1 10 Aim of the project

In this chapter we describe the characteristics of sodium ion selective electrodes (ISEs) in which the ionophore is either a trimethylester or triethylester monoacid derivative of *p*-tert-butylcalix[4]arene (Figure 4 5) Previously it was demonstrated that methyl and ethyl tetraester derivatives of p-tert-butylcalix[4]arene [22], e g **4 (i)** and **4 (ii)**, and hexaester derivatives of p-tert-butylcalix[6]arene [23], were efficient and selective ionophores for Na^+ and Cs^+ selective electrodes, respectively

In contrast to this work, carboxylated PVC has been used previously m ion-selective devices Pungor *et al* reported on the response of potassium membrane electrodes containing valinomycin prepared with carboxylated PVC [24] From impedance and selectivity studies of such membranes, this group concluded that the carboxyl sites are not ionised within the potassium selective membrane phase Further evidence of the notion that the carboxyl groups are fully protonated within the neutral-carrier based ISE membranes was provided by Meyerhoff and coworkers [25] by using pH response studies and IR spectra of the membranes More recently, the behaviour of cation-selective solvent polymeric membranes based on acidic ionophores, such as monensin (contains a carboxyl group), was mvestigated by Schaller [26] Previous work by the same group had demonstrated the beneficial influence of ionic sites on the potentiometric properties of ISEs and were able to show that there is no fundamental difference between charged and neutral carriers with respect to selectivities of ISEs if appropriate ionic additives are used [27] Since charged and neutral ionophores need lipophilic sites of opposite charge for optimum performance, it is possible to discriminate between neutral and charged carrier-related systems as shown recently for anion-selective electrodes based on metalloporphyrins [28] Therefore, Schaller [26] used this principle to investigate monensin On addition of a small amount of cationic additive relative to monensin gives a negative slope for the emf response The anionic additive, on the other hand improves the slope and the selectivity, as it should be for neutral ligands Moreover, they also reported that the neutral ionophore monensm methyl ester has selectivities similar to its carboxyl analog, showing that no negatively charged COO^- groups take part in the

complexation process However, we will see from our results that the monoacid calixarenes used in this study are ionisable carboxylic acid derivatives

^{1}H NMR data indicate that monoacid **4 (iv)** in solution possesses a pinched cone conformation which is more distorted than the cone conformation of esters **4 (i)** and **4 (ii)** [22] This distortion could facilitate intramolecular hydrogen bonding between the carboxylic acid group and the oxygen atom of a nearby ether or ester function X-Ray analysis of **4 (iv)** [22] confirmed the presence of a distorted cone conformation and an intramolecular hydrogen bond Figure 4 6 and Figure 4 7 shows the 3-d energy minimised structure of **4 (iv)** and **4 (ii)** respectively The distances measured are very similar for both compounds The structural and conformational similarities between monoacid **4 (iv)** and tetraesters **4 (i)** and **4 (ii)** suggested that the former should function as a sodium-selective complexing agent in much the same way as the latter This was in fact found to be the case from stability constant measurements in methanol [29] which revealed somewhat stronger binding for **4 (iv)** relative to **4 (ii)** for all alkali cations with, however, a lower selectivity for Na^+ with respect to K^+ (6 3 for **4 (iv)** versus 400 for **4 (ii)**) In contrast, the monoacid was apparently ineffective, compared with **4 (i)** or **4 (ii)** in extracting alkali picrates from aqueous solution into dichloromethane [30] This behaviour in complexation/extraction prompted us to compare the performance of ion-selective electrodes based on monoacid triester **4 (iii)** and **4 (iv)** with the earlier electrodes based on tetraesters **4 (i)** and **4 (ii)** The relatively easy conversion of the methyl and ethyl tetraesters to their equivalent monoacid triesters [22], and the evidence of poor ion extraction by the monoacids from the picrate studies were not in accordance with our observation of very long lifetimes for ion-selective electrodes based on the tetraesters **4 (i)** and **4 (ii)**, in some cases of over a year [31]

The results obtained with monoacid **4 (iii)** and **4 (iv)**, the preparation and conformational properties of which are described in detail elsewhere [22], expand the range of calixarenes suitable for use as ionophores in ISEs to include ionisable carboxylic acid derivatives These results also help to explain the extended lifetimes observed with ISEs based on tetraesters **4 (i)** and **4 (ii)**

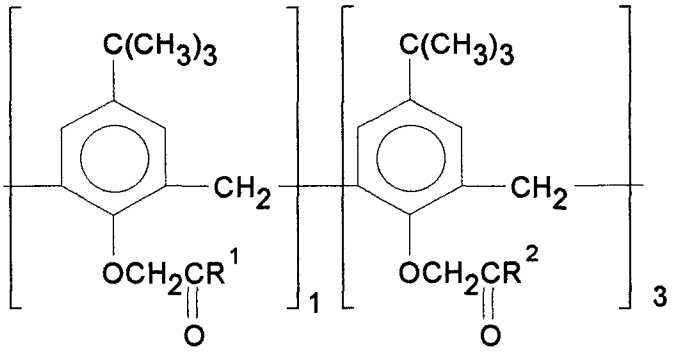

4 (i) $R^1 = OMe$ $R^2 = OMe$

4 (ii) $R^1 = OEt$ $R^2 = OEt$

4 (iii) $R^1 = OH$ $R^2 = OMe$

4 (iv) $R^1 = OH$ $R^2 = OEt$

4 (v) $R^1 = Me$ $R^2 = Me$

Figure 4.5: *Structures of the calixarene compounds*

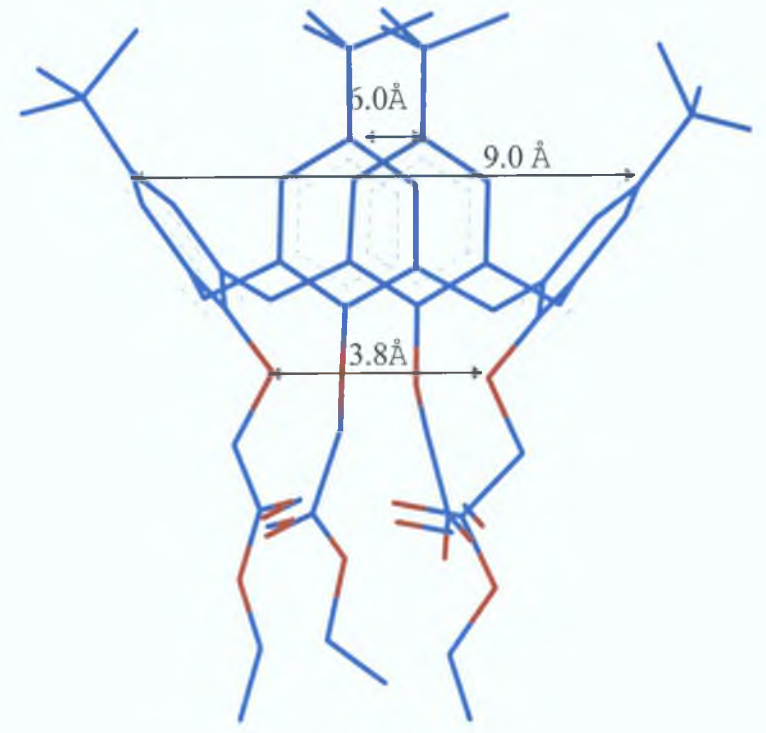

Side view

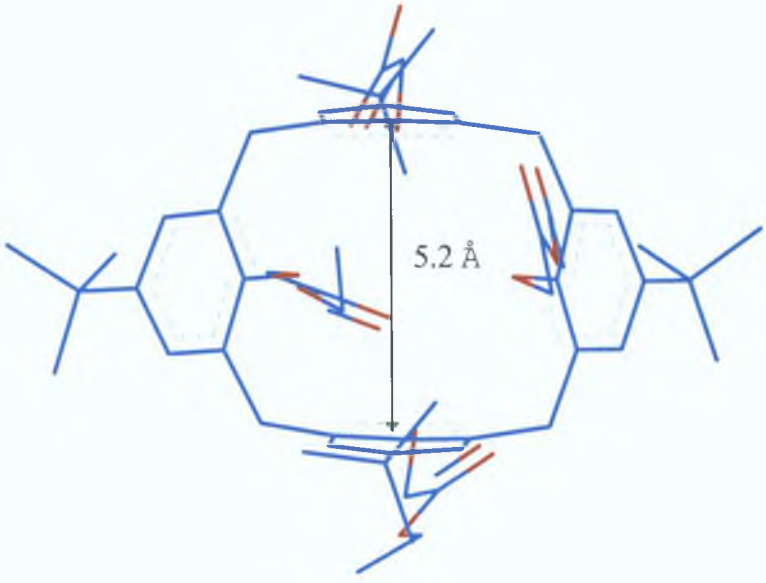

Top view

Figure 4.6: *Energy minimised structure of the triethyl ester monoacid* ***4 (iv)*** *obtained using Hyperchem v.4.0 using* MM^{+}*, showing side and top view.*

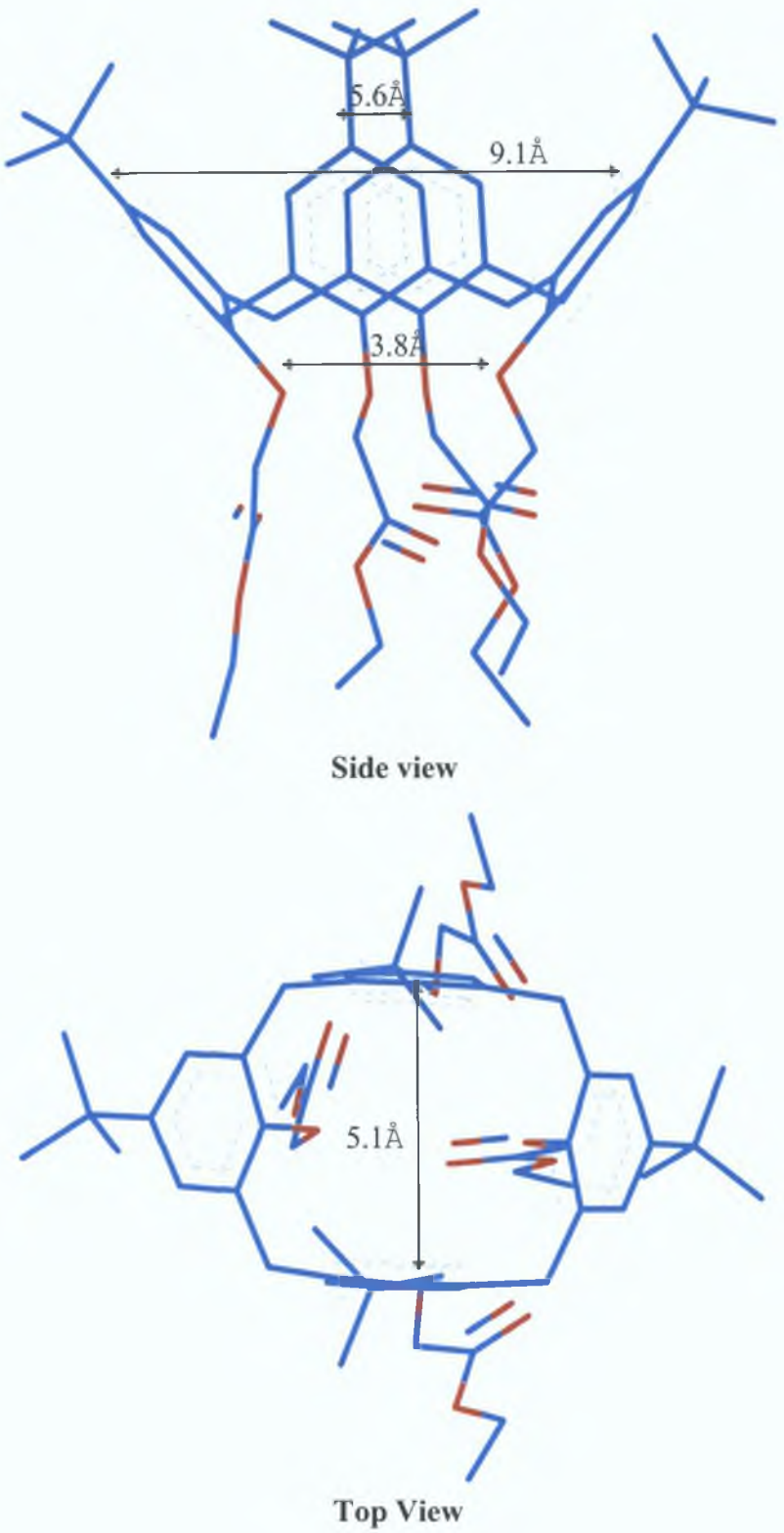

Figure 4.7: *Energy minimised structure of the tetraethyl ester calix[4]arene* ***4 (ii)*** *obtained using Hyperchem v. 4.0 using MM*$^{+}$.

4.2 Experimental

4 2.1 Materials

Ionophores **4 (i)** and **4 (ii)** were prepared by the literature method [32] and ionophores **4 (iii)** and **4 (iv)** as described by Barrett *et al* [22] All alkali and alkaline earth chlorides were of AR grade, obtained from Aldrich or Riedal-de Haen Membrane plasticiser, o-nitrophenyl octyl ether (o-NPOE), ion-exchanger potassium tetra*kis* *p*-chlorophenyl borate (KTpClPB), Poly(vinylchloride) (PVC) and selectophore grade tetrahydrofuran (THF) were obtained from Fluka Deionized Milli Q grade water was used throughout

4.2.2 Equipment

ISE mV measurements were made relative to a Metrohm capillary tip SCE or an Amagruss Refex reference electrode (Castlebar Industrial Estate, Co Mayo, Ireland) using a Hewlett Packard μV meter in high input impedance mode (Model 34401A) The same meter was used along with a flat surface pH glass electrode (No E8087 EDT Instruments Ltd , Dover, UK) for monitoring the release of release of hydrogen ions from PVC-doped membranes Conventional pH measurements were made using a Jenway 3040 Ion Analyser (Jenway Ltd , Essex, UK) and an Orion 9156SC combination glass electrode

The ISE-EMF measurements were carried out on cells of the type

Hg,Hg_2Cl_2 / KCl(satd) / sample / PVC membrane / 0 1M NaCl / AgCl/Ag

Selectivity coefficients were calculated by the separate solution (SS) method in 0.1M solutions of the interfering ions. The divalent selectivities were confirmed by the mixed solution (MS) method using 10^{-1} M fixed interfering ion concentration [3]. Electrode slopes were determined in sodium chloride solutions (10^{-4} M to 10^{-1} M; n=5). Sodium activity coefficients were calculated as described in section 4.1.3. All electrochemical measurements were made at 20±0.5 °C

4.2.3 Electrode fabrication

PVC membrane bench electrodes were prepared as described elsewhere [33]. The PVC cocktail composition was as follows; ligand 2.0 mg; exchanger 0.5 mg; plasticiser 200 mg; PVC 100 mg. The whole cocktail was dissolved with THF and stirred in a sealed container for at least one hour to ensure a homogeneous mixture. The PVC membrane solution was then poured into a glass mould and covered to prevent contamination. Gradual evaporation at room temperature gave a transparent flexible PVC membrane. Discs were cut with a cork borer from master membranes and were securely fastened at the tip the electrode. The internal electrolyte was 0.1 M NaCl. Chloridised silver wires (Sentek, Ltd. Essex, UK) were used as internal reference electrodes. Fabricated electrodes were conditioned for at least 3 hours prior to use in 0.1 M NaCl and stored in 0.1M NaCl between experiments.

4.2.4 Injection experiments

Dynamic responses were estimated by injecting 0.225 mL of a 1M solution of alkali metal and alkaline earth ions (Li^+, Na^+, K^+, Cs^+, Rb^+, H^+, NH_4^+) into a stirred 25 mL aliquot of a $1x10^{-3}$ M NaCl. Transient changes in potential were recorded using a virtual instrument designed with LabView 3.0 and MIO-16 I/O card (National Instruments, Austin, Texas) fitted in a 486-PC. The concentration change in the case

of a sodium injection involves a step change of approximately one order of magnitude These injections are designed to generate an approximate ten-fold excess of the injected ion over the original Na^+ concentration (10^{-3} to 9 91x10^{-3} M)

4.2 5 Membrane dilution experiments

The PVC membrane was prepared so that the concentration of ligand **4 (iii)** was equal to 1 05x10^{-3} M The membrane was then dissolved in THF and an equal volume of plasticiser so that the ligand concentration was halved This dilution was repeated five times up to 1 59x10^{-5} M ligand At each dilution step the slope, d c resistance and selectivity (separate solution method) of electrodes based on the membrane were measured

4.2 6 pH Stability of the ISEs

Combination glass pH electrode (connected to the pH meter), and reference electrode (calomel) and four PVC membrane ISEs based on each ligand were immersed in 10^{-3} M NaCl solution A few drops of lithium hydroxide solution (ca 1M) was added to adjust the solution to pH >10 according to the glass electrode (previously calibrated in pH 4 and pH 10 buffer solutions) The potential of each ISE was measured in sequence against the calomel electrode after allowing 2 minutes for the potentials to stabilise HCl (1M) was then added drop-wise to vary the pH In this way it was possible to monitor simultaneously changes in the solution pH, and any corresponding shift in the PVC membrane potential of the four electrodes in the same solution This experiment was also carried out at 10^{-4}, 10^{-2} and 10^{-1} M NaCl so that the effect of pH on electrode slopes could be investigated

4.2.7 Monitoring proton exchange above PVC membranes

PVC membranes based on ligands **4 (ii)** and **4 (iv)** were made up with the same components and proportions as for the electrodes and were cast in the bottom of a 50 mL beaker using a total mass of components of approximately 1 5 g The membranes obtained were clear and ca 0 5 mm thick 20 mL of 0 1 M LiCl was added to the beaker and the flat-surfaced pH glass combination electrode was positioned about 1 mm above the membrane 0 1 mL of 1 M NaCl was injected into the LiCl solution using a micropipette at a position well removed from the glass electrode, and the electrode output monitored for 8 5 minutes Between experiments, the membranes were soaked for 30 minutes with milli-q water, with the water being renewed every 10 minutes, in order to ensure that any sodium taken up during the experiment was removed before commencing the next experiment

4.3 Results and Discussion

4.3 1 General Characterıstics

Electrodes made from the four lıgands showed slopes ın excess of 50 mV/decade The slopes and selectıvıty data are gıven ın Table 4-1 Selectıvıty coefficıents were estımated agaınst a range of common ınterferents by the mıxed solutıon method (dıvalent interferents) and the separate solutıon methods (monovalent ınterferents) Whıle data obtaıned by these methods are, ın general, not representatıve of the performance of an electrode ın real analytıcal sıtuatıons, they do gıve a general ıdea of the selectıvıty of the electrodes From Table 4-1 ıt would appear that ın unbuffered solutıons,

- all four electrodes are selectıve for sodıum agaınst all ıons ınvestıgated
- there ıs vırtually no dıfference ın the selectıvıty of lıgand **4 (i)** compared to lıgand **4 (iii)**, and of lıgand **4 (ii)** compared to lıgand **4 (iv)**, and,
- lıgands **4 (i)** and **4 (iii)** are more selectıve than lıgands **4 (ii)** and **4 (iv)** towards dıvalent ınterferents such as Mg^{2+} and Ca^{2+}, but the selectıvıty agaınst monovalent ınterferents ıs broadly sımılar for all four lıgands These results are ın agreement wıth previous studıes ınvolvıng the tetraesters whıch showed the tetramethyl ester **4 (i)** to be superıor to the tetraethyl ester **4 (ii)** ın terms of selectıvıty [10,12]

Ligand	**4 (i)**	**4 (ii)**	**4 (iii)**	**4 (iv)**
Slope/mV dec^{-1}	54 4	54 3	54 8	54 1
ion (j)	$\log k^{ij}_{pot}$			
K^+	-2 7	-2 0	-2 6	-2 2
Cs^+	-2 5	-2 1	-2 2	-2 0
Li^+	-2 9	-2 5	-3 2	-3 0
Ca^{2+}	-3 5	-2 6	-3 3	-2 4
Mg^{2+}	-3 7	-2 9	-3 6	-3 1
H^+	-2 0	-2 2	-2 3	-1 5
NH_4^+	-3 5	-2 7	-3 3	-3 1

Table 4-1: *Selectivity coefficients in unbuffered solutions of PVC membrane electrodes incorporating ligands* ***4 (i)-4(iv)*** *Selectivity coefficients were estimated by the separate solution method at $10^{-1}M$ concentrations of primary and interfering ions, divalent selectivities by the mixed solution method (constant $10^{-1}M$ interfering ion)*

Figure 4 8 compares the linear response and limits of detection of electrodes based on the tetramethyl ester **4 (i)**, the trimethyl ester monoacid **4 (iii)** and the tetramethyl ketone **4 (v)** in unbuffered NaCl solutions This shows that the tetramethyl ester produces the best electrode but the differences between the electrodes is very slight, and only apparent at low sodium concentrations (10^{-4}M and below, approximately) From this study it is clear that all three ligands produce electrodes with virtually the same slopes and linear range Electrodes based on all five ligands have limits of detection between 10^{-5}M and 10^{-6}M NaCl, while the slopes vary between 53 and 59 mV/ pNa depending on the batch, age, and experimental method, which is typical for PVC membrane ISEs of this type

The dynamic response of the triethyl ester monoacid **4 (iv)** is shown in Figure 4 9 There is a sharp response (≈54 mV) to the injection of an approximate 10-fold increase in concentration (10^{-3}-9 91x10^{-3} M) This is in agreement with the theoretical value of 56 2 mV for this change in sodium concentration at 20°C The injection of LiCl resulted in a decrease of potential to ca -5 mV This is due to a combination of a decrease in the sodium activity coefficient arising from increased ionic strength on injection of the LiCl and dilution effects The same lack of response was obtained for the other interfering cations (Table 4-2) confirming the excellent selectivity of the monoacid **4 (iv)** for sodium

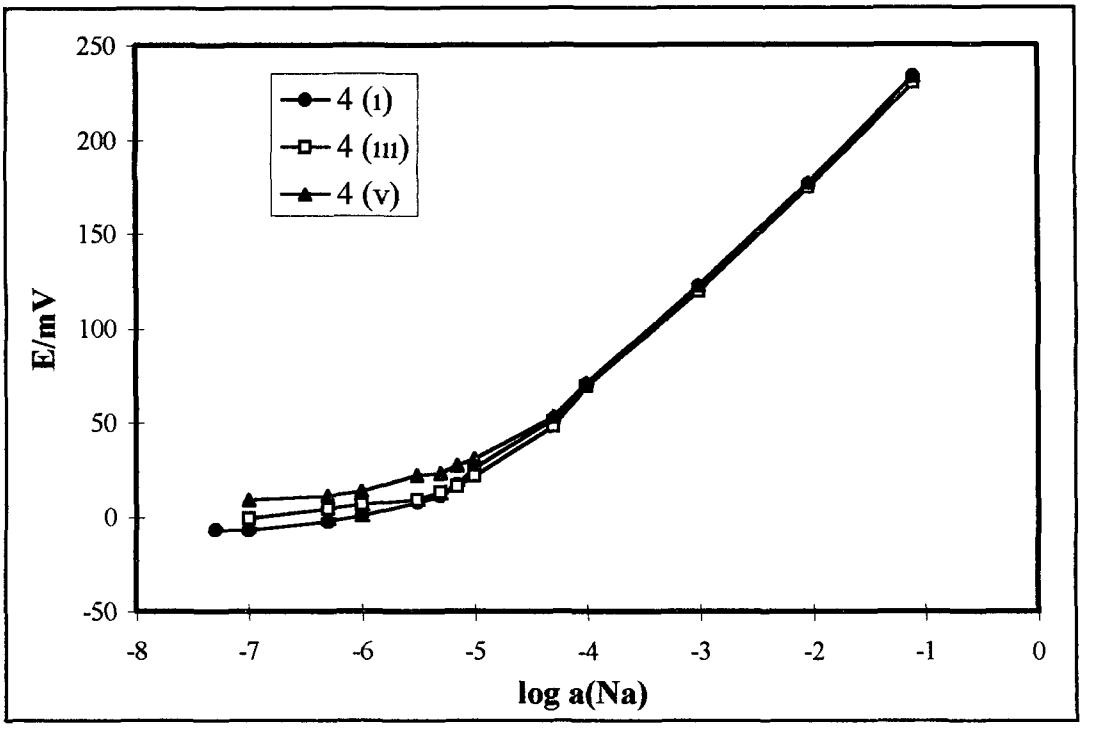

Figure 4.8: *A comparison of the linear response and limits of detection of electrodes based on the tetramethyl ester* ***4 (i)****, the trimethyl ester monoacid* ***4 (iii)*** *and the tetramethyl ketone* ***4 (v)*** *in unbuffered NaCl solutions*

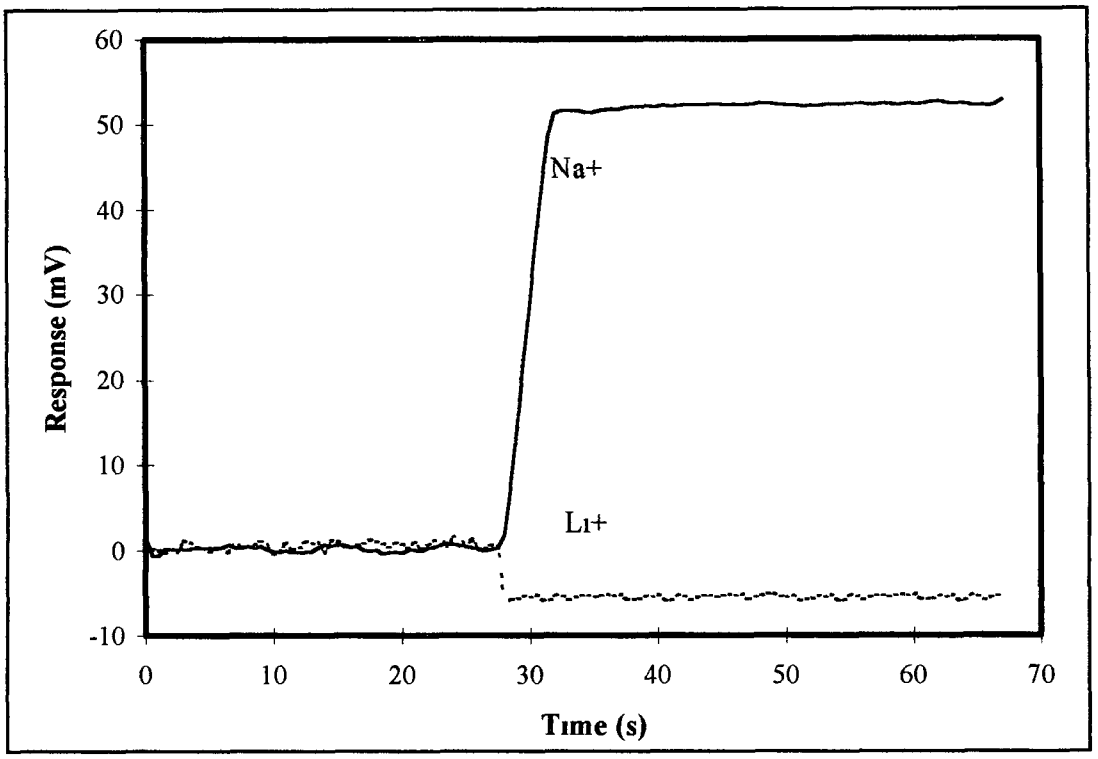

Figure 4.9: *Dynamic response of the triethyl ester monoacid 4 (iv) to injections of 0 225 mL of a 1M solution of alkali metal ions (Na^+ and Li^+ shown here) into a stirred 25 mL aliquot of 1 x 10^{-4}M NaCl which in the case of Na^+ is a ten-fold increase in concentration Transient changes in potential were recorded using a virtual instrument designed with LabView 3 0*

mV Response of the Ligands				
Injected ion	**4 (i)**	**4 (ii)**	**4 (iii)**	**4 (iv)**
Na^+	54	55	54	54
K^+	-5 0	-4 0	-2 5	-8 0
Li^+	-7 0	-5 0	-4 0	-6 0
NH_4^+	-10 0	-6 0	-5 0	-10 0
Rb^+	-6 0	-5 0	-4 0	-10 0

Table 4-2: *mV response of the Ligands to injections of 0 225 mL of a 1M solution of alkali metal ions into a stirred 25 mL aliquot of a 1 x 10^{-4} M NaCl Transient changes in potential were recorded using a virtual instrument designed with LabView 3 0*

4 3 2 Stability

A vital characteristic in any sensor is its stability with respect to time Figure 4 10 compares the stability in electrode slope over a period of 35 days for ISEs based on ligands **4 (i)-4(iv)** This shows the monoacid compounds to be as stable as both the tetramethylester and the tetraethyl ester monoacid In previous studies, our group have attempted to predict the effective lifetime of electrodes based on the tetraesters by means of ligand dilution experiments [31] which involve measuring the membrane resistance as the electrode ages, and relating these resistances to those of membranes with differing ligand concentrations The effect of diluting the concentration of ligand **4 (iii)** (trimethylester monoacid) in a PVC membrane on the membrane resistance, the electrode slope and the electrode selectivity is illustrated in Figure 4 11 These results show that for the first two dilution steps (ligand concentration decreased from 1 05x10^{-3}M to 2 55x10^{-4}M), there is little change in the membrane properties except for a decrease in slope to around 50 mV/pNa A further reduction in ligand concentration to just above 10^{-4}M causes a noticeable increase in membrane resistance, but the selectivity and slope are still relatively unchanged This suggests that while the ion flux at the membrane sample boundary is reduced somewhat due to the lower concentration of carriers, essentially the conditions for ligand-controlled permselectivity still hold However, as the concentration of carriers decreases below 10^{-4} M, the membrane resistance increases sharply, and the electrode slope and selectivity collapses (see Figure 4 11) It therefore follows that electrodes with resistances below the critical resistance should perform satisfactorily, in contrast with those with resistances above it This provides a simple diagnostic test for satisfactory electrode performance, and an approximate indicator of useful device lifetime, assuming that the rate of increase in electrode resistance remains constant

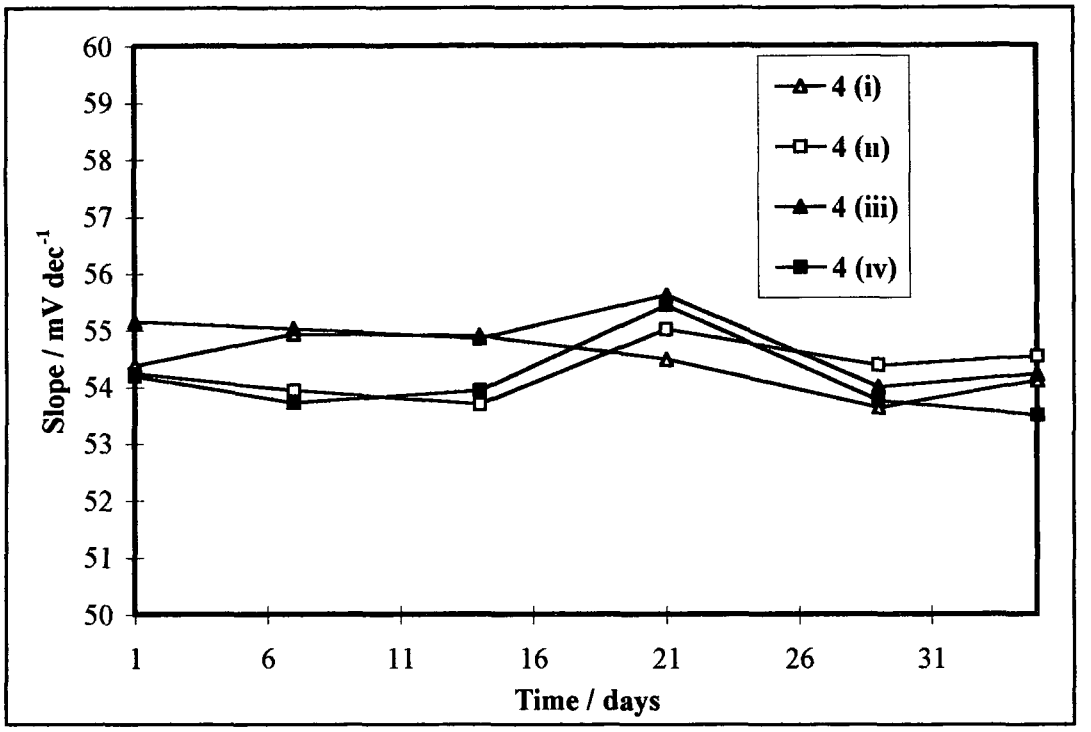

Figure 4.10 *Lifetime studies of the PVC membrane electrodes incorporating ligands 4 (i)-4 (iv) Slopes obtained over the range 1 x 10^{-1}M to 1 x 10^{-4}M NaCl solutions Units are given in mV per decade change in sodium concentration*

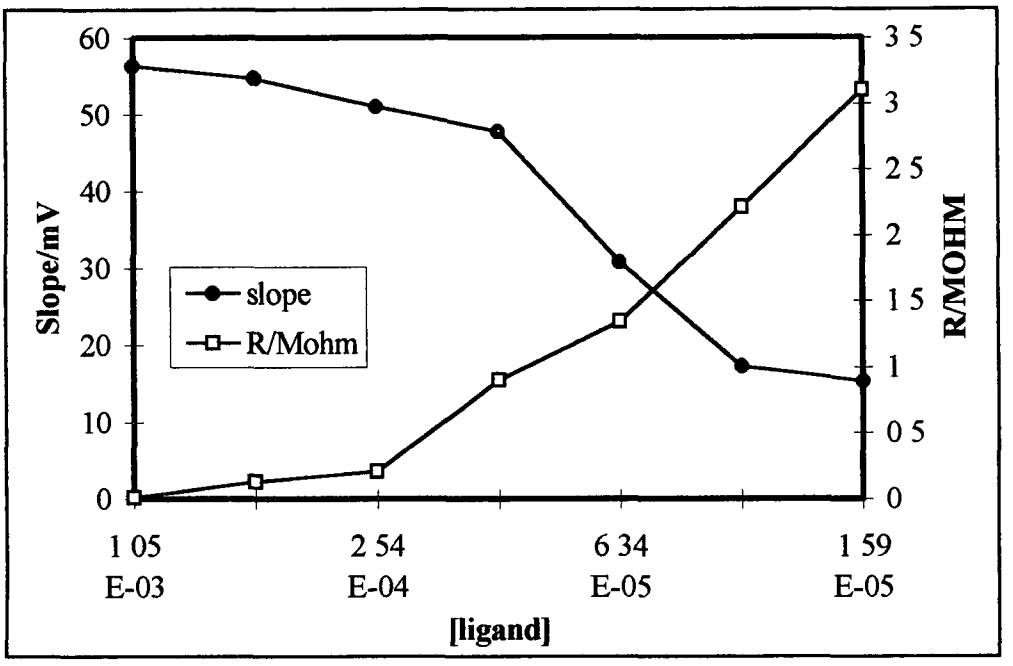

(a)

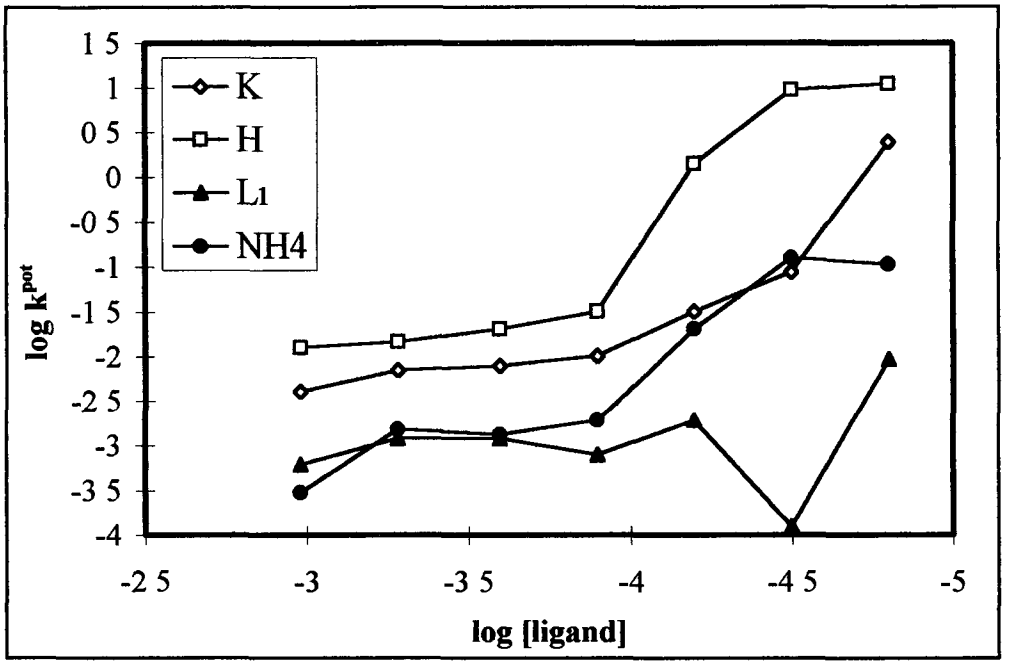

(b)

Figure 4.11: *(a) Variation of electrode slope and electrode DC resistance on dilution of ligand 4 (iii) concentration (b) Effects of electrode selectivity on dilution of membrane components*

In comparison to the tetramethyl ester [31] the resistance of this membrane (trimethyl ester) is lower by two orders of magnitude This is probably due to a different interfacial exchange mechanism or charge transport through the bulk of the membrane involving proton transport The critical concentration of ligand in this research appears to be around 10^{-4} M, which is in agreement with previous studies, [31,34] The concentration of the carrier in the membrane is important in order that there is adequate trans-membrane ionic transport system Membranes based on PVC are permselective to cations even without added ionic sites It is now well documented that anionic impurities originating from the PVC manufacturing process are responsible for permselectivity [35] The concentration of these ionic impurities must not be in excess as compared with the ligand [36] if the ligand characteristics are to predominate Since the concentration of anionic impurities in commercially available PVC was obtained as 6 $3x10^{-5}$M [37], Figure 4 11a shows the breakdown in the expected range of carrier concentration (10^{-4} to 10^{-5} M) Therefore if the concentration of the carrier approaches or falls below the concentration of the impurities present there is a breakdown in electrode slope and selectivity (Figure 4 11)

Given the low rate of leaching of these carriers into aqueous samples as evidenced by the extended lifetimes of the tetraester based electrodes [31], similarly extended lifetimes for the monoacid based electrodes can be predicted, longer than 35 days as demonstrated in this study (Figure 4 10) The main degradation of the tetraester is to the monoacid and at that stage the hydrolysis stops unless extremes of pH are applied The monoacid derivatives have the same properties as the tetraesters and this is the reason for the long sensor lifetime for these devices

4.3.3 pH Stability

All measurements presented above were made in unbuffered salt solutions (pH 5-6 typically) However, given the acidic nature of the monoacid derivatives of the

tetraesters, it is important to compare the pH stability of these ionophores The pK_a of the triethylester monoacid has been reported as 10 25 in methanol [38], and the trimethylester monoacid can be expected to be very similar However, the acidity of these groups at an aquo-boundary can be expected to be enhanced, with the effective pK_a being reduced by perhaps around 2 units [39] due to the better protolytic environment offered by the aqueous environment Hence the performance of electrodes based on the monoacids may change from that of the uncharged neutral carrier form (which is very close to the corresponding tetraester in structure and properties as demonstrated in the results presented above) to that of the deprotonated carboxylate anion In the deprotonated form, a negative charge becomes delocalised on the acid group and can be expected to affect the metal complexation behaviour of the ligand Hence at the aquo-membrane boundary region under increasingly basic conditions the monoacid will tend to be in equilibrium with its deprotonated form

The results of the pH stability experiments are presented in Figure 4 12 and Figure 4 13 The main features can be summarised as follows,

The methyl **4 (i)** and ethyl **4 (ii)** tetraester based electrodes show excellent stability over the pH range investigated (Figure 4 12) In contrast, the monoacid derivatives show peak performance at neutral pH Above this they show a positive shift in potential, beginning at pH 8 The effect of this increase is more pronounced for the trimethyl ester monoacid **4 (iii)** Above pH 10 the increase in potential is not as dramatic

The effect of pH on electrode slope is presented in Figure 4 13 These data suggest that the tetraethyl ester **4 (ii)** based electrode is slightly better than the tetramethyl ester based electrode **4 (i)**, at least at neutral and alkaline pH However, the differences between these electrodes are marginal, and may be largely accounted for by the individuality of each electrode arising from the manual method of construction

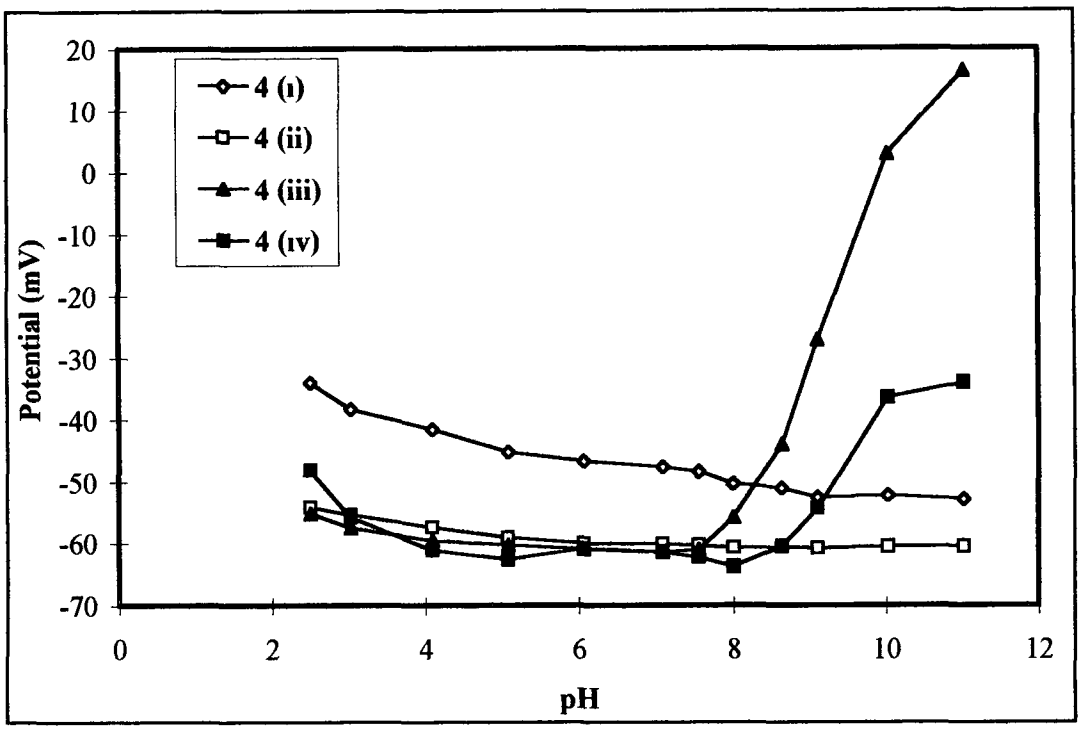

Figure 4.12: *pH stability of the ISEs measured by monitoring simultaneously changes in the solution pH and any corresponding shift in the PVC membrane potential*

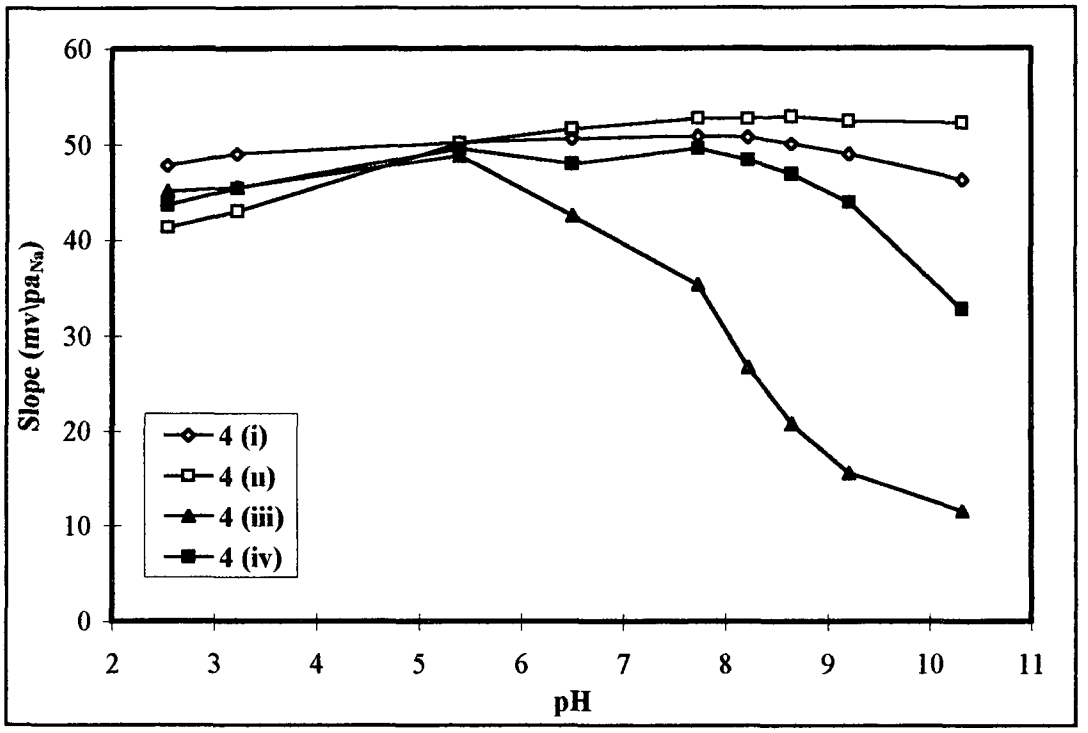

Figure 4.13: *Effect of pH on electrode slope Slopes obtained over the range 1 x 10^{-1}M to 1 x 10^{-4}M NaCl solutions*

With respect to the monoacid derivatives, the slope and linearity are similar at acid and neutral pH to the tetraesters, but diverges strikingly at alkaline pH With monoacid based electrodes, raising the pH above 8 leads to a rapid decrease in electrode slope (see Figure 4 13) Of the two, the triethyl ester monoacid **4 (iv)** is more resistant to pH effects, but even so its slope drops below 40 mV/pNa$^+$ by pH 10 31 The trimethyl ester monoacid shows an even more drastic pH dependence, beginning around pH 6 where the slope begins to decrease and becoming more apparent above pH 8 where the slope is reduced to 10 mV/pNa$^+$ by pH 10 31

From these results, we can broadly classify the effect of pH on the sodium uptake by membranes based on the monoacid ligands as follows,

- at acidic and neutral pH, the sodium response of the monoacid-based electrodes is broadly similar to that of the tetraester based electrodes This suggests that the monoacid ligands are behaving primarily as neutral carriers (i e the complexes are deprotonated)
- on moving to neutral and alkaline pH, complexation is increasingly accompanied by deprotonation Complexation with sodium ions will increase the acidity of the carboxylate group and hence render the proton more labile Evidence in favour of this is provided by the pH response in Figure 4 14 on addition of sodium ions

At more extreme alkaline pH, the monoacid ligands are probably already deprotonated at the aquo-membrane boundary prior to complexation with sodium ions leading to a loss in the proton exchange compensation mechanism (see below) and consequent reduction of potentiometric response It is now clear why the picrate extraction technique does not reveal the ion-sequestering ability of monoacids such as **4 (iii)** and **4 (iv)** The problem arises from the conditions and design of picrate extraction experiments which are indirect measurements based on spectrophotometric detection of the coloured picrate anion in the dichloromethane phase containing the ionophore after shaking with an *alkaline aqueous phase* containing metal picrate The method assumes that extraction of the metal ion from the aqueous phase is accompanied by transfer of the coloured picrate ion to maintain charge neutrality

This is undoubtedly true in many cases, providing a very convenient method for screening ionophores which may complex colourless cations However, under the alkaline conditions usually employed in this test (pH 13), the trends in our results shown in Figure 4 13 show that sodium uptake is almost certainly completely suppressed In addition, an alternative mechanism which involves the release of protons from the dichloromethane phase on complexation will maintain charge neutrality In this case, picrate ion will not be detected in the organic phase even though complexation of the target cation is occurring In contrast to the picrate extraction data, our results with monoacid triester electrodes establish that this ionophore is capable of complexing sodium ions This suggests that a mechanism similar to that just described is occurring, the essential feature being the concomitant release of a proton from the carboxylic acid moiety of **4 (iv)** in the complexation process Hence in the picrate studies, the ion pair transferred into the dichloromethane phase is the metal complex of the carboxylate anion of **4 (iv)** and not the complexed metal picrate

In order to investigate this possibility further, an experiment was designed to monitor the pH in the vicinity of PVC membranes containing the ligands cast on the bottom of a 50 mL beaker after injection of NaCl The results are summarised in Figure 4 14 These clearly show that in the case of the triethylester monoacid-doped PVC, injection of NaCl into a LiCl solution above the membrane resulted in a release of protons from the membrane, which is strong evidence for the proton exchange mechanism presented above In contrast, with the tetraethyl ester, virtually no change in the pH electrode signal occurred on injection of the NaCl solution The mechanism of proton release on complexation with a cation is also employed in chromoionophore studies using chromogenic calixarenes [40] as discussed in Chapter 3 In this case a nitrophenylazophenol calix[4]arene in the presence of a base (tridodecylamine) exhibits a decreases in absorbance at 380 nm and a corresponding increase in absorbance at 520 nm on addition of lithium ions No colour change is observed in the absence of base This colour change arises from acidity of the nitrophenylazophenol group upon metal ion complexation which facilitates the removal of the phenolic proton by the base We believe that a similar mechanism is

facilitating the removal of the proton from the carboxylic acid groups of the monoacid calixarenes in this investigation

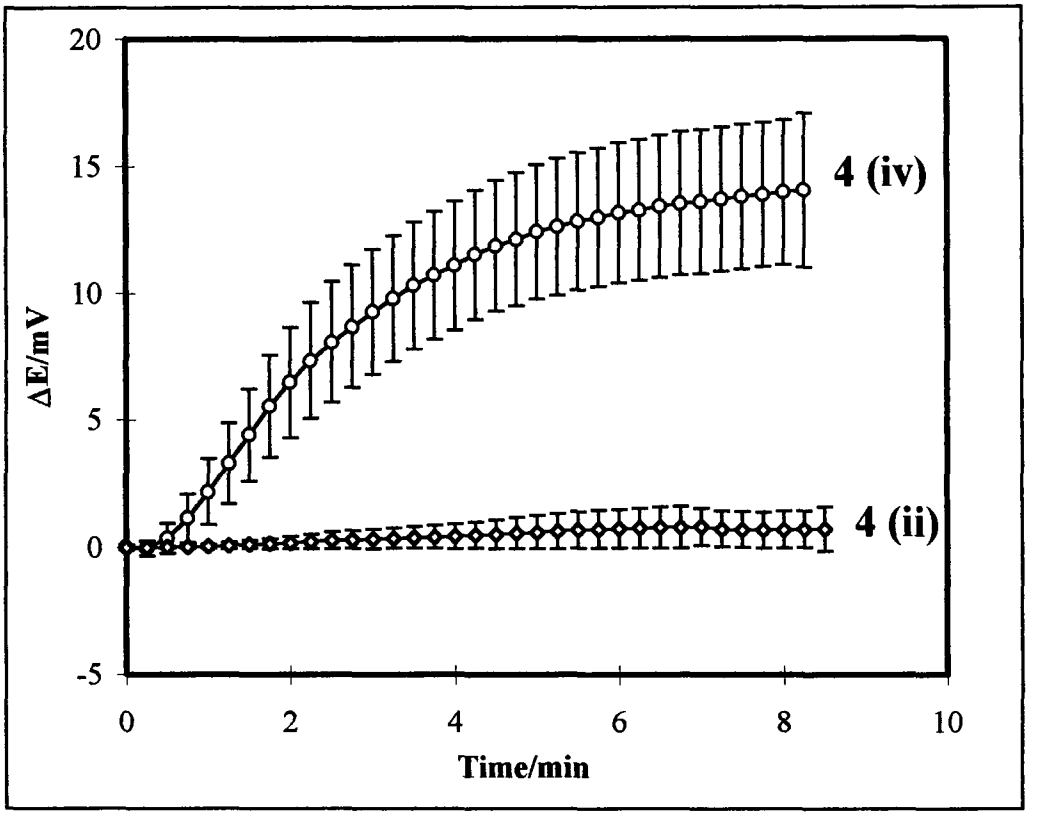

Figure 4.14: *Effect of sodium exchange on pH glass electrode potential for membranes based on the triethyl ester monoacid* ***4 (iv)*** *and tetraethyl ester* ***4 (ii).*** *Data plotted as mean of 5 runs (ligand* ***4 (ii)****) and 8 runs (ligand* ***4 (iv)****) with standard deviations as error bars*

4.4 Conclusions

The results obtained expand the range of calixarene derivatives suitable for use as ionophores in ion-selective electrodes They also explain the extended lifetimes obtained with sodium-selective electrodes based on calixarene tetraesters, despite the relative ease of hydrolysis of these ligands to their monoacid derivatives, as electrodes based on the hydrolysed products **4 (iii)** and **4 (iv)** are shown to have excellent sodium response characteristics in their own right at neutral and acidic pH values The proton mechanism proposed for complexation of metal ions by the monoacid derivatives also explain why ion transport studies based on the conventional picrate extraction method fail to give evidence of ion complexation by these ligands

4.5 References

1 W E Morf, "*Principles of Ion-Selective Electrodes and of Membrane Transport*", Elsiever, Amsterdam, 1981

2 E P Serjeant in "*Potentiometry and Potentiometric Titrations*", Wiley, New York, 1984

3 G J Moody and J D R Thomas, "*Selective Ion Sensitive Electrodes*", Merrow, Watford, 1971

4 D Ammann, W E Morf, P Anker, P C Meier, E Pretsch and W Simon, *Ion-Selective Electrode Rev* , 1983, **5**, 3

5 G J Moody and J D R Thomas, *Selective Electrode Rev* , 1991, **13**, 227

6 J Janata, M Josiwicz and D M DeVaney, *Anal Chem* , 1994, **66**, 207R

7 K M O'Connor, D W M Arrigan and G Svehla, *Electroanalysis*, 1995, **7**, 205

8 D Diamond, in Electrochemistry, Sensors and analysis (Eds M R Smyth and J G Vos), Elsevier, Amsterdam, 1986, 155

9 D Diamond and G Svehla, *Trends Anal Chem* , 1987, **6**, 46

10 D Diamond, G Svehla, E Seward and A M McKervey, *Anal Chim Acta*, 1988, **204**, 223

11 K Kimura, M Matsuo and T Shono, *Chem Lett* , 1988, 615

12 A Cadogan, D Diamond, M R Smyth, M Deasy, M A McKervey and S J Harris, *Analyst*, 1989, **114**, 1551

13 K Cunningham, G Svehla, S J Harris and M A McKervey, *Analyst*, 1993, **111**, 341

14 M Telting Diaz, D Diamond, M R Smyth, E Seward, M A McKervey and G Svehla, *Anal Proc* , 1989, **26**, 29

15 M Telting Diaz, F Regan, D Diamond and M R Smyth, *J Pharm Biomed Anal* , 1990, **8**, 695

16 M Telting Diaz, D Diamond, M R Smyth, E Seward, and M A McKervey, *Electroanalysis*, 1991, **3**, 371

17 M Telting Diaz, F Regan, D Diamond and M R Smyth, *Anal Chim Acta*, 1991, **251**, 149

18 R J Forster, F Regan and D Diamond, *Anal Chem* , 1991, **62**, 876

19 R J Forster and D Diamond, *Anal Chem* , 1992, **64**, 1721

20 D Diamond and R J Forster, *Anal Chim Acta*, 1993, **276**, 75

21 D Diamond, J Lu, Q Chen and J Wang, *Anal Chim Acta*, 1993, **281**, 629

22 G Barrett, V Bohmer, G Ferguson, J F Gallagher, S J Harris, R G Leonard, M A McKervey, M Owens, M Tabatabai, A Vierengel and W Vogt, J Chem Soc , *Perkin Trans 2*, 1992, 1595

23 A Cadogan, D Diamond, M R Smyth, G Svehla, M A McKervey, E M Seward and S J Harris, *Analyst*, 1990, **114**, 1551

24 E Lindner, E Graf, Z Niegreisz, K Toth, E Pungor and R P Buck, *Anal Chem* , 1988, **60**, 295

25 S C Ma, N A Chaniotakis and M E Meyerhoff, *Anal Chem* , 1988, **60**, 2293

26 U Schaller, E Bakker and E Pretsch, *Anal Chem* , 1995, **67**, 3123

27 U Schaller, E Bakker, U Spichiger and E Pretsch, *Anal Chem* , 1994, **64**, 391

28 E Bakker, E Malinowska, R D Schiller and M E Meyerhoff, *Talanta*, 1994, **41**, 881

29 F Arnaud-Neu, G Barrett, S J Harris, M Owens, M A McKervey, M-J Schwing-Weill and P Schwinte, *Inorg Chem* , 1993, **32**, 2644

30 M Deasy, Ph D Thesis, University College Cork, 1988

31 D Diamond and F Regan, *Electroanalysis*, 1990, **2**, 113

32 F Arnaud-Neu, E M Collins, M Deasy, G Ferguson, S J Harris, B Kaitner, A J Lough, M A McKervey, E Marques, B L Ruhl, M J Schwing and E M Seward, *J Am Chem Soc* , 1989, **111**, 8681

33 J Lu, Qiang Chen, D Diamond and J Wang, *Analyst*, 1993, **118**, 1131

34 U Oesch and W Simon, *Anal Chem* , 1980,**52**, 692

35 A van der Berg, PD van der Wal, M Skowronska-Ptasinska, E J R Sudholter, D N Reinhoudt and P Bergveld, *Anal Chem* , 1987, **59**, 2827

36 P Buhlmann, S Yajima, K Tohida and Y Umezawa, *Electrochim Acta*,1995, **40**, 3021

37 M Nagele and E Pretsch, *Mikrochim Acta*, 1995, **121** 269

38 F Arnaud-Neu, G Barrett, S J Harris, M Owens, M A McKervey, M-J Schwing-Weill and P Schwinte, *Inorg Chem* , 1993, **32**, 2644

39 E Bakker, M Lerchi, T Rosatzin, B Rusterholz and W Simon, *Anal Chim Acta*, 1993, **278**, 211

40 M McCarrick, S J Harris, D Diamond, *Analyst*, 1993, **118**, 1127

5. Characteristics of Europium-Selective Electrodes Based on Calixarene Phosphine Oxides.

5.1 Introduction

Inter- and intra-group separations of lanthanides and actinides are among the most difficult of all metal-ion separations and are important processes in strategies for management and storage of high-level radioactive waste and clean-up of decommissioned nuclear facilities [1] Environmental concerns demand that such processes be conducted with stringent attention to safety

Of particular importance in separation processes are liquid-liquid extraction and ion-exchange, both of which involve, in their simplest forms, the transfer of a charged metal ion, or a complex, from a polar aqueous phase (usually highly acidic in nuclear waste) to another immiscible phase with concomitant charge neutralisation Of the various extractants used in actinide process chemistry, neutral organophosphorous compounds are among the most useful [1] The PUREX process for plutonium/uranium separation, for example, is based on the extracting ability of tributylphosphate [2] Efforts to improve the performance of simple monofunctional organophosphorous extractants led to the development of a group of bifunctional analogues which include carbamoylmethylphosphonates [$(RO)_2PO(CO)NR'_2$] (CMPs) and carbamoylmethylphosphine oxides [$R_2POCH_2(CO)NR'_2$] (CMPOs) [3]

In this chapter, an introduction will be given into the complexation of lanthanide ions by calixarenes and this is followed by the experimental procedure and results of potentiometric measurements carried out on PVC membrane electrodes incorporating phosphine oxide derivatives of calixarenes

5.1.1 Lanthanide ions and calixarenes

Calixarenes are an exceptionally interesting group of molecules for investigation as lanthanide ion-binding reagents [4] As cyclic phenolic oligomers, they constitute macrocyclic, multidentate ligands which are readily obtained in ring sizes varying greatly with respect to lanthanide ion radii, and which can be chemically modified at the phenolic oxygen, the aromatic ring and the methylene bridges These molecules can also readily adopt conformations in which all donor atoms can be directed towards a common point However, unlike alkali and alkaline-earth complexation, high selectivity among lanthanide cations is difficult to achieve

Harrowfield *et al* confirmed, for the first time, the ability of the parent phenolic calixarene *p*-t-butylcalix[8]arene to complex lanthanide ions [5] The study was carried out in N,N-dimethylformamide by UV-Vis absorption spectrometry after deprotonation of the ligands using Et_3N in excess and it showed the simultaneous formation of a binuclear and a mononuclear complex of europium This was confirmed by X-ray crystallography Sulphonation of the para position of the phenolic calixarenes leads to water soluble compounds The binding properties of such a tetramer were studied with all the lanthanides [6]

The introduction of functional groups such as esters or amides have led to better complexing agents for lanthanides A 1 1 complex of the *p*-t-butylcalix[4]arene tetradiethylamide has been prepared with $EuCl_3$ [7] The complex is water-soluble, in contrast to the ligand which is sparingly soluble in methanol The ability of *p*-t-butylcalix[4]arene tetracarboxylic acid to bind lanthanides has also been established by extraction experiments, from water to toluene or chloroform [8] The extraction constants of the 1 2 metal ligand complexes for the water-toluene system follow the order Eu > Nd > Yb > Er > La

As a contribution to an EC programme on storage and management of nuclear waste, a number of research groups have been involved in the synthesis of novel calixarenes and have examined their ability to extract selected lanthanides and actinides

As discussed above CMPOs are commonly used as effective extractants for lanthanides and actinides [3,9] This prompted Bohmer and coworkers [10] to introduce CMPO analogous structural elements into calixarenes and to study the extraction behaviour of these compounds in comparison to the usual CMPO (Figure 5 1) All the calix[4]arene derivatives were found to be much better extractants for lanthanides and actinides than CMPO Extraction of Th (IV) and Eu (III) nitrates from 1M aq nitric acid to dichloromethane were studied With equimolar concentrations of metal and ligand (10^{-4} M) the extraction level of thorium is higher than 50% and shows no significant dependence on the length of the alkoxy chain (C_{10}-C_{18}) These CMPO-type calixarenes were able to extract more than 60% of neptunium and 95% of plutonium and americium, even when applied in concentrations as low as 0 001 M

Calixarene tetrahydroxamate were also synthesised as part of the programme to develop cost effective and efficient chelators for the specific removal of actinides [11] This chelator (Figure 5 2) was found to extract thorium (IV) into chloroform from aqueous solutions quite efficiently around pH of 2-3

McKervey *et al* have reported on the synthesis of calixarene derivatives with phosphine oxide derivatives attached to the lower rim [12] and the structures are shown in Figure 5 3 ^{1}H NMR analysis revealed that the p-tert-butyl tetramer **5 (iv)** and its dealkylated counterpart **5 (vii)** exist in stable cone conformations in solution The hexamers and octamers are conformationally mobile at ordinary temperatures as is the case with many larger calixarene derivatives The isolation of good quality crystals of the tetramer phosphine oxide **5 (iv)** offered the opportunity to probe the solid-state structure by X-ray diffraction The molecule exists in a distorted cone conformation which is best described by the angles between the four aromatic rings and the mean plane of the macrocyclic ring methylene groups The methylene carbon atoms are themselves almost coplanar Two opposing aromatic rings are almost normal to one another (96°) while the other two opposing rings are almost parallel (2°)

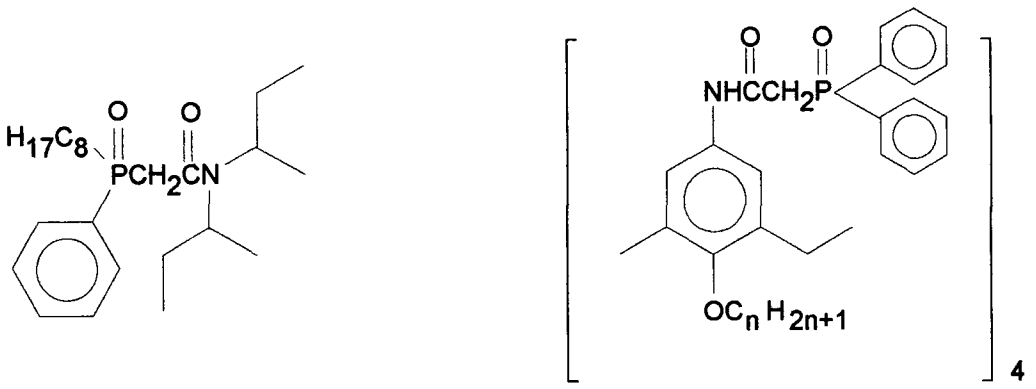

5(i) 5 (ii)

Figure 5.1: *Structures of the carbamoylmethylphosphineoxides (CMPOs) and a calixarene substituted with phosphine oxide acetamide at the upper rim [10]*

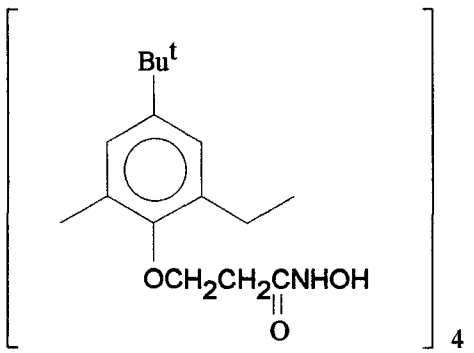

5 (iii)

Figure 5.2: *Structure of the calixarene tetrahydroxamate [11]*

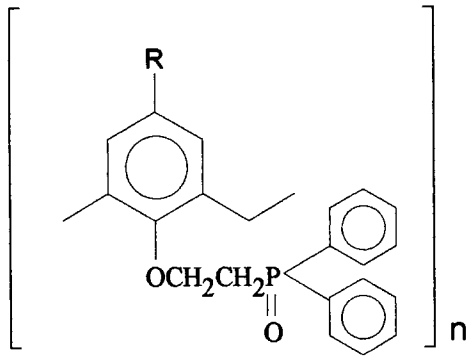

	R	n
5 (iv)	Bu^t	4
5 (v)	Bu^t	6
5 (vi)	Bu^t	8
5 (vii)	H	4
5 (viii)	H	6
5 (ix)	H	8

Figure 5.3: *Structures of the lower rim tetraphosphine oxides [12]*

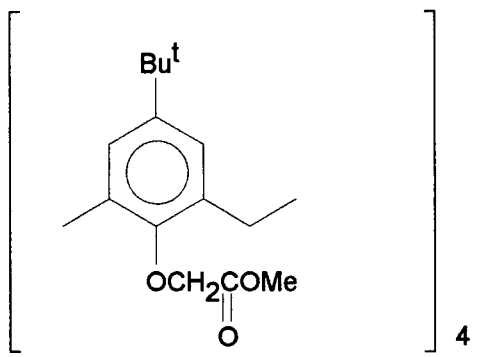

5 (x)

Figure 5.4: *Structure of the tetramethyl ester calix[4]arene*

The confines of the lower hydrophilic cavity are defined by the positions of the four phenolic oxygen atoms and the four phosphine oxide residues, the distortion of the cone being highlighted by the distances, 3 50 Angstroms and 5 22 Angstroms between phenolic oxygen atoms across the cavity

The primary objective was to study the extraction of thorium and europium, the former as a model for tetravalent, and the later as a model for trivalent actinides, and to apply the results to the extraction of simulated nuclear waste containing sodium nitrate and nitric acid Preliminary extractions of thorium (IV) picrate and europium (III) picrate with the calixarene phosphine oxides from neutral aqueous solution into dichloromethane, demonstrated that all compounds were active phase-transfer agents under these conditions However, water at pH 7 provides a very inadequate simulation of the conditions for extracting lanthanides or actinides from strongly acidic nuclear waste Therefore it was decided to study the extraction of metal nitrates from 1 mol dm^{-3} nitric acid into dichloromethane All six of the calixarene derivatives were efficient extractants for thorium (IV) In general the absence of a *p*-t-butyl group significantly increases the extraction efficiency towards thorium Europium was found to be less extracted than thorium

In conjunction with this research carried out by McKervey, it was decided to investigate the selectivity of ion-selective polymeric membrane electrodes based on the calixarene phosphine oxide derivatives, **5(iv), 5 (v) and 5 (vii),** for the detection and estimation of europium The selectivity and response of the electrode containing **5 (iv)** is compared with that of an electrode incorporating the tetramethyl ester calix[4]arene **5 (x).** As far as we are aware, this is the first use of any type of phosphine oxide as a sensor in an ISE and the first report of an ISE for a lanthanide ion

5.2 Experimental

5 2.1 Materials

All alkali chlorides were of analytical reagent grade obtained from Aldrich or Riedel-de Haen Membrane plasticiser, *o*-nitrophenyl octyl ether (*o*-NPOE), ion-exchanger potassium tetrakis(*p*-chlorophenyl)borate (KTpC1PB), poly(vinyl chloride) (PVC) and selectophore tetrahydrofuran (THF) were obtained from Fluka De-ionised Milli-Q grade water was used throughout

5.2.2 Equipment

ISE measurements (in millivolts) were made relative to a Metrohm capillary tip saturated calomel electrode (SCE) with a Hewlett Packard μV meter in high impedance mode (Model 34401A) Computer-based data acquisition was via an MIO-16 I/O card (National Instruments, Austin, Texas, USA) and virtual instrument software developed in-house using the LabView environment (v 3 0) For transient capture and FIA experiments, an acquisition rate of 2 Hz and PC platform of 486-33 MHz was used

The ISE-EMF measurements were carried out on cells of the type

Hg, Hg_2Cl_2/ KCl (satd)/ sample/ PVC membrane/ 0 1M EuCl / $AgCl_2$/Ag

5 2.3 Electrode Fabrication

PVC membrane electrodes were prepared by a standard procedure as described in Chapter 4 The PVC cocktail composition was as follows, ligand 2 0 mg, KT*p*C1PB 1 0 mg, *o*-NPOE 200 mg, PVC 100 mg Discs from the master membrane were securely attached to the tip of a home-made electrode body using a tight-fitting plastic ring and filled with 0 1 M $EuCl_3$ internal electrolyte Chloridised silver wires (Sentek Ltd , Essex, UK) were used for internal contact Fabricated electrodes were conditioned for at least 30 minutes prior to use and stored in 0 1M $EuCl_3$ between experiments Disks cut from the same membrane were used in a flow-cell (FISE 101, EDT Instruments Ltd , Dover, Kent, UK) for FIA experiments

5.2.4 Injection Experiments

Dynamic responses were estimated by injecting 0 225 mL of 1M solutions of the metal ions (Eu^{3+}, Li^{+}, Na^{+}, K^{+}, NH_4^{+}, La^{3+}) into a stirred 25 mL aliquot of a $1x10^{-3}$ M $EuCl_3$ solution producing a ten-fold excess of the injected ion Transient changes in potential were recorded using a virtual instrument designed with LabView 3 0 This experiment was repeated using a similar PVC membrane containing the tetra methyl ester calix[4]arene **5 (x)** which is a known sodium selective ligand

5 2 5 Lifetime experiments

The lifetime of the electrode was studied by periodically re-calibrating the electrode in standard solutions and calculating the response slope over the range 10^{-4} M to 10^{-1} M $EuCl_3$

5 2 6 FIA experiments

A calibration in the range 10^{-2} M to 10^{-4} M was carried out using flow injection analysis The carrier composition was 10^{-7} M $EuCl_3$ in 10^{-1} M KCl, and the calibration standards were prepared so that the ionic strength was also equal to 10^{-1} M using KCl as the ionic strength adjuster Data capture and control of FIA system was effected via a LabView Virtual Instrument front panel [13] An injection volume of 150 µL with a flow rate of 1 mL/minute was used and all injections were carried out in triplicate

5.3 Results and discussion

5 3 1 Comparison of ligand **5(iv)** and **5 (x)**

5 3 1 1 General characteristics

The electrode based on ligand **5 (iv)** showed a sub-Nernstian slope of 15 1 ± 0 8 mV/decade (n=5) $EuCl_3$ over the range studied A possible reason for this is the well known hydrolysis of the lanthanides which results in lower free-ion concentration This interpretation is supported by identical measurements in standards buffered at pH 3 2 with potassium hydrogen phthalate and HCl to suppress the hydrolysis, which resulted in slopes of 18 2 ± 0 4 mV/decade (n=5) This compares very well with the theoretical slope of 19 7 mV/decade for a trivalent ion at 25°C

5 3 1 2 Selectivity coefficients

The selectivity coefficients for this electrode and for comparison, those of the tetramethyl ester calixarene **5 (x)**, are given in Table 5-1 The coefficients were obtained against a range of common interferents by the mixed solution method (divalent interferents) and the separate solution method (monovalent interferents) [14] While data obtained by these methods are, in general, not representative of the performance of an electrode in real analytical situations, they do give a general idea of the selectivity of the electrodes From Table 5-1 it would appear that the electrode shows good selectivity to all the interfering cations examined except Ca^{2+} where the $\log k_{Eu,Ca}^{pot} = 1\ 2$

Ligand	5 (iv)	5 (x)
	$\log k_{ij}^{pot}$	
Na^+	-2 0	0 0
K^+	-2 6	-2 7
NH_4^+	-1 8	-3 5
Li^+	-1 0	-2 9
Ca^{2+}	1 2	-3 5
Mg^{2+}	-2 1	-3 7
Eu^{3+}	0 0	-3 7
La^{3+}	-1 8	-5 1

Table 5-1: *Selectivity coefficients of the PVC membrane electrode incorporating the tetra phosphine oxide (ligand* ***5 (iv)****) and the tetra methyl ester calixarene (ligand* ***5 (x)****) Selectivity coefficients were estimated by the separate solution method at* 10^{-1} *M concentrations of primary and interfering ions, divalent selectivities by the mixed solution method*

In contrast to the well-known behaviour of many tetraester and tetraketone-based electrodes, there is virtually no response to sodium ions (log $k_{Eu,Na}^{pot}$= -2 0) Interestingly, the data suggests that the ligand may be selective within the lanthanide series itself (log $k_{Eu,La}^{pot}$ = -1 8) The results of the injection experiments discussed below also support this evidence of selective complexation within the Lanthanides

5 3 1 3 Stability

A vital characteristic of any sensor is its stability with respect to time The electrode showed good stability over a period of 20 days with the slope (10^{-4}-10^{-1} M $EuCl_3$) never dropping below 15 mV/decade

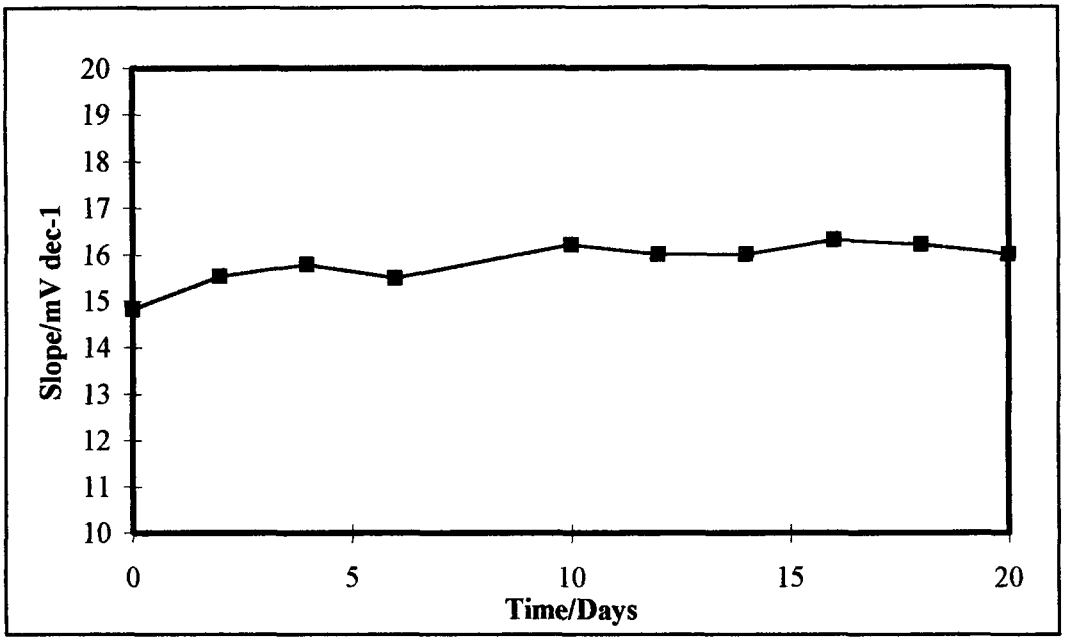

Figure 5.5: *Lifetime studies Slope (mV/decade) vs time for the electrode containing the t-butyl tetraphosphine oxide calix[4]arene* ***5 (iv)*** *Slopes calculated over the* 10^{-1} *M -* 10^{-4} *M concentration range of* $EuCl_3$

5 3 1 4 Injection experiments

The dynamic response of tetraphosphine oxide **5 (iv)** to a ten-fold increase in Eu(III) concentration (10^{-3} M to 10^{-2} M $EuCl_3$) is shown in Figure 5 6 There is a sharp response to the change in concentration of europium up to 17 mV which is almost the theoretical value However, a similar injection of $LaCl_3$ into 10^{-3} M $EuCl_3$ resulted in a smaller increase in potential of 6 mV which supports the separate solution measurements indicating that some selectivity within the lanthanide series may exist For an equivalent sodium injection there was only a slight increase of about 2 mV and similar changes in potential were obtained with injections of other cations (Li^+, Na^+, K^+, NH_4^+ Mg^{2+}, La^{3+}) as shown in Table 5-2, demonstrating that ligand **5 (iv)** is selective for europium Calcium was the only other ion to generate a significant response (15 mV, theoretical response is 29 6 mV/decade at 25°C) Interestingly, these results suggested that the electrode could be used for Ca^{2+} measurements with excellent selectivity against common interferents, particularly Mg^{2+} This was found to be true with the outcome of a calcium selective electrode incorporating ligand **5 (iv)** exhibiting near-Nernstian slopes (26 3 mV/decade) and excellent selectivity against common cations, including magnesium (log $k_{Ca,Mg}^{pot}$ = - 2 6) [15]

For comparison, Figure 5 7 shows the dynamic response of the calix[4]arene tetramethyl ester **5 (x)** based electrode to a ten-fold increase in concentration (10^{-3} M to 10^{-2} M NaCl) As expected, there is a fast, almost theoretical, response to sodium (56 mV) Identical injections of europium and lanthanide produced only a slight increase in potential of around 5 mV These experiments demonstrate the striking difference in selectivity between ligands **5 (iv)** and **5 (x)** This difference in selectivity between the two ligands produced by replacement of the carbonyl groups of ligand **5(x)** by the phosphine oxide groups in ligand **5 (iv)** results in an ionophore that is highly selective for complexation of europium against sodium

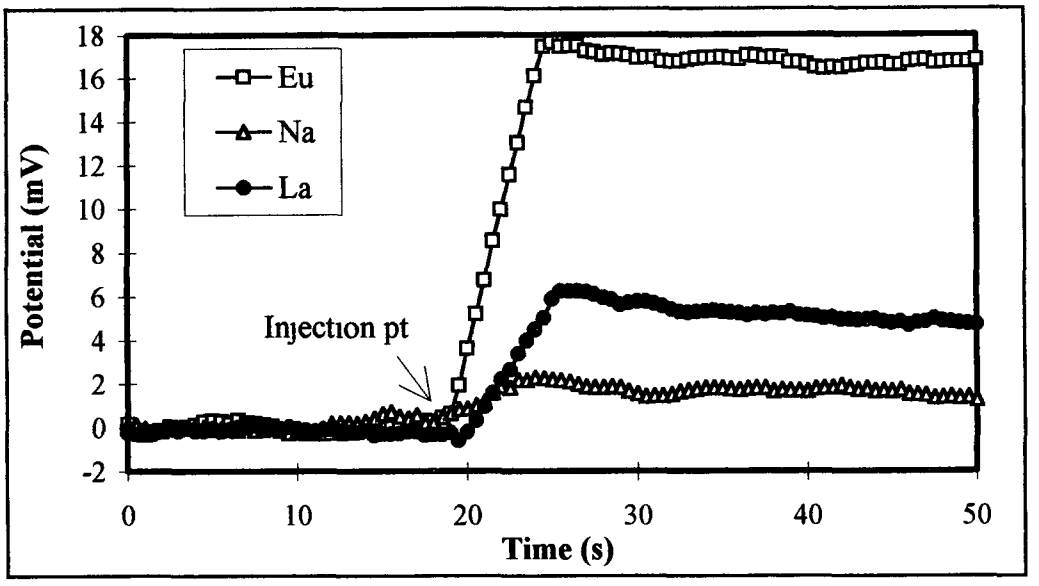

Figure 5.6: *Response of PVC membrane electrode incorporating ligand* ***5 (iv)****, tetraphosphine oxide, to injections of 0 225 mL of a 1M solution of various metal ions into 25 mL of 10^{-3} M $EuCl_3$ solution producing a ten-fold excess of the injected ion Theoretical response is 19 7 mV at 25°C*

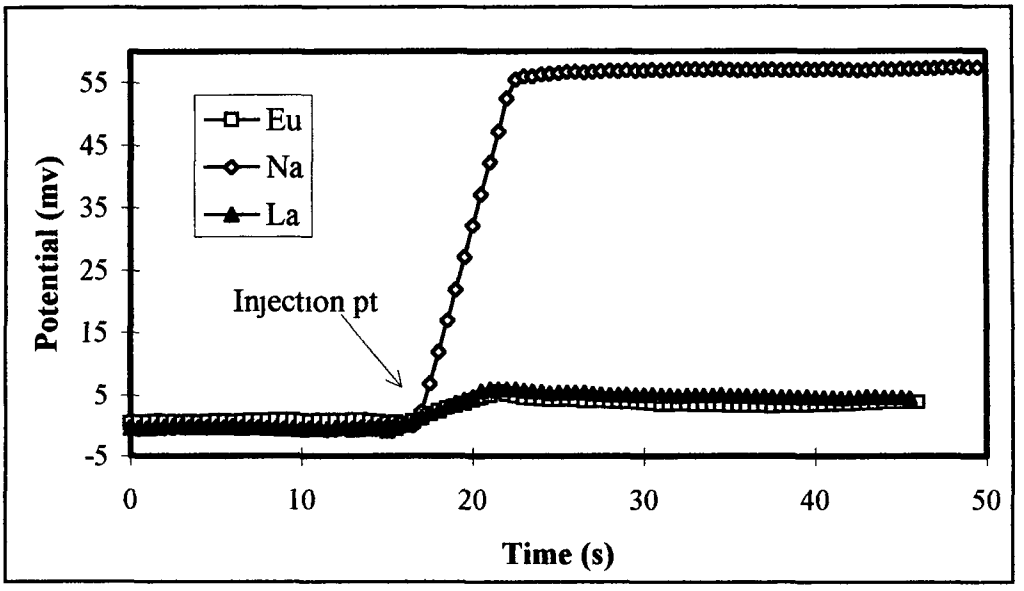

Figure 5.7: *Response of PVC membrane electrode incorporating ligand* ***5 (x)****, tetramethyl ester, to injections of 0 225 mL of metal ion solutions (1 M) into 25 mL of 10^{-3} M NaCl solution producing a ten-fold excess of the injected ion Theoretical response is 59 2 mV at 25°C*

Ligand	5 (iv)	5 (x)
Cations	Change in potential (mV)	
Na^+	1 8	55
K^+	1 0	-5 0
NH_4^+	0 0	-6 0
Li^+	2 2	-6 0
Ca^{2+}	15 0	-4 0
Mg^{2+}	0 0	-4 0
Eu^{3+}	18 0	5 0
La^{3+}	6 0	5 0

Table 5-2: *Change in potential obtained by injecting 225 μL of a variety of metal ions into a 25 mL aliquot of 1 x 10^{-3} M of the primary cation ($EuCl_3$ and NaCl in the case of* ***5 (iv)*** *and* ***5 (x)*** *respectively) causing a ten-fold excess of the injected ion*

5 3 1 5 FIA experiments

Figure 5 8 shows an FIA trace obtained for injections of 10^{-4} M, 10^{-3} M and 10^{-2} M $EuCl_3$ (in 0 1 M KCl) using a carrier of 10^{-7} M $EuCl_3$ and 10^{-1} M KCl at a flow rate of 1 mL /min The peak height increases with increasing concentration and the peak heights are also reproducible The signal is slow to return to baseline for the three concentrations investigated This could be rectified by reducing the size of the sample loop and also by reducing the membrane thickness Increasing the flow rate may also reduce the drift in the signal In Figure 5 9 the response to a ten-fold increase (10^{-4} M to 10^{-3} M) in europium (III) concentration indicates a fast and reproducible response to europium (III) The carrier used in this case was 10^{-4} M $EuCl_3$ and 0 1 M KCl This dynamic response to europium (III) suggests that the sensor could be used in continuous monitoring or automated analysis

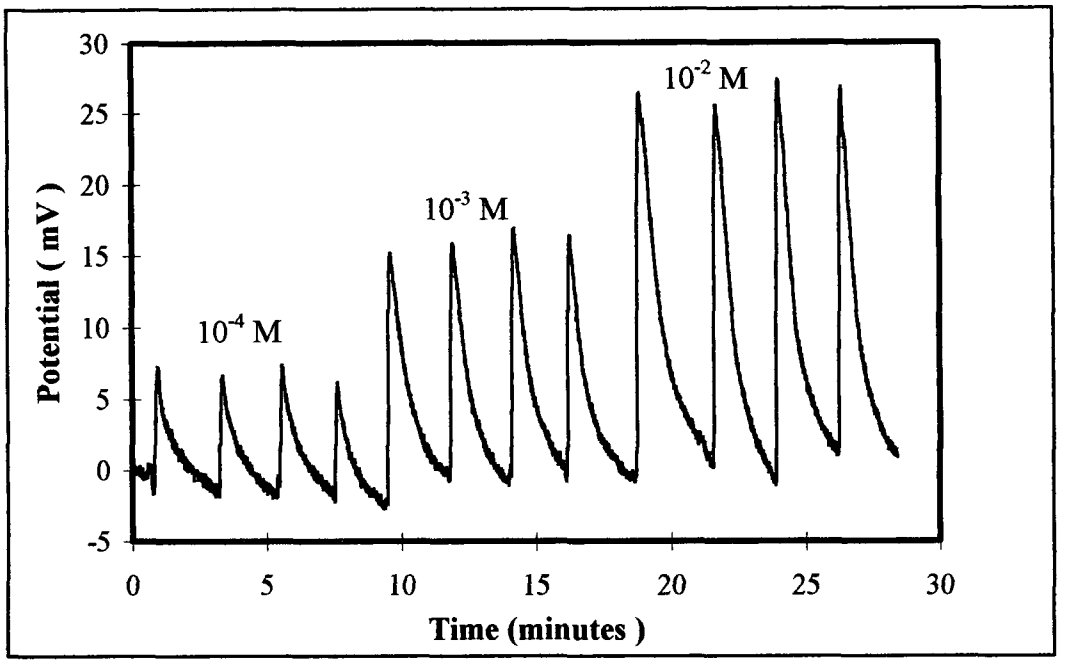

Figure 5.8: *FIA trace obtained for injections of 10^{-4} M to 10^{-2} M $EuCl_3$ (adjusted to an ionic strength of 0 1 M using KCl) with a carrier containing 10^{-7} M $EuCl_3$ and 0 1 M KCl An injection volume of 150 µL with a flow rate of 1 mL /min was used throughout*

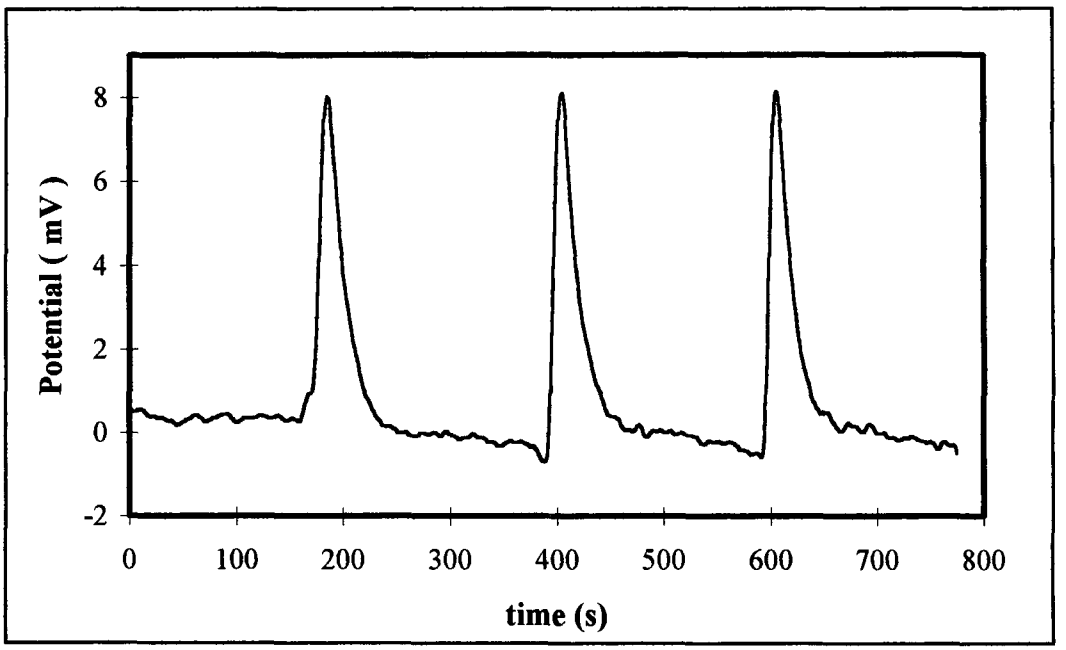

Figure 5.9: *FIA trace showing peaks obtained on injection of 10^{-3} M $EuCl_3$ (adjusted to ionic strength of 0 1 M using KCl) with a carrier containing 10^{-4} M $EuCl_3$ and 0 1 M KCl, resulting in a ten-fold increase in concentration of $EuCl_3$*

5.3.2 Ligands **5 (v)** and **5 (vii)**

The *p-t*-butyl calix[6]arene phosphine oxide **5 (v)** and the dealkylated tetraphosphine oxide **5 (vii)** were also investigated for their selectivity

5 3 2 1 General characteristics

The electrode based on the hexameric phosphine oxide calix[6]arene **5 (v)** gave an average slope of 16 6 ± 0 7 mV/decade $EuCl_3$ over the range studied The average slope for the dealkylated tetramer **5 (vii)** was found to be 17 2 ± 0 6 mV These slopes are slightly higher than that obtained for the *p*-t-butyl phosphine oxide calix[4]arene **5 (iv)** When the calibrations were carried out in buffered solutions, the slopes were improved to 18 2 and 18 5 mV/decade for **5 (v)** and **5 (vii)** respectively (Theoretical slope = 19 7 mV/decade for a trivalent ion at 25° C)

5 3 2 2 Selectivity coefficients

The selectivity coefficients for the two electrodes are shown in Table 5-3 It would appear that the two electrodes are not as selective as ligand **5 (iv)** However the selectivity over calcium is improved with ligand **5 (v)** where the log $k_{Eu,Ca}^{pot}$ = -1 0 The selectivity over sodium is not as good as ligand **5 (iv)** with log $k_{Eu,Na}^{pot}$ values of -0 8 and -0 9 for ligand **5 (v)** and **5 (vii)** respectively Interestingly, the data suggests that the ligand **5 (vii)** may be selective within the lanthanide series itself (log $k_{Eu,La}^{pot}$ = -1 1)

Ligand	5 (v)	5 (vii)
	$\log k_{ij}^{pot}$	
Na^+	-0 8	-0 9
K^+	-0 5	-1 1
NH_4^+	-0 1	-0 9
Li^+	-0 6	0 5
Ca^{2+}	-1 0	0 2
Mg^{2+}	-1 5	-1 8
La^{3+}	-0 6	-1 1

Table 5-3: *Selectivity coefficients of the PVC membrane electrode incorporating the hexaphosphine oxide calixarene (ligand* ***5 (v)****) and the dealkylated tetraphosphine oxide calixarene (ligand* ***5 (vii)****) Selectivity coefficients were estimated by the separate solution method at* 10^{-1} *M concentrations of primary and interfering ions, divalent selectivities by the mixed solution method*

5 3 2 3 Stability

Both electrodes appear to be stable over a period of 20 days with the slope (measured over the range 10^{-4} M-10^{-1} M $EuCl_3$) never falling below 16 mV/decade The variation of the slope with time is illustrated in Figure 5 10

5 3 2 4 Injection experiments

Figure 5 11 shows the dynamic response of the electrode incorporating the hexaphosphine oxide calix[6]arene There is a Nernstian response to both Eu^{3+} and La^{3+} with the potential reaching about 20 mV in each case in contrast to ligand **5 (iv)** where there appeared to be some selectivity within the lanthanide series For an equivalent sodium injection there was only a slight increase in potential up to 4 mV Table 5-4 gives the changes in potential on the injection of other interfering cations The small increase in potential on injection of Ca^{2+} supports the evidence of selectivity over calcium as seen in the selectivity coefficient results

There is a near-theoretical response to Eu^{3+} with ligand **5 (vii)** as shown in Figure 5 12 but there is considerable drift as the membrane potential is decreasing slowly, so ΔE depends on when you measure After 60 seconds the change in potential is approaching 20 mV The same drift in potential occurs on injection of La^{3+} and after 60 seconds the change in potential is equal to 15 mV which suggests selectivity within the lanthanides as was demonstrated in the selectivity coefficient measurements (Table 5-3) On injection of sodium the potential rises to about 7 mV On examination of the data in Table 5-4 there is considerable response to a number of injected ions, namely Li^+ and Mg^{2+} with the potential rising to 16 and 10 mV respectively A large increase in potential occurs on the addition of Ca^{2+} up to 25 mV which is close to the Nernstian response for a divalent cation

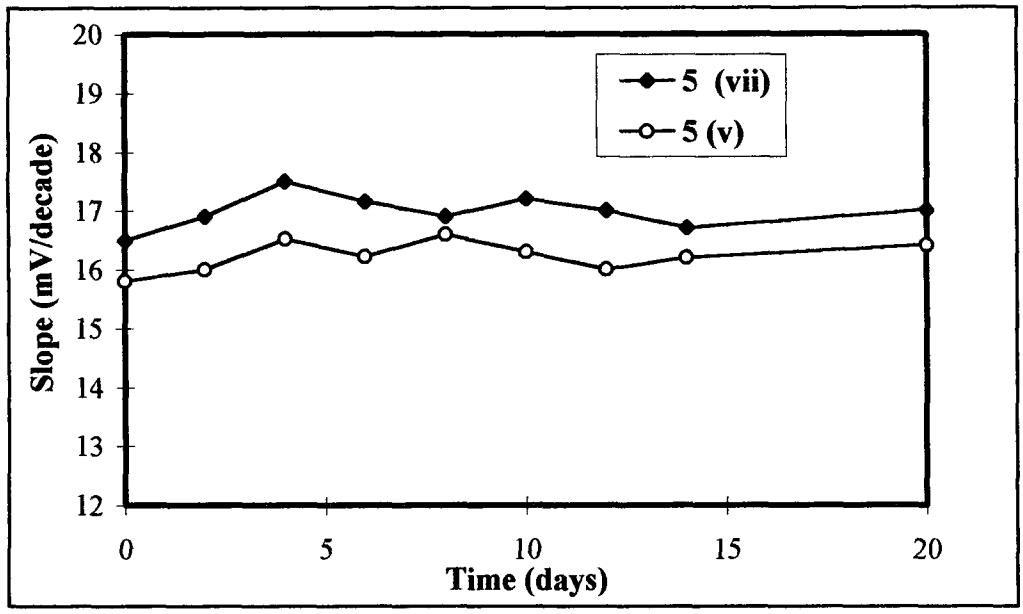

Figure 5.10: *Lifetime studies Slope (mV/decade) vs time for the electrode containing the hexaphosphine oxide calix[6]arene* ***5 (v)*** *and the dealkylated tetramer* ***5 (vii)*** *Slopes calculated over the* 10^{-1} *M -*10^{-4} *M concentration range of* $EuCl_3$

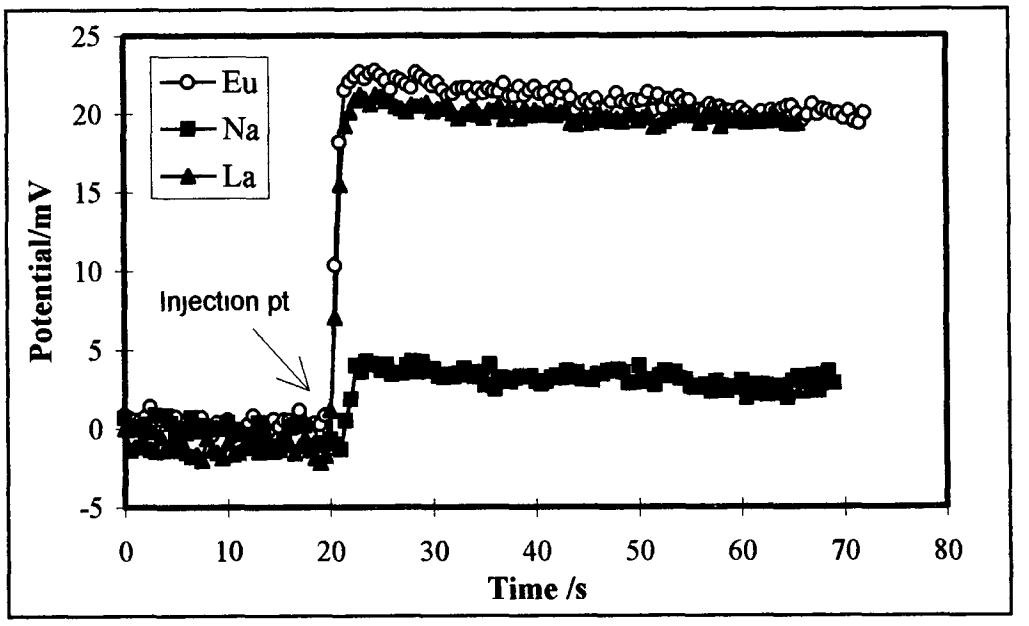

Figure 5.11: *Response of PVC membrane electrode incorporating ligand 5 (v), hexaphosphine oxide, to injections of 0 225 mL of a 1M solution of various metal ions into 25 mL of 10^{-3} M $EuCl_3$ solution producing a ten-fold excess of the injected ion Theoretical response is 19 7 mV at 25°C*

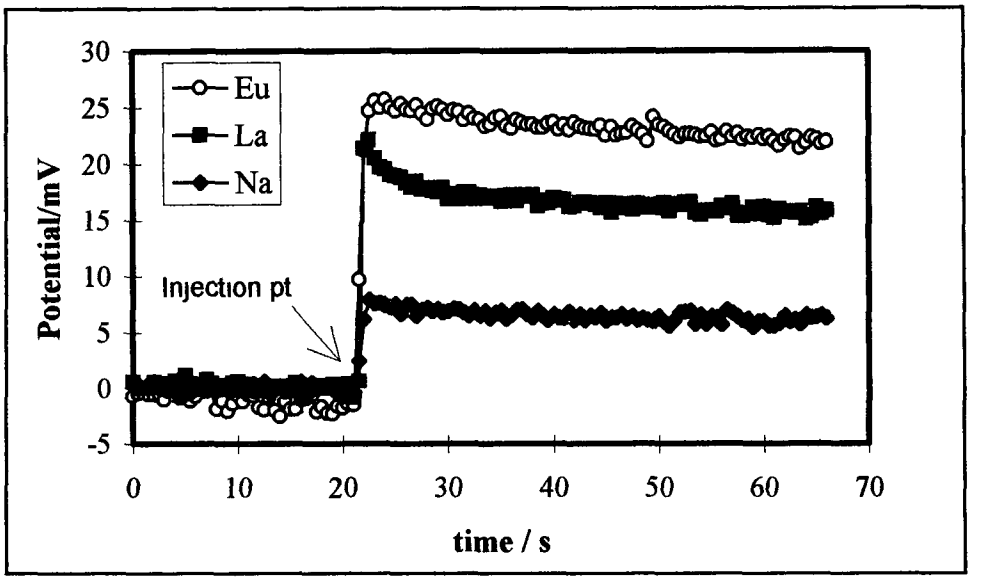

Figure 5.12: *Response of PVC membrane electrode incorporating ligand 5 (vii), dealkylated tetramer, to injections of 0 225 mL of metal ion solutions (1 M) into 25 mL of 10^{-3} M NaCl solution producing a ten-fold excess of the injected ion. Theoretical response is 19 7 mV at 25°C*

Ligand	5 (v)	5 (vii)
Cations	Change in potential (mV)	
Na^+	5 0	7 0
K^+	3 0	4 0
NH_4^+	1 0	5 0
Li^+	-4 0	16 0
Ca^{2+}	2 0	25 0
Mg^{2+}	4 0	10 0
Eu^{3+}	20 0	21 0
La^{3+}	23 0	17 0

Table 5-4: *Change in potential obtained by injecting 225 μL of a 1 M solution of a variety of metal ions into a 25 mL aliquot of 1 x 10^{-3} M of the primary cation ($EuCl_3$) causing a ten-fold excess of the injected ion*

From these results it would appear that the two ligands investigated in this study are not as selective as the *p*-t-butyl phosphine oxide calix[4]arene **5 (iv)** As discussed earlier this ligand has a rigid distorted cone conformation and the orientation of the substituent groups are arranged in such a way that the calixarene can selectively bind Eu^{3+} in the presence of other cations and the results even suggest selectivity within the lanthanide series itself

The energy minimised structure of ligand **5 (iv), 5 (vii)** and **5 (v)** are shown in Figure 5 13, Figure 5 14 and Figure 5 15 respectively, showing the side and top view of the molecules The structure were minimised using Hyperchem v 4 0 which employs molecular mechanics with the force field MM^{+} The following algorithms were also employed, Steepest Decent, Polak-Ribiere and Newton-Raphson Light blue = Carbon atoms, red = oxygen atoms and phosphorous atoms = yellow Hydrogen atoms are not shown for clarity The interatomic distances measured between *p*-t-butyl phosphine oxide calix[4]arene, **5 (iv)**, and the dealkylated tetramer **5 (vii)** illustrate that the molecules are very similar in conformation However, the dealkylated tetramer would result in a molecule that is conformationally mobile due to the lack of the bulky t-butyl groups on the upper rim The groups attached to the lower rim of the calixarene may pass through the annulus of the macrocyclic ring by rotation about the Ar-CH_2 bonds and thereby assume other conformations Therefore, eventhough **5 (iv)** and **5 (vii)** are structurally similar, the conformational mobility of **5 (vii)** would result in a less rigid cavity which may explain the decrease in selectivity observed for this ligand

The hexameric substituted calix[6]arene **5 (v)** results in a cavity of much larger dimensions than the tetramer as shown in Figure 5 15 For example the distance between the phenolic oxygens of the tetraphosphine oxides are 3 6 Å and 5 2 Å for opposing rings, for the hexamer these distances have increased to 12 8 Å and 14 6 Å The decrease in selectivity seen with the hexamer **5 (v)** is probably due to this increased cavity size with the ligand being able to accommodate La^{3+} to much the same extent as Eu^{3+} (Figure 5 11)

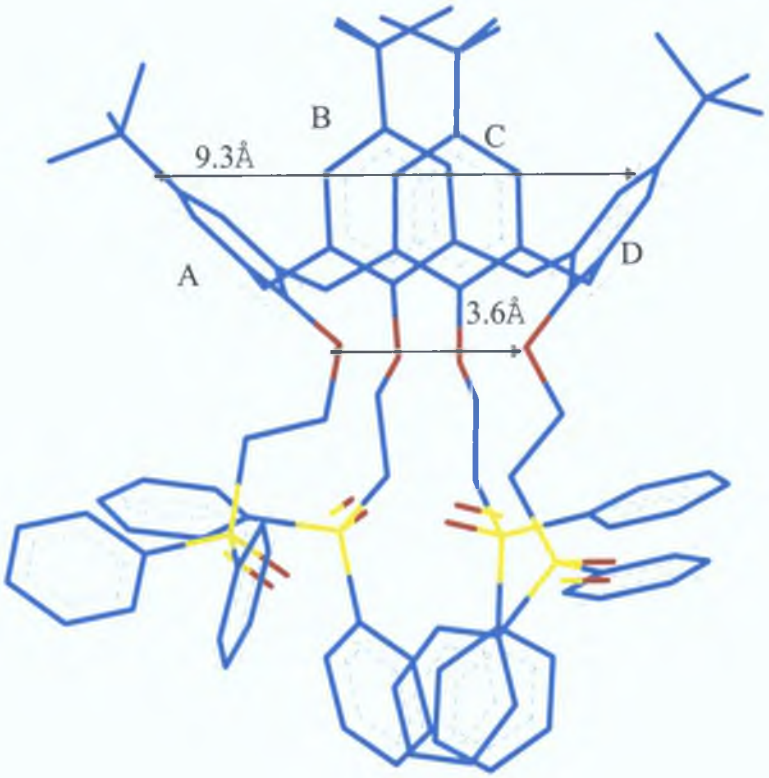

Side view

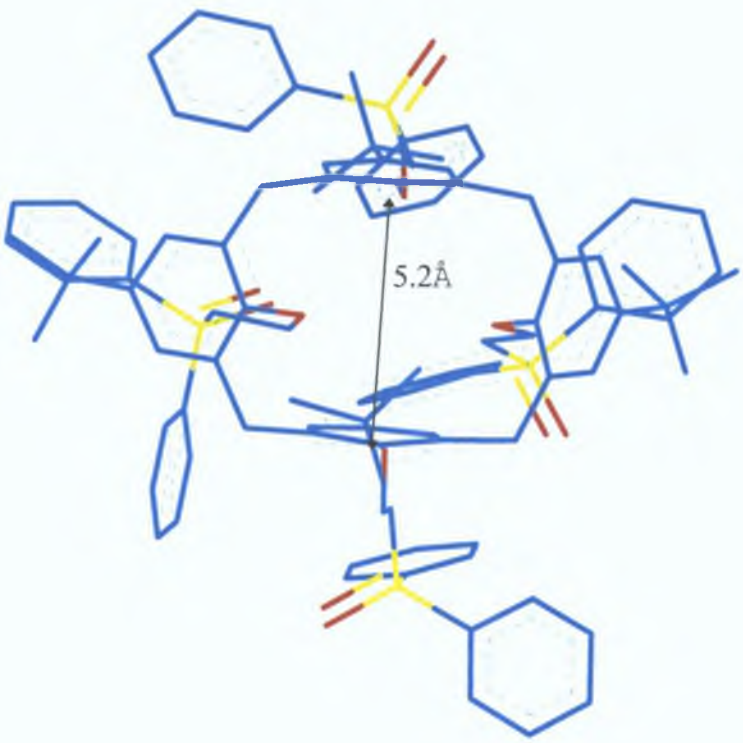

Top view

Figure 5.13: *3-d energy minimised structure of the tetraphosphine oxide calix[4]arene* ***5 (iv)*** *obtained using Hyperchem v.4.0.*

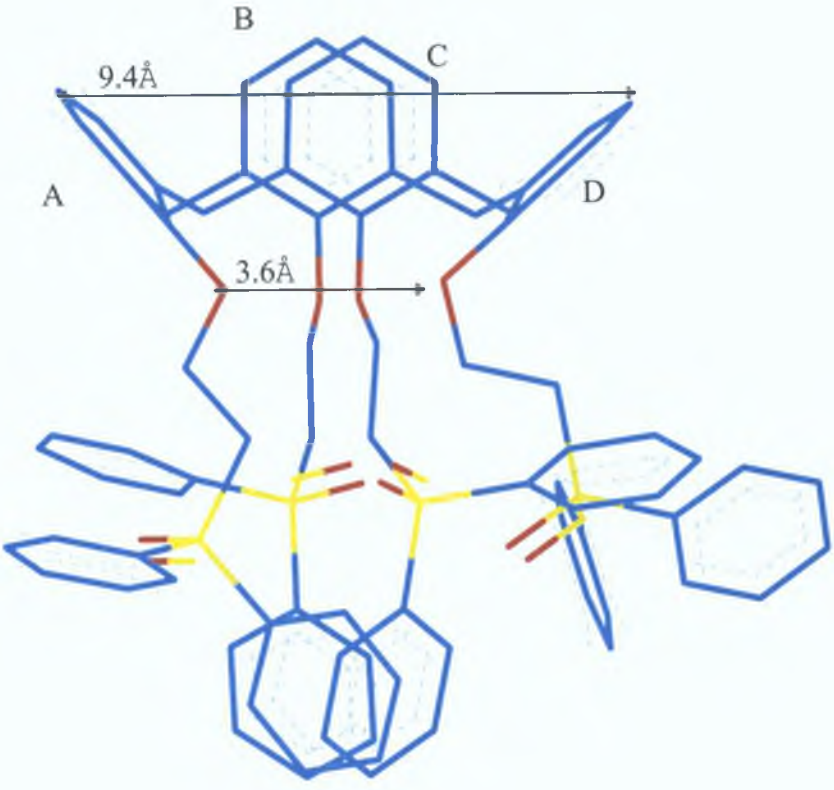

Side view

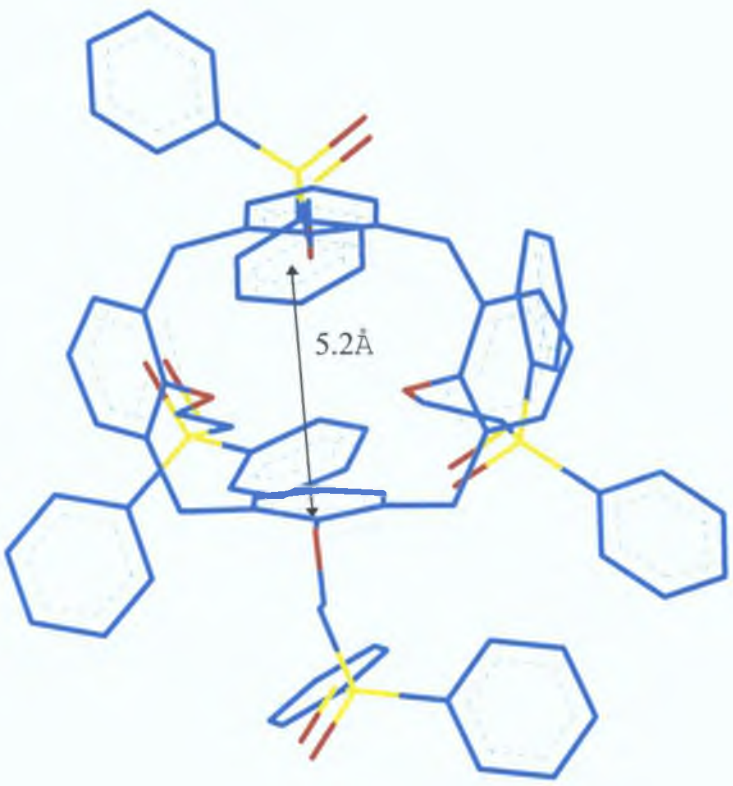

Top view

Figure 5.14: *3-d energy minimised structure of the dealkylated tetraphosphine oxide calix[4]arene* ***5 (vii)*** *obtained using Hyperchem v.4.0.*

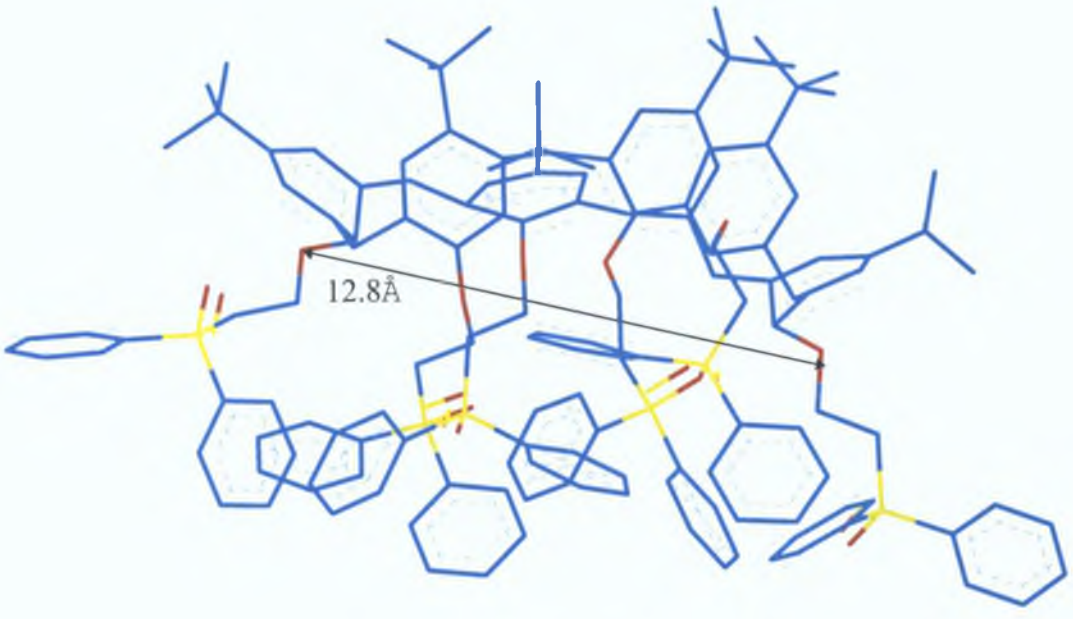

Side view

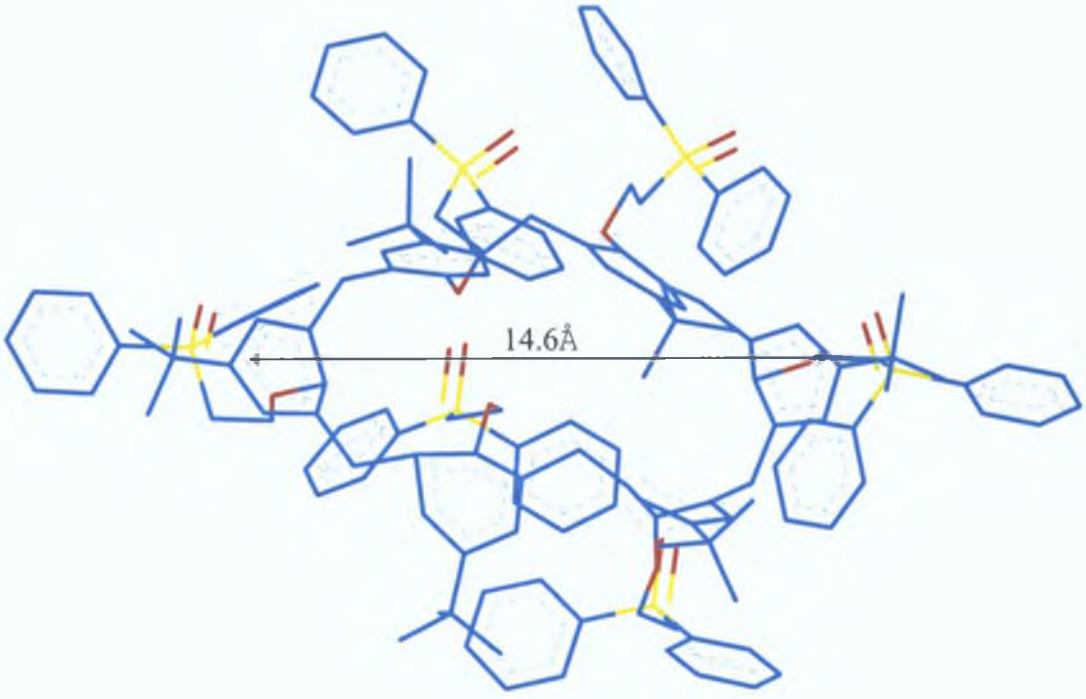

Top view

Figure 5.15: *3-d energy minimised structure of the hexaphosphine oxide calix[6]arene* ***5(v)*** *obtained using Hyperchem v.4.0.*

5.4 Conclusion

In conclusion a PVC membrane electrode based on ionophore **5 (iv)** has been developed which is selective for Eu(III) in the presence of a high background of Na^+ and other common ions The results also suggest that there is selectivity within the lanthanide series itself The dramatic difference in response between ligand **5 (iv)** and **5 (x)** confirms how the complexation ability of calixarenes strikingly depends on the ligating functional groups attached The hexameric form of the phosphine oxide and the dealkylated tetramer are not as selective as **5 (iv)** and this is probably due to their conformation

The determination of lanthanides by this PVC membrane electrode method would have little value in an analytical situation but is very useful as a screening method for the determination of selectivity over other cations which may not appear obvious from extraction data As discussed earlier the low selectivity for calcium of the tetraphosphine oxide prompted our group to investigate this calixarene as a calcium selective ligand which proved to be selective over magnesium and other interfering cations

5.5 References

1 K L Nash, *Solvent Extr Ion Exch*, 1993, **11**, 729

2 J Starry, *Talanta*, 1966, **13**, 42

3 T H Siddall III, *J Inorg Nucl Chem*, 1964, 1991

4 F Arnaud-Neu, *Chem Soc Rev*, 1994, **23**, 235

5 B M Furphy, J M Harrowfield, D L Kepert, B W Skelton, A H White and F R Wilner, *Inorg Chem*, 1987, **26**, 4231

6 I Yoshida, N Yamamoto, F Sagara, K Ueno, D Ishii and S Shinkai, *Chem Lett*, 1991, 2105

7 N Sabbatini, M Guardigli, A Mecati, V Balzani, R Ungaro, E Ghidini, A Casnati and A Pochini, *J Chem Soc, Chem Commun*, 1990, 878

8 R Ludwig, K Inoue and T Yamato, *Solv Extr Ion Exch*, 1993, **11**, 311

9 E P Horwitz, D G Kalina, H Diamond, G F Vandegrift and W W Schulz, *Solv Extr Ion Exch*, 1985, **3**, 75

10 J F Dozol, N Simon, L H Delmau, F Arnaud-Neu, M J Schwing, O Mauprivez, V Bohmer, R A Jakobi and C Gruttner, 3rd International Calixarene Conference, Fort Worth, Texas, Usa, May 1995, (Poster)

11 L Dasaradhi, P Shark, V J Huber, A S Gopalan, P H Smith and G D Jarvinen, 3rd International Calixarene Conference, Fort Worth, Texas, Usa, May 1995, (Lecture)

12 J F Malone, D J Marrs, M A McKervey, P O'Hagan, N Thompson, A Walker, F Arnaud-Neu, O Mauprivez, M J Schwing-Weill, J F Dozol, H Rouquette and N Simon, J Chem Soc, Chem Commun, 1995, 2151

13 F J Saez de Viteri and D Diamond, *Anal Proc*, 1994, **31**, 229

14 G J Moody and J D R Thomas *'Selective Ion-Selective Electrodes'*, Merrow, Watford, 1971

15 T McKittrick, D Diamond, D J Marrs, P O'Hagan and M A McKervey, *Talanta*, 1996, in press